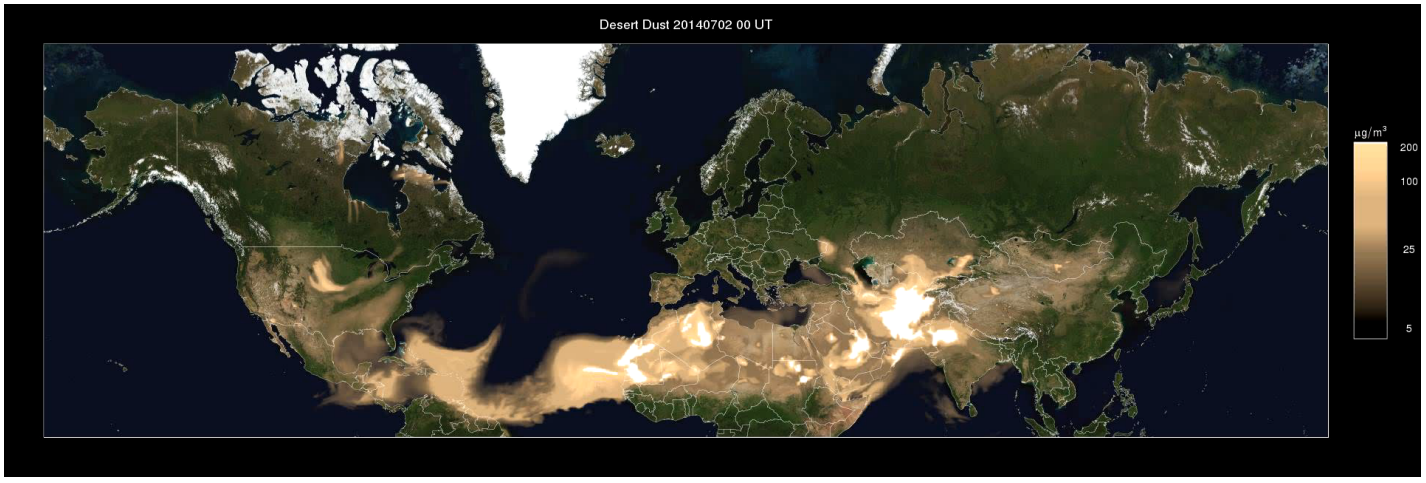
Documentation of the chemistry-transport model

chimere

[version *chimere 2017*]





- This documentation and the model are freely available at the following internet adresse:

```
http://www.lmd.polytechnique.fr/chimere/
```

- CHIMERE is distributed under the GNU General Public License
- Copyright (C) 2017 LMD (CNRS), INERIS, LISA (CNRS)
- For questions, send an e-mail to chimere@lmd.polytechnique.fr
- *Last update of this documentation: March 15, 2017*

Contents

1 Model overview and last changes **11**
- 1.1 Short Description of the model . . . 11
- 1.2 Main characteristics . . . 11
- 1.3 The CHIMERE software . . . 13
  - 1.3.1 The GPL licence . . . 13
  - 1.3.2 Training courses . . . 13
  - 1.3.3 Numerical langage . . . 14
  - 1.3.4 Graphical tool . . . 14
- 1.4 Last changes in version *chimere 2017* . . . 14
- 1.5 How to contact the developers? . . . 16
- 1.6 Acknowledgments . . . 16
- 1.7 About this documentation . . . 17

2 First CHIMERE simulation **19**
- 2.1 Main sources installation . . . 19
- 2.2 The first run tutorial . . . 19
  - 2.2.1 Download required data and programs . . . 20
  - 2.2.2 Simulation configuration . . . 21
  - 2.2.3 Running a simulation . . . 21
- 2.3 Main options in the parameter file . . . 22
- 2.4 The output on screen . . . 29
- 2.5 The output files . . . 29
  - 2.5.1 The chemical and meteorological fields outputs on file "out.[label].nc" . . . 29
  - 2.5.2 The deposition fields outputs on file "dep.[label].nc" . . . 31
  - 2.5.3 The restart fields outputs on file "end.[label].nc" . . . 31
- 2.6 Post-processing the results . . . 31
- 2.7 Some figures to validate your first CHIMERE simulation for the 2009 Test Case . . . 31

3 CHIMERE model source code **35**
- 3.1 CHIMERE general code structure . . . 35
- 3.2 Directories . . . 37
- 3.3 Model Files . . . 37
  - 3.3.1 Scripts . . . 37
  - 3.3.2 Makefile . . . 38
  - 3.3.3 Meteo interface - 1st stage . . . 38
  - 3.3.4 Source directory . . . 39
  - 3.3.5 Dynamic files generated at runtime . . . 40
- 3.4 Parallelism . . . 40
  - 3.4.1 Parallelism optimization in CHIMERE . . . 40
  - 3.4.2 Domains division . . . 41
  - 3.4.3 Recommendations . . . 43

3.5 Routine calls sequence . . . 43
3.5.1 Parameter broadcast . . . 44
3.6 The 'chimere.nml' model namelist . . . 44
3.7 How to add a new diagnostic variable to the code? . . . 47
3.7.1 Compute the variable . . . 47
3.7.2 Declare the variable in chimere_common.F90 . . . 47
3.7.3 Allocate the variable in chimere_allocs.F90 . . . 47
3.7.4 Define the corresponding NetCDF variable . . . 47
3.7.4.1 iniout.F90: create and define attributes . . . 47
3.7.4.2 worker_iniout: read the NetCDF structure for parallel I/O . . . 47
3.7.5 Save the variable to the output file . . . 48

4 Domain, landuse and soil **49**
4.1 The vertical mesh . . . 49
4.1.1 Structure . . . 49
4.1.2 Placing the vertical levels . . . 49
4.2 The horizontal domain . . . 50
4.2.1 Options activation . . . 50
4.2.2 Manual creation of a regular horizontal grid . . . 51
4.2.3 From the ascii grid to a complete geog file . . . 52
4.3 The surface databases . . . 52
4.3.1 Landuse databases . . . 52
4.3.2 The CHIMERE landuse . . . 53
4.3.3 Projection of land-use categories from external databases to CHIMERE . . . 53
4.3.3.1 The GlobCover Land Cover aggregation matrix . . . 53
4.3.3.2 The USGS aggregation matrix . . . 53
4.3.4 The aeolian roughness length interface . . . 54
4.3.5 The erodibility interface . . . 55

5 [chemprep] the chemical preprocessor **57**
5.1 Preparation of new chemical data . . . 57
5.1.1 Available options for the chemistry . . . 57
5.1.2 The make-chemistry.sh script . . . 57
5.2 The preparation of gaseous and aerosol chemistry . . . 58
5.2.1 The input chemistry data files . . . 58
5.2.1.1 The chemical mechanisms . . . 59
5.2.1.2 The ANTHROPIC data files . . . 60
5.2.1.3 The AEROSOL data files . . . 60
5.2.1.4 The MAKEPRI data files . . . 61
5.2.1.5 The REACTIONS data files . . . 61
5.2.1.6 The chemprep.awk program for the gaseous reactions . . . 64
5.2.1.7 The ACTIVE_SPECIES and OUTPUT_SPECIES data files . . . 64
5.2.1.8 The FAMILY data file . . . 66
5.3 The aerosols size distribution calculations . . . 67
5.3.1 Disretization of the size distribution . . . 67
5.3.2 Implementation . . . 67
5.3.3 The log-normal distribution calculation . . . 69
5.4 The preparation of tracers . . . 71

5.4.1 Tracers activation . . . 71
5.4.2 The TRACERS.data data file . . . 71
5.4.3 The chemprep-prep-tracer-data.sh script . . . 71
5.4.4 Calculation of emissions fluxes . . . 72

6 Emissions **73**
6.1 Anthropogenic surface emissions . . . 73
6.1.1 User's precompiled emissions . . . 73
6.1.2 The emiSURF interface . . . 74
6.1.2.1 Step 1 : preprocessing . . . 75
6.1.2.2 Step 2: Horizontal and monthly downscaling with source2chimere.F90 . . . 76
6.1.2.3 Step 3: Downscaling on the vertical dimension and in time with sectoremis.F90 78
6.2 Biogenic emissions . . . 78
6.2.1 Option activation . . . 78
6.2.2 The biogenic emitted species . . . 79
6.2.3 Biogenic emission interface . . . 80
6.3 Sea salt emissions . . . 80
6.3.1 Option activation . . . 80
6.3.2 Sea salt parameterization . . . 80
6.4 Mineral dust emissions . . . 81
6.4.1 Option activation . . . 81
6.4.2 The datasets and input parameters . . . 82
6.4.2.1 The USGS soil texture . . . 82
6.4.2.2 The USGS landuse types . . . 82
6.4.2.3 The aeolian roughness length z_{0s} . . . 83
6.4.2.4 User input parameters . . . 83
6.4.3 Mineral dust fluxes parameterizations . . . 84
6.4.3.1 Weibull distribution for 10m wind speed . . . 84
6.4.3.2 The sporadic effect of rain . . . 85
6.4.3.3 The threshold friction velocities and the drag efficiency . . . 86
6.4.3.4 The soil moisture effect . . . 87
6.4.4 The several mineral dust production schemes . . . 88
6.4.4.1 The [Marticorena and Bergametti, 1995] scheme . . . 88
6.4.4.2 The [Alfaro and Gomes, 2001] scheme . . . 88
6.4.4.3 The [Kok 2014] scheme . . . 89
6.4.5 Vegetation variability . . . 89
6.5 Fire emissions . . . 90
6.6 The resuspension process . . . 90
6.6.1 Option activation . . . 90
6.6.2 Resuspension fluxes estimation . . . 90

7 Depositions **93**
7.1 Dry deposition . . . 93
7.1.1 The deposition velocity for gas and aerosols . . . 93
7.1.2 The aerodynamical resistance, r_a . . . 94
7.1.3 The quasi-laminar layer resistance r_b for gases . . . 94
7.1.4 The surface resistance for gases, r_c . . . 95
7.1.4.1 The stomatal conductance, g_{sto} . . . 96

7.1.4.1.1 The LAI, SAI and phenological factor. . . . 98
7.1.4.1.2 The light factor, f_{light}. . . . 98
7.1.4.1.3 The temperature factor, f_{temp}. . . . 100
7.1.4.1.4 The leaf to air vapour pressure deficit factor f_{vpd}. . . . 100
7.1.4.1.5 The soil water potential factor, f_{SWP}. . . . 101
7.1.4.1.6 The mesophyllic resistance, r_m. . . . 101
7.1.4.2 The non stomatal bulk conductance, G_{ns} 101
7.1.4.2.1 Non stomatal bulk conductance for ozone. . . . 101
7.1.4.2.2 The in-canopy resistance, R_{inc}. . . . 101
7.1.4.2.3 The external leaf uptake resistance, R_{ext}. . . . 102
7.1.4.2.4 Non stomatal bulk conductance for SO_2. . . . 102
7.1.4.2.5 Non stomatal bulk conductance for NH_3. . . . 102
7.1.5 The quasi-laminar layer resistance r_b for aerosols 103
7.1.6 The surface resistance for aerosols, r_s 103
7.1.7 The settling velocity v_s 104
7.2 Wet scavenging 105
7.2.1 Input parameters 105
7.2.2 Wet scavenging for gases 105
7.2.3 Wet scavenging for aerosol 107

8 Initial and boundary conditions **109**
8.1 Options activation 109
8.2 The boundary and initial conditions interface 110
8.2.1 In case of a nested run 111
8.2.2 In case of a climatology use 111
8.3 Available global models climatologies 111
8.3.1 The MACC climatology 112
8.3.2 The LMDz-INCA climatology 112
8.3.3 The GOCART climatology 113
8.3.4 The boundary conditions builder files 114

9 Meteorology **117**
9.1 Meteorological input data 117
9.1.1 Option activation 117
9.1.2 Case of WRF model output 118
9.1.3 Case of any other model output 119
9.2 Diagnostics of parameters: 120
9.2.1 Management of additional parameters 120
9.2.1.1 The friction velocity u_* 120
9.2.1.2 The surface sensible heat flux Q_0 121
9.2.1.3 The Monin-Obhukov length L 122
9.2.1.4 The boundary layer height $\overline{h}$ 122
9.2.1.5 The vertical diffusivity profile K_z 122
9.2.1.6 Urban corrections and other tunable parameters 122
9.2.2 Estimation of the vertical velocity 124
9.2.3 Calculation of the solar zenithal angle 124
9.2.4 Deep convection fluxes 125
9.3 Transport and mixing 128

9.3.1 Horizontal transport . . . 128
9.3.1.1 Option activation . . . 128
9.3.1.2 The transport equation . . . 128
9.3.1.3 Upwind scheme . . . 129
9.3.1.4 Van Leer scheme . . . 129
9.3.1.5 The Parabolic Piecewise Method scheme . . . 130
9.3.2 Vertical transport . . . 130
9.3.2.1 Option activation . . . 130
9.3.2.2 The transport equation . . . 130
9.3.3 Turbulent mixing . . . 131

10 CHIMERE time integration **133**
10.1 The several time-steps . . . 133
10.1.1 The physical time-step . . . 134
10.1.2 The chemical time-step and the CFL criteria . . . 134
10.2 The TWO-STEP time numerical solver . . . 136

11 Gas-phase chemistry **139**
11.1 Option activation . . . 139
11.2 The MELCHIOR mechanims . . . 139
11.2.1 Species list of the reduced MELCHIOR1 gas-phase chemical mechanism . . . 139
11.2.2 Reaction list of the reduced MELCHIOR1 chemical mechanism . . . 140
11.2.3 Species list of the reduced MELCHIOR2 gas-phase chemical mechanism . . . 149
11.2.4 Reaction list of the reduced MELCHIOR2 chemical mechanism . . . 150
11.3 The SAPRC mechanims . . . 154
11.3.1 Species list of the SAPRC-07-A gas-phase chemical mechanism . . . 154
11.3.2 Reaction list of the SAPRC-07-A chemical mechanism . . . 155
11.3.3 Species list of the chlorine SAPRC-07 gas-phase chemical mechanism . . . 163
11.3.4 Reaction list of the chlorine SAPRC-07-A chemical mechanism . . . 163

12 Aerosol chemistry **167**
12.1 The modelled aerosols . . . 167
12.2 Option activation . . . 167
12.3 Aerosols processes . . . 167
12.3.1 Composition and mathematical representation of aerosols . . . 168
12.3.2 Coagulation . . . 168
12.3.3 Absorption . . . 169
12.3.4 Nucleation . . . 170
12.4 Thermodynamic equilibrium . . . 170
12.4.1 Humid diameter and density of aerosols . . . 172
12.5 Multiphase chemistry . . . 172
12.5.1 Sulfur aqueous chemistry . . . 172
12.5.2 Heterogeneous chemistry . . . 172
12.6 Secondary organic aerosol (SOA) . . . 173
12.7 Radiative transfers and photochemical reaction rates . . . 175
12.7.1 Radiative processes in the atmosphere . . . 175
12.7.2 Optical preprocessing using prep_mie . . . 176
12.7.3 Fast-JX initialisation . . . 177
12.7.4 Online calculation of photochemical reaction rates . . . 177

12.7.5 surface albedo . . . 177

13 Additional diagnostic variables **179**
13.1 The optical depth . . . 179
13.2 The lidar vertical profiles . . . 179
13.2.1 Methodology . . . 179
13.2.2 The CHIMERE output results . . . 181

Bibliography **182**

A References using CHIMERE **199**
A.1 Reference papers . . . 199
A.2 List of papers using CHIMERE . . . 199

B History **211**
B.1 Development of the mineral dust emissions . . . 211
B.2 chimere2008 . . . 211
B.3 V200606 . . . 212
B.3.1 Parallelization . . . 212
B.3.2 Toolbox . . . 213
B.3.3 Scripts . . . 213
B.3.4 makefiles changes . . . 213

C Some scripts used in the CHIMERE suite **215**
C.1 The *domains/makeCOORDdomains* script for horizontal grid definition . . . 215
C.2 The *util/define_geom* script for vertical grid definition . . . 216

D How To install NetCDF under GNU/Linux **217**
D.1 Background . . . 217
D.2 Download . . . 217
D.3 Configure NetCDF . . . 217
D.3.1 ifort 64 bit on Intel EMT64 or AMD Opteron . . . 218
D.3.2 gfortran (4.7.2 or later) 64 bit on Intel EMT64 or AMD Opteron . . . 219
D.4 Manually Configure CHIMERE . . . 219

E How To install MPI under GNU/Linux **221**
E.1 Background . . . 221
E.2 LAM/MPI Installation . . . 221
E.3 Testing . . . 222
E.4 Uniprocessor users . . . 222
E.5 Installation from source . . . 223
E.6 Open MPI installation . . . 223

F Notes on using CHIMERE with LAM MPI **225**
F.1 Specific case of single node envrionment . . . 225

G Structure of the CHIMERE netCDF files **227**
G.1 Known issues . . . 227
G.2 EMIS.[domain].[MM].[SPEC].s.nc and EMIS.[domain].[MM].[SPEC].p.nc . . . 227
G.3 exdomout.nc . . . 228
G.4 meteo.nc . . . 230
G.5 AEMISSIONS.nc . . . 232
G.6 BEMISSIONS.nc . . . 234
G.7 BOUN_CONCS.nc . . . 235
G.8 end.nc . . . 235
G.9 Fire emissions EMIS.[domain].[MM].[SPEC].f.nc . . . 240

1 Model overview and last changes

1.1 Short Description of the model

All informations, documentation and code sources are available on the CHIMERE web site:

`http://www.lmd.polytechnique.fr/chimere/`

The CHIMERE multi-scale model is primarily designed to produce daily forecasts of ozone, aerosols and other pollutants and make long-term simulations for emission control scenarios. CHIMERE runs over a range of spatial scales from the hemispheric scale to the urban scale (100-200 Km) with resolutions from 1-2 Km to hundreds Km. On CHIMERE server, documentation and source codes are proposed for the complete multi-scale model. CHIMERE proposes many different options for simulations which make it also a powerful research tool for testing parameterizations, hypotheses. Its use is relatively simple so long as input data is correctly provided. It can run with several vertical resolutions, and with a wide range of complexity. It can run with several chemical mechanisms, simplified or more complete, with or without aerosols.
Currently, the model may be used for:

- Physical and chemical processes research
  - Transport and mixing, turbulence
  - Gas and aerosol chemistry
  - Anthropogenic, biogenic, natural (mineral dust and fires) emissions
  - Dry and wet deposition
- Scenarios and climatologies
  - Past and future emissions impacts
  - Ensemble analysis
- Operational forecast
  - Regional air quality networks (France, Italy, Spain, Netherlands, Portugal etc.)
  - National or Continental institutes (PREV'AIR, MACC, CAMS, etc.)

The main properties of the CHIMERE processes calculations are described in Table 1.1 .

1.2 Main characteristics

CHIMERE is an Eulerian off-line chemistry-transport model (CTM). External forcings are required to run a simulation: meteorological fields, primary pollutant emissions, chemical boundary conditions. Using these input data, CHIMERE calculates and provides the atmospheric concentrations of tens of gas-phase and aerosol species over local to continental domains (from 1 km to few degrees resolution). The key processes affecting the chemical concentrations represented in CHIMERE are: emissions, transport (advection and mixing), chemistry and deposition, as presented in Figure 1.1 . Note that forcings have to be on the same grid and time step as the CTM simulation. In this sense, CHIMERE is not only a chemical model but a suite of numerous pre-processing programs able to prepare the simulation. The model is now used for pollution event analysis, scenario studies,

Process	Methodology
Meteorological forcing	ECMWF, WRF
Landuse	GlobCover or USGS global datasets
Horizontal resolution	from 1km to few degrees
Horizontal advection	upwind, Van Leer or PPM
Vertical advection	upwind or Van Leer
Deep convection	Tiedke scheme
Boundary-layer turbulence	Troen and Mahrt scheme
Anthropogenic emissions	EMEP, HTAP or local inventories
Biogenic emissions	online MEGAN model
Sea salt emissions	Monahan scheme
Mineral dust emissions	Alfaro and Gomes or Kok scheme
Chemical mechanism	SAPRC or MELCHIOR
Aerosols representations	bins
Secondary Organic Aerosols	Pun scheme
Photolytic rates	online FastJX radiative transfer model
Numerical solver	TwoStep solver
Aerosol thermodynamic equilibrium	online ISORROPIA
Dry deposition	Wesely or Zhang parameterization

Table 1.1: *Main properties of the CHIMERE model*

operational forecast and more recently for impact studies of pollution on health ([Valari and Menut, 2010]) and vegetation ([Anav et al., 2011]).

The first model version was released in 1997 and was a box model covering the Paris area including only gas-phase chemistry ([Honoré and Vautard, 2000], [Vautard et al., 2001]). In 1998, the model is implemented for its first forecast version (Pollux) during the ESQUIF experiment ([Menut et al., 2000b]) still over the Paris area ([Vautard et al., 2000]). At the same time, the adjoint model was developed to estimate the sensitivity of concentrations to all parameters ([Menut et al., 2000a]). In 2001, the geographical domain was extended over Europe with a cartesian mesh ([Schmidt et al., 2001]) and the new experimental forecast platform (PIONEER) is set up. In 2003, the experimental forecast became operational with the PREVAIR system operated at INERIS ([Honoré et al., 2008], [Rouïl et al., 2009]). The aerosol module is implemented in 2004 ([Bessagnet et al., 2004]) with further improvements concerning the dust natural emissions and resuspension over Europe ([Vautard et al., 2005b], [Hodzic et al., 2006a] [Bessagnet et al., 2008]) and evaluated against long-term and field measurements ([Hodzic et al., 2005], [Hodzic et al., 2006b]). The development of the mineral dust version started in 2005 ([Menut et al., 2005]). Chemistry was not included in that version and a new horizontal domain had been designed to cover the whole northern Atlantic and Europe, including the Saharan desert and downwind regions. In 2006, an important step is achieved with the development of the parallel version of the model and its first implementation on a massively parallel computer (the ECMWF computer in the framework of the FP6/GEMS project). In 2014 the European dust production model was removed and the African dust production model extent to any domain over the globe. In 2016 CHIMERE is able to run over a hemispheric domain as well as for smaller regions anywhere in the world ([Mailler et al., 2016]).

The CHIMERE model is now considered as a state-of-the-art model. It has been involved in numerous intercomparison studies mainly focusing on ozone and PM_{10} from the urban scale ([Vautard et al., 2007, Van Loon et al., 2007, Schaap et al., 2007]) to continental scale ([Solazzo et al., 2012], [Zyryanov et al., 2012]). Moreover, the model has been mainly applied over Europe, but also more recently over Africa and the North Atlantic for dust simulations, over Central America during the MILAGRO project

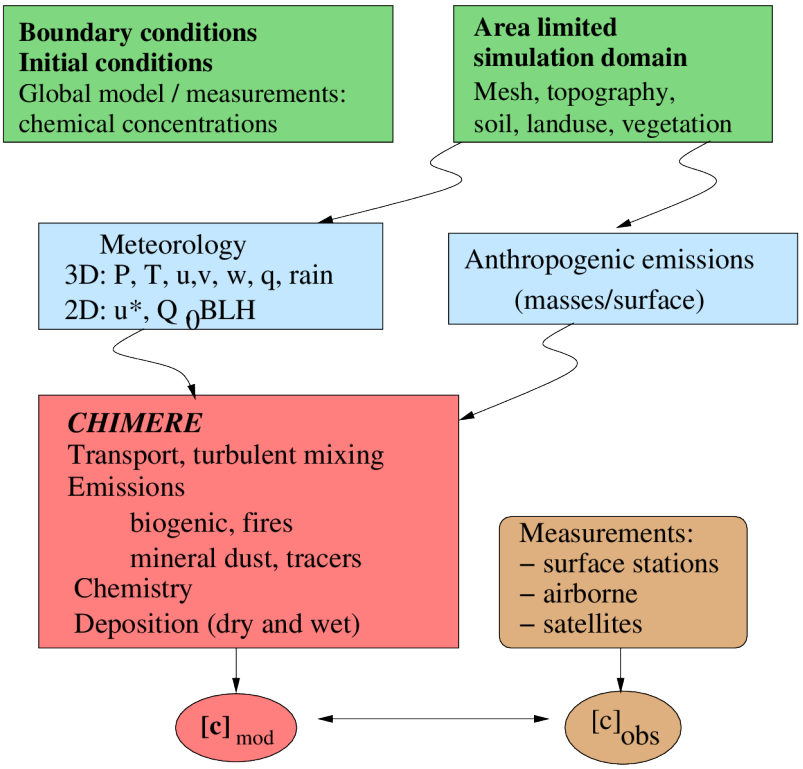


Figure 1.1: *General principle of a chemistry-transport model such as CHIMERE. In the box 'Meteorology', u_* stands for the friction velocity, Q_0 the surface sensible heat flux, L the Monin-Obukhov length and BLH the boundary layer height. c_{mod} and c_{obs} are for the chemical concentrations fields for the model and the observations, respectively.*

to study organic aerosols ([Hodzic et al., 2009], [Hodzic et al., 2010b], [Hodzic et al., 2010a]) and over the US within the AQMEII project ([Solazzo et al., 2012]).

Finally, the development of CHIMERE follows three main rules. First, concentrations of main pollutants are calculated with the best possible accuracy using well evaluated and state-of-the-art parameterisations. Second, a modular framework is maintained to allow updates to the code by developers but also all interested users. Third, the code is kept computationally efficient to allow long-term simulations, climatological studies and operational forecast.

1.3 The CHIMERE software

1.3.1 The GPL licence

In order to facilitate software distribution, CHIMERE is protected under the General Public License. The source code and the associated documentation is available on a web site `http://www.lmd.polytechnique.fr/chimere`. The documentation is both technical and scientific. It includes a chapter dedicated to the set-up of a test case simulation that allows new users to easily carry out a CHIMERE simulation: model configuration and data (meteorology and emissions files) are provided to simulate 2009 winter-time particulate pollution over Europe.

1.3.2 Training courses

In addition, two-day training courses are organised twice a year. Each training course is free of charge for participants and offers a complete training to be able to install the code, launch a simulation and change surface emissions or other parameters in the code.

1.3.3 Numerical langage

The code is completely written in Fortran90, and running scripts are written in shell (using gnu-awk for input datafiles processing). The required software is a Fortran 95 compiler (gfortran is free and efficient, but Makefiles with Intel's ifort compiler options are also provided). The required libraries are NetCDF (either 3.6.x or 4.x.x), PnetCDF, MPI (see below), python, and GRIB API (if you intend to the use the ECMWF meteorological datasets). The model includes tools that can help the user to configure the model's Makefiles for the libraries already installed.
The model computation time for one AMDx64 node of 16 CPUs is 1h30min for 1 month of simulation for the Paris area, at 15 km resolution, the domain size being 45x48x8 with a time step of 360 seconds on average. CHIMERE uses the distributed memory scheme, and MPI message passing library. It is maintened for Open MPI (recommended) and LAM/MPI, but works, with minor changes in the scripts, with MPICH or other MPI compatible parallel environments. The model parallelism results from a Cartesian division of the main geographical domain into several sub-domains, each one being processed by a worker process. Each worker performs the model integration in its geographical sub-domain as well as boundary condition exhanges with its neighbours and file output. To configure the parallel sub-domains, the user has to specify two parameters in the model parameter file: the number of sub-domains for the zonal and meridional directions. The total number of CPUs used is therefore the product of these two numbers.

1.3.4 Graphical tool

For graphical postprocessing, the *CHIMPLOT* software is provided (http://www.lmd.polytechnique.fr/chimplot). It allows making various 1D or 2D plots (e.g., longitude-latitude or time-altitude maps, vertical slices, time series, vertical profiles). One can also overlay multiple fields (e.g., O_3 concentrations, wind vectors, and pressure contours) and perform simple operations such as calculating daily maxima, daily means, vertical or horizontal averaging or integrations.

1.4 Last changes in version *chimere 2017*

The version ***chimere 2017*** contains the following improvements:

- Processes
  - ◇ Several new options are now available for sea salt parameterizations. See section §6.3.
  - ◇ Evaporation of secondary inorganic aerosols takes into account the gas/particle partitioning.
  - ◇ Adjustment of some constants in model parameterizations (cut-off relative humidity for aerosol processes, deep convection activation threshold).
  - ◇ The case of identical horizontal domain to that of WRF is taken into account. In this case the WRF surface pressure is used, rather than extrapolation from the 1st and 2nd CHIMERE layer tops.
- Software
  - ◇ Separation of biogenic and sea salt emissions processing. The resulting emissions are saved respectively in BEMISSIONS.nc and SEMISSIONS.nc files.

- ◇ Changed order of (optional) arguments to chimere.sh; possibility to specify simulation end hour.

- Databases:
  - ◇ New soil categories processing with a high-resolution database for the *GREENFRAC* variable;
  - ◇ The GLCF database is no longer supported.

- Bug fixes:
  - ◇ Urban correction;
  - ◇ CL chemistry for the SAPRC mechanism;
  - ◇ USGS/CHIMERE correspondance for snow/ice;
  - ◇ Deposition cumulation;
  - ◇ Execution flags handling in sequental/parallel/compilation modes;
  - ◇ Simulation end date/hour in the file names;
  - ◇ Reading of a few chimere.par parameters for the 2nd, etc. columns.
  - ◇ *pH* calculation;
  - ◇ Taking into account metal oxydes (e.g. in reactions of SO_2 with Fe and Mn);
  - ◇ Tracers processing.

The version ***chimere 2016a*** contained the following improvements:

- Processes
  - ◇ Domains: Possible use of the model with an hemispheric domain
  - ◇ Mineral dust:
    - ◇ Extension of the dust production model to any domain over the globe.
    - ◇ Addition of a MODIS erodibility database for arid areas
    - ◇ Addition of the production model of [Kok et al., 2014]
  - ◇ Calculation of on-line lidar profiles (Zenith and Nadir)
  - ◇ Humidity impact on aerosol growth
  - ◇ Better estimation of the CFL
  - ◇ Better estimation of the boundary conditions at the model domain top in case of nesting
  - ◇ Use of the MEGAN LAI to have a more realistic dry deposition
  - ◇ New design of the gaseous and aerosols tracers
  - ◇ Addition of a resuspension scheme (active for urbanized areas only)
  - ◇ Addition of chlorine SAPRC-07A mechanism

- Numerics/Software
  - ◇ Removal of the **master** process and use of the **PnetCDF** library to read and write data.
  - ◇ Possible use of the model for several hours in place of several days, with any starting hour
  - ◇ Meteorological and chemical outputs are all in the output file (removal of the meteo file)
  - ◇ Whole code with dynamical arrays allocation
  - ◇ **prepwrf** and **prepemis** are now included into CHIMERE core and being called at each hourly time step.
  - ◇ Every fortran files are now located into the same directory: **src** and every scripts are now located into the same directory: **scripts**. Consequently, the **Makefile** has been simplified and the **compile** script has been removed.
  - ◇ Each aerosol in a single array in the output file (bDUST in place of p01DUST, ... for example)
  - ◇ Removal of the hourly loop within the worker.F90.

- Databases

- ◇ Added landuse and soil types from USGS database (`http://www.usgs.gov`).
- ◇ The aeolian roughness length used is the GARLAP dataset [Prigent et al., 2012].
- ◇ Green fraction from NCAR database (`http://ncar.ucar.edu`).
- ◇ Erodibility from MODIS analysis

1.5 How to contact the developers?

CHIMERE is a National Tool of the French Institut des Sciences de l'Univers, meaning that support has to be provided to the users of model. The model is developed at IPSL/LMD (Palaiseau), INERIS (Verneuil en Halatte) and IPSL/LISA (Creteil) in France.

- **For questions about the model development**:
  Regarding parameterizations or variables choices, you can send an e-mail to the developers:
  chimere@lmd.polytechnique.fr
  This will send an e-mail to: Laurent Menut, Dmitry Khvorostyanov, Myrto Valari, Solène Turquety, Sylvain Mailler (LMD), Bertrand Bessagnet, Augustin Colette, Florian Couvidat, Frédérik Meleux (INERIS) and Guillaume Siour (LISA).
- **For questions about the model use**:
  To share pre- or post-processing tools with the other users, or just present your result, you can register to the chimere users mailing list here:

  `http://www.lmd.polytechnique.fr/chimere/subscribe.php`

  Note that by registering to download the code, you will be automatically registered on the chimere-users mailing list. You can initiate discussions, exchange programs or data between users by using the e-mail adress:
  chimere-users@lmd.polytechnique.fr

1.6 Acknowledgments

The CHIMERE developers acknowledge:

- Gabriele Curci for the biogenic emissions interface
- Richard Engelen for the global concentrations dataset in the framework of the MACC project.
- Eric Chaxel for the WRF model meteorological interface
- Christian Seigneur and Betty Pun (AER) for the reduced SOA scheme,
- Mian Chin and Paul Ginoux (NASA) for the GOCART aerosols concentrations fields used as boundary conditions,
- Sophie Szopa and Didier Hauglustaine (IPSL/LSCE) for the LMDz-INCA gas concentrations fields used as boundary conditions,
- Athanasios Nenes and the ISORROPIA team for the free use of ISORROPIA model,
- Catherine Prigent for the GARLAP aeolian roughness length data.

According to the provided databases you use, please acknowledge in your publications:

- **MACC global dataset as boundary conditions**:
  "This data set was provided by the MACC-II project, which is funded through the European Union Framework 7 programme. It is based on the MACC-II reanalysis for atmospheric composition; full access to and more information about this data can be obtained through the MACC-II web site (`http://www.copernicus-atmosphere.eu`)."

- **Aerodynamic roughness lengths for mineral dust emissions**
  "Comparison of satellite microwave backscattering (ASCAT) and visible/near-infrared reflectances (PARASOL) for the estimation of aeolian aerodynamic roughness length in arid and semi-arid regions by [Prigent et al., 2012, Atmos. Meas. Tech.]."

1.7 About this documentation

In this documentation:

◇ Chapter 2 explains how to install the model from scratch and perform a first run using the prepared test case '2009 winter-time particulate pollution over Europe'.
◇ Chapter 3 (p.35) presents the model sources documentation including the pre- and post-processing interfaces.
◇ Chapter 4 (p.49) and 5 (p.57), explain how the user may define its own model geometry (domain and landuse) and its own configuration for chemistry (gas and/or aerosols, tracers etc.)
◇ Chapters 6 (p.73), 8 (p.109), 9 (p.117), 11 (p.139) describe the treatment (processes and numerics) of the emissions, boundary conditions, meteorology and chemistry.
◇ Appendix presents "how-to" files explaining the way to install libraries such as netCDF and LAM/MPI, and the format of all files used by the model.
◇ A list of published papers about studies using CHIMERE is displayed in chapter A, p.199.

2 First CHIMERE simulation

In the case of a user who never used the CHIMERE model before, this chapter presents how to:

- §2.1: install all softwares prerequisites,
- §2.3: perform a simulation with the pre-defined test case available on the CHIMERE web site
- §2.2: adapt the model top-calling script,
- §2.4: see how are written the results.
- §2.6: post-process the concentrations fields .

2.1 Main sources installation

The CHIMERE model has only been tested on GNU/Linux systems with LAM-MPI and Open MPI message passing libraries. However it should be working on most UNIX systems provided the following software is installed. The foreseenable changes should be related to **shell**, **awk** and **make** syntax, to the **MPI** library used, and also to unformatted binary files which may have to be converted.
The model requires several numerical tools. Their URL adresses are given in Table 2.1 :

- a **Fortran 95** compiler (e.g., **gfortran**)
- GNU **bash** Bourne shell, **awk** and **make**
- Unidata **NetCDF** library (free)
- **PnetCDF** library (free)
- **Open MPI** or **LAM-MPI** software (free)
- The NCO libraries (free)
- python libraries (free)

The installation process of NetCDF and MPI is fully described in **§D, p.217** and **§E, p.221**.
Note that the NetCDF library must be compiled with the same compiler as the CHIMERE model.
If no **bash** is installed, the model may work with a baseline Bourne-shell, but the user may have to edit the scripts to take in account some syntactic features specific to **bash** . The same remark apply to the **awk** and **make** utilities.
The model has been tested with gfortran and ifort compilers.
In the following examples, the **wget** utility is used for downloading, because it is a robust and powerful downloading tool. However, if **wget** is not installed on your system, you can obviously use your favorite browser to download files.

2.2 The first run tutorial

For the first CHIMERE run, we propose to simulate the particulate matter pollution event occurred over Northern Europe in March 2009.
This Test Case simulation is over the European domain called *CONT5* (defined in domains/domainlist.nml, see below) and lasts 8 days starting from March 12 2009. The PM pollution event occurs on March 19 with a maximum at 14h. To drive CHIMERE, WRF model meteorological fields have been prepared. The WRF simulation was driven by the 6-hourly NCEP/AVN analyses with the spectral "nudging" option (grid FDDA).

Models	
WRF model (free)	http://www.wrf-model.org/index.php
ISORROPIA	http://isorropia.eas.gatech.edu
MEGAN	http://www.lar.wsu.edu/megan
Librairies	
Unidata NetCDF library (free)	http://www.unidata.ucar.edu/
PnetCDF library (free)	http://trac.mcs.anl.gov/projects/parallel-netcdf
Open MPI library (free)	http://www.open-mpi.org
Fortran compilers	
gfortran compiler (free)	http://gcc.gnu.org/wiki/GFortran
ifort compiler	http://www.intel.com/cd/software/products/asmo-na/eng/compilers/index.htm
Databases	
EMEP	http://www.emep.int
EDGAR-HTAP	http://edgar.jrc.ec.europa.eu/
GlobCover Portal	http://ionia1.esrin.esa.int
USGS	http://www.usgs.gov
GARLAP	[Prigent et al., 2012]
Green Fraction	http://ncar.ucar.edu
LAI from NASA/EOSDIS	http://www.daac.ornl.gov
Biogenic emissions factor	[Guenther et al., 2006]

Table 2.1: *Useful URL adresses for the development and the use of the CHIMERE model and its modules*

You can see the detailed list of WRF simulation parameters in the output file wrfout*. The model domain covers the Western Europe with a horizontal resolution of 45km and 30 vertical levels.

2.2.1 Download required data and programs

To perform this test case, you need to download the model and some input data archives. To access the source files and databases for the first time, you need to register by filling out the form in the downloads section of the CHIMERE web site:

```
http://www.lmd.polytechnique.fr/chimere/download.php
```

Your data will be examined and if approved you will receive your login/password to access the download page. The script chimere-download.sh is provided to simplify CHIMERE installation. You need to download the script from the web site and to launch it from the directory where you wish to install Chimere.
The script does the following:

1. Prompts you to specify the directory where you would like to store large data files. Creates the model directory and subdirectories for the big files, emissions, output, and the meteorology

2. Downloads the CHIMERE source code and data for the test case: EMEP emissions. In this case, and for their use in a publication, please acknowledge EMEP (Yearly totals), IER (Time variations), TNO (Aerosol emissions), UK Dept of Environment (VOC speciation, [Passant, 2002]). For the users, these data were already preprocessed for Mars and WRF meteorological output for the 5 days of the test simulation.

3. Downloads emission data for other months and the complete emiSURF preprocessor

4. Downloads the boundary and initial conditions

5. Decompresses the downloaded archives to the appropriate directories
6. Moves the archives to the ARCH directory

2.2.2 Simulation configuration

Once the code is downloaded and the mandatory libraries NetCDF, PnetCDF and MPI are installed, the next step is to configure CHIMERE for your system.
CHIMERE uses configuration files that reflect user's requirements and environment. These files reside in ***chimere 2017*** top directory:

- [Makefile.hdr] is a symbolic link to a preformated file, specific to a given compiler. It contains all the information pertinent to your execution environment: compiler options, libraries, etc. Its *BIGARRAY* option determines the memory model used during compilation. You need the 'medium' model if your arrays can exceed 2G (set BIGARRAY=YES). You can activate this option by default if your operating system is 64 bit. In this case you also need to compile your NetCDF libraries with the -mcmodel=medium and -m64 options. Makefile.hdr is included by all subsequent makefiles in CHIMERE source tree, to ensure a consistent compilation.
- [mychimere.sh] contains PATHs to the system software used by CHIMERE: NetCDF and MPI libraries, Fortran compiler, the Makefile.hdr version to use, and the compilation mode (debugging or performance, see below). This file simplifies model portability between different computers, system library versions and Fortran compilers. Once you generated a version of mychimere.sh for a particular system/compiler, you can easily change between them just by changing the symbolic link mychimere.sh to mychimere.sh.[sofware_version]. The mychimere.sh link must be placed into the src directory.
- [chimere.par] is an ASCII file that unites by topic all main parameters of CHIMERE simulations, such as data file locations, domain definitions, physical and numerical options. This file is fully described in Table 2.3 , p.23.

To configure CHIMERE:

- Run config.sh.

```
./config.sh mychimere.sh.gfortran_MyLinuxCluster
```

  This will generate a version of mychimere.sh corresponding to

  - ◇ location of your Fortran compiler
  - ◇ location of your NetCDF package
  - ◇ location of your PnetCDF package
  - ◇ location of your MPI library and executables
  - ◇ if needed, location of your gribex library (for interfaces to meteorologcal datasets in the grib format)

  It will also create a symbolic link mychimere.sh to the newly generated version of the file into the src directory. Later, during CHIMERE compilation with the chimere-compile.sh script and when running the top-calling script chimere.sh, an appropriate symbolic link Makefile.hdr will be created. You can then manually edit src/mychimere.sh to specify the complilation mode: DEVEL for debugging or PROD for performance (the *${my_mode}* variable in src/mychimere.sh).

2.2.3 Running a simulation

- Edit chimere.par to :

- ◇ set up the time span of a run
- ◇ set the cartesian division of the domain (nzdoms and nmdoms)
- ◇ tell CHIMERE the location of pertinent files and directories including the input data that you downloaded:
  - ◇ domain geometry
  - ◇ species list
  - ◇ emission files
  - ◇ boundary conditions files
  - ◇ meteo file
  - ◇ working directory
  - ◇ output directory
- ◇ choose model options

The current model version has been tested with Open MPI. The latter does **not** need to be booted, you can just launch mpirun with your executable. If you are still using LAM MPI, see p. 225.

- Compile CHIMERE:
  All CHIMERE components are compiled with the top-calling script chimere.sh. The flag "c" is used to compile CHIMERE. The compiled code is copied to the exe_${my_mode} directory.
- Run CHIMERE:

  After the compilation you can run chimere.sh to execute the model.
  The general format of chimere.sh script is:

```
./chimere.sh [param_file [task [start_date [nhours [end_date [run_number] ] ] ] ] ]
```

  The command-line arguments are optional: `param_file` is chimere.par by default; `task` is one of: (c)ompilation, (s)equential part, (p)arallel part, (f)lags given in chimere.par (default option). The `run_number`, if specified, overrides values given in the 'runs' row of chimere.par. NEW: The `end_date` (which can be given with trailing two-digit hour) has priority over `nhours`: if it is specified, `nhours` is ignored.
  For instance, for the proposed test case, type the following commands in your terminal:

```
./chimere.sh chimere.par c
./chimere.sh
```

  and see the messages on the screen to check if installation was correctly done.

2.3 Main options in the parameter file

Notes to the top-calling script chimere.sh and the parameter file chimere.par:

- The starting date `di` is an optional argument of the script chimere.sh. For example, for the tutorial test case, the user could launch the script using `chimere.sh chimere.par f 20090312`. If the parameters `di`, `nhours`, etc. are specified as arguments of chimere.sh they have a priority over those given in chimere.par. These parameters can also be specified in chimere.par for each of nested simulations.
- chimere.par also accepts comments (started with '#'), valid bash commands like

```
$(date -u -d "${di} ${ndays} days" +%Y-%m-%d)
```

  and supports simplified date arithmetic, e.g., `(($di - 1))` instead of

```
$(date -u -d "$di 1 days ago" +%Y-%m-%d)
```

- Most of the parameters visible to CHIMERE are specified in chimere.par in the format

```
[$parameter_name] This parameter description  : Value1, Val2,..  ValN
```

  All parameters initialized this way will be visible to the scripts of CHIMERE during simulations.
- Simulation parameters, such as lab, nested, dom, etc., are given as comma-separated values after the colon character (":") in chimere.par. Each column of values corresponds to a different simulation. The user can run multiple simulations with a single call to chimere.sh. The script will subsequently run simulations with parameters defined by the columns whose numbers are listed in the "RUNS" line in the beginning of chimere.par. This is useful when running nested simulations: e.g., the first column corresponds to a course domain, while the second one specifies the fine domain. If for some parameter the number of comma-separated values is less than the number of the simulation requested, the last comma-separated value will be used for that simulation. For instance, you would typically save concentrations to the restart file *end....nc* at the same frequency for all your simulations, thus having only one value of the *$nsconcs* parameter.
- Analysis or forecast mode? ($forecast = 0 or 1) If simulation timing parameters (di, de, dib, deb, dim, dem, dibm, debm) are set to 0 in chimere.par, they will be automatically redefined in scripts/check-dates.sh according to the value of the *$forecast* parameter.
  - ◇ In the analysis mode ($forecast = 0), the run duration is 'nhours', from 'di' to 'di'+'nhours'-24. If a previous simulation is used to force the current one (with initial conditions), it is assumed to have the same duration 'nhours' and to span from 'di'-'nhours' to 'di'-24.
  - ◇ In the forecast mode ($forecast = 1), 'nhours' refers to the maximum forecast time, and the whole simulation period is from 'di' to 'di'+'nhours', i.e., 'nhours'+24. The previous simulation used to force the current one spans from 'di'-1 to 'di'+'nhours'-1.
  - ◇ Typical 'nhours' value is 120 hours for an analysis run and 96 hours for a forecast simulation.
- The Table 2.2 summarizes the links between the user flags and the programs used.

Flag	Action	Script in the **scripts/** directory	Chimere component(s)
imakecompil	Model compilation	chimere-compil.sh	
imakemeteo	Meteorological interface	chimere-meteo.sh	interf-<meteo> and chimere.e
imakeaemis	Anthropogenic emissions	chimere-emis.sh	prep_aemis.e
iusedust	Dust emissions	chimere-run.sh	chimere.e
imakefemis	Fire emissions	chimere-emis.sh	prep_femis.e
iusebound	Inititial and boundary conditions	chimere-bound.sh	prep_bc.e/prep_chimere.e
imakerun	Running Chimere	chimere-run.sh	chimere.e

Table 2.2: *Links between the user's flags and the programs used*

All available options in the chimere.par file are summarized in the Table 2.3.

Table 2.3: List of CHIMERE parameters in the chimere.par file

Flag	**Function**	**Recommended values**
Date/Time management		

Continued on next page

Table 2.3 – continued from previous page

Flag	Function	Recommended values
runs	Number of nested simulations. Give the number of columns you want to activate. Example: the string "1 2" will run the model for the characteristics of the two first columns.	1 2
forecast	Forecast or analysis run 0 = forecast 1 = analysis	1
di	run start date (format YYYYMMDD)	20090101
nhours	run duration (in hours)	240
hour	run start hour	00
de	run end date (0 = auto)	0
endhour	run end hour (0 = auto)	0
CHIMERE Simulation Domain		
nested	Nested run. You have to specify 'no" or "yes" for each simulation column	no, yes
dom	CHIMERE domain. You have to specify the domain name for each simulation column	CONT5, IDF15C
nzdoms	Number of parallel zonal subdomains	5
nmdoms	Number of parallel merid subdomains	3
nlevels	Number of vertical layers	8
top_chimere_pressure	Top layer pressure (mbar)	500
first_layer_pressure	First layer pressure	997
Meteorology Driver		
meteo	Meteo driver (WRF,MM5,ecm)	WRF
metdom	Meteo driver domain	d01, d02
Simulation Output Files		
lab	Simulation label	test1
clab	Coarse domain label	none, test1
accur	Output species detailed (low/full)	low
nsconcs	Conc. save freq. (hr), file end...	24
nsdepos	The deposition fluxes are cumulated every 'nsdepos' values.	2
nframes (future versions)	No. frames per output files (out..nc, etc.)	-
sim	Current run label (output files' ending). The default value will produce an output file with, here for example, the extension *2009010100_2009011100_test1*	dihour_dehour_$lab
Emissions		
emis	Anthropogenic emission source. You have to specify the name of the database you want to use. Default is 'emep'	emep

Continued on next page

Table 2.3 – continued from previous page

Flag	Function	Recommended values
surface_emissions	Use (or not) surface emissions 0 = no 1 = yes	1
point_emissions	Use (or not) point emissions 0 = no 1 = yes	0
fire_emissions	Use (or not) fire emissions 0 = no 1 = yes	1
iusebemis	Use (or not) biogenic emissions 0 = no 1 = yes	1
iusedust	Use (or not) mineral dust emissions 0 = no 1 = yes	1
icuth	u* threshold estimation 0 = [Iversen and White, 1982] scheme 1 = [Shao and Lu, 2000] scheme	1
ifluxv	Dust production model for saltation and sandblasting 0 = [Marticorena and Bergametti, 1995] scheme 1 = [Alfaro and Gomes, 2001] 2 = [Alfaro and Gomes, 2001] + optimization following [Menut et al., 2005] 3 = [Kok et al., 2014] scheme	2
ifecan	Use of soil moisture to inhibit mineral dust emissions, following the [Fecan et al., 1999] scheme 0 = no 1 = yes	1
Boundary conditions		
iusebound	Use and build Boundary conditions 0 = do not use 1 = forced build then use 2 = check if files exist, build only if not existing then use	1
iuseini	Use and build Initial conditions? 0 = do not use 1 = forced build then use 2 = check if files exist, build only if not existing then use	1
Chemistry		

Continued on next page

Table 2.3 – continued from previous page

Flag	Function	Recommended values
mecachim	Chemistry mechanism. [0] = No gas phase chemistry [1] = melchior complete [2] = melchior reduced [3] = SAPRC-07-A	2
aero	Chemically-active aerosols. 0 = no 1 = yes If aero=1, a minimal configuration with NO3, NH4, SO4, PPM, Sec. Org. Aer., WATER is calculated	1
nbins	Number of aerosol size sections. A value between 6 and 10 is recommended	10
seasalt	Include sea salts [0] = none [1] = inert [2] = active (i.e sea salts react with chemistry).	2
isaltp	Sea-salt emission parameterization (0..2)	0
carb	Include carboneceous species [0] = no [1] = yes If yes, OCAR and BCAR are used	1
soatyp	Secondary organic aerosol scheme. This option is active only if aero=1 [0] = no SOA chemistry [1] = simple , [2] = medium [3] = complex	2
trc	Include tracers 0 = no 1 = yes	0
nequil	Gas-particle equilibrium [0] = tabulation [1] = coupling using ISORROPIA on-line	0
npeq	Equilibrium calculation frequency Every 'npeq' physical time-step	1
Pysics options		
iadrydep	Aerosols dry deposition [1] = [Wesely, 1989] scheme [2] = [Zhang et al., 2001] scheme	2
resusp	Resuspension 0 = no 1 = yes	0
Numerical solution parameters		
dtphys	Physical time steps (in mn)	15

Continued on next page

Table 2.3 – continued from previous page

Flag	Function	Recommended values
dtchem	Chemical step (in mn)	5
ngs	Number of Gauss-Seidel iterations	1
nsu	'ngs' values during spinup	5
irs	Number of spinup hours	1
iadv	Advection scheme [0] = upwind [1] = PPM [2] = Van Leer	2
iadvv	Vertical advection scheme [0] = upwind [1] = Van Leer	1
CHIMERE Subgrid Processes		
ideepconv	Deep convection activation 0 = no 1 = yes	1
urbancorr	Urban correction 0 = no 1 = yes	0
ilidar	Lidar profiles (possible diagnostic in output) 0 = no 1 = yes	0
Flags whether to run individual dynamic interfaces and the Core		
imakechemprep	Make chemical input data [0] = No preparation. We consider the directory already exist and is OK [1] = Force building of data [2] = Check is directory exists. If yes, continue.	2
istopchemprep	stop after chemprep stage or not [0] = Prepare the data if necessary and continue. [1] = Prepare the data and forced stop	0
imakemeteo	Run meteo interface? (0-2)	2
imakeaemis	Build anthropogenic emissions? (0-2)	1
imakefemis	Build fire emissions? (0-2)	0
imakerun	Run Chemistry-Transport? (0-1)	1
chimverb	Print on screen verbose or not [0:5]	1
Directories and files (Absolute PATHs here!)		
Simulation Output		
simuldir	Simulation output	/home/user/chimere/$lab
csimuldir	Course run output (for nested run BC)	$simuldir/../$clab
psimuldir	Previous run output (if continue)	$simuldir
Static Data		
bigfilesdir	Big files (AEROMIN.bin, etc)	/home/user/BIGFILES

Continued on next page

Table 2.3 – continued from previous page

Flag	Function	Recommended values
iland_cover	Landuse data [2] = Globcover [3] = USGS	1
landcover_dir	Land Cover directory	$bigfilesdir/LANDCOVER
megan_data	MEGAN data root directory	$bigfilesdir/MEGAN
bcdir	Boundary conditions	$bigfilesdir
bcgas	BC Gaseous Species model name	LMDz4_INCA3_96x95x19_v2013c
bcgasdt	Use of the gaseous species for boundary conditions [0] = no use [1] = use of climatological values [2] = use of time varying values using linear temporal interpolation	1
bcaer	BC non-dust Aerosols model name	LMDz4_INCA3_96x95x19_v2013c
bcaerdt	Use of the aerosols species (except dust) for boundary conditions [0] = no use [1] = use of climatological values [2] = use of time varying values using linear temporal interpolation	1
bcdust	BC Dust model name	GOCART
bcdustdt	Use of the mineral dust species for boundary conditions [0] = no use [1] = use of climatological values [2] = use of time varying values using linear temporal interpolation	1
Dynamic Pre-processors' Data		
Input data		
meteo_DIR	Meteo driver output dir	/home/user/meteo
meteo_file	Meteo file	$meteo_DIR/wrfout_$metdom_$di
wrf_geog	Where is geog from WRF	$meteo_DIR/geo_em_$metdom.nc
emissdir	Anthropic emission directory	
fire_emissdir	Fire emission directory	
Output data		
datadir	Pre-processors input/output directory	$simuldir/data_$dom_$lab
metdir	Dir to store exdomout file	$meteo_DIR/exdomout.$dom
fnmeteo	Meteo out file on chimere 3D grid	$simuldir/meteo.$sim.nc
exdomout	METEO file name	$metdir/exdomout.$sim1.nc
aemisdir	Dir to store anthrpc emiss (stage 2)	$datadir
fnemisa	Anthropic emiss. File (from Stage 2)	$aemisdir/AEMISSIONS.$sim1.nc
fnemisf	Fires emiss. File (from Stage 2)	$datadir/FEMISSIONS.$sim.nc
fnemisb	Biogenic emission File	$datadir/BEMISSIONS.$sim.nc
fnemissalt	Sea salt emission File	$datadir/SEMISSIONS.$sim.nc
fnemisd	Dust emission File	$datadir/DEMISSIONS.$sim.nc

Continued on next page

Table 2.3 – continued from previous page

Flag	Function	Recommended values
iniboundir	Dir to store INI/BOUND files	$simuldir/INIBOUN.$nbins
garbagedir	Log files (compilation)	$chimere_root/compilogs
clean	Clean mode full: all is cleaned except the out files light: only temporary files are removed none: all is keeped	full

2.4 The output on screen

The outputs on screen give the correct reading of input file or not, shows the meteorological pre-processing phase and the CHIMERE simulation itself by printing some variables to give informations about the run. The output on screen may be very simple (with the flag chimverb=0) to very very verbose (with the flag chimverb=5).
After the initialization phase, the outputs on screen have an hourly frequency and are as:

```
DATE          O3      NO2    T_2m(K)    PBLH(m)    w(m/s)    DT(mn)    run(%)    CPU(mn)
2013062600    52.3    0.0      30.5       472.   0.69E-03        5.        0.      13.4
2013062601    52.3    0.0      30.0       470.   0.74E-03       10.        1.      75.8
```

These outputs are:

- The current date in format `yyyymmddhh`
- The first two species defined in the OUTPUT_SPECIES file
- The 2m temperature (in degree)
- The boundary layer height (in meters)
- The vertical wind speed (in m/s) of the first vertical level (typically between 0 to 30 m AGL).
- The integration time-step (in mn)
- The percentage of simulation done (in %)
- The CPU used for each hour of simulation (in mn)

All these values are given for a cell located at the middle of the horizontal domain.

2.5 The output files

Four different output files are delivered:

1. out.[label].nc: contains concentrations fields and meteorology regridded on the CHIMERE mesh
2. dep.[label].nc: contains dry and wet deposition fluxes
3. ini.[label].nc and end.[label].nc: for initialization and restart

They are encoded in the NetCDF format, which presents the following advantages:

- portability among different architectures of computers
- self-documentation since a lot of meta-data are included in the file itself
- direct access

- compatibility with many free or commercial post-processing tools

Moreover, CHIMERE uses a NetCDF convention derived from the one used in NCAR'S WRF mesocscale modelling system, simplifying the toolset for post-processing.

2.5.1 The chemical and meteorological fields outputs on file "out.[label].nc"

Three-dimensional chemical fields are written in an output out.[label].nc file. The selected species correspond to those listed in the OUTPUT_SPECIES parameter file. Default concentrations values are expressed in ppb. These values may be transformed into μg.m^{-3} if the molar mass of each species is added as a second column in the parameter files OUTPUT_SPECIES located in the chemprep directory (the default value is zero). In case of use of FastJX for the photolysis rates, an output of the optical depth for clouds and aerosols is automatically added as output in the out.[label].nc file.
example: In the file chemprep/data/output_species/OUTPUT_SPECIES...: If the line is "`O3 0.`", ozone results will be in ppb. If the line is "`O3 48.`", the results will be in μg.m^{-3}.
Hourly 2-D and 3-D meteorological and turbulence related fields calculated on the CHIMERE grid are also provided in the output *out* file. For an "off-line" run meteorological fields are calculated with the corresponding meteorological model (e.g. WRF) and then interpolated on the CHIMERE grid. Turbulence related fields are calculated with a meteorological diagnostic program embedded in the CHIMERE core. The variables are listed in Table 2.4 .

Table 2.4: List of output meteorological variables

Model variable	**Variable description**	**Units**
Times	Date string	NA
lon	Longitude	degrees-east
lat	Latitude	degrees-north
2-D Variables		
hght	Boundary Layer Height	m
usta	Friction Velocity u_*	m/s
uwta	Convection Velocity w_*	m/s
aerr	Aerodynamic Resistance	s/m
sshf	Surface Heat Flux	W/m^2
slhf	Surface Latent Heat Flux	W/m^2
u10m	10m Zonal Wind Speed	m/s
v10m	10m Meridional Wind Speed	m/s
w10m	10m Vertical Wind Speed	m/s
tem2	2m Temperature	K
soim	Soil Moisture	m^3/m^3
sreh	Surface relative humidity	%
pscf	Surface Pressure	Pa
swrd	Short Wave Radiation	W/m^2
atte	Radiation Attenuation Coefficient	[0-1]
copc	Convective precipitation	kg/m^2/h
lspc	Large Scale precipitation	kg/m^2/h
toppc	Total precipitation	kg/m^2/h
3-D Variables		

Continued on next page

Table 2.4 – continued from previous page

Model variable	Variable description	Units
hlay	Top of Layers' Height	m
thlay	Layers' Thickness	m
winz	Zonal Wind Speed	m/s
winm	Meridional Wind Speed	m/s
winw	Vertical Wind Speed	m/s
temp	Temperature	K
pres	Pression	Pa
airm	Air Density	kg/m^3
sphu	Specific Humidity	kg/kg
clwc	Liquid (+ice) Water Content	kg/kg
cliq	Cloud Liquid Water Mixing Ratio	kg/kg
cice	Ice Liquid Water Mixing Ratio	kg/kg
rain	Rain Water Mixing Ratio	kg/kg
kzzz	Vertical Diffusion Coefficient	m^2/s^2
Deep convection related fields		
dpeu	Entrainement in Updraft	$kg/m^2/s$
dped	Entrainement in Downdraft	$kg/m^2/s$
dpdu	Detrainement in Updraft	$kg/m^2/s$
dpdd	Detrainement in Downdraft	$kg/m^2/s$
flxu	Upward Mass Flux	$kg/m^2/s$
flxd	Downward Mass Flux	$kg/m^2/s$

2.5.2 The deposition fields outputs on file "dep.[label].nc"

This file contains fluxes integrated over the chemical time-step duration. The calculations are done in the model core and are written in independent files. For the dry deposition flux, only the first vertical cell is taken into account. On the other hand, for the wet deposition, fluxes are sumed up the whole column since, in the model, each vertical level may contribute to a net sink. Units of these two integrated fluxes are g/cm^2.

2.5.3 The restart fields outputs on file "end.[label].nc"

The structure of this file is described in **Appendix G.8, p.235**. The main goal of this file is to save all concentrations fields every $nsconcs hours. For example, for a second run following in time the first one, this "end..." file will be link to a "ini..." file and thus used to give realistic initial conditions during the restart.

2.6 Post-processing the results

Apart some configuration files and static data files written in ASCII code, all the input and output files of the model are written in the NetCDF format, using conventions similar to the WRF conventions. Thus the tools described below may be used to process almost any CHIMERE NetCDF file, including meteo files. CHIMERE NetCDF files are suffixed with **.nc**.
You can use the *CHIMPLOT* program to visualize your data, either interactively or producing plots automatically. Interactive visualization is done using a simple graphical user interface running *chimplot.py*. To automate your work you can save a *Template* after plotting a figure and then run a command-line version *chimplotcm.py*

with a datafile of interest and the generated *Template*. There are multiple options running *chimplotcm.py*. Please refer to the *CHIMPLOT* web site for installation and usage guidelines:

```
http://www.lmd.polytechnique.fr/chimplot
```

2.7 Some figures to validate your first CHIMERE simulation for the 2009 Test Case

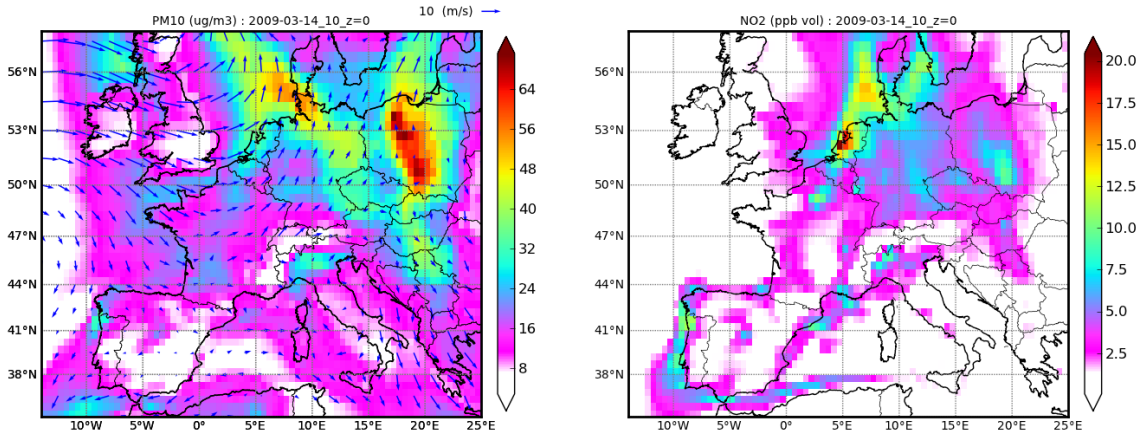
Here we present some figures from the March 2009 test case described in §2. If you used the data available on the CHIMERE website for this test case (the TEST directory when using the chimere-download.sh script), and the simulation parameters set by default in chimere.par, then you should obtain the same figures. The figures shown here were made with *CHIMPLOT*.
To quickly plot these figures with *CHIMPLOT* you can execute the following few lines of *bash* code from the main CHIMPLOT directory ***chimplot***. The code runs the command-line utility *chimplotcm.py*. Sample *CHIMPLOT* Templates PM10_test.par and wind_test.par are provided with the Test Case and can be downloaded on the CHIMERE download page.

```
chimfile=OUTPUTS/Test/out.2009030700_2009031500_Test.nc
chimplotcm.py -fig PM10.png "$chimfile" "PM10_test.par wind_test.par"
```

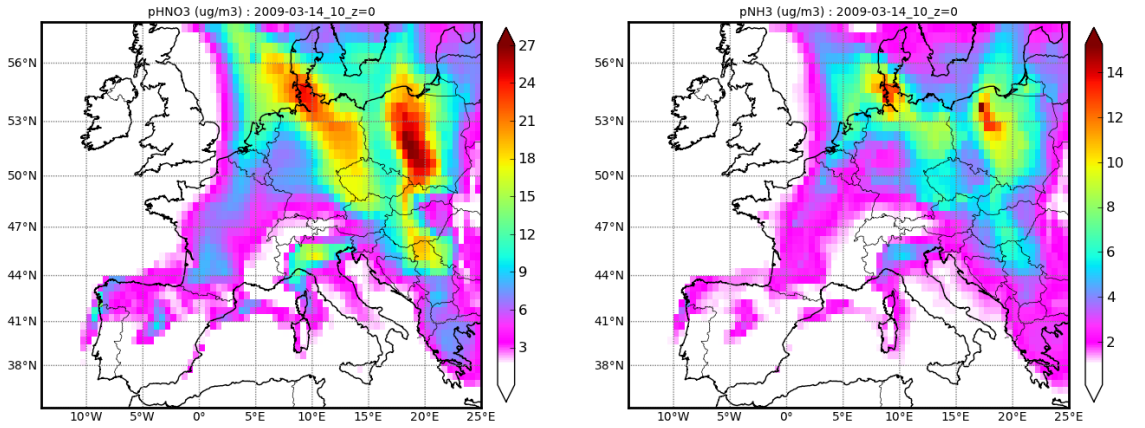
To make other plots automatically from the template PM10_test.par:

```
for v in NO2 pHNO3 pNH3 pH2SO4 pPPM ; do
   chimplotcm.py -varname "['${v}']" -fig ${v}.png ${chimfile} PM10_test.par
done
```

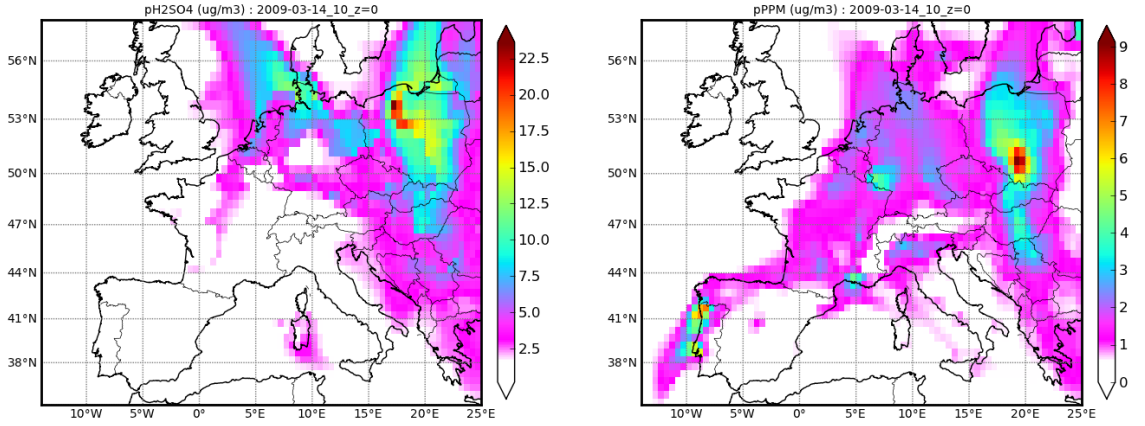
The code above supposes you put the CHIMPLOT template into the BIGFILES directory containing the OUTPUT directory where the out.*nc file is written.
Note: the "-varname" option can only be used with a single template at a time, therefore the second of the above examples (the one with a loop over species) will plot concentration maps without wind vectors. If you wanted to automate the first of the above examples, please check the templates/mk_templ.py script for template generation.



(a) PM_{10} (μg m^{-3}) and NO_2 (ppb) concentrations on March 14, 2009 at 10h



(b) HNO_3 and NH_3 concentrations (μg m^{-3}) on March 14, 2009 at 10h



(c) $H2SO_4$ and PPM concentrations (μg m^{-3}) on March 14, 2009 at 10h

Figure 2.1: Figures to validate the March 2009 Test Case simulation

3 CHIMERE model source code

3.1 CHIMERE general code structure

The general structure of the CHIMERE model is shown in Figure 3.1. Before running the model core (chimere.e executable), a few pre-processors need to prepare the model input data. These are:

- Data generated once per simulation domain ${dom} and put to the domains/${dom} directory:
  - ◇ Domain horizontal coordinates:
    domains/HCOORD/COORD_${dom}
  - ◇ Domain vertical coordinates (see p. 49):
    domains/VCOORD/VCOORD_${nlevels}_${first_layer_pressure}_${top_chimere_pressure}
  - ◇ Land-use categories (see p. 52):
    LANDUSE_[database]_${dom}.nc
  - ◇ Soil categories:
    geog_[database]_${dom}.nc
  - ◇ Biogenic emission factors and leaf-area indices for MEGAN (see p. 78):
    EFMAP_LAI_${dom}.nc
  - ◇ Aeolian roughness length (see p. 81):
    z0_CHIMERE_${dom}_ASCAT.nc
- Data generated once per specified chemistry/aerosol configuration
  - ◇ Chemistry and aerosol parameters (chemprep/inputdataXXXX.X directory, see p. 57)
- Data from the dynamic pre-processors, often generated for every CHIMERE simulation, but any of them can be reused for further simulations by adjusting appropriate flags in chimere.par. The following data are put to the CHIMERE data directory ${datadir} :
  - ◇ Boundary and initial conditions: BOUN_CONCS.${sim}.nc-* for boundary conditions (p. 109) and INI_CONCS.${sim}.nc-* or end.${sim}.nc for initial conditions, depending on whether or not the simulation starts from a restart file (p. 31).

CHIMERE simulation output consists of four NetCDF files in ${simuldir}:

- Output concentrations out.${sim}.nc
- Restart concentrations end.${sim}.nc
- Depositions dep.${sim}.nc
- Meteorological fields diagnozed by CHIMERE out.${sim}.nc (p. 117)

Each pre-processor prepares its data on the CHIMERE grid for the time period and domain to simulate.
The model core organization is described below. The main FORTRAN program src/chimere.F90 initializes and reads all data and then integrates the model for the required time period. The output files are available for post-processing already during simulation. The whole system is driven by the top-level script chimere.sh, which :

- reads parameters of the simulation

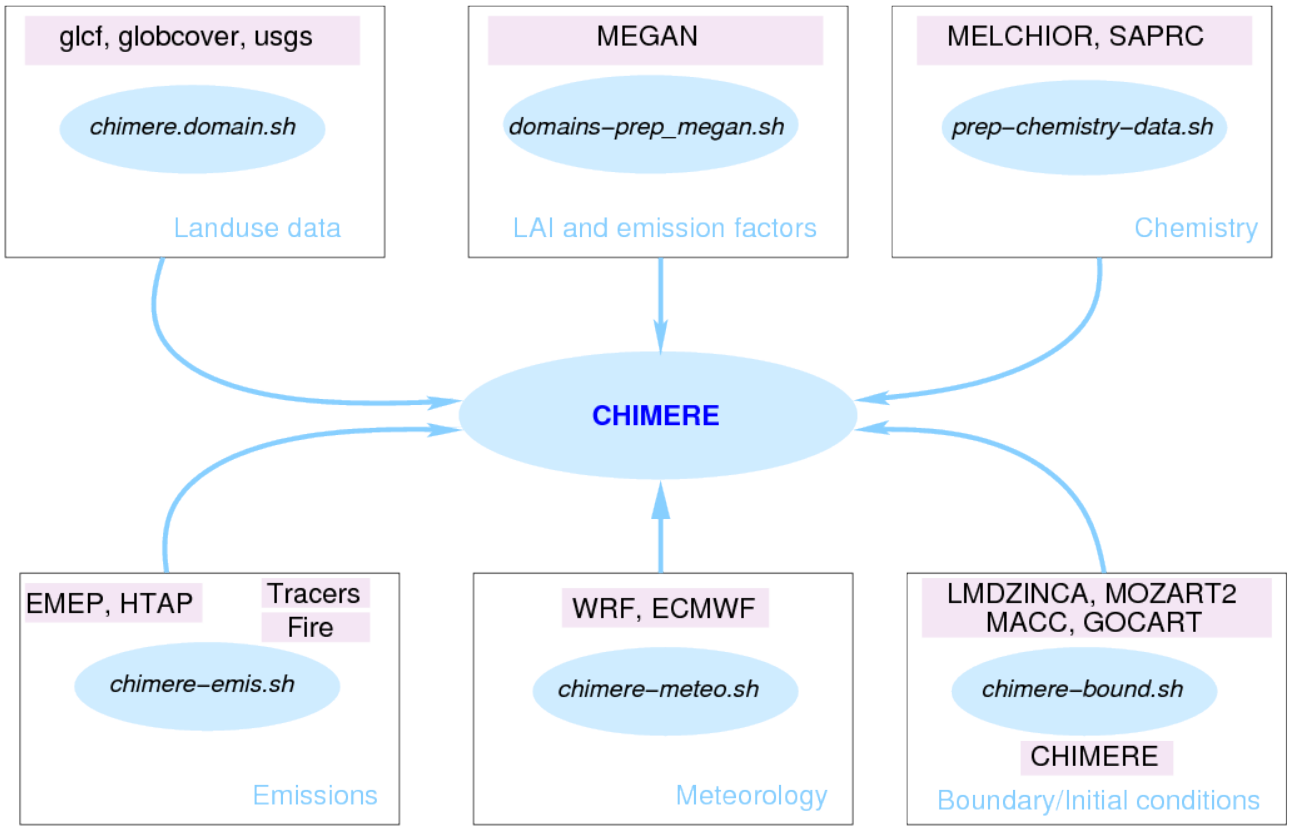


Figure 3.1: *General structure of CHIMERE model*

- links or copies all necessary files into $chimere_tmp where all programs are executed
- compiles the code using the `make` command
- runs the dynamic pre-processor (boundary conditions)
- runs the model core

Before running the top-level script, chimere.par must be edited to specify model options and directories.

Model directories are specified in two different files: data directories are given in chimere.par, while system directories, such as PATHs to NetCDF and MPI libraries, are given in the file mychimere.sh. The latter is activated with a *source* command inside the top-level script chimere.sh. This is done to simplify the model portability between different computers: the user can create one src/mychimere.[System/Compiler].sh version for each computer, each with its own system PATHs and architecture parameters, and then just update a symbolic link src/mychimere.sh -> mychimere.[System/Compiler].sh every time one needs to run CHIMERE on one of those computers. This allows to avoid editing system parameters every time the model is run on a different computer or with a different compiler or library.

The script config.sh automates the task of editing mychimere.sh by searching the installed libraries and Fortran compilers and guiding the user to choose between available versions. When making the choices *it is up to user to ensure that all the components are compiled with the same Fortran compiler!* After the script has finished its work a new version of mychimere.sh is created corresponding to the desired configuration.

3.2 Directories

The $chimere_root top directory contains individual files, the top-level script chimere.sh, and subdirectories. These subdirectories are:

- chemprep/: Contains data files for gas, aerosols and chemical mechanisms.
- domains/: A subdirectory where coordinate files COORD_${dom} and land-use files LANDUSE_[database]_${dom}.nc must be placed for each CHIMERE model domain. This directory contains also the file domainlist.nml where each line corresponds to a model domain.
- makefiles.hdr/: Contains examples of Makefile headers for several architectures and compilers.
- scripts/: Contains the scripts called by the top-level script.
- src/: Contains the model source code.

Other subdirectories are created when running the model:

- exe-${my_mode}/, where ${my_mode} defined in mychimere.sh is the compilation mode, either `PROD` or `DEVEL`, is where all executable files are copied. This directory is used to avoid code recompilation for each run.
- $chimere_tmp/: CHIMERE *temporary directory* defined in chimere.par. This allows several simulations to be subsequently launched from a unique $chimere_root directory, given the name of the temporary directory $chimere_tmp contains either a unique process number (`$$` in the bourne shell) or script execution date and time (default option in chimere.par)[1]. Depending on the $clean option in chimere.par, this directory can be left after a model simulation (especially when debugging) or removed at the end of the top-level script execution. A temporary directory is created for each model run.
  Hint for developpers :
  You can `cd` to $chimere_tmp to modify the model code and test your modifications. The model environment and parameters are defined in files chimere.nml and chimere_params.F90 in $chimere_tmp. To perform a model run without the overhead of replaying the boundary conditions, and especially for debugging, you can type the following commands in a Terminal:

```
source src/mychimere.sh
cd $chimere_tmp
ulimit -s unlimited
make && time ${my_mpirun} -np N ./chimere.e
```

  with N = number of subdomains
- $simuldir/: An *output* directory where simulation output files are created during the run. The PATH to this directory is given in chimere.par (variable $simuldir). It does not need to be created before the run.

3.3 Model Files

3.3.1 Scripts

Three main steps are accomplished by the top-level script chimere.sh. All the scripts called by chimere.sh ÑĄan be found in the scripts/ directory.

1. Preparation of landuse and chemical data files:

[1] If you loop over chimere.sh though, you will need separate $chimere_root directories to run simultaneous simulations.

- define_params.sh calls read-params.sh and check-dates.sh to inititalize simulation parameters.
- make-chemistry.sh calls chemprep-prep-chemistry-data.sh, chemprep-prep-tracer.sh, chemprep-prep-boun-data.sh, chemprep-check_consistency.sh, and chemprep-copy-chemresults.sh rebuild a chemical mechanism (see explanations p.57).
- chimere-domain.sh prepares the domain data generated by the static pre-processors. It calls domains-makeCOORDdomains.sh, domains-prep_geog.sh, domains-prep_landuse.sh, domains-prep_megan.sh, and domains-prep_z0.sh (see explanations p.49).
- domains-define_geom.sh is an utility script that defines the vertical grid. It creates a file with hybrid sigma-p coefficients defining the grid (see explanations p.49).

2. The sequential part chimere-step1.sh:

   - chimere-init.sh inherits the variables defined in chimere.par and initializes other simulation parameters used by other scripts.
   - chimere-compil.sh is called to compile the model code.
   - chimere-bound.sh launches the initial / boundary conditions interfaces.
   - chimere-meteo.sh launches the meteorological interfaces other than WRF and prepares the namelist for the meteo-prepwrf module.
   - chimere-run1.sh launches the model core execution for the sequantial part

3. The parallel part chimere-step2.sh:

   - chimere-step2.sh calls the parallel part of CHIMERE that requires several processors. The separation onto sequential and parallel parts is done to avoid the loss of computing time by requesting many processors on a cluster to run sequential programs.

3.3.2 Makefile

The code is built according to src/Makefile. To ensure consistency, the Makefile calls a top-level header Makefile.hdr, which specifies all the user installation details. Makefile.hdr is a symbolic link to one of the predefined headers located in makefiles.hdr subdirectory.

3.3.3 Meteo interface - 1st stage

The interface discribed below is for WRF, and ECMWF (defined as `[$meteo] : ecm` in chimere.par) mesoscale modelling systems. Note that the WRF interface does not require COORD_${medom} files, since domain grid coordinates can be found in WRF output NetCDF files, while ECMWF interface requires LSMORO file as described below.

I. scripts/

   - chimere-meteo.sh: script to prepare meteorological interface.
   - meteo-interf-${meteo}: scripts to run the meteorological interface

II. meteo_domains/ecm

   - LSMORO_ecm${metdom}.GRB: contains the coordinates of the ecm file, Geopotentiel and Land_sea mask at the ground.

III. src/

- ${meteo}_consts.F90: defines the physical constants used by prep${meteo}.F90.
- meteo-prep${meteo}.F90: read WRF or ECMWF standard output files and perform interpolations to the horizontal CHIMERE model grid. NEW: For WRF model this is part of the model core, while for other meteorological interfaces these are separate programs meteo-prep${meteo}.e called by the scripts meteo-interf-${meteo}.
- meteo-${meteo}_par.F90: describe input and output variables for meteo-interf-${meteo}. Should be edited depending on the available variables in the meteo output file.
- meteo-prep_bilin.F90: bilinear interpolation subroutine used in the meteo interface meteo-prep${meteo}.F90.
- subs.F90: contains various helper subroutines.
- interp_tools.F90: subroutines to calculate the weighting coefficients for horizontal interpolation.
- io.F90: I/O subroutines.
- calendar.F90: calendar subroutines.
- ncvar.F90: netcdf I/O subroutines.
- pncvar.F90: parallel netcdf I/O subroutines.

IV. $chimere_tmp/

- ${chimere_tmp}/metargs-${meteo}: ASCII files generated by the top-level script (scripts/chimere-meteo.sh). Passed to meteo-interf-${meteo}. Contain parameters used by meteo-prep${meteo}.F90.
- ${chimere_tmp}/meteo-prep${meteo}.nml: namelist generated by meteo-interf-${meteo} and containing input parameters for meteo-prep${meteo}.F90.

3.3.4 Source directory

All the model sources are in the src/ directory.

1. chimere_params.F90 module.
2. chimere.F90 is the main program. Compiled to chimere.e and called by the execution script.
3. chimere_common.F90 module describes all the variables shared by the workers, type definitions, and memory allocation subroutines.
4. worker.F90 is the main subroutine called by chimere.F90.
5. chimere_consts.F90 module holds most of the physical and mathematical constants used in the model.
6. worker_message_subs.F90 module contains the message passing (MPI) subroutines used to exchange the data between the parallel subdomains.
7. ini*.F90 are initialization subroutines executed once by the rank 0 process.
8. readhour.F90, renewhour.F90 provide the model with hourly meteo and boundary conditions.
9. outprint.F90, write*.F90 periodically save the model results to files.
10. is*.f contains the ISORROPIA thermodynamic model. Unmodified ISORROPIA library. Called by workers, but has its own namespace.
11. fjx*.F90 contains the Fast-JX model. Called by workers, but has its own namespace.
12. prep_*emis.F90 is the standard emission interface (anthropic, fire, tracers).

13. prep_bc.F90 is the boundary and initial conditions interface for the coarse (non-nested) runs. Compiled to prep_bc.e and called by the top-level script before the model core.

14. prep_chimere.F90 is the boundary and initial conditions interface for the nested runs. Compiled to prep_chimere.e and called by the top-level script before the model core.

15. prep_mie.F90 used to intialize (read inputfile) the Fast-JX model. Compiled to prep_mie.e and called by the top-level script before the model core.

16. other.*.F90 are helpers for initialization subroutines used by the model core.

3.3.5 Dynamic files generated at runtime

All the following files can be found in the $chimere_tmp/ directory.

1. Dynamic parameters All these files are created and moved into the $chimere_tmp/ directory before the model run.

   - ${chimere_tmp}/prep_bc.nml: namelist generated by the top-level script to drive prep_bc.e.
   - ${chimere_tmp}/prep_chimere.nml: namelist generated by the top-level script to drive prep_chimere.e.
   - ${chimere_tmp}/prepemis.nml: namelist generated by the top-level script to drive the prep_aemis, prep_temis and prep_femis modules of the CHIMERE core.
   - ${chimere_tmp}/prep_mie.nml: namelist generated by the top-level script to drive prep_mie.e.
   - ${chimere_tmp}/chimere.nml: namelist containing most of the runtime parameters for the model.

2. Dynamic data files All these files are created in the datadir/ directory during the model run.

   - ${datadir}/exdomout/exdomout.${sim}.nc: output NetCDF file generated by meteo-interf-${meteo} with interfaces for models other than WRF. Contains meteo variables interpolated to CHIMERE horizontal grid.
   - ${datadir}/AEMISSIONS.${sim}.nc: NetCDF file generated by the anthropogenic emissions interface. Contains hourly anthropogenic emissions.
   - ${datadir}/BEMISSIONS.${sim}.nc: NetCDF file generated by the model core to save the biogenic emissions calculated during the simulation.
   - ${datadir}/FEMISSIONS.${sim}.nc: NetCDF file generated by the model core to save the fire emissions calculated during the simulation.
   - ${datadir}/BOUN_CONCS.${sim}.nc-*: NetCDF file(s) generated by the boundary/initial conditions interface. Contain hourly lateral and top concentrations.
   - ${datadir}/INI_CONCS.${sim}.nc-*: NetCDF file(s) generated by the boundary/initial conditions interface. Contain initial concentrations.

3.4 Parallelism

3.4.1 Parallelism optimization in CHIMERE

In previous CHIMERE versions, the parallelizazion was done as following:

- One master process that read input data and wrote output files.

- Several worker processes related to subdomains. Each worker was in charge of computations on its subdomain only.

The master process was an intermediary between input/output files and workers, e.g., reading meteorology from a weather forecast model and sending it to workers.
In order to optimize the interactions, the master process has been removed, and each worker process now directly communicates with external files. This is implemented using the parallel input/output routines of the Parallel-Netcdf library [Li et al., 2003] (Figure 3.2). Note that the parallel netcdf library is the one of the *Argonne National Laboratory*:
`http://trac.mcs.anl.gov/projects/parallel-netcdf`.
This handles classic-format NetCDF files (rather than the *unidata* NetCDF4 library working with NetCDF-4 format files).

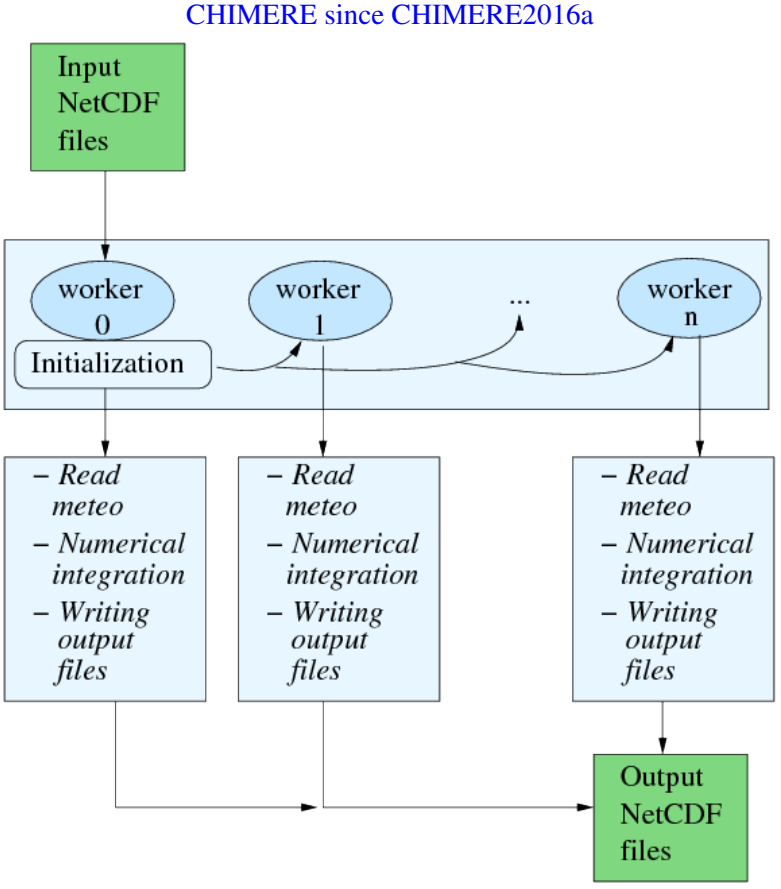


Figure 3.2: *Interaction between master and workers processes and input and output files. Note that workers processes also communicate with each other and that these interraction are not represented here.*

3.4.2 Domains division

Only the model core (chimere.e) has been parallelized so far, while CHIMERE preprocessing tasks (i.e., prior to chimere.F90 call), such as the boundary condition interface, remain sequential.

To allow for a parallel execution of CHIMERE by several processors, the main domain is horizontally divided in rectangular subdomains. This cartesian division is performed in the main execution script, which takes as inputs the user-defined parameters **nzdoms** and **nmdoms**, numbers of subdomains in each dimension. Then the main execution script launches **nzdoms*nmdoms** chimere.e processes in parallel, through the MPI command

```
mpirun -np nzdoms*nmdoms ./chimere.e
```

Processes are called **workers**. There are as many workers as CHIMERE subdomains.
In a first order analysis, we could consider that :

1. all workers read the chimere.nml namelist
2. worker 0 performs all initializations
3. worker 0 broadcasts initialization data to other workers (see Section 3.5.1)
4. all workers work on their own subdomains
5. each worker writes its portion of the results to the corresponding sections in the output files

Since CHIMERE has been parallelized, the computation of transport terms needed additional interactions. A worker process requires not only its subdomain's data but also a stripe of boundary data belonging to its neighbours. The reason is that to calculate a target value at point **(i,j)**, you need values for all surrounding points from **(i-3,j-3)** to **(i+3,j+3)**. So, steps 3 and 4 in the the algorithm above become:

3. worker 0 broadcasts intialization data *plus a surrounding "halo"*, to other workers
4. all workers work on their own subdomain *but communicate with other workers to update their surrounding "halo"*

In fact, to calculate a target value at point **i** and time **tn+1**, you need source values at point **i-3, i-2, i-1**, at time **tn+1**, and source values **i, i+1, i+2, i+3** at time **tn**. You cannot simply calculate target values at time **tn+1** from a set of source values at time **tn**. That is, to start the calculation of the 5th line of a subdomain, you need to know the new values of the 3 last pixels of the 5th line of its left neighbour. This is done by setting a dependency relationship between lines, and by copying the 3 last pixels of a line to the halo of the corresponding line in the right-hand subdomain. This copy occurs for each line of each subdomain, thus at a frequency much higher than the fine time step.
What we have just explained in the previous paragraph for the **i** direction also applies to the **j** direction. The dependancy relationship in both directions leads to a straightforward conclusion : *it is impossible to parallelize CHIMERE.*
We have practically solved the problem by starting the computation of each row of subdomains as if it were an independant domain, with no upper and lower neighbour, exactly as we do for the main domain in the sequential scheme. But at the end of each fine time step, we update their upper and lower halos. This provides a reasonnable smoothing between subdomains, albeit not being numerically identical to the sequential scheme. This leads to an imperceptible numerical difference between the results of the sequential model and those of the parallel model, showing patterns parallel to the X direction when we display the difference. The amplitude of the discrepancy is negligible, it damps very quickly, and we have never observed the development of numerical instabilities from these patterns.

3.4.3 Recommendations

The optimal number of subdomains **nzdoms*nmdoms** results from a tradeoff between the true computing time and the time wasted in message passing between processes. The message passing time is roughly proportional to the perimeters of the subdomains, and the true computation time to their area. For a 80*80 domain and the gas-only version, you will waste CPU time in message passing if you go beyond 4*4 subdomains. On the other hand, the same 80*80 simulation including aerosol chemistry, sea salts, and 3 Gauss-Seidel iterations should still be efficient with 8*8 subdomains.
It is the user's responsibility to try with an increasing number of subdomains (and an increasing number of processors, of course) in a typical model configuration and to decide of the best choice.

3.5 Routine calls sequence

The general schematic diagram of calls of the CHIMERE model src/chimere.F90 is given in Figure 3.3. Only major routines are cited, not the utility ones.

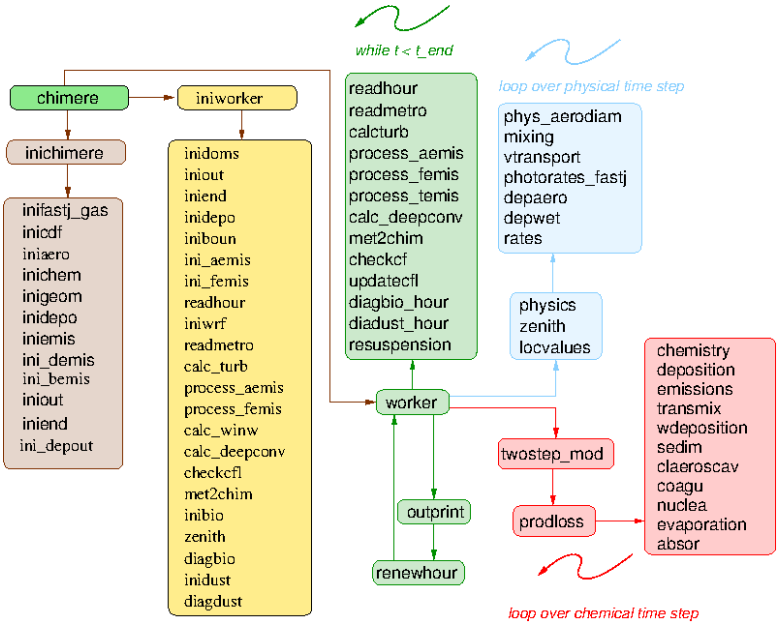


Figure 3.3: *Detailed list of CHIMERE routines and time loops*

1. The main program chimere.F90 first calls the chimere.nml reading routine read_chimere_nml on all processors. Then the worker 0 calls the initialization routines (in inichimere.F90 and further calls) where all "static data" are read and many variables defined. At the end of the initialization step, data are broadcasted from worker 0 to other processors (see Section 3.5.1).

2. Then all processors call successively the iniworker.F90 and worker.F90 subroutines which will

   (a) initialize arrays and ouput files

   (b) reads hourly data every hour (routine readhour.F90)

   (c) loops on the coarse time step,

   (d) outputs results on files (routine outprint.F90) and

(e) shifts hourly data (routine renewhour).

3. At each *hourly* model time step, one needs hourly data for the start and the end of the hour in order to linearly interpolate, for meteo data, boundary conditions, biogenic and anthropogenic emissions. The code keeps only these two instants in memory. Within the coarse time step, the locvalues.F90 routine is called in order to assign all variables that will be kept constant during the *physical* time step (linearly interpolated meteo data, reaction rates etc...), and a loop on the *fine* time step is carried out, with a call to the numerical solver twostep_mod.F90.

4. The twostep_mod.F90 routine calls the core routine prodloss.F90 which calculates, for all processes, the loss and production terms and sums them up. Thus prodloss.F90 calls emissions.F90 (emission terms), transmix.F90 (transport and mixing terms), chemistry.F90 (chemical terms), deposition.F90 and wdeposition.F90 (dry and wet deposition terms). For aerosol species prodloss.F90 calls sedim.F90 (sedimentation terms), evaporation.F90 (evaporation terms) end nucelation.F90 (nucleation term).

3.5.1 Parameter broadcast

Once the worker 0 has finished the initialization step, parameters are broadcasted to other workers. This is done by the call to the broadcast_all_once subroutine (worker_message_subs module), from the inidoms subroutine. The broadcast_all_once subroutine will perform the following operations:

- Initialization of worker 0 domain parameters with the domains_init subroutine (pncvar module) (e.g., number of zonal cells, number of meridian cells, longitude, latitude, sub-domain indexes within the entire domain).
- These domain related parameters are then scattered from worker 0 to the other workers (subroutine scatter_params).
- All parameters are broadcasted from worker 0 to other workers (e.g., array size, time parameters).
- Now that all workers knows all parameters, they are able to allocate array with a call to the worker_allocall subroutine (chimere_common module).
- Once array are allocated on all workers, the worker 0 may broadcast the array data (subroutine bcast_arrays) and types structure for species, output and emissions (subroutine bcast_types). Note that spatialized arrays do not require to be broadcast entirely (e.g., xlong, xlati, dland) as each worker only need to know the part of the array related to its subdomain. These arrays are then scatter from worker 0 to other workers using mpi_send / mpi_recv.
- Finally, the subroutine domains_init is called by non-zero workers.

After the call to the broadcast_all_once subroutine, the worker 0 has transmitted every information that he has acquire during the intialization step, to the other workers. From this point, communications among workers will mainly consist in halos updates at each time steps.
Note that each workers, allocate arrays on its own subdomain only. However, workers sometimes require information over the whole domain, thus some variables are allocated over the whole domain. Such variables, related to the whole domain, always have the "entire_domain" suffix in their names.

3.6 The 'chimere.nml' model namelist

A CHIMERE run consists in several actions which are performed in the top-level script:

- running the interfaces,
- building the namelists and
- executing ./chimere.e.

For the model execution, many input files are necessary. After running the interfaces, they are listed in the chimere.nml model namelist. This list also contains the output file names and directories.

This section describes all files and user choices listed in this namelist. All these input files must be present in the temporary directory before running the executable chimere.e. The top-level script assembles these files in the temporary directory automatically. Here are some of the namelist parameters specified in chimere.par:

- $chimere_root: the model directory
- $chimere_tmp: the simulation directory
- $simuldir: the output results directory
- $inputdata: an example of chemistry data directory automatically created by the chemprep script. Note that this directory is created before the run and placed in $chimere_root/chemprep/inputdata
- $dom: an example of simulation horizontal domain
- $sim=$di$hour_$de$hour_$lab: the full simulation label containing starting and ending simulation dates
- $lab: the name of the simulation

The necessary parameters and input files are listed below. For each file, we describe its "common name", the complete path and its function.

Parameter	Value	Type
version	'chimere'	The model version
idatestart	2008062100	The starting date and hour of the simulation
nhourrun	240	The number of hours of the simulation
iopinit	1	The use of initial conditions
imakerun	1	Make the run or not
iusebemis	1	Build biogenic emissions or not
iusedust	1	Build dust emissions or not
iusebound	1	Build and use boundary conditions or not
icuth	1	The ustar threshold parameterization
ifluxv	2	The sandblasting flux parameterization

These parameters are integer and describes the starting date and duration (in hours) of the simulation. The other flags are the choices to make regarding the initial conditions, biogenic emissions, mineral dust emissions, the use of boundary conditions, and the parameterizations included in the mineral dust module.

Parameter	Value	Type
fnoutspec	'$inputdata/OUTPUT_SPECIES.full'	Name of output species (here, if the user wants all species in output)
fnspec	'$inputdata/ACTIVE_SPECIES'	all active species names
fnchem	'$inputdata/CHEMISTRY'	preprocessed reactions
fnstoi	'$inputdata/STOICHIOMETRY'	stoichiometric coefficients
fnrates	'$inputdata/REACTION_RATES'	tables of reaction rates
fnfamilies	'$inputdata/FAMILIES'	Definition of families
fnaerosol	'$inputdata/AEROSOL'	aerosols; number of bins, molar weights
fnaeromin	'$inputdata/AEROMIN.bin'	Parameters for ISORROPIA scheme for aerosols
fnaeroorg	'$inputdata/AEROORG.bin'	Parameters for the SOA scheme
fnprim	'$inputdata/PRIMARY'	Size distribution of aerosols
fnsemivol	'$inputdata/SEMIVOL'	Semivolatile aerosols parameters
fnanthro	'$inputdata/ANTHROPIC'	List of anthropic emitted species
fnfires	'$inputdata/FIRES'	List of fires emitted species
fnbiogen	'$inputdata/BIOGENIC'	List of biogenic emitted species
fndepoespe	'$inputdata/DEPO_SPEC'	coefficients for calculation of resistances / species
fndepopars	'$inputdata/DEPO_PARS'	landuse coefficients for dry deposition
fnwetd	'$inputdata/WETD_SPEC'	wet deposition species and parameters

The files in the '$inputdata/' directory are created by the chemprep/ programs during the first model run for each new set of chemistry options. This includes the active species names, the output species, the stoichiometric coefficients, tables of reaction rates, definition of families, the photolysis rates computed by FastJ, the number of bins, molar weights of aerosols. The specific AEROMIN.bin and AEROORG.bin are binary files for the ISOROPIA and SOA chemical schemes, respectively.

Parameter	Value	Type
fnlanduse	'${dom}/LANDUSE_[database]_${dom}.nc'	Landuse in the CHIMERE classes
fniVCO	'VCOORD/VCOORD_${nlevels}_${first_layer_pressure}_${top_chimere_pressure}'	Vertical coordinates
fniMGNEF	'${dom}/EFMAP_LAI_{dom}.nc'	LAI and emission factors
fnigeo	'${dom}/geog_[database]_${dom}.nc'	Soil categories
fniz0	'${dom}/z0_CHIMERE_${dom}_ASCAT.nc'	Aeolian roughness length
fnisolspe	'chemprep/dustdata/dustdata-soil.asc'	Soil data for dust emissions

The files in the domains directory depend only on the horizontal grid. They are automatically generated in the beginning of a simulation for each new domain.

Parameter	Value	Type
fnmetraw	'${datadir}/exdomout.${sim}.nc'	Input: Meteo fields on the native meteo model vertical grid
fnbounconc	'${datadir}/BOUN_CONCS.${sim}.nc'	Input: boundary conditions
fnemisa	'${datadir}/AEMISSIONS.${sim}.nc'	Input: antrhopogenic emissions
fnemisf	'${datadir}/FEMISSIONS.${sim}.nc'	Input: Fires emissions
fnoBIO	'${datadir}/BEMISSIONS.${sim}.nc'	Output: Biogenic emissions
fnoDUST	'${datadir}/DEMISSIONS.${sim}.nc'	Output: Mineral dust emissions
fninit	'${outputdir}/ini.${sim}.nc'	Output: Initial conc fields
fnout	'${outputdir}/out.${sim}.nc'	Output: Simulation conc fields
fnconcs	'${outputdir}/end.${sim}.nc'	Output: Last conc fields (used for restart)
fndepos	'${outputdir}/dep.${sim}.nc'	Output: Deposition fluxes

Note that the complete format of the main output files is more precisely described in §2.5,p.29.

3.7 How to add a new diagnostic variable to the code?

These are brief guidelines to adding a new diagnostic variable to the code. As an example let us examine how the `atb_mol_nad` variable is implemented.

3.7.1 Compute the variable

This is done in a subroutine called from the worker subroutine, e.g.,

```
if (ilidar == 1) call lidar
```

In our example, the molecular attenuated backscatter signal `atb_mol_nad` is computed in the lidar subroutine called from worker.

3.7.2 Declare the variable in chimere_common.F90

We need both the variable itself and its structure in the output NetCDF file:

```
real(kind=iprec),allocatable,dimension(:,:,:,:)  :: atb_mol_nad
....
type(ncvar_type)                                 :: var_atb_mol_nad
```

3.7.3 Allocate the variable in chimere_allocs.F90

```
allocate( atb_mol_nad(nzonalmax,nmeridmax,nverti,nwl) )
```

3.7.4 Define the corresponding NetCDF variable

3.7.4.1 iniout.F90: create and define attributes

Output NetCDF variables are currently created using the traditional NetCDF library:

```
integer :: out_atb_mol_nad_varid
....
ncstat=nf90_def_var(out_ncid,'atb_mol_nad',NF90_DOUBLE,
    & d_dimids,out_atb_mol_nad_varid)
....
ncstat=nf90_put_att(out_ncid,out_atb_mol_nad_varid,'units', &
    '[m-1 sr-1]')
ncstat=nf90_put_att(out_ncid,out_atb_mol_nad_varid,'long_name', &
    'ATB molec nadir')
```

3.7.4.2 worker_iniout: read the NetCDF structure for parallel I/O

Once the NetCDF file is created, and the variable is defined using the standard NetCDF library, its structure can be read with the pncvar module routine for future input/output:

```
call pncvar_get_var_info(out_nc, 'atb_mol_nad', var_atb_mol_nad)
```

3.7.5 Save the variable to the output file

In the outprint subroutine, the variable's portion of each subdomain is written to the output file, using the pncvar_put_var subroutine of the pncvar module:

```
toprint4d(:,:,:,:)=real(atb_mol_nad(1:nzonal,1:nmerid,1:nivout,1:nwl))
call pncvar_put_var(domains, var_atb_mol_nad, toprint4d, &
       rank, (/nzonal,nmerid,nivout,nwl,1/), (/iprint+1/))
```

4 Domain, landuse and soil

For each simulation, several input data files are needed to describe the vertical mesh, the horizontal domain and its properties (landuse, soil texture and roughness length). If the creation of the vertical mesh is simple, the generation of all surface data is much more complex and needs a complete chain of pre-processors. In this chapter, all the steps are described for:

- §4.1: the vertical mesh
- §4.2: all files describing the surface data

4.1 The vertical mesh

4.1.1 Structure

The vertical mesh of CHIMERE is completely independent on the horizontal domain. The model uses any number of vertical layers, described in hybrid sigma-p coordinates. The pressure in hPa at the top of each layer k is given by the following formula:

$$P_k = a_k 10^5 + b_k P_{surf}. \tag{4.1}$$

P_{surf} is the surface pressure and the coefficients a_k and b_k are calculated by the geom.awk script, called from chimere-domain.sh via define_geom.sh. The a_k and b_k coefficients ($1 \leq k \leq nlayer$) are written to the VCOORD file which is then stored in the domains/VCOORD/ directory of the chimere root directory, and in the domains/ subdirectory of the temporary chimere directory.
The generation of the VCOORD file depends on three parameters of the chimere.par file :

```
[nlayer_chimere]       Number of vertical layers           : 20
[top_chimere_pressure] Top layer pressure (mbar)           : 200
[first_layer_pressure] First layer pressure (sigma * 1e3)  : 997
```

with:

1. *nlayer_chimere* is the number of vertical layers needed,
2. *top_chimere_pressure* is the pressure of the top of the domain (mbar), and
3. *first_layer_pressure* is the pressure of the top of the lowest chimere level, expressed in $\sigma * 10^3$ units. For example, if `$first_layer_pressure` is set to 997, the thickness of the first layer (in pressure) will be equal to $(1 - 0.997)\, P_{surf} \simeq 3\,\mathrm{hPa}$.

4.1.2 Placing the vertical levels

Since version 2014, the algorithm for positioning the vertical levels has changed: up to version 2013b, the layer thickness was increasing exponentially from ground level to the top of model. Even though this permitted to

have a good resolution within the PBL, layers inside the free troposphere had thicknesses reaching several kilometers, which hinders the representation of long-range transportation of anthropogenic of natural contamination plumes (e.g. dust layers).
Since version 2014a, the algorithm coded in scripts/domain-geom.awk produces a VCOORD file in which the thickness of the layers increase exponentially with height in the lowest 200 hPa of the atmosphere, and have constant thickness (in pressure coordinates) from 200 hPa to the top of the model. The number n_{200} of layers in the lowest 200 hPa of the model is determined so that:

1. No layer is thicker than its upper neighbour. Since the layer thickness increase exponentially from $k = 1$ to $k = n_{200}$ and is constant from $k = n_{200} + 1$ to $k =$`$nlayer_chimere`, this condition is equivalent to imposing that layer n_{200} is not thicker than layer $n_{200} + 1$

2. n_{200} is the highest possible value such that condition 1 is verified

These two conditions are coded in scripts/domain-geom.awk and produce a VCOORD file that ensures a fine vertical resolution for the lowest atmospheric layers while not having too thick layers close to model top. Another script scripts/domain-geom-verbose.awk is also provided in order to make a (relatively) user-friendly output on the screen so that the user can check whether the vertical resolution obtained with their parameters is reasonable. A sample output of scripts/domain-geom-verbose.awk is as follows:

```
Vertical layers will be as follows :
lowest model layer will be  5 hPa thick
will have  6  layers below 800 hPa
           2  layers from 800 hPa to  500 hPa
k    ca        cb         p(hPa)       thk(hPa)
  1  0.00000   0.99500    995.00000     5.00000
  2  0.00902   0.97705    986.07113     8.92887
  3  0.02513   0.94500    970.12617    15.94496
  4  0.05389   0.88777    941.65206    28.47411
  5  0.10525   0.78555    890.80371    50.84835
  6  0.19697   0.60303    800.00000    90.80371
  7  0.34848   0.30152    650.00000   150.00000
  8  0.50000   0.00000    500.00000   150.00000
```

Users may want to generate their own VCOORD files depending on their modelling priorities (long-range transport, urban boundary layer . . .). To do that, the easiest possibility is to modify the geom.awk script according to one's needs.

4.2 The horizontal domain

4.2.1 Options activation

The first step for the horizontal properties of the simulation is to define the grid: the longitudes and latitudes of the grid cells centers.

```
[dom]             CHIMERE domain                 : MEDC1b
[metdom]          Meteo driver domain            : d01
[bigfilesdir]     Big files (AEROMIN.bin, etc)   : my-BIGFILES-directory
[iland_cover]     Globcover(2)/USGS(3)          : 3
[landcover_dir]   Land Cover directory           : {bigfilesdir}/LANDCOVER
[wrf_geog]        Where is geog from WRF         : {meteo_DIR}/WPS/geo_em.{metdom}.nc
```

This definition of the horizontal grid is possible following two ways:

- Direct use of the WRF grid (if WRF was the model used for the meteorological forcing)
- Creation of a new grid

This choice is simply done by specifying or not the existenz of a WRF geog file. This is done with the line containing the flag wrf_geog in the chimere.par file. The test is performed by the scripts/chimere-domain.sh script.

1. If the WRF geog file is used, a large part of preprocessing has not to be done. Note that, in this case, the surface database is forced to USGS, even if the user has selected another database with the flag iland_cover.

2. If the WRF file is not used, the pre-processor has to create a file describing the horizontal mesh. This file is named domains/HCOORD/COORD_$dom and the user can create this file by himself or use the script dedicated to its creation. This creation is done automatically and the user has just to give some soimple informations about the grid. These informations must be filled in the domains/domainlist.nml namelist file.

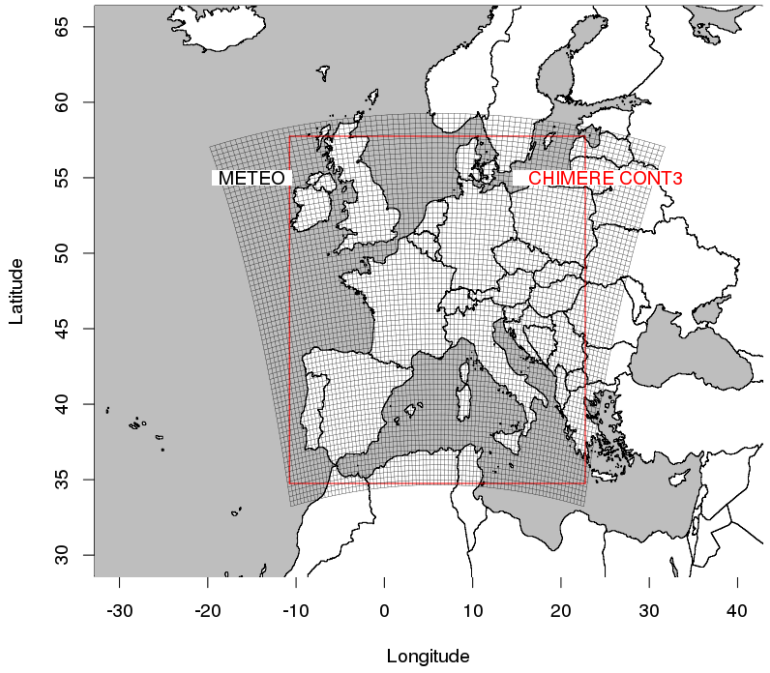


Figure 4.1: *Examples of horizontal domains. The dots represent the MM5 EUR1 grid cells centers and the rectangle represents the boundaries of the CHIMERE CONT3 domain.*

4.2.2 Manual creation of a regular horizontal grid

For example, the line describing the CHIMERE 'CONT3' domain corresponds to the mesh displayed in the Figure 4.1. The first column, the $dom is a name given by the user to the model horizontal grid/domain. The other columns are the number of cells in the x-direction, the number of cells in the y-direction, and the coordinates of the South-West cell center, as follows:

```
domain      NX  NY  DX    DY   XMIN    YMIN
CONT1       65  33  0.5   0.5  -10.0   40.5
CONT3       67  46  0.5   0.5  -10.5   35.0
CONT4       70  44  0.5   0.5  -10.5   36.0
CONT5       79  47  0.5   0.5  -14.0   35.0
FRA10      101 111 0.15   0.1   -5.0   41.0
```

If, however, the simulation domain is not regular in terms of latitude and longitude, the user has to provide himself a correct domains/HCOORD/COORD_$dom file. Note that a domain that is regular in terms of distance (e.g., 3x3 km) is **not** regular in terms of latitude/longitude.
The flag dom in chimere.par indicates the name to use with the script scripts/chimere-domain.sh, launching the tool scripts/domains-makeCOORDdomains.sh and generates the grid (ascii format) domains/HCOORD/COORD_$dom file.

4.2.3 From the ascii grid to a complete geog file

If a geog file is not provided, the user can define its own grid. Since the version 2016, the CHIMERE model directly reads surface informations with the equivalent of the WRF geog format. This means that if the geog is not provided, but only coordinates or a COORD file, it is necessary to rebuilt a geog file.
This is done in the script scripts/chimere-domain.sh, launching the scripts/scripts/domains-prep_geog.sh. In order to have a complete dataset, this program uses the COORD file and the USGS database to have all necessary informations for CHIMERE.

4.3 The surface databases

When the first step for the creation of the horizontal grid is done, several scripts are launched by the scripts/chimere-domain.sh to create additional databases:

1. **Landuse:** The scripts/domains-prep_landuse.sh creates all landuse data files needed for depositions and biogenic emissions.
2. **LAI:** The scripts/domains-prep_megan.sh creates MEGAN biogenic emission factors and leaf-area indices on the domain grid.
3. **Roughness length:** The scripts/domains-prep_z0.sh creates z_0 roughness length database for the mineral dust emissions calculations
4. **Erodibility:** The scripts/domains-prep-erodib.sh reads a provided MODIS database and extract erodibility values (between 0 and 1) on the CHIMERE grid. These values are used for the mineral dust emissions but only over arid areas.

4.3.1 Landuse databases

For the landuse, the user has the choice between three differents databases:

1. **The GlobCover Land Cover**:
   The GlobCover is a global land cover map at 10 arc second (300 meter) resolution [Bicheron et al., 2011]. It contains 22 global land cover classes defined within the UN Land Cover Classification System (LCCS). GlobCover database is based on the ENVISAT satellite mission's MERIS sensor (Medium Resolution Image Spectrometer) Level 1B data acquired in Full Resolution (FR) mode with a spatial resolution of

300 meters. GlobCover LC was derived from an automatic and regionally-tuned classification of a time series of MERIS FR composites covering the period December 2004-June 2006. Table 4.2 shows the 22 GlobCover classes.
Data are in the file globcover_freshwater.nc

2. **The U.S. Geological Survey:**
The U.S. Geological Survey (USGS) land cover is a global land cover map at 30 arc second (1 km) resolution. It contains 24 global land cover classes defined within the UN Land Cover Classification System (LCCS). USGS database is based on the data set derived from 1 km Advanced Very High Resolution Radiometer (AVHRR) data spanning a 12 month period (April 1992-March 1993). This data was generated by the U.S. Geological Survey's (USGS) National Center for Earth Resources Observation and Science (EROS), the University of Nebraska-Lincoln (UNL) and the Joint Research Centre of the European Commission, [Loveland et al., 2000]. Table 4.3 shows the 24 USGS classes.
Data are in the file usgs_soil_landuse.nc

In these files, an additional class "inland water" has been added to the classifications to distinguish between the sea water and fresh water. This was needed to avoid model emissions of sea salt over the fresh water surfaces. The separation was done using a land-sea mask. So instead of the original 22 GlobCover classes or 24 USGS classes, CHIMERE land use pre-processor takes 23 or 25 classes, respectively (see Table 4.2 and Table 4.3).

4.3.2 The CHIMERE landuse

The CHIMERE model is using its own landuse categories: only 9 different categories, to speed-up the calculations for the dry deposition, mainly. Its is thus necessary to build the landuse database on the CHIMERE grid but also to built some agregation table to link the databases landuse to the CHIMERE landuse.
The CHIMERE landuse categories are presented in Table 4.1

Category Number	Description	Category Number	Description
1	Agricultural land / crops	6	Shrubs
2	Grassland	7	Needleaf forest
3	Barren land/bare ground	8	Broadleaf forest
4	Inland Water	9	Ocean
5	Urban		

Table 4.1: *Landuse categories used in CHIMERE*

4.3.3 Projection of land-use categories from external databases to CHIMERE

In order to project the values in the several databases, some factors are applied. The factors were arbitrarily defined and are presented in the following tables. They correspond to ascii datafile, easily modified by the user.

4.3.3.1 The GlobCover Land Cover aggregation matrix

This matrix is reported in the file domains/LAND_AGGREGATION_GLOBCOVER.

4.3.3.2 The USGS aggregation matrix

This matrix is reported in the file domains/LAND_AGGREGATION_USGS.

```
CROP GRAS BARR IWAT URBA SHRB CONI DECI OCEA
1.00 0.00 0.00 0.00 0.00 0.00 0.00 0.00 0.00    1 Post-flooding or irrigated cropland
1.00 0.00 0.00 0.00 0.00 0.00 0.00 0.00 0.00    2 Rainfed cropland
0.64 0.12 0.00 0.00 0.00 0.12 0.06 0.06 0.00    3 Mosaic cropland (50-70\%) / vegetation (20-50\%)
0.40 0.20 0.00 0.00 0.00 0.20 0.10 0.10 0.00    4 Mosaic vegetation (50-70\%) / cropland (20-50\%)
0.00 0.00 0.00 0.00 0.00 0.00 0.00 1.00 0.00    5 Broadleaved evergreen or semi-deciduous forest (>5m)
0.00 0.00 0.00 0.00 0.00 0.00 0.00 1.00 0.00    6 Closed broadleaved deciduous forest (>5m)
0.00 0.00 0.00 0.00 0.00 0.00 0.00 1.00 0.00    7 Open broadleaved deciduous forest/woodland (>5m)
0.00 0.00 0.00 0.00 0.00 0.00 1.00 0.00 0.00    8 Closed needleleaved evergreen forest (>5m)
0.00 0.00 0.00 0.00 0.00 0.00 1.00 0.00 0.00    9 Open needleleaved deciduous or evergreen forest (>5m)
0.00 0.00 0.00 0.00 0.00 0.00 0.50 0.50 0.00    10 Closed to open mixed broadleaved and needleleaved forest
0.00 0.40 0.00 0.00 0.00 0.30 0.15 0.15 0.00    11 Mosaic forest or shrubland (50-70\%) / grassland (20-50\%)
0.00 0.60 0.00 0.00 0.00 0.20 0.10 0.10 0.00    12 Mosaic grassland (50-70\%) / forest or shrubland (20-50\%)
0.00 0.00 0.00 0.00 0.00 1.00 0.00 0.00 0.00    13 Shrubland
0.00 1.00 0.00 0.00 0.00 0.00 0.00 0.00 0.00    14 Herbaceous vegetation
0.00 0.25 0.00 0.00 0.00 0.25 0.25 0.25 0.00    15 Sparse (<15\%) vegetation
0.00 0.00 0.00 0.00 0.00 0.00 0.00 1.00 0.00    16 Closed to open broadleaved forest regularly flooded
0.00 0.00 0.00 0.00 0.00 0.40 0.00 0.60 0.00    17 Closed broadleaved forest / shrubland permanently flooded
0.00 0.40 0.00 0.00 0.00 0.00 0.30 0.30 0.00    18 Grassland / woody vegetation regularly flooded
0.00 0.00 0.00 0.00 1.00 0.00 0.00 0.00 0.00    19 Urban areas >50\%
0.00 0.00 1.00 0.00 0.00 0.00 0.00 0.00 0.00    20 Bare areas
0.00 0.00 0.00 0.00 0.00 0.00 0.00 0.00 1.00    21 Water bodies
0.00 0.00 1.00 0.00 0.00 0.00 0.00 0.00 0.00    22 Permanent snow and ice
0.00 0.00 0.00 1.00 0.00 0.00 0.00 0.00 0.00    23 Inland water
```

Table 4.2: *Projection factors from the Globcover database to CHIMERE.*

```
CROP GRAS BARR IWAT URBA SHRB CONI DECI OCEA
0.00 0.00 0.00 0.00 1.00 0.00 0.00 0.00 0.00    1 Urban and Built-up Land
0.80 0.20 0.00 0.00 0.00 0.00 0.00 0.00 0.00    2 Dryland Cropland and Pasture
0.50 0.50 0.00 0.00 0.00 0.00 0.00 0.00 0.00    3 Irrigated Cropland and Pasture
0.50 0.50 0.00 0.00 0.00 0.00 0.00 0.00 0.00    4 Mixed Dryland/Irrigated Cropland and Pasture
0.00 1.00 0.00 0.00 0.00 0.00 0.00 0.00 0.00    5 Cropland/Grassland Mosaic
0.50 0.00 0.00 0.00 0.00 0.00 0.25 0.25 0.00    6 Cropland/Woodland Mosaic
0.00 1.00 0.00 0.00 0.00 0.00 0.00 0.00 0.00    7 Grassland
0.00 0.00 0.00 0.00 0.00 1.00 0.00 0.00 0.00    8 Shrubland
0.00 0.50 0.00 0.00 0.00 0.50 0.00 0.00 0.00    9 Mixed Shrubland/Grassland
0.00 0.00 0.00 0.00 0.00 1.00 0.00 0.00 0.00    10 Savanna
0.00 0.00 0.00 0.00 0.00 0.00 0.00 1.00 0.00    11 Deciduous Broadleaf Forest
0.00 0.00 0.00 0.00 0.00 0.00 1.00 0.00 0.00    12 Deciduous Needleleaf Forest
0.00 0.00 0.00 0.00 0.00 0.00 0.00 1.00 0.00    13 Evergreen Broadleaf
0.00 0.00 0.00 0.00 0.00 0.00 1.00 0.00 0.00    14 Evergreen Needleleaf
0.00 0.00 0.00 0.00 0.00 0.00 0.50 0.50 0.00    15 Mixed Forest
0.00 0.00 0.00 1.00 0.00 0.00 0.00 0.00 0.00    16 Water Bodies
0.00 0.00 0.00 0.00 0.00 1.00 0.00 0.00 0.00    17 Herbaceous Wetland
0.00 0.50 0.00 0.00 0.00 0.00 0.25 0.25 0.00    18 Wooden Wetland
0.00 0.00 1.00 0.00 0.00 0.00 0.00 0.00 0.00    19 Barren or Sparsely Vegetated
0.00 0.00 0.00 0.00 0.00 1.00 0.00 0.00 0.00    20 Herbaceous Tundra
0.00 0.00 0.00 0.00 0.00 0.00 0.50 0.50 0.00    21 Wooded Tundra
0.00 0.25 0.00 0.00 0.00 0.25 0.25 0.25 0.00    22 Mixed Tundra
0.00 0.00 1.00 0.00 0.00 0.00 0.00 0.00 0.00    23 Bare Ground Tundra
0.00 0.00 0.00 0.00 0.00 0.00 0.00 0.00 0.00    24 Snow or Ice
0.00 0.00 0.00 0.00 0.00 0.00 0.00 0.00 0.00    25 Playa
0.00 0.00 0.00 0.00 0.00 0.00 0.00 0.00 0.00    26 Lava
0.00 0.00 0.00 0.00 0.00 0.00 0.00 0.00 0.00    27 White sand
0.00 0.00 0.00 0.00 0.00 0.00 0.00 0.00 1.00    28 Ocean
```

Table 4.3: *Projection factors from the USGS database to CHIMERE.*

4.3.4 The aeolian roughness length interface

A z_0 file is required to compute mineral dust emission along with USGS landuse. The z_0 file will be created by the program domains-extract_z0.F90, called by the script domains-prep_z0.sh, itself called by chimere-domain.sh script. If the file already exist or if $iusedust is "0", the z_0 file will not be created.

The domains-extract_z0.F90 program will use the 6km spatial resolution GARLAP (Global Aeolian Roughness Lengths from ASCAT and PARASOL) dataset from [Prigent et al., 2012] (file z0_CHIMERE_usgs_ASCAT_m.nc) to create the z_0 file. The z_0 output file will contain aeolian roughness length values along with landuse index and landuse percentage, for each landuse category and for each soil types over the given CHIMERE domain.

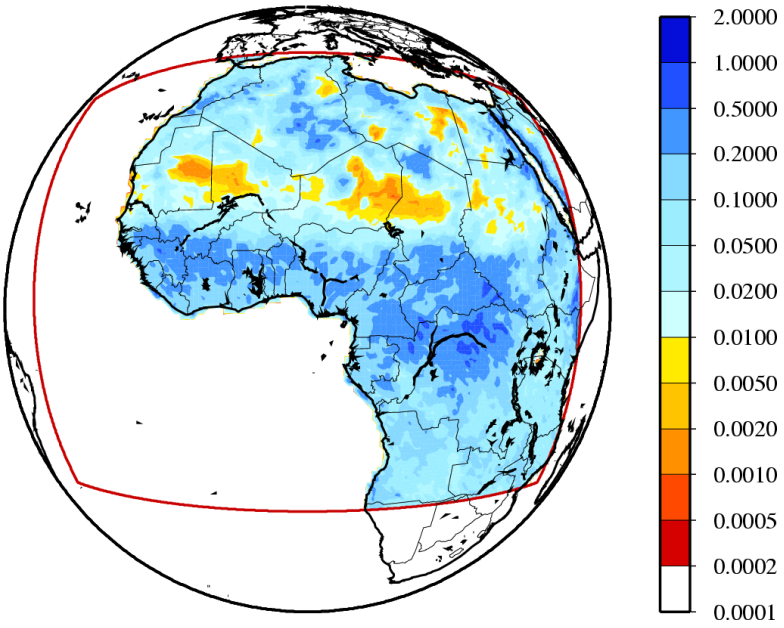


Figure 4.2: *Example of aeolian roughness length z_0 derived from GARLAP dataset and projected on a CHIMERE grid.*

4.3.5 The erodibility interface

The script chimere-domain.sh also calls the script domains-prep-erod.sh to project MODIS erodibility factor on the CHIMERE grid. An example of output is presented in Figure 4.3 .

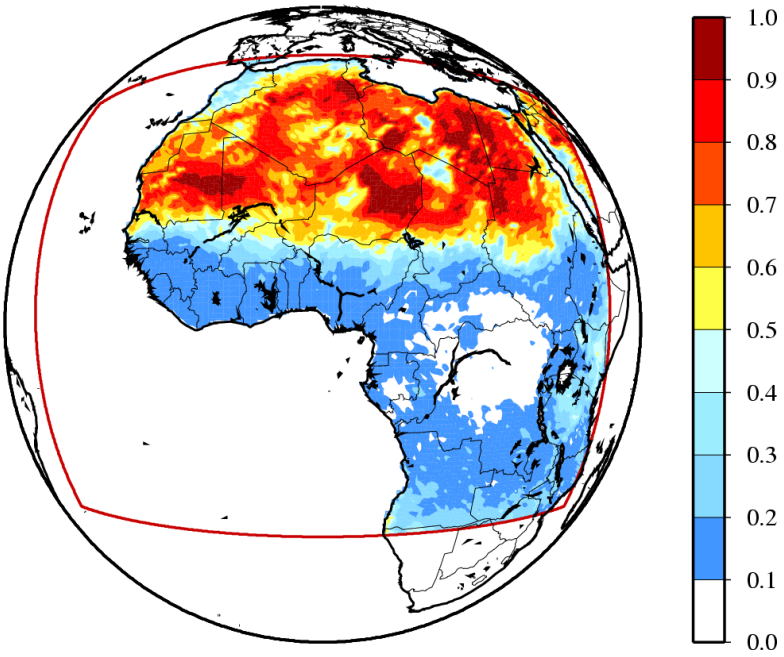


Figure 4.3: *Example of erodibility factor derived from MODIS dataset and projected on a CHIMERE grid.*

5 [chemprep] the chemical preprocessor

5.1 Preparation of new chemical data

5.1.1 Available options for the chemistry

CHIMERE uses a chemical pre-processor to prepare all necessary informations about the chemistry, both for gaseous species and aerosols. This allows to have a very flexible code where the chemistry has not to be hardcoded in Fortran and in the model itself.
The preparation of the chemistry is done before a simulation and only if the data directory is not existing yet:

- When the script chimere.sh is launched, the availability of chemistry input files corresponding to the specific simulation is checked. If the data already exist, the run continues.
- If not, the script scripts/make-chemistry.sh creates all prerequesite files in a new directory called something like:
  chemprep/inputdata.2110011210.10
  In this new directory, all input files required by CHIMERE for a simulation are stored. The arguments called labchem (following the string inputdata) correspond to the simulation options having an impact on the files preparation. labchem is designed as:
  labchem=$mecachim $aero $seasalt $carb $trc $soatyp $iusedust $iadv $iadvv .$nbins
  For example and for a simulation with only gas-phase chemistry and no aerosols, but with a passive gaseous tracer, the directory created will have the label *"1000001000.0"*. This is with this code that the model is able to detect if the chemical files are already available or not. All these parameters are described in the 'chimere.par' file in section 2.3, p.22.
- If a new simulation with the same options is launched or in case of a restart, the files will be used as it: the code will check automatically the existenz of the directory. If the main run options change, the script will automatically be launched to create new files.

If the chemistry directory already exists but the user wants to reprocess it, he can force the building of the whole chemistry by changing the option imakechemprep in the chimere.par parameter file. It is also possible to launch the model to only make the 'chemprep' stage and stop the code by changing istopchemprep. This allows to manually modify the created files (but of course this is not recommended). The possible options are (with in red, the recommended option to save in your chimere.par file):

imakechemprep = 0 : No preparation. We consider the directory already exist and is OK
= 1 : Force building of data
= 2 : Check is directory exists. If yes, continue.
istopchemprep = 0 : Prepare the data if necessary and continue.
= 1 : Prepare and forced stop.

5.1.2 The make-chemistry.sh script

If imakechemprep is 1 or 2, the model will launch automatically the make-chemistry.sh script (contained in the chimere.sh main model script). The main role of make-chemistry.sh is to launch the following scripts:

1. scripts/chemprep-check_consistency.sh:
   check consistency between the several user parameters

2. scripts/chemprep-prep-chemistry-data.sh:
   make the new inputdata directory and all files to create. This script is the main chemprep script.

3. scripts/chemprep-prep-boun-data.sh:
   prepare some data files linking the selected model species for the simulation and the available data contained in the climatological files for the boundary conditions.

4. scripts/chemprep-copy-chemresults.sh:
   at the end, copy the new data files in the inputdata directory.

The first script, scripts/chemprep-check_consistency.sh is very simple and only designed to check is the user's options are logical. The last script, scripts/chemprep-copy-chemresults.sh is also simple and just dedicated to copy all the new files into the new inputdata directory.
The main part of the work is done by the scripts/chemprep-prep-chemistry-data.sh scripts, which makes concatenations of already existing files and calls programs. This script is fully described in the next section 5.2.
The script chemprep-prep-tracer-data.sh adds parameters of gaseous and particulate tracers to the data files describing parameters of the chemistry mechanism, depositions, and output.This script is fully described in the next section 5.4.

5.2 The preparation of gaseous and aerosol chemistry

The script scripts/chemprep-prep-chemistry-data.sh is the one making all new required files. There is three main steps in this scripts:

1. Concatenate already existing ascii files

2. Run the src/chemprep-distrib.F90 program for the calculation of the aerosol size distribution

3. Run the src/chemprep-families.F90 programs to create model species families, following the user choices.

5.2.1 The input chemistry data files

All necessary chemistry files are already prepared. The main goal of the scripts/chemprep-prep-chemistry-data.sh is to concatenate the files depending on the user's options. If the user wants to make a simulation without aerosol for example, only the gaseous files will be used.
The complete list of input ascii files is in the following Table 5.1 .
Note that some files are more detailed in other sections of this documentation:

- The FastJ files are detailed in the section 12.7, p.175.
- The dry deposition files DEPO_SPEC.$meca depends on the chemical mechanism used, and, thus, the list of active model species. The constants are necessary for the calculation of the quasi-laminar layer resistance r_b for gases. The details are given in Table 7.1 , p.95.
- The DEPO_PARS.univ is not dependent on the chemical mechanim used and is described in Table 7.3 , p.98.
- The wet deposition file WETD_SPEC.univ is detailed in Table 7.4 , p.106.

In Table 5.1 , there are two kinds of data files:

File name	Content	Format	Changeable
AEROMIN.bin	Constants for ISORROPIA	binary	no
AEROORG.bin	Constants for ISORROPIA	binary	no
FJX_spec_$meca.dat	Parameters for FastJX	ascii	no
FJX_scat-cld.dat	Cloud scattering data for FastJX	ascii	no
FJX_scat-UMa.dat	Parameters for FastJX	ascii	no
input-fastj.txt	Parameters for FastJX	ascii	yes
atmos_std.dat	Temperature and ozone climatology for FastJX	ascii	no
DEPO_SPEC.$meca	Dry deposited species	ascii	yes
WETD_SPEC.univ	Constants for the wet deposition	ascii	yes
BIOGENIC.univ	List of biogenic active species	ascii	yes
DEPO_PARS.univ	Constants for the dry deposition calculation	ascii	yes
SEMIVOL.univ	Constant for the semi-volatils species	ascii	yes
ANTHROPIC.*	List of anthropogenic species	ascii	yes
AEROSOL.*	Characteristics of aerosols	ascii	yes
MAKEPRI.*	List of mean mass median diameters for emitted aerosols	ascii	yes
REACTIONS.*	List of chemical reactions	ascii	yes

Table 5.1: *List of primary data files in the chemprep/data directory.*

- The data files with the extension "univ" are not dependent on the chemical mechanism used
- The datafiles "ANTHROPIC", "REACTIONS", "DEPO_SPEC.$meca" and "MAKEPRI" directly depend on the chemical mechanism used and thus of the chemical model species.

The BIOGENIC.univ file contains the list of the model species considered as biogenic, i.e with possible emissions calculated using the MEGAN model. More details about these species are given in section 6.2, p.78.
The SEMIVOL.univ file contains parameters for the semi-volatil species. This datafile is read in the program src/inichem.F90 and it contains the informations described in Table 5.2.

5.2.1.1 The chemical mechanisms

Three mechanisms are available in *chimere 2017*:

1. MELCHIOR1: the reduced version of the MELCHIOR mechanism, described in section 11.2.2, p.140
2. MELCHIOR2: the complete version of the MELCHIOR mechanism, described in section 11.2.4, p.150
3. SAPRC: The SAPRC-07-A chemical mechanism, described in section 11.3.4, p.163

These files must be modified by the user before the run of chemprep. Their format is detailed in the next sections.
The main principle of the chemprep pre-processor is to concatenate these files, depending on the user's options. For example:

- A simulation with only the gaseous species and the SAPRC mechanism:
  ANTHROPIC=ANTHROPIC.saprc
- A simulation with gas and aerosols, including SOA calculation:
  ANTHROPIC=ANTHROPIC.saprc + ANTHROPIC.aero + ANTHROPIC.med

Name	p0L	a0L	t0L
AnA0D	$1.0.10^{-10}$	0.	298.
AnA1D	$1.0.10^{-10}$	0.	298.
AnA2D	$1.0.10^{-10}$	0.	298.
AnBmP	2.10^{-3}	18772.	298.
AnBIP	$2.6.10^{-7}$	18772.	298.
BiA0D	$1.0.10^{-10}$	0.	298.
BiA1D	$1.0.10^{-10}$	0.	298.
BiA2D	$1.0.10^{-10}$	0.	298.
BiBmP	$6.6.10^{-4}$	18772.	298.
ISOPA1	$1.9.10^{-3}$	18772.	295.
ISOPA2	$1.0.10^{-5}$	18772.	295.
BiBhP	$1.0.10^{-10}$	0.	298.
BiBIP	$1.0.10^{-10}$	0.	298.
SOA	$1.00.10^{-10}$	0.	298.00
BaP	$9.34.10^{-7}$	11488.	283.15
BbF	$2.05.10^{-7}$	10541.	283.15
BkF	$7.00.10^{-7}$	10194.	283.15

Table 5.2: *Parameters needed for the semi-volatil compounds and the Secondary Organic Aerosols (SOA) formation. These species are not dependent on the chemical mechanism, their reactions being added whatever the chemical mechanism chosen.*

5.2.1.2 The ANTHROPIC data files

This file is only a list of model species names. For gaseous species, the model species name may be 'APINEN', 'C2H4' etc. The important point is to have these species as in the chemical mechanism file.
For aerosols, the model species are always considered with three modes:"_fin", "_coa" and "_big". For example, OCAR will be defined in the ANTHROPIC file as OCAR_fin and OCAR_coa. This specific management of the aerosol model species name is due to the emissions inventories often delivered with these three modes. This is also to allow to have a flexible aerosol size distribution, with a number of bins changeable by the user.

5.2.1.3 The AEROSOL data files

These files are also a list of model species names but with more informations for each species. For example, the data file AEROSOL.aero.med contains the informations:

```
PPM         1    100.      1
AnA1D       2    168.      1
AnBmP       2    152.      1
BiA1D       2    170.      0
BiBmP       2    236.      0
ISOPA1      2    177.      0
H2SO4       3    96.       1
HNO3        3    62.       1
NH3         3    18.       1
WATER       4    18.       1
```

with the columns:

1. The model species name (without the extension, being here representative of the aerosol without any consideration on its size distribution). This is the table aeroname(nkc) in the model.

2. The type of aerosol. Four types are currently defined in the model:

   (a) ntypesp = 1: the primary species

(b) ntypesp = 2: the semi-volatile organic species

(c) ntypesp = 3: the semi-volatile mineral species

(d) ntypesp = 4: the similar water species

This is the table ntypesp(nkc) in the model.

3. The molar mass. When this molar mass is not known (as for PPM), the value of 100 is put in this file. This is the table conmw(nkc) in the model.

4. The "origin" of the chemical species. Three types are defined and used in the model core:

   (a) 0 = biogenic

   (b) 1 = anthropogenic

   (c) 2 = mineral

   This is the table origin(nkc) in the model.

5.2.1.4 The MAKEPRI data files

All aerosols are considered with a size distribution. This size distribution is always considered as tri-modal. The MAKEPRI are designed to give informations about these three modes. The user can directly change these values.
For example, the mineral dust are defined with the following constants in MAKEPRI.dust:

```
DUST_fin  DUST  1 1.5e-6 1.7
DUST_coa  DUST  1 6.7e-6  1.6
DUST_big  DUST  1 14.2e-6 1.5
```

where:

1. `DUST_fin`: The species name and its extension to know if we are defining the fine, coarse or big mode.

2. `DUST`: The model species name finally used in CHIMERE

3. `1`: An indicator to recognize:

   (a) 1 = the aerosols with a classical log-normal distribution

   (b) 2 = a specific distribution for sea salt (following the recommendations of [Monahan, 1986])

4. `1.5e-6`: the mean mass median diameter (in meters)

5. `1.7`: the width of the distribution σ (no unit)

All MAKEPRI files are concatened and then read by the src/chemprep-distrib.F90 program.

5.2.1.5 The REACTIONS data files

All lot of REACTIONS files are available, each one listing chemical reactions. These files represent (i) the gaseous mechanisms, (ii) the types of aerosols the user wants in its simulation.
The choice was made to have a chemical mechanim in *human readable format*. This allows the user to simply modify a REACTION file or add a new one. But a specific syntax was defined and has to be respected.
For example, the first lines of the REACTIONS.univ.melchior2 data file are:

```
#    Inorganic chemistry    #
#############################

O3+NO->NO2             k(T)=Aexp(-B/T),A=1.8e-12,B=1370
O3+NO2->NO3            k(T)=Aexp(-B/T),A=1.2e-13,B=2450
O3+OH->HO2             k(T)=Aexp(-B/T),A=1.9e-12,B=1000
O3+HO2->OH             k(T)=Aexp(-B/T),A=1.4e-14,B=600
NO+HO2->OH+NO2         k(T)=Aexp(-B/T),A=3.7e-12,B=-240
NO2+OH+M->HNO3         k(T,M)=mtroe(3.4e-30,0,3.2,4.77e-11,0,1.4,0.30)
NO3+HO2->NO2+OH        k=4e-12
NO3+H2O2->HNO3+HO2     k=2e-15
```

where:

1. The **first column** is the chemical reaction. This reaction is written as:
   A1 + A2 -> α1 B1 + α2 B2
   The A_i species are the reactants (max=4), the B_i species are the products and the α_i are the stoechiometric coefficients of each B_i. The A_i must be active species, and can be repeated as many times as desired.

2. The **second column** is the reaction rate. The chemprep.awk program will interpret automatically the form of the reactions rate, considering its formulation follows the rule described in Table 5.3. The mathematical expressions for reaction rates (the K's and J's) can take more than 20 forms.

Note there are other rules and possibilities:

- Each line is considered as a reaction except blank lines or lines starting with a "#" sign (left for comments).
- Species names must contain at most 15 characters.
- There are special species whose concentration is only prescribed in the model. These are:
  1. H2O (water vapor),
  2. N2 (molecular nitrogen),
  3. O2 (molecular oxygen),
  4. M (80% N2 + 20% O2).

  Their values are given by the meteo data. Reaction with these species is possible with no constraint. Changes in these "prescribed species" imply several modifications in the model and are not an easy issue.
- Reactants can also be one (or several) of the prescribed species (H2O, N2, O2 or M).
- Syntax like A1+A2-A3 is NOT allowed
- Only species which are *consumed* at least once in the mechanism will be considered as **active species** in the model. If the user intends to use a species which results of chemical reactions but is not a reactant in any reaction, she (he) should add an artificial reaction to the mechanism, for instance A->X (A is the concerned product), with a negligible reaction rate, i. e. k=1e-10 (s-1).
- The mathematical expressions for reaction rates (the K's and J's) can take 20 forms, but here only a limited number is available. The table below shows the available possibilities, together with associated syntax.
- For the reaction rate #5 (the photolysis reactions), *label* is a label standing for recognition of chemprep in the FJX_j2j.dat file.
- The reaction rate type #13 is the aggregation of the ozone photolysis with reactions with atomic oxygen. The photolysis rates must be those of ozone only, hence the budget reaction is O3->2*OH.
- The reaction rate #14 corresponds to a specific Fall-off expression to apply to the reaction NO2+OH+M $\rightarrow$ HNO3

This is possible to change or add reactions. This is also possible to add a new reaction rate type. In this case, the user must change several programs:

1. Add this new type description in the code chemprep.awk
2. Define the number of constant ltabrate in the program src/inichem.F90
3. Add the new mathematical expression in the program src/rates.F90

Table 5.3: List of possible chemical reactions

Type number	**Name**	**Mathematical expression**	**syntax in REACTIONS file**
1	Constant K	K	k=*value*
2	Simplified Arrhenius	K=Aexp(-B/T)	k(T)=Aexp(-B/T), A=*value*, B=*value*
3	Arrhenius	K=Aexp(-B/T)(300/T)**N	k(T)=Aexp(-B/T)(300/T)**N, A=*value*, B=*value*, N=*value*
4	Troe or Falloff	K=K_0*f**Z/(1+M*(K_0/K_∞)) K_0=A_0exp(-B_0/T)(300/T)**N_0 K_∞=A_∞exp(-B_∞/T)(300/T)**N_∞ Z=1/(1+(Log10(M*K_0/K_∞))**2) M=air-density	K(T,M)=troe(A_0,B_0,N_0,A_∞,B_∞,N_∞,f)
5	Photolysis	J=J(Z)	J(Z)=photorate(*label*)
6	Special type	K=K_1*K_2/(1+K_2) K_1=A_1exp(-B_1/T) K_2=A_2exp(-B_2/T)	k(T)=SPECIAL_1(A_1, B_1, A_2, B_2)
7	Special type	K=K_1/(1+K_2) K_1=A_1exp(-B_1/T) K_2=A_2exp(-B_2/T)	k(T)=SPECIAL_2(A_1, B_1, A_2, B_2)
8	Special type	K=2*sqrt(f1*f2*f3*f4/((1+f3)*(1+f4))) f1=A_1exp(-B_1/T) f2=A_2exp(-B_2/T) f3=A_3exp(-B_3/T) f4=A_4exp(-B_4/T)	k=SPECIAL_3(A_1,B_1,A_2,B_2,A_3,B_3,A_4,B_4)
9	Special type	K=2*sqrt(f1*f2)*(1-sqrt(f3*f4))*(1-f4)/(2-f3-f4) f1=A_1exp(-B_1/T) f2=A_2exp(-B_2/T) f3=A_3exp(-B_3/T) f4=A_4exp(-B_4/T)	k=SPECIAL_3(A_1, B_1, A_2, B_2, A_3, B_3, A_4, B_4)
10 to 12	Not used		
13	Aggregated ozone photolysis	J=J0*H2O/(H2O+M*(0.02909*exp(70/T) +0.06545*exp(110d0/T))) H2O=water vapor (molec/cm3) M=air density (molec/cm3)	J(T,Z,H2O)=photorate(O3)
14	Modified Troe	Like Type #4 (Troe) but: Z=1/(1+((Log10(M*K_0/K_∞)-0.12)/1.2)**2)	K(T,M)=troe(A_0,B_0,N_0,A_∞,B_∞,N_∞,f)
15	NO2/HONO Heterogeneous reaction	ks=0.5*depo(NO2) at level 1	ks=0.5*depo(NO2)
16 to 20	Not used		
26	Special type	k(T)=k_0(T)+k_3(T)[M]/(1+k_3(T)[M]/k_2) k_0(T)=A1exp(-B_0/T) k_2(T)=A1exp(-B_2/T) k_3(T)=A1exp(-B_3/T) M=air-density	k(T)=saprc_2(A_0, B_0, A_2, B_2, A_3, B_3)

Continued on next page

Table 5.3 – continued from previous page

Type number	Name	Mathematical expression	syntax in REACTIONS file
27	Special type	k(T)=k_1(T)+k_2(T)[M] k_1(T)=A1exp(-B_1/T) k_2(T)=A1exp(-B_2/T) M=air-density	k(T)=saprc_1(A_1, B_1, A_2, B_2)
29	Troe or Falloff for SAPRC	K=K0*f**Z/(1+M*(K0/K_∞)) K0=A0exp(-B0/T)(300/T)**N0 K_∞=A_∞exp(-B_∞/T)(300/T)**N_∞ Z=1/(1+(Log10(M*K0/K_∞)/N)**2) M=air-density	K(T,M)=troe_saprc(A_0,B_0,N_0,A_∞,B_∞,N_∞,f,N)

5.2.1.6 The chemprep.awk program for the gaseous reactions

The scripts/chemprep.awk program is the interpreter able to convert the 'human readable' chemsitry files into the CHIMERE chemistry files.
The characteristics of this program are:

- Input data: the REACTIONS ascii file
- Output data:
  1. the .species file: This file lists the gaeseous active species. This list is merged with the aerosol list in scripts/chemprep-prep-chemistry-data.sh to produce the ACTIVE_SPECIES file.
  2. the CHEMISTRY file: This is the original REACTIONS but with only the reactants and products and the code number of the reaction.
  3. the STOICHIOMETRY file: Same as CHEMISTRY, but for the stoechiometric coefficients values
  4. The REACTION_RATES file: Same as CHEMISTRY, but for the reactions rates
  5. The FJX_j2j.dat file: Information for the FastJX model for photolysis
  6. The FAMILIES file: List of species in families.

If the user wants to add a new reaction type, it is necessary to define a new syntax (as explained in Table 5.3) and to add a piece of code in this program. The way is to write the test to recognize the reaction type. For example and for the reaction reate #3, corresponding to the "complete Arrhenius" rate, the code is:

```
# Type 3: Complete Arrhenius

$2 ~ /k\(T\)=Aexp\(-B\/T\)\(300\/T\)\*\*N,/ {
 split($2,w,/(=|,)/)
 printf(nofreac" 3 "w[4]" "w[6]" "w[8]"\n") >> "REACTION_RATES"
}
```

5.2.1.7 The ACTIVE_SPECIES and OUTPUT_SPECIES data files

The output files are directly in the model to know the list of chemically active species (including the gases and aerosols) and the species to write in the out.[label].nc results file.
The ACTIVE_SPECIES contains the following informations:

```
1 APINEN 2 1
2 AnA1D 2 1
3 AnA1DAQ 2 1
...
207 p10ISOPA1 2 1
208 p10H2SO4 2 1
209 p10HNO3 2 1
210 p10NH3 2 1
211 p10WATER 2 1
```

where the beginning of the file lists the gaseous species and the end lists the aerosols species. The model considering that one bin of one aerosol is a specific species to transport, all aerosols are defined with the syntax: p<number of the bin><species name>.
This file is read by the program src/inichem.F90 and the four columns correspond to:

1. The number of the species
2. The name of the species
3. The number of the horizontal transport scheme to use for this species (the flag iadv)
4. The number of the vertical transport scheme to use for this species (the flag iadvv)

For the definition of the species to write as output at the end of a simulation, two data files are created:

- OUTPUT_SPECIES.full: contains all chemical species used in the model for the simulation
- OUTPUT_SPECIES.low: contains a reduced list of the chemical species (not all gaseous species and not the binned aerosols)

The choice between these two options is made in the chimere.par file with the option:

```
[$accur]    Output species detailed (low/full)              : full
```

The syntax of the OUTPUT_SPECIES files is:

```
O3   0.
NO2     0.
NO      0.
PAN     0.
...
p01BCAR 100.
p01DUST 100.
p01OCAR 100.
p01PPM 100.
p01SALT 58.5
p01AnA1D 168.
p01AnBmP 152.
...
```

with:

1. The first column is the model species name
2. The second column is the molar mass of the species
   - For gases:
     - ◇ with 0, the result in output is expressed in ppb
     - ◇ with a prescribed molar mass value, the result is automatically converted and written in μg m^{-3}

- For aerosols, the results are always in μg m^{-3}.
  - ◇ If the molar mass is known (for inorganic species), its value is used,
  - ◇ else a fake value of 100 is used.

5.2.1.8 The FAMILY data file

There is a possibility of defining families. These are groups of species whose concentration sum can be output in the model. However these families are only used in outputs, not in the chemistry itself.

- The **gaseous species families** have to be manually defined in the chemprep/data/FAMILIES* files, corresponding to the chemical mechanism used.
- The **aerosol species families** are automatically calculated by the src/chemprep-distrib.F90 program. The program is designed to produce families for:
  - ◇ All aerosols in order to have one species for the whole size distribution. For example, for a simulation with ten bins:

    ```
    10 pDUST p01DUST p02DUST p03DUST p04DUST p05DUST p06DUST
     p07DUST p08DUST p09DUST p10DUST
    ```

    where pDUST is the sum of all p*DUST species (one concentration per bin).
  - ◇ PM25: all aerosols with a mean mass median diameter less than 2.5 μm
  - ◇ PM10: all aerosols with a mean mass median diameter less than 10 μm
  - ◇ The relative parts of anthropogenic and biogenic PM25 and PM10, called PM25ant, PM25bio, PM10ant and PM25bio.

Many families are already defined, corresponding to the most often use in chemical composition studies. For example, the parameter file FAMILIES.gasp.melchior2 contains the following families for the gaseous species:

```
TOTPAN=PAN+toPAN
NOX=NO+NO2
OX=NO2+O3
HOX=OH+HO2+CH3O2+CH3COO+oRO2+oPAN+oRN1+obio
NOY=NO+NO2+NO3+N2O5+N2O5+HNO3+PAN+oPAN+oRN1+ISNI+CARNIT+HONO
ROOH=CH3O2H+obioH+PPA+oROOH
HCNM=C2H6+C2H6+NC4H10+NC4H10+NC4H10+NC4H10+C2H4+C2H4+C3H6+C3H6
    +C3H6+OXYL+OXYL+OXYL+OXYL+OXYL+OXYL+OXYL+OXYL+C5H8+C5H8+C5H8+C5H8+C5H8
    +APINEN+APINEN+APINEN+APINEN+APINEN+APINEN+APINEN+APINEN+APINEN+APINEN
```

Other families are automatically defined for aerosols, namely PM25 and PM10. For example, with 10 bins, there are 48 aerosol sections to cumulate to finally have the concentration of the anthropogenic part of PM25.

```
48 PM25ant p01BCAR p02BCAR p03BCAR p04BCAR p05BCAR p06BCAR p01OCAR p02OCAR
   p03OCAR p04OCAR p05OCAR p06OCAR p01PPM p02PPM p03PPM p04PPM p05PPM p06PPM
   p01AnA1D p02AnA1D p03AnA1D p04AnA1D p05AnA1D p06AnA1D p01AnBmP p02AnBmP
   p03AnBmP p04AnBmP p05AnBmP p06AnBmP p01H2SO4 p02H2SO4 p03H2SO4
   p04H2SO4 p05H2SO4 p06H2SO4 p01HNO3 p02HNO3 p03HNO3 p04HNO3 p05HNO3
   p06HNO3 p01NH3 p02NH3 p03NH3 p04NH3 p05NH3 p06NH3
```

In the CHIMERE output file call out.<label>.nc, the hourly three-dimensional fields of O_x and NO_x, for example, are directly available. For the aerosols, the results are then written for each bin (i.e p01DUST p02DUST p03DUST...) and for the total mass of this aerosols pDUST.

	N= 3	N= 4	N= 5	N= 6	N= 7	N= 8	N= 9	N= 10	N= 11	N= 12	N= 13	N= 14	N= 15	N=
1	0.01	0.01	0.01	0.01	0.01	0.01	0.01	0.01	0.01	0.01	0.01	0.01	0.01	0.0
2	2.50	0.16	0.06	0.04	0.03	0.03	0.03	0.02	0.02	0.02	0.02	0.02	0.02	0.0
3	10.00	2.50	0.40	0.16	0.09	0.09	0.06	0.05	0.05	0.04	0.03	0.03	0.03	0.0
4	40.00	10.00	2.50	0.63	0.27	0.27	0.16	0.11	0.11	0.08	0.06	0.06	0.05	0.0
5	/	40.00	10.00	2.50	0.83	0.83	0.40	0.23	0.23	0.16	0.12	0.12	0.09	0.0
6	/	/	40.00	10.00	2.50	2.50	1.00	0.52	0.52	0.32	0.21	0.21	0.16	0.1
7	/	/	/	40.00	10.00	5.00	2.50	1.14	1.14	0.63	0.40	0.40	0.27	0.2
8	/	/	/	/	40.00	10.00	5.00	2.50	2.50	1.25	0.73	0.73	0.48	0.3
9	/	/	/	/	/	40.00	10.00	5.00	5.00	2.50	1.35	1.35	0.83	0.5
10	/	/	/	/	/	/	40.00	10.00	10.00	5.00	2.50	2.50	1.44	0.9
11	/	/	/	/	/	/	/	40.00	20.00	10.00	5.00	3.97	2.50	1.5
12	/	/	/	/	/	/	/	/	40.00	20.00	10.00	6.30	3.97	2.5
13	/	/	/	/	/	/	/	/	/	40.00	20.00	10.00	6.30	3.9
14	/	/	/	/	/	/	/	/	/	/	40.00	20.00	10.00	6.3
15	/	/	/	/	/	/	/	/	/	/	/	40.00	20.00	10.0
16	/	/	/	/	/	/	/	/	/	/	/	/	40.00	20.0
17	/	/	/	/	/	/	/	/	/	/	/	/	/	40.0

Table 5.4: Values of the diameter bins obtained for $D_{min} = 0.01\,\mu\text{m}$, $D_{max} = 40\,\mu\text{m}$, and twelve different values of N.

5.3 The aerosols size distribution calculations

5.3.1 Disretization of the size distribution

The CHIMERE model accounts for the size distribution of the aerosols using a size-bin approach: the aerosol particles for each of the model species are distributed in N size bins, covering a diameter range from D_{min} to D_{max}. Given these three user-defined parameters, a preprocessor compute a sequence $(d_i)_{i=1,N+1}$ of cutoff diameters that meets the following requirements:

- $2.5\,\mu\text{m}$ and $10\,\mu\text{m}$ are retained as cutoff diameters: two indices $i1$ and $i2$ such that $d_{i1} = 2.5\,\mu\text{m}$ and $d_{i2} = 10\,\mu\text{m}$ must exist
- The sequence of the cutoff diameters covers exactly the size interval requested by the user: $d_1 = D_{min}$ and $d_{N+1} = D_{max}$

The first requirement is set to allow a meaningful evaluation of $PM_{2.5}$ and PM_{10} in the model, since these quantities are typically available from routine measurements.
The default (and recommended) values of the extreme diameters are $D_{min} = 0.01\,\mu\text{m}$ and $D_{max} = 40\,\mu\text{m}$. Using these values, the produced size distributions for various values of the number of intervals N are shown in Tab. 5.4 according to the requested number of bins, N. If $N \geq 12$, then the ratio of two successive cut-off diameters is always such as $d_{i+1}/d_i \leq 2$: all particles within a single size bin have comparable diameters at least within a factor 2, which is a good way to ensure that all the size-depending processes affecting the aerosols (sedimentation, coalescence etc.) are treated in a realistic way. However, when calculation speed is a critical requirement, for example for operational prevision, the number of size bins could be lowered to $N = 6$, still ensuring that $d_{i+1}/d_i \leq 4$

5.3.2 Implementation

The following calculation steps are performed in the src/chemprep-distrib.F90 program:

1. The size distribution depending on the distribution range and the number of bins, $nbins$
2. The log-normal distribution to project the three emitted modes into the $nbins$ bins

This program is launched by the scripts/chemprep-prep-chemistry-data.sh and some parameters are available in the script: the user can change some values but it is strongly recommended to keep the values as it. These values are:

```
# cut1 and cut2 forced the size distribution
cut1=2.5
cut2=10.

# dmin and dmax (micrometers) are used as tuner parameter to adjust the aerosol
# distribution (they are not the min and max cut off diameter !!)
dmin=0.05
dmax=40.
```

where:

- `cut1` and `cut2` ensures to have a size distribution with an exact cut-off for $PM_{2.5}$ and PM_{10}.
- `dmin=0.05` and `dmax=40` are the boundaries of the size distribution, in μm (and not the first and last mean mass median diameters).

This program has the following specifications:

1. **Input:** the MAKEPRI file and the options cut1, cut2, dmin and dmax
2. **Output:**
   (a) The AEROSOL file: The definition of the bins sizes and cut-off.
   (b) The PRIMARY file: The definition of the log-normal distribution to reaffect the three modes (fine, coarse and big) into the models bins.

This size distribution is used by the model with the AEROSOL file. An example is given below for a distribution of 10 bins.

```
# Number of sections D(2.5) D(10.0)
          10           6           8
 0.3906250E-07  0.7812500E-07  0.1562500E-06  0.3125000E-06
 0.6250000E-06  0.1250000E-05  0.2500000E-05  0.5000000E-05
 0.1000000E-04  0.2000000E-04  0.4000000E-04
# Name of aerosol components, properties (no blank line a the end!)
# NAME          TYPE   Molar mass     Origin [0=bio,1=anth,2=mineral]
BCAR            1      100.               1
DUST            1      100.               2
OCAR            1      100.               1
PPM             1      100.               1
SALT            1      58.5               0
AnA1D           2      168.               1
AnBmP           2      152.               1
BiA1D           2      170.               0
BiBmP           2      236.               0
ISOPA1          2      177.               0
H2SO4           3      96.                1
HNO3            3      62.                1
NH3             3      18.                1
WATER           4      18.                1
```

An example of an aerosol size distribution is presented in Figure 5.1.

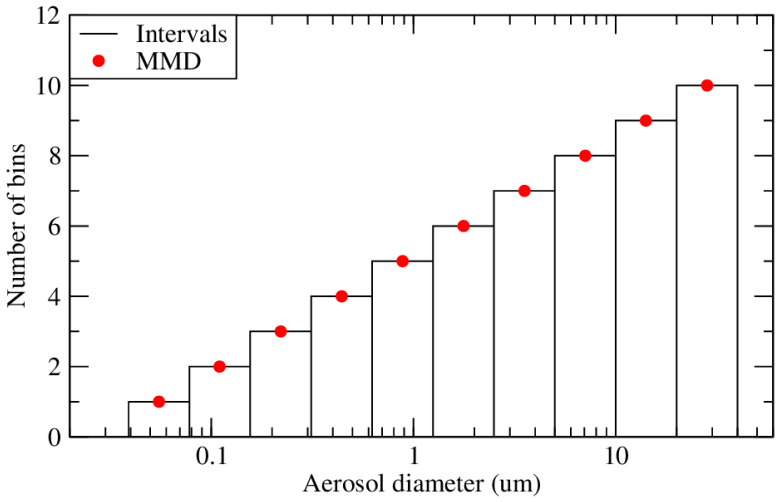


Figure 5.1: *Example of an aerosol size distribution with ten bins. The intervals represent the boundaries of the distribution (nbins+1 values) and the red dots represent the Mean Mass Median Diameter (MMD) of the distribution (nbins values).*

5.3.3 The log-normal distribution calculation

The second output of the src/chemprep-distrib.F90 program is the log-normal distribution coefficients to estimate the aerosols emitted fluxes from their three main modes to the model bins. This distribution is calculated as:

$$n(D_p) = \frac{N}{\sqrt{2\pi} D_p ln\sigma_c} exp\left(-\frac{(lnD_p - lnD_c)^2}{2ln^2\sigma_c}\right) \tag{5.1}$$

where:

- D_p the mean mass median diameter of the CHIMERE size distribution (e.g. 10 bins)
- D_c the mean mass median diameter of the raw modes (i.e fine, coarse and big)
- σ_c the standard deviation of each D_c

For a simulation with the parameters already defined in the model, the aerosols are currently defined as in the Table 5.5 .

The results of the $n(D_p)$ values are displayed in Figure 5.2 .

These data are written as output in the PRIMARY file as:

Aerosol	Name	Fine D_p (σ)	Coarse D_p (σ)	Big D_p (σ)
	Anthropogenic emissions			
H2SO4	Primary sulfuric acid	0.2 (2.5)		
OCAR	Primary organic carbon	0.11 (1.6)	4.0 (1.1)	
BCAR	Primary black carbon	0.11 (1.6)	4.0 (1.1)	
PPM	Primary particulate matter	0.2 (2.5)	4.0 (1.1)	
	Sea salt emissions			
SALT	Total dry sea salts		M86	
H2SO4	Sulfate fraction of sea salts		M86	
NA	Sodium fraction of sea salts		M86	
HCL	Chloride fraction of sea salts		M86	
WATER	Water fraction of sea salts		M86	
	Mineral dust emissions			
DUST	Mineral dust	1.5 (1.7)	6.7 (1.6)	14.2 (1.5)

Table 5.5: *Aerosols emissions with the three modes describing their size distribution: fine, coarse and big. The mean mass median diameter D_p is expressed in μm, σ is unitless.*

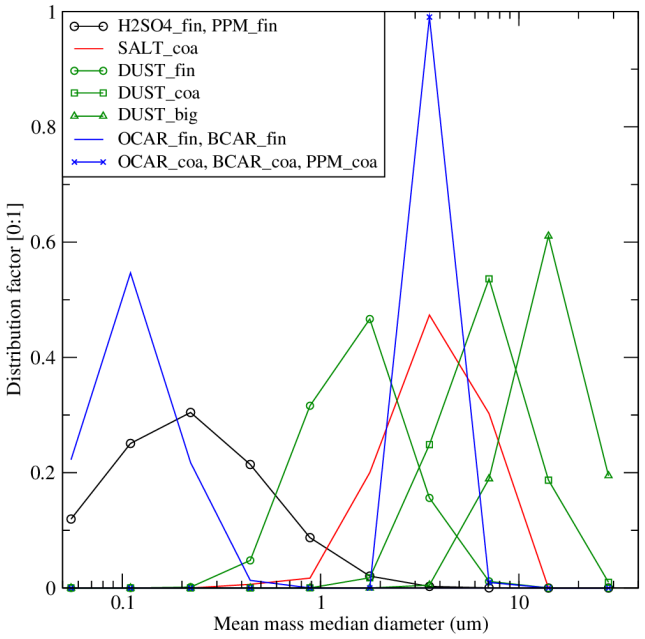


Figure 5.2: *Distribution factors used to project the three aerosol emitted modes on the CHIMERE bins size distribution.*

```
          11
H2SO4_fin       H2SO4           1          0.20000E-06          0.25000E+01
SALT_coa        SALT            2          0.10000E+01          0.10000E+01
DUST_fin        DUST            1          0.15000E-05          0.17000E+01
DUST_coa        DUST            1          0.67000E-05          0.16000E+01
DUST_big        DUST            1          0.14200E-04          0.15000E+01
OCAR_fin        OCAR            1          0.11000E-06          0.16000E+01
BCAR_fin        BCAR            1          0.11000E-06          0.16000E+01
PPM_fin         PPM             1          0.20000E-06          0.25000E+01
OCAR_coa        OCAR            1          0.40000E-05          0.11000E+01
BCAR_coa        BCAR            1          0.40000E-05          0.11000E+01
PPM_coa         PPM             1          0.40000E-05          0.11000E+01
 0.1195939E+00  0.2506953E+00  0.3044555E+00  0.2142743E+00  0.8734840E-01
   0.2059794E-01  0.2804594E-02  0.2200042E-03  0.9919314E-05  0.2564
548E-06
```

where the first line is the number of aerosols needing a redistribution, the second block represents the aerosols and the last block represents the distribution coefficients calculated using the Equation 5.1 .

5.4 The preparation of tracers

5.4.1 Tracers activation

It is possible to add passive tracers in the simulation. In this model version, the coding is simplified for the user and only one data file has to be managed, the chemprep/data_trc/TRACERS.data. This file is read by the script chemprep-prep-tracer-data.sh if the flag <$trc> is set to one in the chimere.par file as:

```
   [trc]       Include tracers?     : 1
```

5.4.2 The TRACERS.data data file

The parameter file chemprep/data_trc/TRACERS.data contains informations as follows:

```
# Name Type    Lon.   Lat.   First date  Last date    Mass(ton)   Zmin(m)  Zmax(m)
GTRC1   1    12.631  35.516  2009010101    2009010312 1000.       0.      2000.
PTRC1   2     9.416  42.833  2009010101    2009010312 1000.       0.      1000.
PTRC2   2     9.416  42.833  2009010101    2009010312 1000.    1000.      2000.
```

where all informations are given line by line. There is one line per tracer. If it is necessary to emit the same tracer at the same location but at two different time periods, the user have to write the line two times. Each line must contain the following informations:

1. The name of the tracer. In this example, there is one gaseous tracer (GTRC1) and two particulate tracers (PTRC1 and PTRC2)
2. The tracer type: 1 = gaseous species; 2 = aerosol
3. The longitude of the emission (in decimal degrees)
4. The latitude of the emission (in decimal degrees)
5. The starting date of the emission (format YYYYMMDDHH)
6. The ending date of the emission (format YYYYMMDDHH)
7. The mass of the emission (integrated over the whole period and the atmospheric column)
8. The starting altitude of the emission (in meters)
9. The ending altitude of the emissions (in meters)

5.4.3 The chemprep-prep-tracer-data.sh script

This script adds parameters of gaseous and particulate tracers to the data files describing parameters of the chemistry mechanism, depositions, and output. At the end the new files created are: FAMILIES.trcgas, ANTHROPIC.trc, REACTIONS.trc, OUTPUT_SPECIES.trc, AEROSOL.trc, MAKEPRI.trc, DEPO_SPEC.trc and WETD_SPEC.trc
Some parameters are available in the script:

```
# The fake aerosols molar mass in g/mol
aeromolmass=100.

# Mean mass median diameter (m) of the three aerosols modes: fine, coarse and big
d_fin=1.5e-6
d_coa=6.7e-6
d_big=14.2e-6
sig_fin=1.7
sig_coa=1.5
sig_big=1.6
```

By default, we consider that the aerosol tracers have the same characteristics than the mineral dust. This may change by the user. A change in these values will impact the size distribution of the tracers, then their transport and deposition.
Finally, this script creates or concatenate the necessary parameters files for the chemistry. Even if thse tracers are not chemically active, it is necessary to put their characteristics into all chemical files in order to consider they are active species in the model. To emulate this, a fake reaction is added in the CHEMISTRY file as:

```
     echo {trc_spec}"->X    k=1e-18"                  >> REACTIONS.trc
```

For the dry and wet deposition of geaseous tracers, it is considered that the tracer has the same characteristics as SO2 (the tracers being often used for volcano transport studies).

5.4.4 Calculation of emissions fluxes

The emissions fluxes are hourly calculated in the *chimere 2017* code and in the program src/prep_temis.F90. The tabulated mass is linearly splitted between the several emissions time period and over the vertical interval. The three modes are projected into the model size distribution bins considering the following percentages of mass: 30% in the fine mode, 40% in the coarse mode and 30% in the big mode. This may be changed in the model code with the following lines:

```
  mdistrib(1)=0.3d0
  mdistrib(2)=0.4d0
  mdistrib(3)=0.3d0
```

6 Emissions

CHIMERE accounts for most possible types of emissions. While the anthropogenic and fire emissions need to be processed before the beginning of the simulation, all the other types of emissions (mineral dust, biogenic emissions, sea-salt emissions and tracers) are estimated by the CHIMERE main program itself during the simulation.
The emissions fluxes calculations are described in:

1. §6.1, p.73: anthropogenic emissions
2. §6.2, p.78: biogenic emissions
3. §6.3, p.80: sea salt emissions
4. §6.4, p.81: mineral dust emissions
5. §6.5, p.90: vegetation fires emissions
6. §5.4, p.71: tracers emissions (in the chemprep chapter)
7. §6.6, p.90: the resuspension

6.1 Anthropogenic surface emissions

There are two options on how anthropogenic emissions may be handled by the CHIMERE model. But at the end, the simulation needs to have a AEMISSIONS.${sim}.nc file with the format described *Appendix G.5, p.232*. The two possible ways are:

1. The user can pre-process anthropogenic emissions from an inventory of his/her own choice. The important point is to finally create a NetCDF file following the AEMISSIONS.${sim}.nc format.
2. Alternatively, the CHIMERE team develops and distributes an anthropogenic surface emission preprocessor called emiSURF that, based on a top-down approach, calculates hourly emission fluxes on the CHIMERE grid and the period of the simulation. The input data are either the EMEP or the HTAP databases. The output of this model can be processed by the anthropogenic emission pre-processor now embedded in the CHIMERE core (module prep_aemis.F90), which generates directly the AEMISSIONS.${sim}.nc file.

6.1.1 User's precompiled emissions

The user can produce his/her own AEMISSIONS.${sim}.nc file. This file must contain hourly emission fluxes on the CHIMERE 3-D grid for all gases and aerosol species involved in the chemical mechanism of the CHIMERE simulation (MELCHIOR or SAPRC) in molecules·cm^{-2}·s^{-1} (see Table 6.1 for the list of the required species). Aerosol fluxes need also to be converted to virtual "molecule-like" units in this anthropogenic emission input file considering a fictitious molar mass equal to 100g·mol^{-1}. The conversion coefficient from mass unit to CHIMERE model unit is 6.022×10^{23} mol^{-1}/(100g·mol^{-1}). In this case the user should set the

[$imakeaemis] flag at 0, so that "prep_aemis.F90" module subroutines are not invoked, and provide the appropriate [$aemisdir] and [$fnemisd] paths pointing to the AEMISSIONS.${sim}.nc file in the "chimere.par" file.

MELCHIOR2

NO	Nitrogen monoxide
NO2	Nitrogen dioxide
HONO	Nitrous acid
SO2	Sulphur dioxide
NH3	Ammoniac
CO	Carbon monoxide
CH4[1]	Methane
C2H6	Ethane
NC4H10	n-Butane
C2H4	Ethene
C2H6	Ethane
C3H6	Propene
C5H8	Isoprene
OXYL	o-Xylene
HCHO	Formaldehyde
CH3CHO	Acetaldehyde
CH3COE	Methyl ethyl Ketone
APINEN	α-pinene

AEROSOLS

PPM_fin[2]	Primary particulate matter
PPM_coa[3]	Primary particulate matter
PPM_big[4]	Primary particulate matter
H2SO4_fin[5]	Primary sulfuric acid
BaP_fin [5]	Benzo(a)pyrene
BbF_fin[5]	Benzo(b)fluoranthene
BkF_fin[5]	Benzo(b)fluoranthene
OCAR_fin[5]	Primary organic carbon
BCAR_fin[5]	Primary black carbon

SAPRC

CH4[1]	Methane
CO	carbon monoxide
HONO	Nitrous acid
NO	itrogen monoxide
NO2	itrogen dioxide
SO2	Sulphur dioxide
ACET	Acetone
ALK1	Ethane
ALK2	Propane
ALK3	Alkans 2.5x10^3 <k_{OH}< 5x10^3
ALK4	Alkans 5x10^3<k_{OH}<1x10^4
ALK5	Alkans 1x10^4<k_{OH}
ARO1	Aromatiques k_{OH}<2x10^4
ARO2	Aromatiques k_{OH}>2x10^4
BALD	Aromatic aldehydes
CCHO	Acetaldehyde
C2H4	Ethen
GLY	Glyoxal
HCHO	Formaldehyde
MEOH	Methanol
MACR	Methacrolein
OLE1	Alkens k_{OH}<7x10^4
OLE2	Alkens k_{OH}>7x10^3
CRES	Phenols and Cresols
PRD2	Ketones (k_{OH}>0.7x10^4 ppm^{-1}.mn^{-1})
RCHO	Lumped C3+ Aldehydes
C5H8	Isoprene
APINEN	α-pinene
ACYE	Acetylen
BENZ	Benzen
AACD	Acetic Acid
IPRD	Lumped isoprene product species
NH3	Amoniac

[1] Zero in this model version
[2] $\phi < 2.5\ \mu$m
[3] $2.5 < \phi < 10\ \mu$m
[4] $\phi > 10\ \mu$m
[5] Assumed to be in the fine mode

Table 6.1: *Gas and particle emissions required for MELCHIOR and SAPRC*

6.1.2 The emiSURF interface

For simulations over Europe, the starting point are annual national emission totals from the EMEP database (EMEPCWEST [Vestreng et al., 2005]) available at the web site http://www.emep.int. Additional data for benzo(a)pyrene, benzo(k)fluoranthene and benzo(b)fluoranthene (respectively BaP, BkF and BbF) can be requested on the EMEP-MSCEAST web site http://www.msceast.org. Annual totals for European countries are provided per SNAP sector in Mg·year^{-1}·grid cell area^{-1} over the 50x50 km resolution EMEP grid. The following pollutants are available: NO_x, SO_x, NMVOC, CO, NH_3, PM_{coarse} and $PM_{2.5}$, where PM_{coarse}=PM_{10}-$PM_{2.5}$. Inventory data must be obtained from the EMEP for each year and copied to the

annual-EMEP50x50/50x50new/data_expert directory. Please see the README file with the instructions how to obtain the data.
The processing of the annual totals to compute hourly fluxes over the CHIMERE 3-D grid for all the chemical species of the corresponding mechanism consists of three main steps in the emiSURF model (Figure 6.1).
For simulations over other parts of the world, the user can use the HTAP emissions inventory (http://edgar.jrc.ec.europa.eu/national_reported_data/htap.php). These emissions are available as monthly totals per activity sectors and at global scale and at 0.1^ox0.1^o resolutions.

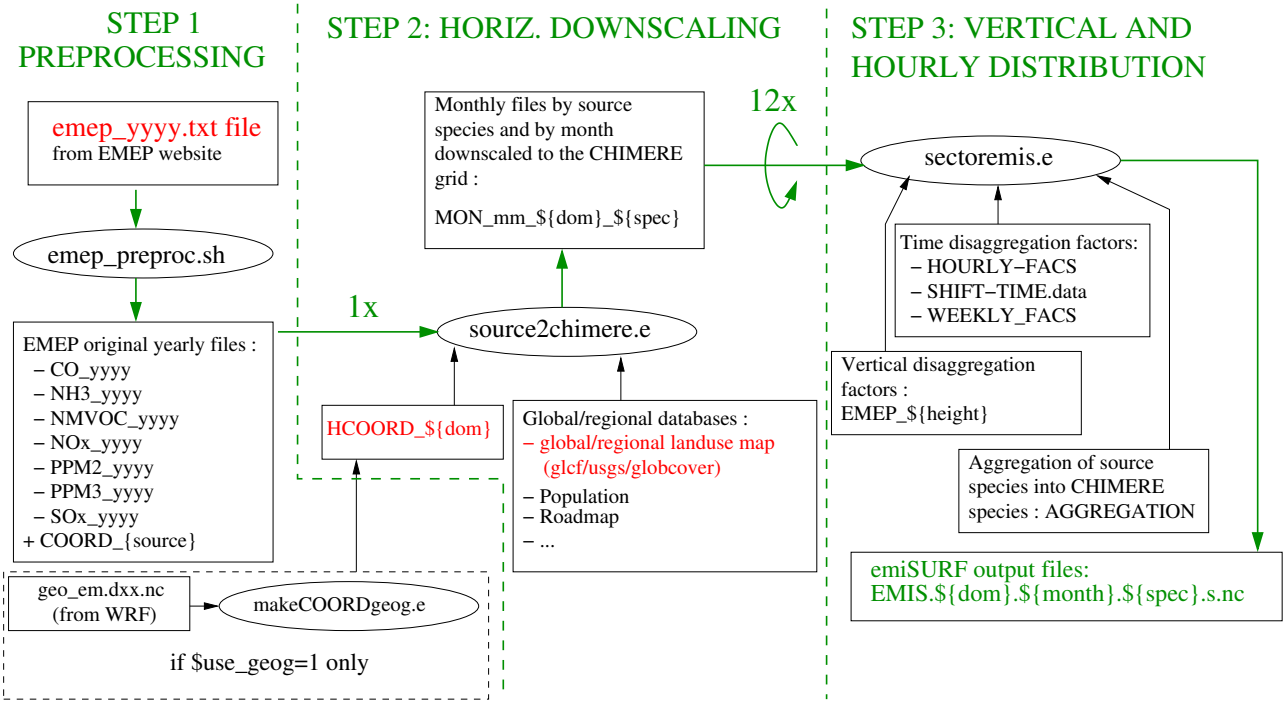


Figure 6.1: *Top-down processing of EMEP anthropogenic emissions with the emiSURF interface*

6.1.2.1 Step 1 : preprocessing

Producing the HCOORD file In earlier versions of CHIMERE and emiSURF, the user had to provide the HCOORD_${dom} ascii file containing the lat-lon coordinates of the grid cell centers for the simulation domain.
It is still possible to produce manually this HCOORD_${dom} file, but in the new CHIMERE and emiSURF version, another, easier alternative is proposed to the WRF users who wish to use for their CHIMERE simulation the same horizontal domain as for their WRF simulation: in this case, a program, makeCOORDgeog.e is provided and run automatically at the beginning of the emisurf.sh script (see 6.1). This script reads the geo_em.dxx.nc file (produced by the WPS module of WRF) and converts it into a CHIMERE-friendly HCOORD_${dom} file. To activate this option, the following flags shall be set in the emisurf.sh script :

```
export use_geog=True
export geogfile=[path to the geog file]
```

geogfile needs to contain the absolute link to the geog file from WRF, e.g. /home/user/wrfoutputs/geo_em.d01.nc.

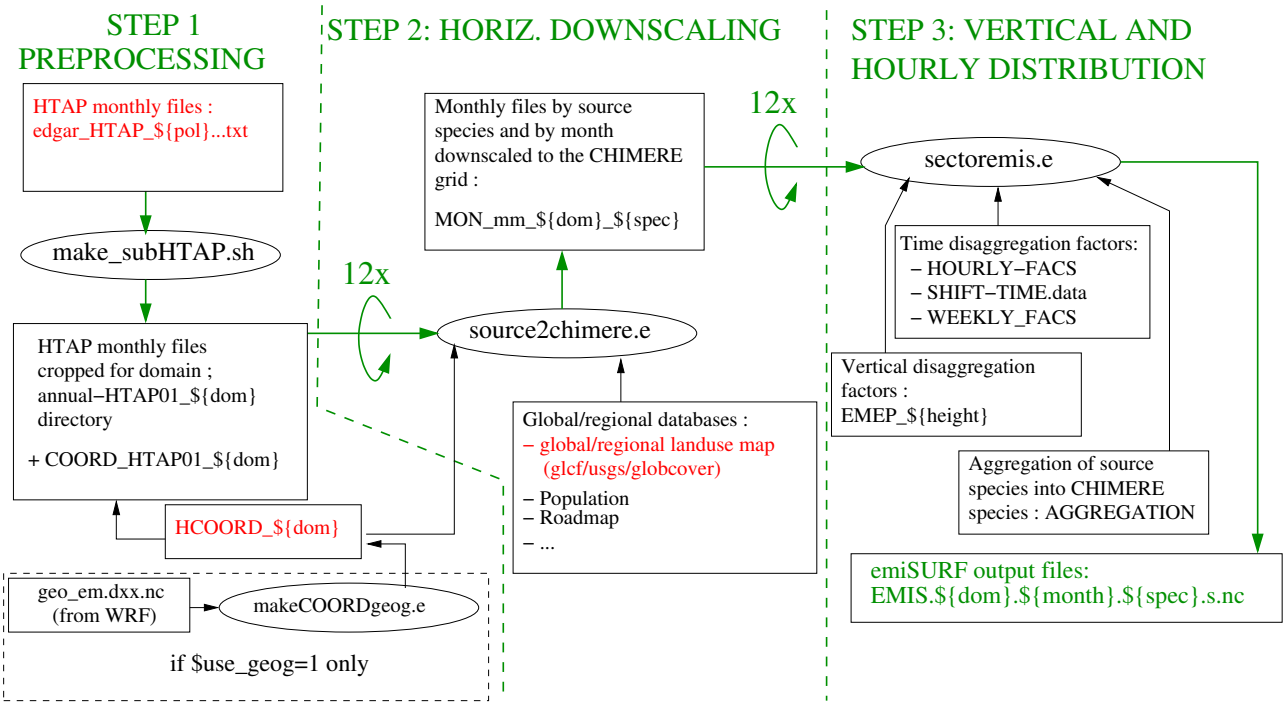


Figure 6.2: *Top-down processing of HTAP anthropogenic emissions with the emiSURF interface*

The user also needs to initialize carefully the *is_polar* flag, with *is_polar=True* if the WRF input domains contains the south and/or the north pole, *is_polar=False* otherwise.

Preprocessing the emission files

1. Case 1: If the emissions are computed from the EMEP emission inventory (see Figure 6.1), the emep_preproc.sh bash shell reads the annual inventory data and creates one file per pollutant: NO_x, SO_x, NMVOC, CO, NH_3, PPM2 = PM_{coarse} and PPM3 = $PM_{2.5}$. The header of these files reads as follows:

```
COUNTRY_ID, WE_EMEP_cell_ID, SN_EMEP_cell_ID,SNAP1,...SNAP10
```

   Emission fluxes are in Mg·year^{-1}·EMEP grid cell area^{-1} (Fig. 6.1).

2. Case2: If the emissions are computed from the HTAP emission inventory (see 6.2), the initial HTAP global files are reformatted and cropped to a lat-lon subdomain of the globe largely including the CHIMERE simulation domain : this step permits to reduce the computation time for treatment of these emissions by source2chimere.F90 by keeping only the useful part of this huge global emission set.

6.1.2.2 Step 2: Horizontal and monthly downscaling with source2chimere.F90

Spatial allocation of surface emissions on the CHIMERE grid is based on landuse data. Three databases are implemented in the current version of emiSURF:

- globcover at 10 arc second (≈300m) resolution developed under the European Space Agency initiative (http://due.esrin.esa.int/page_globcover.php). This option is activated by setting *lu_source="globcover"* in the emisurf.sh script.

- usgs data at 1km resolution, with 24 USGS landuse categories, as used in the WRF meteorological model. This option is activated by setting *lu_source="usgs"* in the emisurf.sh script.

In earlier versions of the emisurf preprocessor, emissions for all the SNAP sectors were performed based on a classification among four landuse types: urban, crop, water or forest. On the new version, two other proxies are proposed for the spatial allocation of the emissions : population density and road map. However, only the landuse map is a mandatory input for source2chimere. Population density and road map are used as described below, and only for SNAP sectors 2 (residential emissions) and 7 (road traffic). Donwscaling using population density as a proxy is activated if pop=1 in emisurf.sh. Downscaling using road map is activated if road=1.

- SNAP sector 2 : if pop=1, emissions from SNAP sector 2 (mostly residential fuel burning) are downscaled using the population density as a proxy for gas species, and a different factor for particulate species, taking into account the fact that wood burning for residential heating occurs predominantly in sparsely populated areas rather than in dense urban areas. If pop=0, then emissions from SNAP sector 2 are downscaled according to the landuse data.

- SNAP sector 7 : if road=1, then emissions from SNAP sector 7 (traffic emissions) are downscaled using the road map data as a proxy. If road=0 but pop=1, then these emissions are dowscaled according to the population density. Otherwise, if road=0 and pop=0, then the emissions from road traffic are downscaled according to the landuse.

Apart from this spatial redistribution, source2chimere.F90 also performs, if needed, the allocation of the yearly EMEP emissions towards monthly totals and produces spatially downscaled emission data on the CHIMERE for each month of the year. It is worth noting at that point that the process depends on the emission inventory used :

- If the emission inventory used is the EMEP emissions inventory, which are annual, the spatial downscaling is performed once and for all by source2chimere.F90. After this process of spatial downscaling, redistribution towards monthly emissions is performed based on seasonal factors provided by the Institute of Energy Research for each country and SNAP sector (see the inputdata/SEASONAL-FACS_<POL> file).

- If the emission inventory used in the HTAP inventory, the emissions are already provided on a monthly basis. Therefore, the spatial downscaling needs to be performed separately for each of the 12 months of the year : to produce emissions for a complete annual cycle, source2chimere.F90 needs to be run once for each of the 12 months.

These two cases are managed automatically by the emisurf.sh script : if the emissions are produced from the EMEP inventory, then source2chimere.F90 is run only once and produces monthly emission files for each contaminant and each activity sector. This reduces very much the computation time for this step. If on the other hand the emissions are computed from the HTAP dataset, then source2chimere.F90 is run 12 times (once for each month of the year), and the downscaling is performed separately for each of these 12 months, which can be time-consuming depending on the domain size.

6.1.2.3 Step 3: Downscaling on the vertical dimension and in time with sectoremis.F90

- A time-shift on the data is applied to take into account the time zone and daylight saving information for each country.
- 24-hour profiles for each day of week and for each SNAP sector are applied over the emissions to obtain hourly data. These variations follow the guidelines provided by the Institute for Energy Economics and Rational Use of Energy, University of Stuttgart; [Ebel et al., 1994].
- Hourly emissions from all SNAP sectors, gridded over the CHIMERE simulation domain are aggregated to a single flux per emitted pollutant.
- Chemical speciation operates on the emitted pollutants at two stages. "Inventory" pollutants (i.e PPM2, PPM3, NO_x, CO, SO_x, NH_3, CH_4 and NMVOC) split into "real" compounds with ratios depending on the SNAP activity sector. At a second stage, "real" compounds split into "model" compounds depending on the chemical mechanism (Melchior or SAPRC). This process is described in the AGGREGATION_$mechanism files found in the "inputdata" directory. Differences between the two chemical mechanisms apply only to the NMVOC species.
  - NO_x: For all SNAP sectors 90% of NO_x emissions is assigned to NO, 9.2% to NO_2 and 0.8% to HONO [Kurtenbach et al., 2001]. Depending on the country, NO_x emissions in the EMEP inventory may include soil NO biogenic emissions in the "Agriculture" sector. The user should be carful not to doublecount NO soil emissions when running the biogenic emissions pre-processor embedded in the CHIMERE model (Sect. 6.2).
  - SO_x: For all SNAP sectors, 99% of SO_x is assigned to SO_2 and 1% to sulphuric acid (H_2SO_4) in the particulate phase.
  - NMVOC: For both mechanisms (Melchior and SAPRC) NMVOC emissions first split into 221 "real" compounds of the british PORG speciation depending on the SNAP sector [Passant, 2002]. Then, a two-step procedure aggregates "real" VOC compounds to a smaller set of VOC classes which correspond directly to the specific compounds of the MELCHIOR or SAPRC chemical mechanism, following the Middleton methodology [Middleton et al., 1990]. Following this procedure, "real" compounds are lumped together into "model" compounds using a reactivity weighting factor which depends on the relative OH radical rate constants of the "real" and "model" compounds. The user should bear in mind that the same reactivity weighting factors are used on emissions for all countries, which represents a significant source of uncertainty in the spatial distribution of VOC emissions.
  - AEROSOLS: The coarse and fine fractions of particles (PPM2 and PPM3 respectively) split into PPM_coa and PPM_fin, BCAR_coa and BCAR_fin and OCAR_coa and OCAR_fin at ratios depending on the SNAP activity sector.

  Note that the speciation of the carbonaceous species has changed since the 2014 model version. When the $carb parameter is set to 1 in chimere.par, the anthropogenic species are separated into PPM, OCAR, and BCAR in CHIMERE. Otherwise, if carb=0, the non-carbonaceous species PPM are mixed with OCAR and BCAR resulting in the species called TPPM. For all the activity sectors H_2SO_4 emissions (1% of the total SO_x) is attributed to the fine mode H_2SO_4_fin.

6.2 Biogenic emissions

6.2.1 Option activation

The biogenic emissions fluxes are calculated if the flag iusebemis is one in the chimere.par file as:

```
[iusebemis]   Need biogenic emissions? (1/0)  : 1
```

The biogenic emissions are estimated using the MEGAN model after [Guenther et al., 2006]. They are calculated on-line in the model and are hourly written in the dedicated output file BEMISSIONS.nc by the src/write_bemis.F90 routine. Its format is described in Appendix G.6, p.234.

6.2.2 The biogenic emitted species

Model species name	Real species
NO	Nitrogen monoxide
C5H8	Isoprene
APINEN	α-pinene
BPINEN	β-pinene
LIMONE	Limonene
TERPEN	Terpene (Lumped class)
OCIMEN	Ocimene (Lumped class)
HUMULE	Humulene (Lumped class)

Table 6.2: *List of the biogenic emitted species with the MEGAN parameterization.*

In the complete version of the model, the model needs as input the species listed in Table 6.2. The MEGAN model (v. 2.04) exploits most recent measurements in a gridded and canopy scale approach, more appropriate for use in CTMs since it estimates the effective burden of gases that mix and react in the boundary layer. Estimates of biogenic VOCs from vegetation and NO emissions are calculated as :

$$ER_i = EF_i \times \gamma_i(T, PPFD, LAI) \times \rho_i \tag{6.1}$$

where ER_i ($\mu g.m^{-2}.h^{-1}$) is the emission rate of species i, EF_i ($\mu g.m^{-2}.h^{-1}$) is an emission factor at canopy standard conditions, γ_i (unitless) is an emission activity factor that accounts for deviations from canopy standard conditions, and ρ_i is a factor that accounts for production/loss within canopy. The canopy standard conditions relevant for this study are defined as: air temperature (T) of 303 K, photosynthetic photon flux density (PPFD) of 1500 $\mu mol.m^{-2}.s^{-1}$ at the top of the canopy, leaf area index (LAI) of 5 $m^2.m^{-2}$ and a canopy with 80% mature, 10% growing and 10% old foliage. The MEGAN model parameterizes the bulk effect of changing environmental conditions using three time-dependent input variables specified at top of the canopy: temperature (T), radiation (PPFD), and foliage density (LAI). The production/loss term within canopy is assumed to be unity ($\rho = 1$). The equation can then be expanded as:

$$ER_i = EF_i \times \gamma_{T,i} \times \gamma_{PPFD} \times \gamma_{LAI} \tag{6.2}$$

The MEGAN model provides input EF and LAI data over a global grid, herefater projected on the CHIMERE model grid. The current available choice for EFs is restricted to following species: isoprene, α-pinene, β-pinene, myrcene, sabinene, limonene, δ^3-carene, ocimene, and nitrogen oxide. EF's are static and refer to years 2000-2001. They are obtained summing up over several plant functional types (e.g. broadleaf and needle trees, shrubs, etc...). LAI database is given as a monthly mean product derived from MODIS observations, referred to base year 2000. Hourly emissions are calculated using 2-m temperature and short-wave radiation from a meteorological model output. The optimal choice for this work is the 150" resolution products proposed in the MEGAN inventory. The daily PPFD and temperature, which are representative values of the simulation, are set to the fixed values of 400. $\mu mol.m^{-2}.s^{-1}$ and 297 K, respectively.
Terpene and humulene emissions are not calculated in this model version and are set to zero.

6.2.3 Biogenic emission interface

The biogenic emissions are calculated following two steps:

1. **Interpolation of the raw global data on the CHIMERE grid:**
   - The original database is constituted of:
     (a) The emission factors data are netcdf files called <spec>all200021.nc.
     Those files must be stored in $bigfilesdir/MEGAN/NETCDF_150sec/EF/EFMT21b.
     (b) LAI data are 12 netcdf files of the format laivyyyymm.nc (one per month).
     The files must be stored in $bigfilesdir/MEGAN/NETCDF_150sec/LAI/LAI20.
   - The program remap_ef.F90 called by prep_megan.sh interpolates original global MEGAN emission factors and LAI data on the CHIMERE grid for the required domain. prep_megan.sh is called by make-chemgeom.sh, so these calculations can be done only once for a given domain.
   - The output file is called EFMAP_LAI_<domain>.nc and is put to the domains directory. It contains emission factors for each MEGAN species, as well as 12 LAIs for each month as 2D variables on the Chimere grid for the given domain.
2. **On-line hourly calculation of biogenic fluxes:**
   Module diagbio_megan in src/diagbio_megan.F90 contains subroutine megan_bioemis called from src/worker_bio.F90 that calculates emission rates for the nine afore-mentioned MEGAN species (re-distributed into the six CHIMERE species) using parameterizations of the original MEGAN code. The module also contains the data used for the calculations.

6.3 Sea salt emissions

6.3.1 Option activation

Sea salt emission parameterizations compute the flux of sea salt particle number in particles m^{-2} s^{-1} μm^{-1} as a function of $\mathbf{r}$ the particle radius and of $\mathbf{U_{10}}$ the wind speed at 10 m in m s^{-1}.
The sea salt emissions fluxes are calculated if the flag seasalt is one or two in the chimere.par file as:

```
[seasalt]   Include sea salts? (0..2)                : 1
[isaltp]   Sea-salt emissions parameterization (0..2) : 0
```

The values of the flag seasalt are:

- seasalt=0: no sea salt
- seasalt=1: inert sea salt
- seasalt=2: chemically active sea salt

6.3.2 Sea salt parameterization

NEW: From version *chimere2017*, sea salt emissions can be calculated with several parameterizations according to the value of the *isaltp* parameter in chimere.par. The parameterizations available are:

- For isaltp=0, the parameterization of [Menut et al., 2013a]
- For isaltp=1, the parameterization of [Monahan, 1986]

Option	Model species name	Real species name
if seasalt=1		
	SALT_coa	Total dry sea salts
if seasalt=2		
	NA_coa	Sodium fraction of sea salts
	HCL_coa	Chloride fraction of sea salts
if seasalt=1 or 2		
	H2SO4_coa	Sulfate fraction of sea salts
	WATER_coa	Water fraction of sea salts

Table 6.3: *List of the sea salt emitted species.*

- For isaltp=2, the parameterization of [Monahan, 1986] completed by the parameterization of [Martensson et al., 2003]

Following [Monahan, 1986]:

$$\frac{dF}{dr} = 1.373 U_{10}^{3.41} r^{-3} (1 + 0.057 r^{1.05}) 10^{1.19 e^{-B^2}} \tag{6.3}$$

$$B = \frac{0.38 - log(r)}{0.65} \tag{6.4}$$

F is the flux of sea salt particle number in particles m^{-2} s^{-1} μm^{-1}, **r** the particle radius in μm and $\mathbf{U_{10}}$ is the wind speed at 10 m in m s^{-1}.

6.4 Mineral dust emissions

The mineral dust emissions are calculated on-line and the fluxes are written as an output. This calculation needs for several surface and soil databases. Since the 2016a version, these databases are global: this allows to calculate mineral dust emissions in every location in the world. The only current limitation is the mandatory use of the USGS database in order to be able to estimate soil and surface properties.
The calculation of mineral dust emissions are done following several steps:

1. section 6.4.1, p.81: Activation of the options in the chimere.par parameter file
2. section 6.4.2, p.82: Preparation of the required surface and soil informations from global databases
3. section 6.4.3, p.84: Calculation of the mineral dust fluxes in CHIMERE.

6.4.1 Option activation

To activate the calculation of dust emissions, some options have to be selected in the chimere.par file:

```
[iusedust]   Mineral dust emissions? (0/1/2)       : 1
[icuth]      u* threshold scheme                   : 1
[ifluxv]     vertical flux scheme                  : 3
[ifecan]     Use of soil moisture [1] or not [0]   : 1
```

Their values are explained in the section 2.3, p.22.
Dust emissions are managed and calculated in mainly three programs in CHIMERE:

1. src/chimere_params.F90: constant parameters needed for the dust production schemes
2. src/ini_demis.F90: initialization of tables, read input data
3. src/worker_dust.F90: calculation of dust fluxes

6.4.2 The datasets and input parameters

Before a simulation, some datasets are needed on the CHIMERE simulation grid. These datasets are explained in Table 6.4. Note that explanations about the use of these datasets are also in [Menut et al., 2013b].

Parameters	Units	Time variability
USGS soil texture	% clay, % silt, % sand	constant
USGS landuse types	%	constant
Aeolian roughness length z_0	cm	constant
Vegetation fraction	%	variable (monthly)
10m wind speed	m/s	variable (hourly, on-line)

Table 6.4: *Mandatory informations for the mineral dust emissions fluxes calculations*

6.4.2.1 The USGS soil texture

The soil is represented by relative percentages of sand, silt and clay for each model cell. The USGS database, called STATSGO-FAO, is used and 19 different soil types are recorded in the global database. This is a global dataset used in meteorological modeling and which may be used for global and regional dust transport modelling and the data are available at *http://soils.usda.gov/survey/geography/*.
It provides soil texture characteristics over longitude/latitude regular grids. The native resolution of the dataset is $0.0083\ ^o \times 0.0083\ ^o$. In order to have homogeneous datasets, the STATSGO-FAO data are regridded into the CHIMERE simulation grid, retaining the dominant feature as presented in Figure 6.3.

The soil types in the two datasets are listed in Table 6.5 together with their relative percentage of clay, silt, salt and sand (coarse and fine-medium). Note that STATSGO-FAO does not contain salts and that fine-medium sand and coarse sand are distinguished according to criteria detailed in [Tegen et al., 2002]. With this approach clay loams are considered as highly unlikely to contain coarse sand and sandy clay loam can contain both coarse and medium fine sand. The textural triangle is based on measurements performed by wet sedimentation techniques which break the soil aggregates leading to high amounts of loose clay particles that generally form aggregates of larger size and that may not be encountered in natural soils. Following [Tegen et al., 2002] clay is in the form of aggregate in loamy sands and it is reassigned to the silt fraction.

6.4.2.2 The USGS landuse types

Landuse data describe the surface occupation (wood, mountains, lakes, etc.) and is typically used to prescribe some properties in meteorological models, such as the roughness length, z_0. For each land use type, a z_0, is typically prescribed. Dynamical roughness lengths based on land use types are not appropriate for use in dust emission parameterizations.
For mineral dust emission calculations, the landuse is typically used to provide a desert mask specifying what surface is potentially erodible. Global or regional models typically consider arid and semiarid categories from a landuse database to identify potential dust source areas. Here, to complement the STATSGO-FAO soil dataset, we use the USGS landuse dataset with a high horizontal resolution ($0.0083\ ^o \times 0.0083\ ^o$). As in the case of the

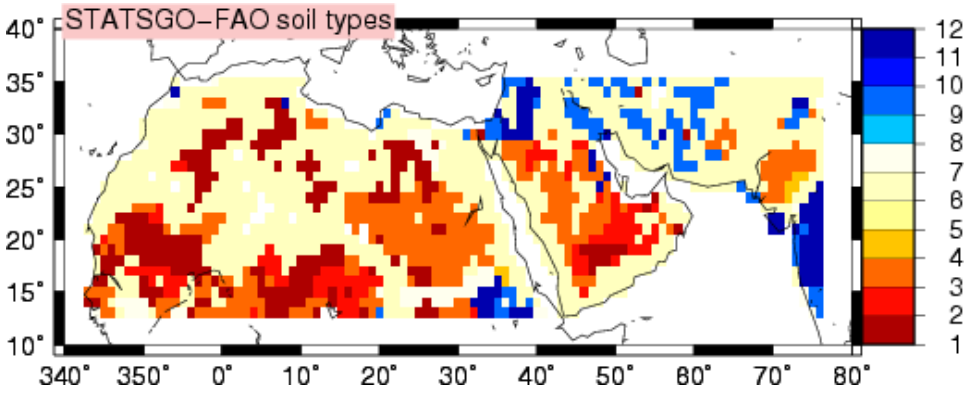


Figure 6.3: *The STATSGO-FAO soil types data regridded to $1^o \times 1^o$ resolution. The values correspond to the surface types explained in the Table 6.5. For each cell, only the most important relative surface is displayed.*

STATSGO-FAO dataset, we calculated the relative surface of the landuse types. The erodible land use types considered were scrublands (8) and barren soil (19). This may appear as a limiting choice but this corresponds to the most important landuse classes able to produce dust in Northern Africa. This constitutes the desert mask as presented in Figure 6.4.

6.4.2.3 The aeolian roughness length z_{0s}

The aeolian roughness length used in CHIMERE is the GARLAP (Global Aeolian Roughness Lengths from ASCAT and PARASOL) dataset. [Prigent et al., 2012] uses a bi-linear regression between in situ measurements on one hand and visible/near-infrared observations (PARASOL: Polarization and Anisotropy of Reflectances for Atmospheric Sciences coupled with Observations from a Lidar) and satellite microwave backscattering (ASCAT: Advanced SCATterometer) data on the other hand in order to create a new dataset of aeolian roughness length with a 6 km spatial resolution: GARLAP (Global Aeolian Roughness Lengths from ASCAT and PARASOL).

6.4.2.4 User input parameters

Several input parameters are available before a simulation. These parameters are listed in Table 6.6. They are considered as constant during the whole simulation. It is possible (but not recommended) to change these values in the src/chimere_params.F90. It is then necessary to recompile the model.

Table 6.6: List of tunable parameters for the mineral dust emissions fluxes

Name	Type	Value
nmode	number of emissions modes for mineral dust	3
nmineral	number of emitted soil particles	5
nsoildmax	number of bins for the soil size distribution	20000
soil_dmin	soil size distribution min (cm)	10^{-4}
soil_dmax	soil size distribution max (cm)	2.10^{-1}
rop	particle density (g cm-3) i.e quartz	2.65
umin	Min wind speed for the 'Owen' effect (cm.s-1)	21.0
woff	Wind offset to smooth Richardson numbers (m/s)	0.5
Mineralogy of soil types		

Continued on next page

Table 6.6 – continued from previous page

Name	Type	Value
mineral_dp	Mean Mass Median diameter of	
	coarse sand (cm)	0.0690
	fine medium sand (cm)	0.021
	silt (cm)	0.0125
	clay (cm)	0.0002
	salt (cm)	0.052
mineral_sig	σ of	
	coarse sand	1.6
	fine medium sand	1.8
	silt	1.6
	clay	2.
	salt	1.5
Weibull distribution		
nwb	Number of values for the distribution	12
kref	Width of the distribution	3
Erodibility		
perod_veg	vegetalized areas	1.0
perod_urb	urbanized areas	1.0
ifit	reduce z0 in Europe or not	0
Snow and water in soil coverage		
snow_th	Snow cover if more that [snow_th] cm	0.1
minsurf_th	No flux if more than (minsurf_th x 100) % of water	0.
% of flux in the three modes (only for [Marticorena and Bergametti, 1995] scheme)		
cad1	% in the fine mode	0.2
cad2	% in the coarse mode	0.6
cad3	% in the big mode	0.2
Parameters for the [Alfaro and Gomes, 2001] scheme		
e1	Binding energies (g.cm2/s2)	3.61
e2	Binding energies (g.cm2/s2)	3.52
e3	Binding energies (g.cm2/s2)	3.46
div1	Factor for binding energies (g.cm2/s2)	2.0
div2	Factor for binding energies (g.cm2/s2)	2.0
div3	Factor for binding energies (g.cm2/s2)	2.0
Parameters for the [Kok et al., 2014] scheme		
kok_ds	Constant (μm)	3.4
kok_sigmas	Constant (ad)	3.0
kok_cv	Constant (μm)	12.62
kok_lambda	Constant (μm)	12.0

6.4.3 Mineral dust fluxes parameterizations

The mineral dust fluxes calculation may be splitted into two parts: (i) numerous parameterizations dedicated to the wind speed, precipitation and soil knowledge, (ii) the mineral dust flux itself. In this section, the firts part of schemes is described.

1. The possibility to better taken into account the mean wind speed by using a Weibull distribution
2. The possibility to take into account the effect of rain on erodible surfaces
3. The calculation of the threshold friction velocities and the drag efficiency
4. The possibility to take into account the soil moisture effect (independently of precipitation)

Category	% CS	% FMS	% silt	% clay	% salt	α	Soiltype
1	46	46	5	3	0	2.e-6	sand
2	41	41	18	0	0	2.e-6	loamy sand
3	29	29	32	10	0	2.e-6	sandy loam
4	0	17	70	13	0	2.e-6	silt loam
5	0	10	85	5	0	2.e-6	silt
6	0	43	39	18	0	2.e-6	loam
7	29	29	15	27	0	2.e-6	sandy clay loam
8	0	10	56	34	0	2.e-6	silty clay loam
9	0	32	34	34	0	2.e-6	clay loam
10	0	52	6	42	0	2.e-6	sandy clay
11	0	6	47	47	0	2.e-6	silty clay
12	0	22	20	58	0	2.e-6	clay
13	0	0	0	0	0	2.e-6	organic material
14	0	0	0	0	0	2.e-6	water
15	0	0	0	0	0	2.e-6	bedrock
16	0	0	0	0	0	2.e-6	other (land-ice)
17	0	0	0	0	0	2.e-6	playa
18	0	0	0	0	0	2.e-6	lava
19	0	0	0	0	0	2.e-6	white sand
99	0	0	0	0	0	2.e-6	ocean

Table 6.5: *Description of the USGS soil types. CS = Coarse sand; FMS = Fine medium sand. Note that only the first 12 soiltype are really used in the mineral dust fluxes calculation. The α value is not used in this model version (but here just for consistency with older model version).*

6.4.3.1 Weibull distribution for 10m wind speed

The interest of the specific Weibull distribution to represent wind speed variability was extensively discussed by numerous authors such as [Pavia and O'Brien, 1986], [Pryor et al., 2005] and [Cakmur et al., 2004]. In order to build a distribution for a chosen wind speed value, representing the mean value for a specific area and period, the probability density function is expressed as:

$$p(|U|) = \frac{k}{A}\left(\frac{|U|}{A}\right)^{k-1} exp\left[-\left(\frac{|U|}{A}\right)^{k}\right] \tag{6.5}$$

where k is a dimensionless shape parameter and A is a scale parameter related to the mean of the distribution (in our case the modelled wind speed for each cell and each modelled hour).

6.4.3.2 The sporadic effect of rain

In this model version, we include the possibility to immediately inhibit dust erosion in case of sudden rainfall in western Europe: the modelled soil moisture will actually increase, thereby inhibiting dust erosion but, sometimes, this increase occurs only many hours after the start of precipitations. For dust erosion, two additional processes have to be taken into account:

- The dust erosion must be set to zero during a precipitation (convective or stratiform) event,
- The dust erosion must restart very slowly after a precipitation event, the soil being potentially crusted.

A simple function describing a factor f_p is applied to moderate the dust emissions fluxes when a precipitation is diagnosed as:

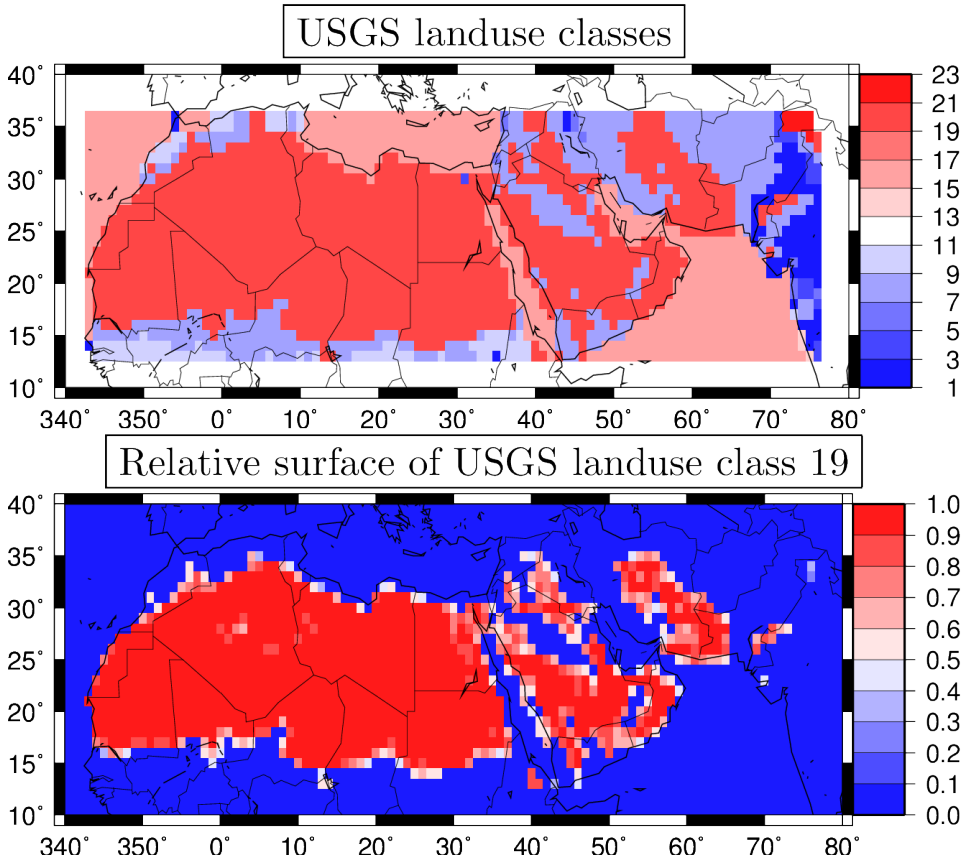


Figure 6.4: *[top] the USGS landuse classes (from 1 to 23) over the domain: (1) urban and built-up land, (2) dryland cropland and pasture, (3) irrigated cropland and pasture, (4) mixed dryland/irrigated cropland and pasture, (5) cropland/grassland mosaic, (6) cropland/woodland mosaic, (7) grassland, (8) shrubland, (9) mixed shrubland/grassland, (10) savanna, (11) deciduous broadleaf forest, (12) deciduous needleleaf forest, (13) evergreen broadleaf forest, (14) evergreen needleleaf forest, (15) mixed forest, (16) water bodies, (17) herbaceous wetland, (18) wooded wetland, (19) barren or sparsely vegetated, (20) herbaceous tundra, (21) wooded tundra, (22) mixed tundra, (23) bare ground tundra. [bottom] The relative percentage of USGS class 19 surface (for barren soils). This class is used as a desert mask for the dust fluxes calculation when using the USGS data.*

$$f_p = E_{dust} \times \left(1 - exp\left(\frac{-\alpha \times \Delta t_p}{\tau}\right)\right) \tag{6.6}$$

with α a constant factor set to α=6, Δt_p the time since the last precipitation event and τ the period after which the surface mineral dust fluxes E_{dust} is fully taken into account, considering that the inhibiting effect of precipitation is finished. For this study, t is in hours and τ=24. This function is displayed in Figure 6.5.

6.4.3.3 The threshold friction velocities and the drag efficiency

The saltation flux F_h is non-zero only if $u_* > u_*^T(D_p)$ for a given soil particle diameter D_p. u_*^T is the threshold friction velocity depending on D_p, the soil particle diameter, z_0, the 'aeolian' roughness length and z_{0s}, the 'smooth' roughness length.
The 'smooth' threshold friction velocity u_*^{Ts} is estimated following [Shao and Lu, 2000]:

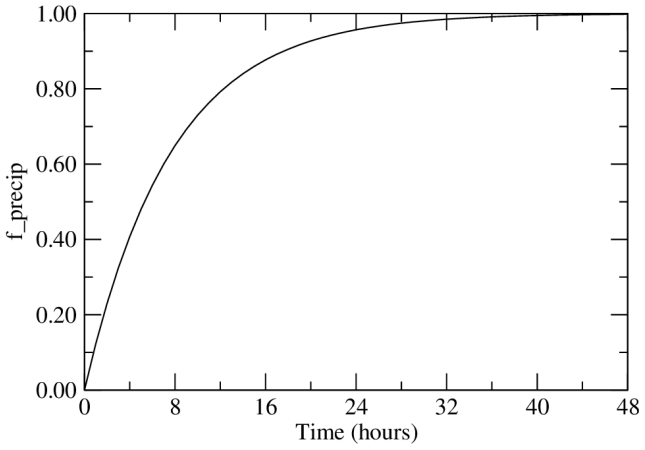


Figure 6.5: *Function defined to moderate the mineral dust emissions fluxes after a precipitation event.*

$$u_*^{Ts}(D_p) = \sqrt{a_n \left(\frac{\rho_p g D_p}{\rho_{air}} + \frac{\gamma}{\rho_{air} D_p} \right)} \tag{6.7}$$

with the constant parameters $a_n = 0.0123$ and γ=300 kg m^{-2}. The particle density, ρ_p=2.65 10^3 kg m^{-3} is chosen to be representative of quartz grains.
The threshold friction velocity, u_*^T, is expressed as:

$$u_*^T(D_p) = \frac{u_*^{Ts}(D_p) \times q}{f_{\text{eff}}(z_0, z_{0s})} \tag{6.8}$$

with q a soil moisture correction. f_{eff} represents the drag efficiency, i.e a function depending on z_0, the 'aeolian' roughness length and z_{0s}, the 'smooth' roughness length which is expressed as:

$$f_{\text{eff}} = \left[1 - \left(\frac{ln(z_0/z_{0s})}{ln(0.35[(0.1/z_{0s})^{0.8}])} \right) \right] \tag{6.9}$$

This function takes into account the non erodible elements dissipating a part of the wind momentum that will not be available for saltation.

6.4.3.4 The soil moisture effect

The soil moisture effect is mainly taken into account following the [Fecan et al., 1999] parameterization. This scheme considers that soil moisture will increase the treshold friction velocity, u_*^T, used to determine if erosion occurs or not. To distinguish between soil conditions, the dry and wet treshold friction velocities are defined, and noted u_*^{Td} and u_*^{Tw}, respectively. u_*^{Tw} is estimated as a possible increase of u_*^{Td} as:

$$u_*^{Tw} = f(w) \times u_*^{Td} \tag{6.10}$$

In the model, the dry treshold friction velocity, u_*^{Td} is calculated following the scheme of [Shao and Lu, 2000]. The $f(w)$ factor is estimated as:

$$\begin{cases} f(w) = 1 & \text{for } w < w' \\ f(w) = \left[1 + A\,(w - w')^{b'} \right]^{0.5} & \text{for } w > w' \end{cases} \tag{6.11}$$

where A and b' are constant to estimate. w (in kg.kg^{-1}) is the gravimetric soil moisture and w' corresponds to the minimum soil moisture from which the threshold velocity increases. The values of A, b' and w' are dependent on the soil texture. Using measurements data, [Fecan et al., 1999] showed that the value of w' is mainly dependent on the clay content of the soil and proposed the following fit:

$$w' = 0.0014(\%clay)^2 + 0.17(\%clay) \tag{6.12}$$

The constants are fixed as A=1.21 and b'=0.68. Note that in Equation 6.11, the gravimetric soil moisture w has to be expressed in %, w' being in % in Equation 6.12.

6.4.4 The several mineral dust production schemes

Three different Dust Production Models are implemented:

1. The [Marticorena and Bergametti, 1995] scheme: it uses the [White, 1986]'s equation and distribution of emitted mass fluxes into the three emissions modes is constant
2. The [Alfaro and Gomes, 2001] scheme: it uses the [Marticorena and Bergametti, 1995] scheme for saltation and the vertical flux is estimated using cohesion kinetic energies scheme. A numerically optimized version presented in [Menut et al., 2005] is proposed.
3. The [Kok et al., 2014] scheme: the vertical dust flux is directly diagnosed for one emissions mode.

6.4.4.1 The [Marticorena and Bergametti, 1995] scheme

The vertically integrated saltation flux is estimated using the [White, 1986]'s equation:

$$F_h(D_p) = \frac{K\rho_{air}}{g\ u_*^3}\left(1 - \frac{u_*^T}{u_*}\right)\left(1 + \frac{u_*^T}{u_*}\right)^2 \tag{6.13}$$

where u_* is the "saltation" friction velocity, i.e the friction velocity calculated using the roughness length, z_0, following [Marticorena and Bergametti, 1995]. u_*^T is the threshold friction velocity depending on the soil particle diameter size D_p and z_0. Following [Marticorena and Bergametti, 1995], we consider the air density as constant with ρ_{air}=1.227 kg.m^{-3}, and used the constant value $K = 1$.
The scheme is designed to estimate one saltation flux. The corresponding vertical flux is estimated by using constant α values displayed in Table 6.5 for each soil type. The vertical flux is then projected into three modes using constant percentages between fine, coarse and big modes.

6.4.4.2 The [Alfaro and Gomes, 2001] scheme

In order to estimate size resolved vertical dust fluxes, i.e sandblasting fluxes, the [Alfaro and Gomes, 2001] DPM is used with the numerical optimization described in [Menut et al., 2005]. The sandblasting flux is computed based on the partitioning of the kinetic energy of individual saltating aggregates and the cohesion energy of the populations of dust particles. This model assumes that dust emitted by sandblasting is characterized by three modes whose proportion depends on the wind friction velocity. From wind tunnel measurements performed on two natural soils from semi arid regions, [Alfaro et al., 1998] consider these three modes as independent of the soil types. They described the three modes using log-normal distributions with diameters d_1=1.5 10^{-6}m, d_2=6.7 10^{-6}m and d_3=14.2 10^{-6}m and their associated standard deviation, respectively σ_1=1.7, σ_2=1.6 and σ_3=1.5. Based on this model, as soil aggregate size or wind speed increases, kinetic energy becomes able to release first particles of the coarsest mode that are associated with the lowest cohesion energy, then particles from the intermediate population, and finally the finest particles. It also implies that for a specific wind speed

and soil size distribution, the dust flux may be zero even if the saltation process occurs. In order to apportion the available kinetic energy between the three modes, a constant cohesion energy e_i is associated to each mode values. The numerical values of e_i were determined by adjusting the predicted aerosols size distribution to those measured in wind tunnel under different wind conditions, using an iterative least square routine. In this study, the values recommended by [Alfaro and Gomes, 2001] are used: e_1=0.376, e_2=0.366 and e_3=0.346 kg m^2 s^{-2}.
The kinetic energy is expressed as a function of the soil particle diameter after [Alfaro et al., 1997] and [Shao and Lu, 2000]:

$$e_c = \rho_p \frac{100\pi}{3} D_p^3 \left(u_*\right)^2 \tag{6.14}$$

It is compared to the cohesion energy of the three aerosol modes in order to compute the proportion $p_i(D_p)$ of these three modes in the total dust size-distribution. By integrating equation 6.14 over the three aerosols modes, the total sandblasting flux may be written:

$$F_{v,m,i}(D_p) = \int_{D_p^{min}}^{D_p^{max}} \frac{\pi}{6} \rho_p \, \beta \, \frac{p_i(D_{p,i}) d_{m,i}^3}{e_i} dF_h(D_{p,i}) \tag{6.15}$$

where i=1,N_{class} is the number of intervals discretizing the soil size distribution in the range $[D_p^{min} : D_p^{max}]$ and $d_{m,i}$ the mean mass diameter, [Menut et al., 2005].

6.4.4.3 The [Kok 2014] scheme

In this model version, the Kok mineral dust emissions parameterization is proposed, in addition to the [Marticorena and Bergametti, 1995] and [Alfaro and Gomes, 2001] schemes. To activate this scheme, simply select the flag ifluxv=3 in the chimere.par file.
The Kok scheme is fully described in [Kok et al., 2014]. The vertical dust flux is calculated as:

$$F_d = C_d \times f_{bare} \times f_{clay} \times \frac{\rho_a \left(u_*^2 - u_{*t}^2\right)}{u_{*st}} \times \left(\frac{u_*}{u_{*t}}\right)^{C_\alpha \frac{u_{*st} - u_{*st0}}{u_{*st0}}} \tag{6.16}$$

The flux is calculated only if $u_* > u_{*t}$. The threshold friction velocity, u_{*t}, is calculated using the [Iversen and White, 1982] or the [Shao and Lu, 2000] scheme. The corresponding u_{*st} is this friction velocity but for a standard atmospheric density ρ_{a0}=1.225 kg m^{-3}:

$$u_{*st} = u_{*t} \times \sqrt{\frac{\rho_a}{\rho_{a0}}} \tag{6.17}$$

u_{*st0} represents u_{*st} for an optimally erodible soil and was chosen as u_{*st0}=0.16 m s^{-1} in [Kok et al., 2014].
The dimensionless coefficient C_α is chosen as C_α=2.7.
The dust emission coefficient C_d represents the soil erodibily as:

$$C_d = C_{d0} \times exp\left(-C_e \frac{u_{*st} - u_{*st0}}{u_{*st0}}\right) \tag{6.18}$$

with the constant dimensionless coefficients C_e=2.0 and C_{d0}=4.4 10^{-5}.
The vertical dust flux is integrated over the whole size distribution. This flux is thus redistributed into the model dust size distribution as:

$$\frac{dV_d}{dlnD_d} = \frac{D_d}{c_v} \left[1 + erf\left(\frac{ln(D_d/D_s)}{\sqrt{2}\, ln\sigma_s}\right)\right] exp\left[-\left(\frac{D_d}{\lambda}\right)^3\right] \tag{6.19}$$

with V_d the normalized volume of mineral dust aerosols for each mean mass median diamter D_d, C_v=12.62 μm, σ_s=3.0, D_s=3.4 μm and λ=12.0 μm.

6.4.5 Vegetation variability

The density of the vegetation cover has an impact on the dust emissions flux [Wolfe and Nickling, 1993] and the seasonal variation of vegetation affects the aeolian roughness length [Prigent et al., 2005]. As the z_0 dataset is representative of northern winter months only [Prigent et al., 2012], it does not take into account vegetation variations. Therefore, we weight the z_0 by the green fraction coefficient of the current month, provided by NCAR, divided by the green fraction coefficient of January. This is a simple correction that induce a monthly variability in mineral dust emissions.

6.5 Fire emissions

To account for fire emissions in the CHIMERE simulations, the following lines need to informed in chimere.par:

- $fire_emissions should be set to 1;
- $fire_emissdir is the name of the directory where fire emissions are stored;
- $fnemisf is the name of the output emission file.

Species list is the same as the anthropogenic one in the current version.
Fire emissions have to be provided in the following file format:

- One netcdf file per species and per month;
- Hourly emissions gridded on the simulation domain;
- Emissions are only provided for grid cells with non zero values, as a list of sources
- List of variables:
  - lon: Longitude grid (2D)
  - lat: latitude grid (2D)
  - ilatsources: latitude index of non-zero sources (1D=sources)
  - ilonsources: longitude index of non-zero sources (1D=sources)
  - SPEC: hourly emissions for species SPEC (3D=hours,days,sources) in molecule/cm2/s

Example netcdf file header for CO is given in **Appendix G.9**.

6.6 The resuspension process

The resuspension process is considered as an emission process in the model.

1. chimere.par: to activate or not the resuspension
2. src/resuspension.F90: the Fortran code, to estimate the resuspension fluxes, in the model core and on-line.

6.6.1 Option activation

```
   [resusp]      Resuspension [1] or not [0]   : 0
```

6.6.2 Resuspension fluxes estimation

The resuspension process is important for particulate matter and may induce a large increase of the emission flux in case of dry soils, for locations where traffic and industries produce available particles. This resuspension process is considered as different and complementary of the aeolian erosion process (leading to mineral dust emissions). In this model version, the resuspension flux is active only for cells containing an urbanized surface. The formulation is derived from the bulk formulation originally proposed by [Loosmore, 2003]. The resuspension rate λ, in s^{-1}, is expressed as:

$$\lambda = 0.01 \frac{u_*^{1.43}}{\tau^{1.03}} \tag{6.20}$$

where τ is the time after the start of resuspension. This time is taken into account considering the particles are first deposited then resuspended. The detail of the processes leading to resuspension are essentially unknown, and we assume here that the available concentration of particulate matter does only depend on the wetness of the surface. In this empirical view, the resuspension flux is assumed to be:

$$F = P \times f(w) \times u_*^{1.43} \tag{6.21}$$

where $f(w)$ is a function of the soil water content and P is a constant tuned in order to approximately close the PM10 mass over Europe. The value of P was estimated in [Vautard et al., 2005a] and was found to give a correct amount of additionnal PM_{10}. In this model version, P is approximated as P=170 μgm^{-2}h^{-1} if we consider European mean conditions with a soil water content of 25% and a friction velocity of u_*=0.5 m.s^{-1}. The soil water function $f(w)$ is estimated as:

$$f(w) = \frac{soim_s - g_{soim}}{soim_s - soim_t} \tag{6.22}$$

where $soim_t$ is a soil moisture treshold chosen as $soim_t$=0.1. $soim_s$ is the maximum of soil moisture ponderated by the ratio of water and soil densities, as:

$$soim_s = soim_{max} \times \frac{D_{water}}{D_{soil}} \tag{6.23}$$

with $soim_{max}$ a constant, representing the maximum sol moisture value and, here, chosen as $soim_{max}$=0.3. D_{water} is the water density (assumed to be unity) and D_{soil} is the dry porous soil density. D_{soil} is itself estimated as:

$$D_{soil} = (1 - satsm) \times D_{mine} \tag{6.24}$$

with $satsm$=0.4 the saturation volumetric moisture content and D_{mine}=2.5, the non porous soil density. Those global resuspended flux has to be projected into the aerosol size distribution.
In the absence of any information, this resuspension flux is calculated only for model cells having a non-zero urban landuse. This flux is thus ponderated in the whole cell by considering the relative surface of the urban area. Another hypothis is that the flux is affected into the PPM emissions, considering that this contribution is mainly primary particulate matter emissions (such as industries). Finally, the flux is projected into the model size distribution considering that 2/3 of the flux is in the fine mode, 1/3 in the coarse mode and zero in the big mode. This assumption may be changed bu the user directly in the src/resuspension.F90 program as:

```
    rflux(1) = 2d0/3d0*rcumul
    rflux(2) = 1d0/3d0*rcumul
    rflux(3) = dzero
```

7 Depositions

7.1 Dry deposition

7.1.1 The deposition velocity for gas and aerosols

The dry deposition process is commonly described through a resistance analogy proposed by [Wesely, 1989]. These resistances are not expressed in the same way, considering gas or particles as displayed in Figure 7.1 .

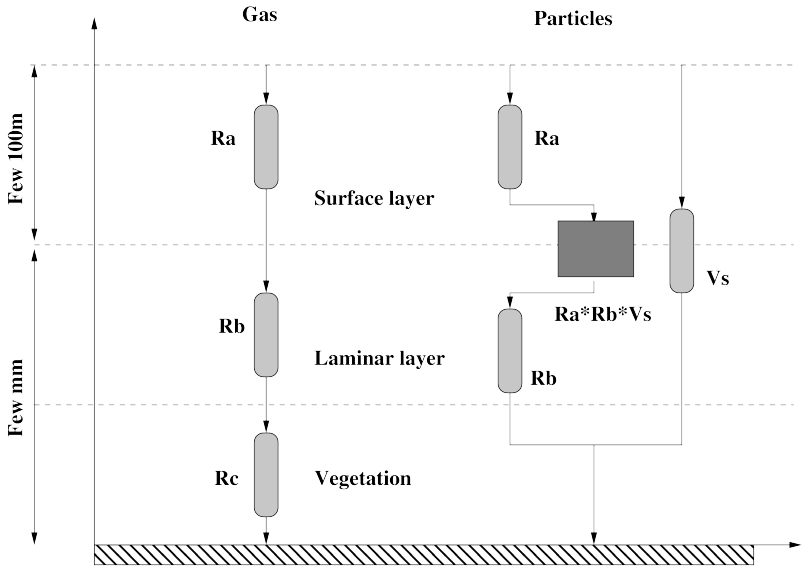


Figure 7.1: *Main principle of dry deposition for gas and particles. For each model species, three resistances are estimated: deposition occurs if the sum of all these resistances is low. For particles, the settling velocity is added.*

The deposition process is a sink and only acts on a concentration c along the vertical, as:

$$\Delta c = \frac{\partial}{\partial z}(v_d.c) \tag{7.1}$$

with v_d the dry deposition velocity. For each gaseous species or particles, the deposition is due to three different processes. First, the turbulent diffusivity is needed to estimate the aerodynamical resistance, r_a. Second, the diffusivity near the ground, in the "laminar" layer, is needed to estimate the surface resistance r_b. Third, for gaseous species only, the species water solubility is needed to estimate the canopy resistance r_c. For particles, there is no solubility, the particle is subject to gravity, falling with a settling velocity v_s.
The dry deposition velocity (in m s^{-1}) for gaseous species is expressed as:

$$v_d = \frac{1}{r_a + r_b + r_c} \tag{7.2}$$

For aerosols, two formulations are implemented in the model:

Following [Wesely, 1989]:

$$v_d = v_s + \frac{1}{r_a + r_b + r_a r_b v_s} \tag{7.3}$$

Following [Zhang et al., 2001]:

$$v_d = v_s + \frac{1}{r_a + r_s} \tag{7.4}$$

with r_s the surface resistance, depending on the vegetation type.
In CHIMERE, all dry deposition calculations are done in:

- Input parameters are initialized in routine inidepo.F90.
- At the coarse time step frequency, deposition velocities are calculated in routine depvel.F90 for gases and depaero.F90 for aerosols.
- Deposition fluxes are calculated at the fine time step frequency in routine deposition.F90.

7.1.2 The aerodynamical resistance, r_a

The aerodynamical resistance r_a depends on several turbulent parameters, such as the Monin-Obukhov length L, the friction velocity u_*, and the dynamical roughness length z_{0m}. This resistance is calculated in the calc_turb.F90 routine based on the Monin-Obukhov similarity theory with the Businger's formulation of the stability-dependent temperature profile function $\phi_T(\zeta)$. The reference height z_r is taken in the middle of the first vertical model layer of thickness H_1: $z_r = H_1/2$. Depending on the atmospheric surface layer stability,

$$\begin{cases} r_a &= \frac{1}{k u_*}\left[\ln\left(\frac{z}{z_{0m}}\right) + 4.7(\zeta_r - \zeta_0)\right] & (\text{stable}, \mathrm{L} \geq 0) \\ &= \frac{1}{k u_*}\left[\ln\left(\frac{z}{z_{0m}}\right) + \ln\left(\frac{(\eta_0^2+1)(\eta_0+1)^2}{(\eta_r^2+1)(\eta_r+1)^2}\right) + 2\left(\tan^{-1}\eta_r - \tan^{-1}\eta_0\right)\right] & (\text{unstable}, \mathrm{L} < 0) \end{cases} \tag{7.5}$$

where $\eta_0 = (1 - 15\zeta_0)^{1/4}$, $\eta_r = (1 - 15\zeta_r)^{1/4}$ and $\zeta_0 = z_0/L$, $\zeta_r = z_r/L$, k=0.41 the von Karman constant. z_0 depends on the fraction of land-use for each category and on the season.

7.1.3 The quasi-laminar layer resistance r_b for gases

The quasi-laminary boundary layer resistance r_b for gases is calculated in depvel.F90. It is estimated following [Hicks et al., 1987], as:

$$r_b = \frac{2}{k u_*}\left(\frac{S_c}{P_r}\right)^{2/3} \tag{7.6}$$

where k the Karman number (here k=0.41), S_c and P_r are the Schmidt and turbulent Prandtl numbers, respectively. The Prandl number is constant and set to Pr=0.72. The Schmidt number is defined as:

$$S_c = \frac{\nu}{D_i} \tag{7.7}$$

where ν is the kinematic viscosity of air. Its value is fixed as ν=0.15 cm^{2}s^{-1} for a reference atmosphere of T=20^{o}C and P=1 atm. D_i is the molecular diffusivity of the species i. This molecular diffusivity is estimated as the diffusion coefficient ratio of water to the pollutant i, following [Erisman et al., 1994].

$$D_i = \frac{D_{H2O}}{D_{gx}} \tag{7.8}$$

with D_{H2O}=0.25, the molecular diffusivity of water. For gaseous species, the molecular diffusivity is expressed as:

$$D_{gx} = \sqrt{\frac{dMx}{18}} \tag{7.9}$$

with dMx the molar mass of the model species. Being 'model species' dependent, one file per chemical mechanism is defined for these parameters. They are listed in the chemprep/data/DEPO_SPEC.meca ascii file. As an example, and for the MELCHIOR1 mechanism, the Table 7.1 presents these parameters values. This file is read in the routine inidepo.F90.

Species	dMx	dHx	$df0$	$dRwat$	Species	dMx	dHx	$df0$	$dRwat$
'charspec'	'rMx'	'rHx'	'rf0'	'rRwat'	'charspec'	'rMx'	'rHx'	'rf0'	'rRwat'
O3	48	0.01	1	2000	BUO2H*	64	1e5	0	1e-20
SO2	64	1e5	0	1.e-20	CH4COX*	64	1e5	0	1e-20
NO2	46	0.01	0.1	2000	CH3O2C*	64	1e5	0	1e-20
NO	30	2e-3	0	2000	CH4CHX*	64	1e5	0	1e-20
NH3	17	1e+5	0	1e-20	OXYLH1*	64	1e5	0	1e-20
HCL	36.5	2.05e+6	0	1e-20	MEMALH*	64	1e5	0	1e-20
HCHO	30	6e3	0	1e-20	MEMAH2*	64	1e5	0	1e-20
CH3CHO	44	14	0	1e-20	PEROX*	64	1e5	0	1e-20
CH3COE	72	13	0	1e-20	MACO2H*	64	1e5	0	1e-20
CH3COY	86	74	0	1e-20	CH4COZ*	64	1e5	0	1e-20
GLYOX	58	3.6e5	0	1e-20	APIO2H*	64	1e5	0	1e-20
MGLYOX	72	3.2e4	0	1e-20	obioH*	64	1e5	0	1e-20
MEMALD	98	70	0	1e-20	oROOH*	64	1e5	0	1e-20
MVK	70	70	0	1e-20	PANH*	64	1e5	0	1e-20
MAC	70	70	0	1e-20	AnA2D	186.	2.6e16	0	1e-20
PAN	109	3.6	0.1	1e-20	AnA1D	168.	1.5e10	0	1e-20
MACPAN	161	1.7	0.1	1e-20	AnA0D	142.	3.5e5	0	1e-20
MEMPAN	161	1.7	0.1	1e-20	AnBIP	167.	0.01	0	1e-20
toPAN	161	1.7	0.1	1e-20	AnBmP	152.	0.01	0	1e-20
HONO	47	1e5	0.1	1e-20	BiA2D	186.	1.6e11	0	1e-20
HNO3	63	1e14	0	1e-20	BiA1D	170.	2.9e10	0	1e-20
H2O2	34	1e5	1	1e-20	BiA0D	168.	1.9e6	0	1e-20
CH3O2H*	64	1e5	0	1e-20	BiBmP	236.	0.01	0	1e-20
PPA*	64	1e5	0	1e-20	ISOPA1	177.	1e5	0	1e-20
ETO2H*	64	1e5	0	1e-20	ISOPA2	177.	1e5	0	1e-20

Table 7.1: *The (chemprep/data/DEPO_SPEC.meca) data file. The main characteristics of the dry deposited species with their names, dMx the molar mass of the model species, dHx the effective Henry's law constant (M atm^{-1}) for the gas, df0 the normalised (0 to 1) reactivity factor for the dissolved gas. Note that all peroxides (with *) are treated as SO_2. $dRwat$ is a resistance to the solution of gases in water', en s m^{-1} and is not used in the current model version.*

7.1.4 The surface resistance for gases, r_c

This resistance acts only for gaseous species. Its formulation follows [Erisman et al., 1994] and the developments made in the EMEP model ([Emberson et al., 2000], [Simpson et al., 2003], [Simpson et al., 2012]). It uses a number of different other resistances accounting mainly for stomatal and surface processes which are again dependent on the land use type and season. Necessary chemical parameters for the calculation of r_c are also taken from [Erisman et al., 1994] except for carbonyls ([Sander et al., 1999]; [Baer and Nester, 1992]) and peroxide species ([Hall et al., 1999]). dHx and $df0$, presented in Table 7.1, are used for the mesophyllic resistance value as described in [Seinfeld and Pandis, 1998]).

The general formulation for this surface resistance is proposed by [Erisman et al., 1994]:

$$r_c = \left[\frac{1}{r_{sto} + r_m} + \frac{1}{r_{inc} + r_{soil}} + \frac{1}{r_{ext}} \right]^{-1} \tag{7.10}$$

where:

- r_{sto} the canopy stomatal resistance
- r_m the mesophyll resistance
- r_{soil} the soil resistance
- r_{inc} the in-canopy aerodynamic resistance
- r_{ext} the canopy cuticle or external leaf resistance

Some specific cases are defined:

- Over water surfaces: r_c=r_{wat}
- Over bare soils: r_c=r_{soil}
- Over snow cover: r_c=r_{snow}

In CHIMERE this resistance is formulated following [Simpson et al., 2003] using a distinction between the 'bulk canopy resistance' R (and the associated conductance $G_c = 1/R$) and the 'unit-leaf-area' resistance r (and the associated conductance $g = 1/r_{sto}$). Using these notations, the bulk canopy conductance is expressed as:

$$G_c = LAI \times g_{sto} + G_{ns} \tag{7.11}$$

where LAI is the Leaf Area Index (in $m^2.m^{-2}$), g_{sto} the stomatal conductance, G_{ns} the bulk non-stomatal conductance.
Two special cases are defined:

- For sub-zero surface temperature, the surface resistance reduces to:

$$r_c = r_{low} = 1000 \exp(-(T_s + 4)) \tag{7.12}$$

  Note that CHIMERE uses the 2m temperature as a 'surface temperature'. The temperature in Equation 7.12 is in ^{o}C.
- Under classical meteorological conditions, the surface resistance for HNO_3 is zero. To ensure model calculations stability, a minimum value of r_c=1 $s.m^{-1}$ is defined:

$$r_c^{HNO_3} = \max(1, r_{low}) \tag{7.13}$$

7.1.4.1 The stomatal conductance, g_{sto}

The stomatal conductance g_{sto} is estimated using the model of [Emberson et al., 2000]:

$$g_{sto} = g_{max} \times f_{phen} \times f_{light} \times \max(g_{min}, (f_{temp} \times fVPD \times f_{SWP})) \tag{7.14}$$

The parameters are:

- g_{max} is the maximum daytime stomatal conductance in mmol O_3 m^{-2} s^{-1}. To use it as a conductance and with the appropriate units, the unit conversion is made: g_{max}=$g^m_{max} RT/P$. At standard temperature and pressure, RT/P is assumed to be 1/41000. With the main units in CHIMERE being centimeters, the factor equals 410.

- g_{min} is the minimum daytime stomatal conductance. It depends only on the vegetation type.
- f_{phen} is the relative conductance determined by leaf/needle age
- f_{light} is the relative conductance determined by irradiance
- f_{temp} is the relative conductance determined by temperature
- f_{VPD} is the relative conductance determined by the leaf-to-air vapour pressure deficit (VPD)
- f_{SWP} is the relative conductance determined by the soil water potential (SWP). Note that in CHIMERE, the value of this parameter is the one chosen in [Emberson et al., 2000], i.e. f_{SWP}=1.

All the relative factors are comprised between 0 and 1. The g_{min} and g_{max} factors are constant and depend only on the vegetation type. They are specified in the model file chemprep/data/DEPO_PARS.univ as a function of the vegetation type. This file uses the 16 EMEP vegetation types (Table 7.3). Note that only the first 10 vegetation types are really used, since the last 6 categories have $g_{max} = 0$.

1	CF	T/B conif	9	GR	Grass
2	DF	T/B decid	10	MS	Med. scrub
3	NF	Med. needle	11	WE	wetlands
4	BF	Med. Broadleaf	12	TU	Tundra
5	TC	T/B crop	13	DE	Desert
6	MC	Med. crop	14	W	Water
7	RC	Root crop	15	ICE	Ice
8	SNL	Moorland	16	U	Urban

Table 7.2: *List of acronyms used in the deposition parameters data file. T/B stands for "temperate or boreal", Med for Mediterranean.*

The stomatal conductance was estimated for ozone only in [Emberson et al., 2000]. In order to derive a value for all other gaseous model species, the conductance value for ozone is scaled using the ratio of the diffusivities in the air of ozone and of another model species:

$$g^x_{sto} = g^{O_3}_{sto} \times \sqrt{\frac{dMO_3}{dMx}} \tag{7.15}$$

Here the ratio of diffusivities denoted 'facD' in the code and calculated in inidepo.F90 follows the Graham's Law of effusion:

$$\frac{\text{Rate of effusion of gas 1}}{\text{Rate of effusion of gas 2}} = \sqrt{\frac{M_2}{M_1}} \tag{7.16}$$

The tabulated parameters listed in Table 7.3 are:

- gmax: Maximum stomatal conductance (mmol O_3 m^{-2} s^{-1})
- gmin: Minimum daytime stomatal conductance observed under field conditions
- deptmin, deptopt and deptmax: Temperature boundaries to define the temperature factor. In this formulation, deptmax is not used.
- depalph: factor used with the PAR to moderate the light on leaves.
- depvpd1 and depvpd2: Threshold values (in kPa) for the minimum and maximum values of the leaf-to-air vapour pressure deficit (VPD)
- depsgs and depegs: (defined as SGS50 and EGS50 in [Simpson et al., 2012]). Start and end of the growing season at latitude 50^{o}N
- depsgl and depegl: duration of the start and end of the growing season
- deplai1 and deplai2: LAI min and max

	CF	DF	NF	BF	TC	MC	RC	SNL	GR	MS	WE	TU	DE	W	I	U
Gmax [1]	160	134	180	200	300	156	360	60	270	213	0	0	0	0	0	0
Gmin [1]	0.1	0.13	0.13	0.03	0.01	0.019	0.02	0.01	0.01	0.014	0	0	0	0	0	0
Tmin [1]	1	6	4	4	12	0	8	1	12	4	0	0	0	0	0	0
Topt [1]	18	20	20	20	26	25	24	18	26	20	20	20	20	20	20	20
Tmax [1]	36	34	37	37	40	51	50	36	40	37	40	40	40	40	40	40
alpha [1]	83e-4	6e-3	13e-3	9e-3	9e-3	48e-4	23e-4	9e-3	9e-3	12e-3	0	0	0	0	0	0
VPDmax [1]	0.6	0.93	0.4	1.8	0.9	1.0	0.31	88.8	1.3	1.3	88.8	88.8	88.8	88.8	88.8	88.8
VPDmin [1]	3.3	3.4	1.6	2.8	2.8	2.5	2.7	99.9	3.0	3.0	99.9	99.9	99.9	99.9	99.9	99.9
SGS [2]	0	90	0	0	105	150	130	0	0	0	0	0	0	0	0	0
EGS [2]	366	300	366	366	197	300	250	366	366	366	366	366	366	366	366	366
SGS length [2]	192	30	180	180	70	70	35	192	180	1	1	1	1	1	1	1
EGS length [2]	96	90	180	180	22	44	65	96	180	1	1	1	1	1	1	1
LAI min [1]	3.4	3.5	3.5	3.5	0	0	0	2.0	2.0	2.5	0	0	0	0	0	0
LAI max [1]	4.5	5.0	3.5	3.5	3.5	3.0	4.2	3.0	3.5	2.5	0	0	0	0	0	0
PHENa [1]	0.2	0.3	0.3	0.3	0.1	0.1	0.2	0.1	1	0.2	1	1	1	1	1	1
PHENb [1]	130	50	110	110	0	0	20	0	0	130	0	0	0	0	0	0
PHENc [1]	130	50	150	150	45	45	45	45	0	130	0	0	0	0	0	0
Zcanopy [0]	20	20	20	20	1	2	0.5	1	1	2	0	0	0	0	0	0
RGSO3 [1]	200	200	200	200	200	200	200	400	1000	200	2000	400	2000	2000	2000	400
RGSSO2 [1]	0	0	0	0	0	0	0	0	0	0	1	500	1000	1	100	400
so2RH [1]	0.85	0.85	0.85	0.85	0.75	0.75	0.75	0.75	0.75	0.75	0	0	0	0	0	0

Table 7.3: *Dry deposition constants set in chemprep/data/DEPO_PARS.univ dependingon the vegetation type: (0) estimated for CHIMERE; (1) taken from the EMEP model documentation (EMEP website); (2) EMEP data with corrections applied for the growing season for the DF type: EGS=300 instead of 270, SGS_len=30 instead of 56.*

- depphe0, depphe1, depphe2: phenological factors
- zcanopy: Canopy height (m)
- RGSO3 and RGSSO2: Ground surface resistance for O_3 and SO_2.
- so2rh: a threshold to estimate if the conditions are wet or dry for the SO_2 deposition.

7.1.4.1.1 The LAI, SAI and phenological factor. To take into account the vegetation growth variability in the deposition velocity calculation, the Leaf Area Index (LAI), the Surface Area Index (SAI) and the phenological factor f_{phen} are estimated.
There are two ways to estimate these parameters in the model. If the MEGAN scheme is used, the LAI is simply read from its database. The phenological factor is thus interpreted as the green fraction factor provided in the landuse file (from WRF or a database such as GLOBCOVER).
If these data are not available in the datasets used with CHIMERE, they are estimated using simple functions as described in [Emberson et al., 2000]. For the LAI, this fit uses minimum and maximum values of the growing season for each vegetation type. Between these values, a simple function is applied as explained in Figure 7.2 (left).The phenology factor is also a simple function, depending only on three constant parameters (for each vegetation type): depphe0, depphe1, depphe2. The function is shown in Figure 7.2 (right): it reaches its maximum of 1 between PHENb and PHENc, while its minimum value PHENa depends on the vegetation type and varies from 0.1 to 0.3.
The SAI (surface area index) is defined in terms of LAI: SAI is set to the LAI value within the growing season and 1 outside the growing season.

7.1.4.1.2 The light factor, f_{light}. The light factor, g_{light}, depends on the vegetation type. It is first needed to calculate the direct, I_{dir}, and diffuse, I_{diff}, solar irradiance (W m^{-2}), and the solar elevation, $\sin\beta$. In

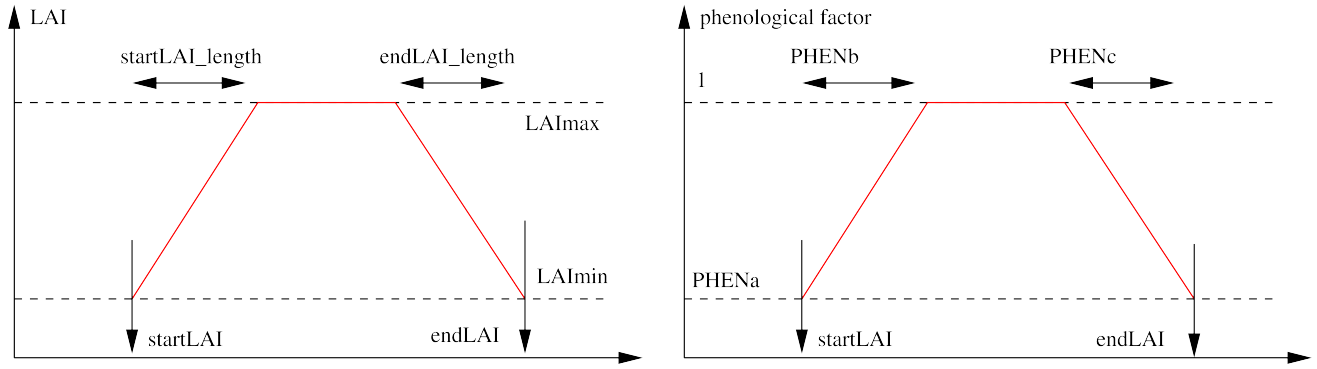


Figure 7.2: *Function used to define the hourly variability of the LAI and the phenological function. The required parameters are shown using their names in the model: SGS and EGS for the start and end of the growing season, LAImin and LAImax for the minimum and maximum of LAI value, SGSlength and EGSlength for the length of the start and end of the growing season. The phenological parameters are PHENa, PHENb, and PHENc to define the minimum value, the length, the start, and the end of the season.*

CHIMERE, the beam radiation, b_{rad}, (*beamrad*) is calculated as:

$$b_{rad} = 4.57 \times A_r \times 1069 \times \exp\left(\frac{-0.21}{cz}\right) \tag{7.17}$$

where cz is the cosinus of the zenithal angle ($\cos\theta$), 4.57 is a conversion factor to convert the irradiances from W m^{-2} to μ mol m^{-2} s^{-1}, A_r (*atte*) is the radiation attenuation calculated as:

$$A_r = \exp(-0.11 \times AOD^{0.67}) \tag{7.18}$$

The solar irradiances are thus estimated as:

$$I_{dir} = A_r \times cz \tag{7.19}$$

$$I_{diff} = I_{dir} \times C \tag{7.20}$$

C being a constant as C=0.13. This constant could probably be variable, this parameter being the impact of the water content in the whole atmospheric column.
Using these irradiances, the LAI and PAR are estimated as:

$$LAI_{sun} = \left(1 - \exp\left(\frac{-0.5 \times LAI}{cz}\right)\right) \times \frac{cz}{\cos(\alpha)} \tag{7.21}$$

In the CHIMERE model, we assume that $\cos(\alpha)$=0.5, corresponding to a constant inclination of leaves in the canopy of 60^o. The relative part of the shaded LAI is estimated as a fraction of LAI_{sun} as:

$$LAI_{shade} = LAI - LAI_{sun} \tag{7.22}$$

For the PAR, the coefficients PAR_{sun} and PAR_{shade} are calculated as:

$$\begin{aligned} PAR_{sun} &= \frac{\cos(\alpha)}{\cos(\theta)} \times I_{dir} + PAR_{shade} \\ PAR_{shade} &= I_{diff} \times \exp\left(-0.5 \times LAI^{0.7}\right) \\ &+ 0.07 \times I_{dir} \times (1.1 - 0.1 \times LAI) \\ &\times \exp(\sin\beta) \end{aligned} \tag{7.23}$$

with $\sin\beta = \cos\theta$. Finally, the f_{light} factors for the sun and shade light conditions are estimated as:

$$\begin{aligned} g_{light,shade} &= 1 - \exp\left(-\alpha \times PAR_{shade}\right) \\ g_{light,sun} &= 1 - \exp\left(-\alpha \times PAR_{sun}\right) \end{aligned} \tag{7.24}$$

with α a factor for each vegetation type. This factor (depalph in the model) is tabulated (see Table 7.3).
The complete f_{light} factor is finally:

$$f_{light} = \frac{g_{light,sun} \times LAI_{sun} + g_{light,shade} \times LAI_{shade}}{LAI} \tag{7.25}$$

To avoid division by zero, the LAI is here chosen as $LAI = \max(LAI, 1.e-20)$.

7.1.4.1.3 The temperature factor, f_{temp}. The temperature factor is estimated between two extrema of temperatures, T_{min} and T_{max}, or between T_{min} and a temperature of maximum conductance, T_{opt}. For all vegetation types, this temperature factor is always between 0 and 40^{o}C. For temperature below 0^{o}C or above 40^{o}C, the stomata are considered to be closed, and r_{sto} is set to a large value to avoid the deposition this way.
In [Emberson et al., 2000], this factor is estimated as:

$$f_{temp} = 1 - \left[\frac{T - T_{opt}}{T_{opt} - T_{min}}\right]^2 \tag{7.26}$$

with T the 2m temperature in ^{o}C. To ensure correct values of r_{sto} at various simulated T_{2m}, T is estimated as:

$$\begin{aligned} T_1 &= \max(T_{min} + 0.1, T_{2m}) \\ T &= \min(T_1, 2 \times T_{opt} - T_{min} - 0.1) \end{aligned} \tag{7.27}$$

7.1.4.1.4 The leaf to air vapour pressure deficit factor f_{vpd}. The leaf-to-air vapour pressure deficit (VPD) describes the difference between the vapor pressure inside the leaf compared to that of the air. This factor varies between 1 (high deficit, VPD$_{max}$, denoted depvpd1 in the code) and 0.1 (low deficit, VPD$_{min}$, denoted depvpd2 in the code). Between VPD$_{max}$ and VPD$_{min}$, a linear dependence is assumed. The current VPD value (vpdkPa in the model) is calculated hourly as:

$$VPD = (1 - rh/100) \times es \tag{7.28}$$

with rh the relative humidity in %, and es, in mbar (denoted vapp in the model) is calculated as:

$$es = 100. \times 6.11 \times \exp\left[\frac{17.27 \times T_{2m}}{T_{2m} - 35.86}\right] \tag{7.29}$$

The factor of 100 is to convert es to Pa (instead of hPa=mbar). In this equation, the 2m temperature is in K. The surface relative humidity is between 0 and 1 in the model and is estimated in calc_turb.F90.
Depending on the relative values of VPD and VPD$_{min}$, VPD$_{max}$ (in kPa, a factor 10^3 is thus applied), the f_{vpd} factor is estimated as:

$$\begin{cases} f_{vpd} = 1 & \text{if } VPD \geq VPD_{max} \\ f_{vpd} = 0.1 & \text{if } VPD \leq VPD_{min} \\ f_{vpd} = 1 - \dfrac{(VPD_{max} - VPD)(1 - 0.1)}{VPD_{max} - VPD_{min}} & \text{if } VPD_{max} \geq VPD \geq VPD_{min} \end{cases} \tag{7.30}$$

7.1.4.1.5 The soil water potential factor, f_{SWP}. The f_{SWP} represents the evolution of the water in soil. The soil water potential (in MPa) can be deduced from soil water content values. In the current scheme, its value is set to the constant f_{SWP}=1.

7.1.4.1.6 The mesophyllic resistance, r_m. The mesophyllic resistance r_m is calculated for each deposited species and follows the expression in [Seinfeld and Pandis, 1998] as:

$$r_m = \frac{1}{3.3 \times 10^{-4} \times dHx + df0 \times 100} \tag{7.31}$$

with dHx the effective Henry's law constant (M atm^{-1}) for the gas and $df0$ the normalised (0 to 1) reactivity factor for the dissolved gas (values are displayed in Table 7.1). Over vegetation canopies, corrections have been implemented according to [Zhang et al., 2001], [Giorgi, 1986] and [Peters and Eiden, 1992].

7.1.4.2 The non stomatal bulk conductance, G_{ns}

Non stomatal conductances are explicitly calculated for O_3, SO_2 and NH_3. For all other gaseous species, the conductance value is estimated by interpolating the values found for O_3 and SO_2 as:

$$\left\{ \begin{array}{rcl} G^i_{ns,dry} & = & 10^{-5} \times dH \times G^{SO_2}_{ns,dry} + df0 \times G^{O_3}_{ns} \\ G^i_{ns,wet} & = & 10^{-5} \times dH \times G^{SO_2}_{ns,wet} + df0 \times G^{O_3}_{ns} \end{array} \right. \tag{7.32}$$

where dH and $df0$ are the effective Henry's law constant and the normalised reactivity factor, respectively. For all model species, these values are displayed in Table 7.1.

7.1.4.2.1 Non stomatal bulk conductance for ozone. After [Emberson et al., 2000], this conductance is expressed as:

$$G^{O_3}_{ns} = SAI \times g_{ext} + \frac{1}{R_{inc} + R^{O3}_{gs}} \tag{7.33}$$

where: g_{ext} is the external leaf uptake conductance, R_{inc} the in-canopy resistance and R^{O3}_{gs} the ground surface resistance (tabulated as a function of the vegetation type in Table 7.3).
Low temperature conditions are taken into account to modify the R^{O3}_{gs} values as:

$$R^{O3}_{gs} = R^{O3}_{gs} + R_{low} + 2000\delta_{snow} \tag{7.34}$$

In the current model version, the presence of snow is not taken into account and a fixed value of δ_{snow}=0 is implemented. This may change in a future version.

7.1.4.2.2 The in-canopy resistance, R_{inc}. The in-canopy aerodynamic resistance R_{inc} represents the deposition to soils and under canopy. [Erisman et al., 1994] explains that it can represent $\approx 20\%$ of O_3 and SO_2 dry deposition. In this model version, this resistance is calculated only for ozone. This resistance uses the friction velocity and the canopy height z_c (in meters). z_c is tabulated independently of the season and latitude in the current model version, as displayed in Table 7.3.

$$R_{inc} = 100. \times \frac{b \times SAI \times z_c}{u_*} \tag{7.35}$$

where 100 is a factor to convert m to cm, b=14 m^{-1}.

7.1.4.2.3 The external leaf uptake resistance, R_{ext}. Several formulations are proposed in the litterature for this resistance. A complete scheme is proposed by [Erisman et al., 1994] to represent the deposition of soluble gases at wet surfaces, for example for SO_2.
For SO_2, this resistance, in s.m^{-1}, is thus derived as:

$$\begin{cases} R_{ext} & = 1 & \text{during or just after precipitation} \\ & = 25000\ \exp(-0.0693\ rh) & \text{at rh} < 81.3\% \\ & = 0.58 \times 10^{12}\ \exp(-0.278\ rh) & \text{at rh} > 81.3\% \end{cases} \tag{7.36}$$

In CHIMERE, this resistance is defined in a simpler way after [Emberson et al., 2000]:

$$R_{ext} = 2500 s.m^{-1} \tag{7.37}$$

Expressed in terms of conductance, using the SAI dependency and converted to cm.s^{-1}, this leads to:

$$g_{ext} = \frac{1}{25} \tag{7.38}$$

7.1.4.2.4 Non stomatal bulk conductance for SO_2. This conductance for sulphur dioxide is controlled by wetness and NH_3 surface concentrations. This estimation uses the 'acidity ratio' (denoted 'acraloc' in CHIMERE) as:

$$a_{SN} = 0.6 \times \frac{[SO_2]}{[NH_3]} \tag{7.39}$$

Using this ratio, the F_{SN} is defined as:

$$\begin{cases} F_{SN} & = \exp(-2 + a_{SN}) & \text{if } a_{SN} < 2 \\ & = 1 & \text{if } a_{SN} \geq 2 \end{cases} \tag{7.40}$$

and used in the following relationship to estimate $R_{ns}^{SO_2}$:

$$\begin{cases} R_{ns,dry}^{SO_2} & = & R_d \times F_{SN} + R_{low} + 2000 \times \delta_{snow} \\ R_{ns,wet}^{SO_2} & = & R_w \times F_{SN} + R_{low} + 2000 \times \delta_{snow} \end{cases} \tag{7.41}$$

with R_d=180 s.m^{-1} and R_w=100 s.m^{-1}.

7.1.4.2.5 Non stomatal bulk conductance for NH_3. The acidity ratio is also used to estimate this conductance as:

$$\begin{cases} R_{ns}^{NH_3} & = \beta \times F_1 \times F_2 & \text{for } T_s > 0 \\ & = 200 & \text{for } -5 < T_s \leq 0 \\ & = 1000 & \text{for } T_s \leq -5 \end{cases} \tag{7.42}$$

β is a constant as β=0.0455 and the two functions are:

$$\begin{cases} F_1 & = & 10 \times log(T_s + 2) \times \exp\left(\dfrac{100 - RH}{7}\right) \\ F_2 & = & 10^{-1.1099 a_{SN} + 1.6769} \end{cases} \tag{7.43}$$

where RH is here the surface relative humidity in %. For this chemical species, there is no dependency on the wet or dry atmospheric conditions and the final resistance is:

$$R_{ns} = \frac{1}{G_{ns}^{NH3}} \tag{7.44}$$

7.1.5 The quasi-laminar layer resistance r_b for aerosols

For aerosols, the quasi-laminar resistance completely differs from that of gases. It is calculated in the depaero.F90 routine. A complete discussion on mecanistic processes of dry deposition is available in [Petroff et al., 2008a] and [Petroff et al., 2008b]. This resistance depends on the particle diameter and is given by:

$$r_b = \frac{1}{u_* \left(S_c^{-2/3} + 10^{-3/S_t} \right)} \tag{7.45}$$

with S_t the Stokes number and S_c the Schmidt number (dimensionless) as:

$$S_c = \frac{\nu_{air}}{D_i} \tag{7.46}$$

with ν_{air} the kinematic viscosity of air (in $m^2.s^{-1}$) and D_i the diffusivity in air of the particle. In case of aerosols, this diffusivity is considered as a Brownian diffusion and is estimated using the Stokes-Einstein relation as:

$$D_i = \frac{k_B \times T \times C_c}{3 \times \pi \times \mu_{air} \times D_p} \tag{7.47}$$

with k_B the Boltzmann constant, $k_B = 1.38065 \times 10^{-23}$ $J.K^{-1}$ (with 1 J = 1 $kg.m^2.s^{-1}$).
The kinematic viscosity ν_{air} is calculated using the value of the dynamic viscosity μ_{air} (in $kg.m^{-1}.s^{-1}$):

$$\nu_{air} = \frac{\mu_{air}}{\rho_{air}} \tag{7.48}$$

The calculation of the dynamic viscosity is possible using a large number of fitted data. In the model, the Sutherland relation is used.

$$\mu = \mu_0 \frac{T_0 + C}{T + C} \left(\frac{T}{T_0} \right)^{3/2} \tag{7.49}$$

with the references values for air: T_0=291.15 K, C=120 K and μ_0=18.27 10^{-6} Pa.s (i.e. $kg.m^{-1}.s^{-1}$).
The dimensionless Stokes number is calculated as:

$$S_t = \frac{v_s \times u_*^2}{g \times \nu_{air}} \tag{7.50}$$

with v_s the settling velocity, itself depending on the aerosol mass median diameter, D_p.

7.1.6 The surface resistance for aerosols, r_s

This formulation follows the scheme of [Zhang et al., 2001]. This surface resistance is calculated as:

$$r_s = \frac{1}{\epsilon_0 \times u_* \times R_1 \times (E_B + E_{IM} + E_{IN})} \tag{7.51}$$

with:

- ϵ_0 is a constant set to ϵ_0=3, for all landuse categories.
- R_1 a correction factor describing the relative amount of aerosols sticking at the surface
- E_B collection efficiency from Brownian diffusion
- E_{IM} collection efficiency from impaction

- E_{IN} collection efficiency from interception

The R_1 factor is estimated following [Slinn, 1982]:

$$R_1 = \exp(-St^{1/2}), \tag{7.52}$$

where this factor is applied only for particles with $D_p > 5\mu m$.
For Brownian diffusion, the resistance is estimated as:

$$E_B = Sc^{-\gamma} \tag{7.53}$$

where γ is a constant depending on the landuse type. In the model, this constant varies between 0.54 and 0.58. For the impaction, the resistance can have a lot of definitions, depending on the landuse. By default, the resistance value used is:

$$E_{IM} = \left(\frac{St}{\alpha + St}\right)^2 \tag{7.54}$$

The α values are landuse dependent and are tabulated following [Zhang et al., 2001]. In this model version, a distinction is made between northern and southern hemisphere, in order to use the correct α for a specific modelled day.
For specific vegetation types, the formulation is changed. For high vegetation (such as forests), the resistance proposed by [Giorgi, 1986] is used:

$$E_{IM} = \left(\frac{St}{0.6 + St}\right)^{3.2} \tag{7.55}$$

For grassland vegetation, a parameterization is proposed by [Davidson et al., 1982]:

$$E_{IM} = \frac{St^3}{St^3 + 0.753\ St^2 + 2.796\ St - 0.202} \tag{7.56}$$

Finally, the collection efficiency from interception is calculated as:

$$E_{IM} = \frac{1}{2}\left(\frac{D_p}{A}\right)^2 \tag{7.57}$$

with A a characteristic diameter given for landuse and seasonal categories.

7.1.7 The settling velocity v_s

The settling velocity represents the effect of gravity on particles and is calculated in depaero.F90 as:

$$v_s = \frac{1}{18}\frac{D_p^2\ \rho_p\ g\ C_c}{\mu} \tag{7.58}$$

with ρ_p, the particle density (chosen as ρ_p=2.65 g cm^{-3} for mineral dust), D_p the mass median diameter of particles, C_c a slip correction factor accouting for the non-continuum effects when D_p becomes smaller and of the same order of magnitude as the mean free path of air, λ, [Seinfeld and Pandis, 1998]. g is the gravitational acceleration with g=9.81 m s^{-2}, μ the dynamic viscosity (here the air dynamic viscosity is set to μ_{air}=1.8 $\times$ 10^{-5} kg m^{-1} s^{-1}).
The slip correction factor C_c is estimated as:

$$C_c = 1 + \frac{2\lambda}{D_p}\left[1.257 + 0.4\ \exp\left(-\frac{1.1 D_p}{2\lambda}\right)\right] \tag{7.59}$$

with λ the mean free path of air, in meters, estimated as:

$$\lambda = \frac{2\mu_{\text{air}}}{p\sqrt{\frac{8M_{\text{air}}}{\pi RT}}} \tag{7.60}$$

where M_{air} is the molecular mass of dry air (here 28.8 g mol^{-1}), T the temperature (K), p the pressure (Pa), μ the air dynamic viscosity and R the universal gas constant.

7.2 Wet scavenging

When the aerosol option is selected in chimere.par, scavenging for gas/aerosols in clouds or rain droplets is taken into account. The calculation is done in several routines:

1. inidepo.F90: Read the input parameters
2. depwet.F90: Calculation of the deposition fluxes

7.2.1 Input parameters

In the inidepo.F90, parameters are read for the wet scavenging of gas and particles. These parameters are stored in the chemprep/inputdata/WETD_SPEC.univ. This parameter file is explained in Table 7.4 .
In the depwet.F90, some constants are hardcoded and are explained in Table 7.5 .

7.2.2 Wet scavenging for gases

The wet scavenging of gases is divided into two processes: the gases in clouds and the gases into the rain droplet below the cloud.
For the **gases in clouds**, nitric acid, ammonia in the gas phase are scavenged by cloud droplets. This process is assumed to be revertible. Moreover, for in-cloud scavenging, dissolved gases in a non precipitating cloud can reappear in the gas phase due to cloud dissipation. Equilibrium between dissolved gases concentration and gas-phase concentrations follow [Seinfeld and Pandis, 1998].
For a gas denoted A and the processes between gas and aqueous phases, there are two simultaneous reactions occurring:

$$A^g \rightarrow^{k+} A^{aq}; A^g \leftarrow^{k-} A^{aq} \tag{7.61}$$

The constants k^- and k^+ (s^{-1}) are estimated following the relations:

$$k^- = \frac{6w_l\rho_a}{\rho_e D}\left(\frac{D}{2D_A^g} + \frac{4}{c_A\alpha_A}\right)^{-1} \tag{7.62}$$

$$k^+ = \frac{600}{RH_AT}\left(\frac{D}{2D_A^g} + \frac{4}{c_A\alpha_A}\right)^{-1} \tag{7.63}$$

with ρ_e and ρ_a the water and air densities, respectively, in kg m^{-3}, w_l the liquid water content (kg kg^{-1}), D the droplet mean diameter (m), c_A the mean molecular velocity of the gas A (ms^{-1}), D^g the molecular diffusion of the gas A in air (in m^2 s^{-1}) and α_A the gas A accomodation coefficient. H is the Henry's constant (M atm^{-1}), T the air temperature (K) and R the molar gas constant.
For the **gases in rain droplets below the clouds**, the dissolution of gases in precipitating drops is assumed to be irrevertible, both for HNO_3 and NH_3. The scavenging coefficient is expressed as:

Species	Type	In cloud scavenging constants			Molar mass
'charspec'	'itywet'		'wetdk'		'dMx_wet'
Gaseous species					
HNO3	1	2.0e-3	0.	0.10	63.0
NH3	1	2.0e-3	0.	0.10	17.0
H2O2	1	2.0e-3	0.	0.18	34.0
HCL	1	2.0e-3	0.	0.10	36.5
Aerosol species					
H2SO4AQ	2	0.	1.	0.	96.9
HNO3AQ	2	0.	1.	0.	62.0
NH3AQ	2	0.	1.	0.	18.0
SOAAQ	2	0.	1.	0.	250.0
AnA0DAQ	2	0.	1.	0.	142.0
AnA1DAQ	2	0.	1.	0.	168.0
AnA2DAQ	2	0.	1.	0.	186.0
AnBmPAQ	2	0.	1.	0.	152.0
AnBIPAQ	2	0.	1.	0.	167.0
BiA0DAQ	2	0.	1.	0.	168.0
BiA1DAQ	2	0.	1.	0.	170.0
BiA2DAQ	2	0.	1.	0.	186.0
BiBmPAQ	2	0.	1.	0.	236.0
ISOPA1AQ	2	0.	1.	0.	177.0
ISOPA2AQ	2	0.	1.	0.	177.0
PPMAQ	2	0.	1.	0.	199.0
BaPAQ	2	0.	1.	0.	252.0
BbFAQ	2	0.	1.	0.	252.0
BkFAQ	2	0.	1.	0.	252.0
SALTAQ	2	0.	1.	0.	58.5
OCARAQ	2	0.	1.	0.	100.0
BCARAQ	2	0.	1.	0.	100.0
NAAQ	2	0.	1.	0.	23.0
HCLAQ	2	0.	1.	0.	25.5
H2O2	2	1.	7.45e4	0.	38.0
SO2	2	1.	1.51e-2	1.	64.0

Table 7.4: *Parameters for the wet deposition with their model species names, charspec, the type of the species, in cloud scavenging constants and the molar mass.*

Constant	Significance	Value
diff	Molecular diffusivity of the species	0.25 10^{-4} (m^2 s^{-1})
Rg	Universal gas constant	8.205 10^{-2} (m^3.atm.kmol^{-1}.K^{-1})
wated	Water density	1.0
diami	Minimal diameter for droplets	0.03 10^{-3} (cm)
diamf	Maximal diameter for droplets	1.2 10^{-2} (cm)
ccloud	volume fraction of cloud in the cell (for cumulus)	0.3 (g/m3)
Fc	Surface of the cell covered by clouds	1.0
pcpth	Precipitation threshold	10^{-8} (g/cm2/s)
cwth	Cloud liquid water content threshold	10^{-11} (kg/kg)
Eff	Default scavenging efficiency	1.0

Table 7.5: *Constants used for the calculation of the wet scavenging fluxes for gas and aerosols*

$$\Gamma = \frac{pD_g}{6.10^5 u_g D^2}(2 + 0.6R_e^{1/2}S_c^{1/3}) \tag{7.64}$$

p being the precipitation rate (mm h^{-1}), D_g the molecular diffusion coefficient ($m^2 s^{-1}$), u_g the raindrop velocity (m s^{-1}), Re and Sc respectively the Reynolds and Schmidt numbers of drops. [Mircea and Stefan, 1998] and references therein give relationships between u_g and hydrometeor diameter for various types of precipitation. In the model, sulfur dioxide and hydrogen peroxide are also scavenged by precipitation.

7.2.3 Wet scavenging for aerosol

For **particles** in **clouds**: Deposition of particles is assumed to be proportional to amount of water lost by precipitations. The deposition flux is written as:

$$\left[\frac{dQ_l^k}{dt}\right] = -0.01\frac{\epsilon_l P_r}{w_l h} Q_l^k \tag{7.65}$$

with p_r being the precipitation rate released in the grid cell (kg m^{-2} s^{-1}), w_l the liquid water content (kg m^{-3}), h the cell thickness (cm) and ϵ an empirical uptake coefficient (in the range 0 - 1) currently assumed to be 1. l and k are respectively the bin and composition subscripts.
For **particles** in **rain droplets below the clouds**: Particles are scavenged by raining drops. Following [Henzig et al., 2006], a polydisperse distribution of raining drops is applied:

$$N(R) = \text{norm} \times 1.98 \times 10^{-5} P^{-0.384} R^{2.93} \exp\left[-(5.38 P^{-0.186} R)\right] \tag{7.66}$$

where

$$\text{norm} = 1.047 - 0.0436 \ln P + 0.00734 (\ln P)^2 \tag{7.67}$$

with P the precipitation rate in mm/h and R the radius of the droplet.

$$\left[\frac{dQ_l^k}{dt}\right] = -Q_l^k \int_R \pi R^2 u_g(R) E(R, r_l) N(R) \mathrm{d}R \tag{7.68}$$

with R, the radius of the raindrop (in m), r_l the radius of the particle (in m), u_g the terminal drop velocity (in m/s), E(R,r_l) the collision efficiency of a particle with a raindrop, N(R) (in m^{-4}) the raindrop size distribution.

8 Initial and boundary conditions

While some regional chemistry transport model rely on observation-based boundary concentrations, the CHIMERE strategy relies exclusively on simulations from global models. The added value in geographical and temporal variability as well as the larger number of chemical species available argue in favour of this second option, despite the increased sensitivity of the limited area CTM to any bias in the large scale forcing data. In order to cope with possible limitations in the global model forcing, we choose to increase the modularity of the global to regional nesting by allowing the use of several sources of boundary conditions (i.e. simulations from different models), or even combinations of such sources.

8.1 Options activation

It is possible to run the model without any boundary or initial conditions. But the best way is to use available informations, coming from previous simulations or other models outputs.

```
[nested]      Nested run? (yes/no)                                : no, yes
[dom]         CHIMERE domain                                      : CONT5, IDF15C
[iusebound]   Use and build Initial & Boundary conditions?        : 2
```

The initial and boundary conditions are different all along the run but their preparation is managed in the same way. The main difference is that the **initial conditions** are necessary for the first time-step only but over the whole simulation domain when the **boundary conditions** are necessary every hour but only for the model cells surrounding the simulation domain.
These several options are summarized in Figure 8.1 .
These options correspond to:

- Initial conditions:
  - ◇ iusebound=0 : all chemical species are set to zero at the first time-step
  - ◇ iusebound=1 or 2
    - ◇ Use climatological data if the simulation starts (no end.nc file available)
    - ◇ Use the previous simulation if the run is chained (end.nc file available)
- Boundary conditions:
  - ◇ iusebound=0 : all chemical species are set to zero around the domain and during the whole simulation
  - ◇ iusebound=1 or 2
    - ◇ Use climatological data if nested=no
    - ◇ Use another CHIMERE simulation if nested=yes

If iusebound=1 or 2 and if nested=no, it is necessary to provide the path where the global datafiles are stored: bcdir, together with a label pointing towards the relevant source (INCA, MACC, GOCART) as the name of the subdirectory where global data where extracted. The source of boundary data can be a composite of several global models for gas, dust and non-dust aerosol by using the right flags: bcgas, bcdust, and bcaer. And for each of these flag the user can indicate whether climatological data (monthly means) are desired (with bcgasdt,

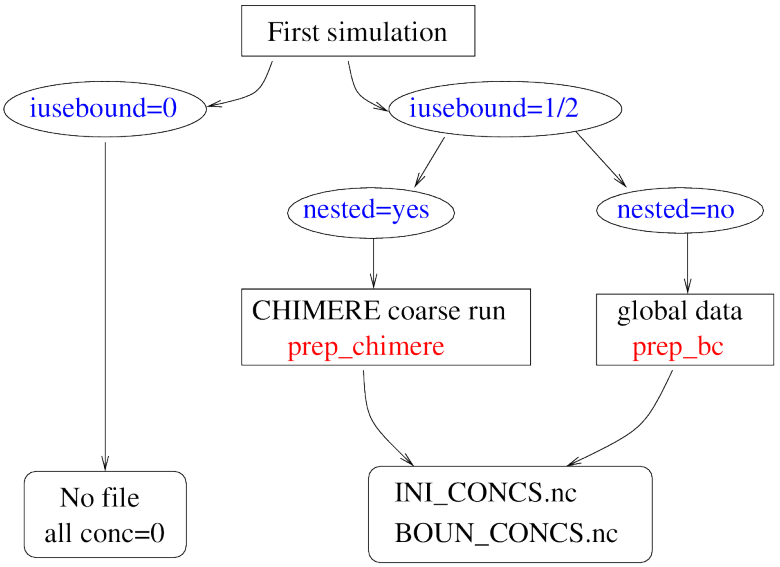


Figure 8.1: *Flowchart of the several options to build the initial and boundary conditions.*

bcaerdt, or bcdustdt = 0), or if a higher temporal frequency is available (setting these flags to 1) in that case the fortan code extract automatically the highest available temporal resolution.
The use of these conditions is managed by the following options available in the chimere.par file:

```
[bcdir]      Boundary conditions    : {bigfilesdir}
[bcgas]      BC Gaseous Species              : LMDz4_INCA3_96x95x19_v2013c
[bcgasdt]    No gas bc (0), Climatological (1) or time varying  (2) : 1
[bcaer]      BC non-dust  Aerosols           : LMDz4_INCA3_96x95x19_v2013c
[bcaerdt]    No aer bc (0), Climatological (1) or time varying  (2) : 1
[bcdust]     BC Dusts      : GOCART
[bcdustdt]   No dust bc (0), Climatological (1), time varying  (2)  : 1
```

8.2 The boundary and initial conditions interface

After reading the chimere.par file, and if the boundary conditions are activated, the script scripts/chimere-bound.sh will prepare required data. There is mainly two options:

1. This is not a nested simulation: the script scripts/chemprep-prep-boun-data.sh is launched during the chemprep stage. Then the script scripts/chimere-bound.sh launchs the program src/prep_bc to extract the global climatological data.

2. This is a nested simulation: the script scripts/chimere-bound.sh launchs the program src/prep_chimere to read the previously done coarse CHIMERE simulation.

At the end of preparation of these files, the results are stored in a dedicated directory defined in the chimere.par file:

```
# Please make sure that $iniboundir is the same for the coarse and all nested runs !!
[$iniboundir] Dir to store INI/BOUND files : ${simuldir}/../INIBOUN.${nbins}
```

with several files, depending on the simulated period and named:

1. INI_CONCS.nc-<speciestype> for the initial conditions
2. BOUN_CONCS.nc-<speciestype> for the boundary conditions

with <speciestype> the three flags: gas, aer and dust. A list of these files is also generated in order to have the exact name of the files to open during the CHIMERE simulation.

8.2.1 In case of a nested run

If the flag nested=yes, the concentrations fields from a previous coarse CHIMERE simulation are used both for initial and boundary conditions. The complete extraction is performed with the src/prep_chimere program. This program will prepare the initial and boundary conditions files using an existing out.[coarse-label].nc simulation output.
For the initial conditions: if the simulations starts, the concentrations of the coarse run are interpolated into the nested domain. If this is a restart simulation, the previous simulation created a end.nc file. This file is renamed as ini.nc file and read durectly during the initialization phase of CHIMERE by the program src/iniconc.F90. The format of this end.nc file is fully described in **Appendix G.8, p.235**.
For the boundary conditions, the src/prep_chimere program interpolates the coarse simulation on the nested domain with an hourly frequency. In this case, the calculations are relatively fast, the model species being the same between the coarse and the nested, thus not needing chemical conversions.

8.2.2 In case of a climatology use

If the simulation if not a nested run, it is necessary to read climatological data to ensure realistic initial and boundary conditions. The calculations are done by the script scripts/chimere-bound.sh launching the src/prep_bc.F90 program.
By reading the arguments in the chimere.par file, the script scripts/chimere-bound.sh will link towards the right type of input data for each type of compound (gas, aer, dust). If several sources are required, the boundary condition extraction will be performed sequentially before being merged into a single file. In the case of time varying data, the script will try to locate the boundary conditions of the relevant years. Otherwise, for climatological data, the code looks for monthly data in the "clim" subdirectory. The boundary condition year is then handled as "0000".
The geometrical extraction as well as unit conversion is ultimately performed in the src/prep_bc.F90 program. This code is generic and ignores the origin of the input data as long as the correct input format is provided. It can handle any temporal resolution of the boundary conditions and makes the difference between climatological and time-varying fields by checking whether the boundary condition year is "0000".

8.3 Available global models climatologies

Three sources of boundary conditions were kindly made available by global chemistry-transport modelling groups to the CHIMERE users:

1. The MACC climatology
2. A climatology from the global model LMDZ-INCA
3. A climatology from the global model GOCART

Their main characteristics are summarised below. The users are invited to take good care of acknowledging the work of their global modelling colleagues in their products and publications.
All the global fields provided for download are monthly climatologies (ie. averages over several years for a given month of the year) but the code has the capacity to use time-varying boundary conditions if the user has such fields available (see section 8.2).

8.3.1 The MACC climatology

The global chemical reanalysis produced as part of the MACC II project (Monitoring Atmospheric Composition and Climat II) is available. The global MACC service provides a 5-years reanalysis for the period 2004-2009 of trace gases and aerosol concentrations. A global monthly climatology at a resolution of 1.125^o is made available to CHIMERE users.
The MACC modelling system relies on the coupled IFS-Mozart [Horowitz, 2003] modelling and assimilation system for reactive gases and on the MACC prognostic aerosol module for particulate matter.
Detailed validation of the MACC reanalysis can be found at:
http://www.copernicus-atmosphere.eu/services/aqac/global_verification/validation_reports/ .
For users, in case of publication using these MACC data, please add in your acknowledgements:

> *This data set was provided by the MACC-II project, which is funded through the European Union Framework 7 programme. It is based on the MACC-II reanalysis for atmospheric composition; full access to and more information about this data can be obtained through the MACC-II web site http://www.copernicus-atmosphere.eu).*

The list of chemical species available in the MACC reanalysis is given in the list below.

- BC ..... Black carbon
- BIGALK ..... Lumped alkans C>3
- BIGENE ..... Lumped alkenes C>3
- C10H16 ..... lumped monoterpense
- C2H6 ..... Ethane
- CH2O ..... Formaldehyde
- CH3CHO ..... Acetaldehyde
- CH4 ..... Methane
- CO ..... Carbon monoxide
- DUST1 ..... Desert dusts (0.03-0.55 μm)
- DUST2 ..... Desert dusts (0.55-0.9 μm)
- DUST3 ..... Desert dusts (0.9-20 μm)
- GLYOXAL ..... Glyoxal
- H2O2 ..... Hydrogen peroxide
- HNO3 ..... Nitric acid
- ISOP ..... Isoprene
- NH3 ..... Ammonia
- NO2 ..... Nitrogen dioxide
- O3 ..... Ozone
- OM ..... Particulate organic matter (0.1-1 μm)
- PAN ..... Peroxy acetyl nitrate
- SO2 ..... Sulfur dioxide
- SO4 ..... Sulfate
- TOLUENE ..... Toluene

8.3.2 The LMDz-INCA climatology

The historical and still commonly used set of boundary conditions is provided by the LMDz-INCA model (Laboratoire de Météorologie Dynamique General Circulation Model coupled with INCA: Interaction with Chemistry and Aerosols). The original INCA model is described in ([Hauglustaine et al., 2004] and [Folberth et al., 2006]) while developments related to aerosol modelling are presented in ([Bauer et al., 2004], [Schulz et al., 2006] and [Balkanski et al., 2007]). The specific version presented here is LMDZ4-INCA3 with the nitrate chemistry introduced in [Hauglustaine et al., 2014]. It has 96x96 horizontal grid points and 19 vertical levels.
The list of chemical species available in the LMDz4-INCA3 model is given below. An example of surface ozone concentrations modelled with LMDz-INCA and MACC is presented in Figure 8.2 .

- ALKAN ..... Lumped alkans C > 3
- AROM ..... Lumped aromatics
- BC ..... Black carbon
- C2H4 ..... Ethylene
- C2H6 ..... Ethan
- C3H6 ..... Propen
- CH2O ..... Formaldehyde
- CH3CHO ..... Acetaldehyde
- CH4 ..... Methane
- CNO3 ..... Coarse Nitrate (2.5-5 μm)
- CO ..... Carbon monoxide
- DUST ..... Desert dusts (1-10 μm)
- H2O2 ..... Hydrogen peroxide
- HNO3 ..... Nitric acid
- NH3 ..... Ammonia
- NH4 ..... Particulate ammonium (0.1-1 μm)
- NO2 ..... itrogen dioxide
- NO3 ..... Particulate nitrate (0.1-1 μm)
- O3 ..... Ozone
- OC ..... Particulte organic carbon (0.1-1 μm)
- PAN ..... Peroxy acetyl nitrate
- SO2 ..... Sulfur dioxide
- SO4 ..... Sulfate

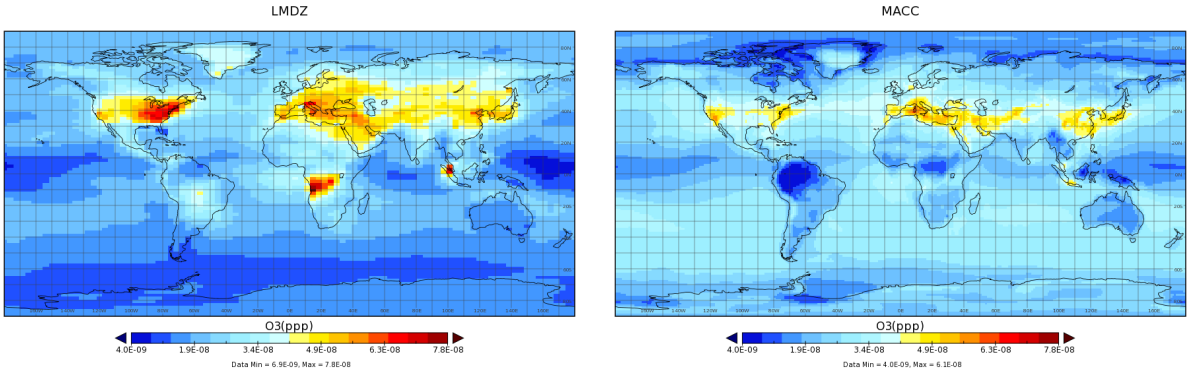


Figure 8.2: *Surface ozone concentrations modelled with LMDz-INCA and MACC for july.*

8.3.3 The GOCART climatology

The Global model GOCART (NASA,[Ginoux et al., 2001]) was historically the only source of boundary conditions for particulate matter, it can still be used in combination with other sources for gaseous boundary conditions.
The list of chemical species available in the GOCART model is given in the list below. For each species, the size distribution is given in μm. An example of surface mineral dust concentrations modelled with GOCART and MACC is presented in Figure 8.3 .

- DUST1 ..... Desert dusts (0.2-0.36)
- DUST2 ..... Desert dusts (0.36-0.6)
- DUST3 ..... Desert dusts (0.6-1.2)
- DUST4 ..... Desert dusts (1.2-2)
- DUST5 ..... Desert dusts (2-3.6)
- DUST6 ..... Desert dusts (3.6-6)
- DUST7 ..... Desert dusts (6-12)
- HBBC1 ..... Hydrophobic black carbon (0.02-0.06)
- HBBC2 ..... Hydrophobic black carbon (0.06-0.18)
- HBBC3 ..... Hydrophobic black carbon (0.18-0.54)
- HBBC4 ..... Hydrophobic black carbon (0.54-1.62)
- HBBC5 ..... Hydrophobic black carbon (1.62-4.86)
- HBBC6 ..... Hydrophobic black carbon (4.86-14.58)
- HBOC1 ..... Hydrophobic organic carbon (0.02-0.06)
- HBOC2 ..... Hydrophobic organic carbon (0.06-0.18)
- HBOC3 ..... Hydrophobic organic carbon (0.18-0.54)
- HBOC4 ..... Hydrophobic organic carbon (0.54-1.62)
- HBOC5 ..... Hydrophobic organic carbon (1.62-4.86)
- HBOC6 ..... Hydrophobic organic carbon (4.86-14.58)
- HLBC1 ..... Hydrophylic black carbon (0.02-0.06)
- HLBC2 ..... Hydrophylic black carbon (0.06-0.18)
- HLBC3 ..... Hydrophylic black carbon (0.18-0.54)
- HLBC4 ..... Hydrophylic black carbon (0.54-1.62)
- HLBC5 ..... Hydrophylic black carbon (1.62-4.86)
- HLBC6 ..... Hydrophylic black carbon (4.86-14.58)
- HLOC1 ..... Hydrophylic organic carbon (0.02-0.06)
- HLOC2 ..... Hydrophylic organic carbon (0.06-0.18)
- HLOC3 ..... Hydrophylic organic carbon (0.18-0.54)
- HLOC4 ..... Hydrophylic organic carbon (0.54-1.62)
- HLOC5 ..... Hydrophylic organic carbon (1.62-4.86)
- HLOC6 ..... Hydrophylic organic carbon (4.86-14.58)
- SULF1 ..... Sulfates (0.02-0.06)

- SULF2 ..... Sulfates (0.06-0.18)
- SULF3 ..... Sulfates (0.18-0.54)
- SULF4 ..... Sulfates (0.54-1.62)
- SULF5 ..... Sulfates (1.62-4.86)
- SULF6 ..... Sulfates (4.86-14.58)

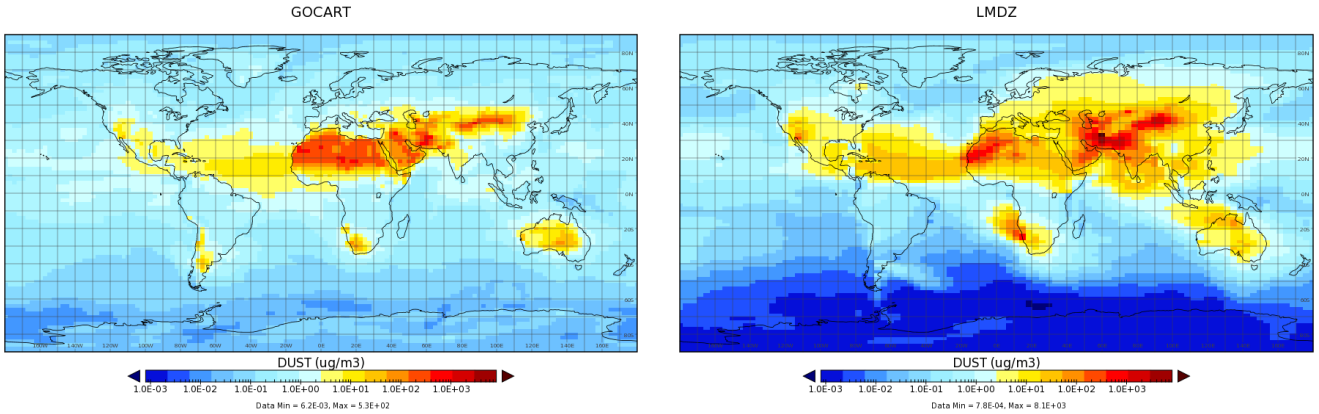


Figure 8.3: *Surface mineral dust concentrations modelled with GOCART and LMDzINCA for july.*

8.3.4 The boundary conditions builder files

In case of use of a climatology, it is necessary to prepare a 'builder' file. The main goal is to be able to convert the global files model species into the CHIMERE model species. It is also necessary to manage the several units available, the type of the species (gaseous or aerosol). This part is managed with the scripts/chemprep-prep-boun-data.sh script.

The file XXX_builder (XXX is the name of a global concentrations dataset, GOCART, LMDZ-INCA or MACC at the moment) is used to build the interface between XXX and CHIMERE species. These files are split in 5 files types.

- For gas species : XXX_builder.meca where meca represents the chemical mechanism name (SAPRC/MELCHIOR1/MELCHIOR2)
- For SOA : XXX_buider.aer.soa where soa represents the SOA mechanism used (simple/medium/complex)
- For dust : XXX_buider.dust if the DUST specie are taken into account
- For primary aerosol species : XXX.car if the carbonaceous species are taken into account and ppmcarb if there are no carbonaceous species.
- For sea salts : xxx_builder.nacl if the sea salts are taken into account

Should any modification be added to the chemical scheme, these builders have to be modified accordingly. For example, the builder for LMDz-INCA and the SAPRC chemical mechanism is chemprep/boundaries_spec/INCAv2012_builder.saprc as:

```
# Coarse species, typde, number of corresponding CHIMERE species,
# and for each species: name, molar mass, conversion factor
ALKAN     gas  1    ALK3   59.    1.
AROM      gas  1    ARO2  119.    1.
C2H4      gas  1    C2H4   28.    1.
C2H6      gas  1    ALK1   30.    1.
C3H6      gas  1    OLE1   72.    1.
CH2O      gas  1    HCHO   30.    1.
CH3CHO    gas  1    CH3CHO 44.    1.
CH4       gas  1    CH4    16.    1.
CO        gas  1    CO     28.    1.
H2O2      gas  1    H2O2   34.    1.
HNO3      gas  1    HNO3   63.    1.
NH3       gas  1    NH3    17.    1.
NO2       gas  1    NO2    46.    1.
O3        gas  1    O3     48.    1.
PAN       gas  1    PAN   100.    1.
SO2       gas  1    SO2    64.    1.
```

All global forcing data are given in netcdf format with one file per month. Additional information on the input data are provided in the netcdf attributes for each variable. The most important attributes are "unit":

- **ppp** for part per part (mixing ratio),
- **ppb** for part per billion of 1e9 ppp,
- **ug** for micro-gram per cubic meter)

"typ" indicates if the variable is a gas ("gas"), desert dust ("dust") or non-dust aerosol ("aer"). The molar mass as used in the global model should also be provided.
In addition to concentration fields, the input files have latitude and longitude coordinates as well as the vertical grid (either 3D pressure on model levels or surface pressure + alpha and beta coefficients for the sigma-p grid). Would some conversion be required to provide concentrations in ppb to Chimere from the native unit in the global model (e.g. μg m^{-3}), the 3D temperature field is also requested in order to derive air density. Alternatively a constant and 3D uniform temperature of 15^{o}C is used.
The correspondence between the chemical species of the global model and Chimere is handled in the chemprep part of the code. This way, it is possible to use any source of input data for any of the chemical mechanism of Chimere.
It is also **possible to add a new global dataset**: Basic netcdf manipulation using NCO or CDO tools should allow advanced users to convert any global model fields into the appropriate format following the structure of the existing forcings and keeping one file per month, even if high frequency data are available. A new builder also needs to be written for each type of forcing.

9 Meteorology

The meteorological data are used three different times in CHIMERE:

1. **§9.1: Input data**:
   CHIMERE being an off-line model, input meteorological fields are necessary. These input data have to be reformatted to be read by CHIMERE.

2. **§9.2: Diagnostic parameters**:
   Many meteorological parameters are required for a CHIMERE simulation. Depending on the input meteorological driver, they are not always available as input. Thus, in CHIMERE, a diagnostic program may be activated to parameterize the necessary but not provided parameters.

3. **§9.3: Transport and mixing**:
   Once all meteorological data are available, they are used to mix and transport chemical species during the simulation.

9.1 Meteorological input data

CHIMERE is driven by meteorological fields from regional models, such as WRF or AROME or global models such as ECMWF-IFS. Since the CHIMERE 2016 version, there is two different ways for the meteorological data management:

- WRF:
  If the meteorological model is WRF, the output file is directly and completely read in CHIMERE, during the simulation. There is no pre-processing in that case.
- AROME, ECMWF or another:
  Several pre-processor are proposed to homogeneize these various data and deliver a standard meteorological file to be read by the CHIMERE core: the NetCDF file exdomout.nc.

9.1.1 Option activation

The choice of the meteorological driver is done in the chimere.par file. Pre-processors are already developed and proposed with the CHIMERE code for the meteorological models WRF, MM5 and ECMWF/IFS.

```
# Meteorology Driver
   [meteo]     Meteo driver (WRF,MM5,ecm)    : WRF
```

Depending on this choice, the user have to write the path of its meteorological files:

```
   [meteo_DIR]   Meteo driver output dir    : <my_WRF_output_directory>
   [meteo_file]  Meteo file                 : ${meteo_DIR}/WRFOUTan_${dom}_${dim}.nc
   [wrf_geog]    Where is geog from WRF     : ${meteo_DIR}/geo_em_${metdom}.nc
```

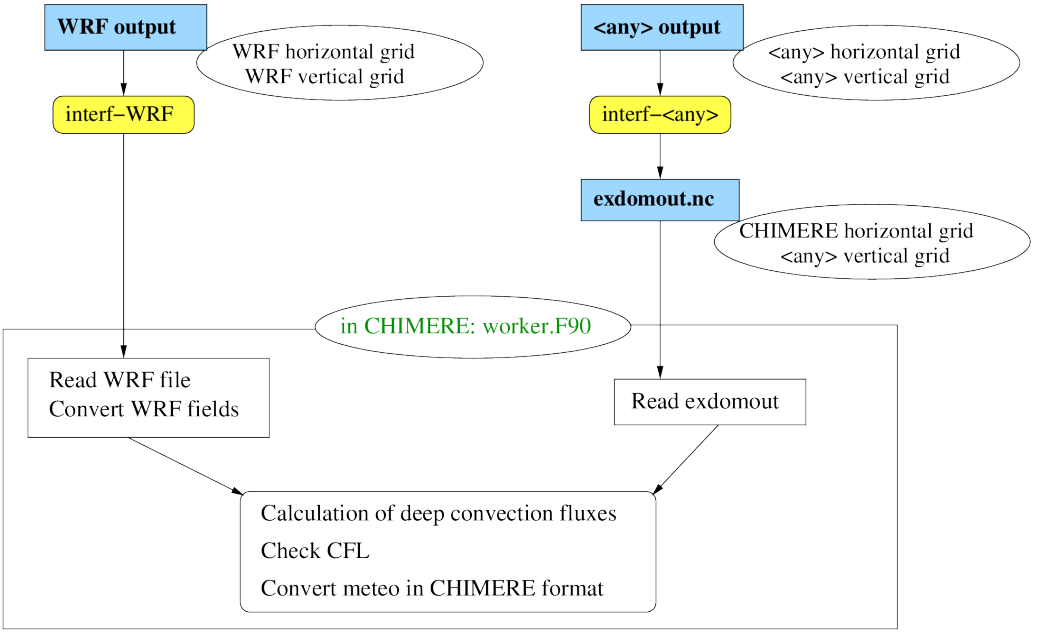


Figure 9.1: *Flow chart of the meteorological CHIMERE pre-processor.*

9.1.2 Case of WRF model output

Most of users are using the WRF model as meteorological driver for CHIMERE simulation. This is certainly the best choice, because:

- WRF is a state of the art model, with many improvements every year
- All validation tests made by the CHIMERE developers are done always using the last WRF version
- CHIMERE is now able to run directly on the WRF grid, avoiding spatial interpolation of all meteorological fields.
- The future developments for CHIMERE will be the on-line coupling between WRF and CHIMERE. All users already using WRF will be able to easily switch to the on-line version.

In preparation of the future on-line WRF-CHIMERE version, many changes were done in CHIMERE. The main goal was to have the complete WRF meteorology inside CHIMERE. This is why the previous pre-processors programs are now integrated in the hourly integration time-step of CHIMERE. The flowchart of this new set-up is presented in Figure 9.1 (left part).
All the programs dedicated to the WRF outputs treatments are in the src/meteo-prepwrf.F90 program. This program will directly read all necessary meteorological variables used in CHIMERE. Note that several assumptions are made in this program and are likely to change the results:

- Following the WRF-ARW documentation (but not the WRF output value), we use always the constant T00=+300 to get the total potential temperature.
- When sea ice is present, an artificial coverage of 10cm of snow is added in order to retrieve the correct albedo. There is no impact on the result (the meteorology being done) but this is a correction for the albedo used later for FastJX.
- A minimum of specific humidity is forced to avoid division by zero: min=10^{-6}kg/kg

9.1.3 Case of any other model output

In case of not using WRF, the user can use already prepared programs (in case of MM5 or ECMWF) or prepare by himself new codes.
If the [meteo] flag in chimere.par is MM5 or ecm, the programs already exist and will be automatically used. If the user wants to use another model, he has to prepare by himself an input file having the format of the exdomout.nc file described in Appendix G.3, p.228
For the the preparation of this exdomout.nc, the script scripts/chimere-meteo.sh calls a program named src/interf-[meteo]. This script calls the prep[metname].F90 fortran program to prepare a generic exdomout.nc file, as presented in Figure 9.1.
The programs such as src/prep-ecm.F90 and src/prep-mm5.F90 read the raw meteorological model output and does several operations:

- It transforms original meteorological variables given on the meteo model grid, at a frequency that is not necessarily one hour, to standard variables given on the CHIMERE horizontal grid as hourly values.
- The operations performed are horizontal and temporal interpolation, wind vector rotation, transformation from perturbation and mean values to the total ones, etc., depending on the original data format.
- Note there is no vertical interpolation (from the meteo file to CHIMERE) to conserve the full vertical resolution, for a better accuracy on turbulent diagnostics made later in CHIMERE (see §9.2)

Table 9.1 lists the variables which must or can be output by the interpolation stage.

CHIMERE name	Variable	Dimension	Units
Mandatory Variables			
lon	longitude of gridpoints	2D	degrees_east
lat	latitude of gridpoints	2D	degrees_north
tem2	2m Temperature	2D	K
soim	Soil moisture	2D	m^3/m^3
rh2m	2m Relative humidity	2D	0-1
lspc	Large-scale Precipitation	2D	$kg/m^2/hour$
copc	Convective Precipitation	2D	$kg/m^2/hour$
temp	Temperature	3D	K
cliq	Cloud liquid water content (excluding rain water)	3D	Kg/Kg
sphu	Specific humidity	3D	kg/kg
pres	Pressure	3D	Pa
alti	Altitude of half layer	3D	m
winz	Zonal component of the wind	3D	m/s
winm	Meridional component of the wind	3D	m/s
swrd	Short Wave Radiation	2D	W/m^2
Optional Variables			
lwrd	Long Wave Radiation	2D	W/m^2
weas	Water equiv. accum. snow depth	2D	mm
sshf	Surface sensible heat flux	2D	W/m2
slhf	Surface latent heat flux	2D	W/m2
usta	Friction velocity	2D	m/s
hght	Boundary layer height	2D	m
snow	Snow depth	2D	cm
psfc	Surface pressure	2D	Pa
rain	rain water profile	3D	Kg/Kg
cice	ice profile	3D	Kg/Kg

Table 9.1: *Mandatory and optional variables in exdomout.nc meteo file. Note that all meteorological 3D variables must be provided at half-layers levels. If the optional variable are not provided by the raw meteorological model, there are intialized to zero and diagnosed if possible.*

The programs are provided for MM5, WRF and IFS/ECMWF.

9.2 Diagnostics of parameters:

The second stage of the meteorological fields treatment is directly in the CHIMERE model, and during the hourly integration phase. Note that compared to the previous versions of CHIMERE, all these programs replace the *diagmet* programs.
All programs are called by the worker.F90 routine and are:

- readmetro: routine for the hourly reading of the *exdomout.nc* file (in meteorological fields are not from WRF model)
- calc_turb: calculation of turbulence on raw meteo profiles
- calc_winw: calculation of the vertical wind speed on chimere profiles
- calc_deepconv: calculation of deep convection fluxes (if required by the user)
- checkcfl: Estimation of the adaptative time-step
- met2chim: Conversion of units from the meteo format to the specifc CHIMERE format (molecules, centimeters and seconds).

9.2.1 Management of additional parameters

These calculations are done in the src/calc_turb.F90 routine. The first calculation is done to estimate several meteorological parameters, mandatory for CHIMERE but not always available with the meteorological input files. These parameters correpond to the optional parameters listed in Table 9.1. The calculations are done using the meteorological fields provided in the *exdomout.nc* file, i.e already projected on the horizontal CHIMERE grid but still on the native meteo model vertical grid.
The availability of these parameters is checked during the reading of the exdomout.nc file or directly into the WRF file. If the parameters exist, they are not recalculated, contrarily to the previous versions of CHIMERE where it was a user's option. Indeed, we consider that if the variables exist, they correspond to recent parameterization in the meteorological model used and are consistent with other variables. They thus have to be keep.
The following variables are calculated:

1. the friction velocity u_* and the bulk Richardson number R_{iB},
2. the surface sensible heat flux Q_0,
3. the Monin-Obukhov length L ,
4. the vertical convective velocity w_*,
5. the boundary layer height $\overline{h}$,
6. the vertical diffusivity profile K_z.

9.2.1.1 The friction velocity u_*

The friction velocity u_* is used for the deposition and calculation of diffusivities. It is a particularly sensitive parameter for ozone in summer through the calculation of the aerodynamic resistance r_a. Friction velocity is thus sensitive to the land use type, which is critical to deposition. In large scale meteorological models, roughness lengths are often too coarse for the implementation of high-resolution deposition. Therefore an update of u_* is

proposed following the [Louis et al., 1982] formulation which is particularly robust. We recommend to use this alternative formulation, no matter whether u_* is available in the input fields, in order to have a deposition that is consistent with the high-resolution land use.

$$u_* = \sqrt{C_{DN}^2 \, F_m \, |U|^2} \tag{9.1}$$

with $|U|$ the mean wind speed at 10 m above ground level, F_m is the [Louis et al., 1982] stability function and C_{DN} the momentum transfer coefficient as:

$$C_{DN} = \frac{k}{ln\left(\frac{z}{z_{0m}}\right)} \tag{9.2}$$

with k=0.41 the Karman constant, z the altitude where the wind speed $|U|$ is known and z_{0m}, the momentum roughness length. The momentum stability function F_m is estimated depending on the bulk Richardson number, R_{ib}, value. R_{ib} is estimated at each altitude z as:

$$R_{ib}(z) = \frac{g \, z}{\overline{\theta_v(z)}} \frac{\overline{\theta_v(z)} - \overline{\theta_v(z_0)}}{|U(z)|^2} \tag{9.3}$$

with g=9.81 m^2 s^{-2} the gravitational acceleration and θ_v the virtual potential temperature in Kelvin.

- In unstable cases, if $R_{ib} < 0$:

$$F_m = 1 - \frac{2b \, R_{ib}}{1 + 3b \, c \, C_{DN}^2 \cdot \sqrt{\frac{z}{z_{0m}}} \sqrt{|R_{ib}|}} \tag{9.4}$$

- In stable cases, if $R_{ib} > 0$:

$$F_m = \frac{1}{1 + \frac{2b \, R_{ib}}{\sqrt{1 + d \, R_{ib}}}} \tag{9.5}$$

with the constant $b = c = d$=5. In neutral case, i.e R_{ib}=0, F_m=1.

9.2.1.2 The surface sensible heat flux Q_0

The surface sensible heat flux, Q_0, is used to compute w_* and therefore mixing, and the height of the boundary layer. In fact only the virtual heat flux is required, which can be recomputed from an empirical formula [Priestley, 1949] using temperatures in the first model layers. This formula is not very accurate. It is strongly advised to use heat fluxes from the meteorological model if available. If the surface sensible heat flux Q_0 is provided by the meteorological model, it is directly used for the computation of the convective velocity w_*:

$$w_* = \left(\frac{g \, Q_0 \, \overline{h}}{\rho \, C_p \, \overline{\theta_v}}\right)^{1/3} \tag{9.6}$$

where $\overline{h}$ is the convective boundary layer height, C_p the specific heat of air at constant pressure, $\overline{\theta_v}$ the mean virtual potential temperature in the first model vertical level.

9.2.1.3 The Monin-Obhukov length L

The Monin-Obhukov length is estimated as:

$$L = \frac{-\overline{\theta_v}\, u_*^3}{k\, g\, Q_0} \tag{9.7}$$

9.2.1.4 The boundary layer height $\overline{h}$

The boundary layer height ($\overline{h}$) is derived from different formulation depending on the atmospheric static stability. When stable, i.e when $L > 0$, $\overline{h}$ is estimated as the altitude when the Richardson number reaches a critical number here chosen as R_{ic}=0.5, following [Troen and Mahrt, 1986].
In unstable situations (i.e. convective), $\overline{h}$ is estimated using a convectively-based boundary layer height calculation. This is based on a simplified and diagnostic version of the approach of [Cheinet and Teixeira, 2003] which consists in the resolution of the (dry) thermal plume equation with diffusion. The in-plume vertical velocity and buoyancy equations are solved and the boundary layer top is taken as the height where calculated vertical velocity vanishes. Thermals are initiated with a non-zero vertical velocity and potential temperature departure, depending on the turbulence similarity parameters in the surface layer.

9.2.1.5 The vertical diffusivity profile K_z

Once the depth of the boundary layer is computed, vertical turbulent mixing can be applied following the K-diffusion framework following the parameterisation of [Troen and Mahrt, 1986], without counter-gradient term. In each model column, the diffusivity coefficient profile K_z (m^2 s^{-1}) is calculated as:

$$K_z = k w_s \frac{z}{\overline{h}} \left(1 - \frac{z}{\overline{h}}\right)^2 \tag{9.8}$$

where w_s is a vertical scale given by similar formulas:

- In the stable case (when the surface sensible heat flux is negative):

$$w_s = \frac{u_*}{(1 + 4.7 z/L)} \tag{9.9}$$

- In the unstable case:

$$w_s = (u_*^3 + 2.8\, e\, w_*^3)^{1/3} \tag{9.10}$$

where $e = max(0.1, z/\overline{h})$. A minimal K_z is assumed, with a value of 0.01 m^2 s^{-1} in the dry boundary layer and of 1 m^2 s^{-1} in the cloudy boundary layer. K_z is capped to a maximal value of K_z=500 m^2 s^{-1} to avoid unrealistic mixing. Above the boundary layer, a fixed value of K_z=0.1 m^2 s^{-1} is prescribed. As for many CTMs considered as numerically diffusive, horizontal turbulent fluxes are not considered.

9.2.1.6 Urban corrections and other tunable parameters

Finally, all three-dimensional meteorological fields are averaged over the CHIMERE vertical grid. Note that several fixed parameters are present in this src/calc_turb.F90 routine. They were chosen are the more realistic as possible and it is not recommended to modify these values. These constant valeus are listed in Table 9.2.
Note that a urban correction is available in the model. This is very simple and just implemented to retrieve some observed trends in urban areas: less surface wind speed and more surface sensible heat flux.
This option may be activated with in the chimere.par parameter file as:

```
   [urbancorr]    Urban correction [1] or not [0]    : 0
```

Parameter	Value	Description	Unit
pblmin	20.	Minimum PBL height	m
vkminup	0.1	Minimum Kz above PBL	m2/s
addwind	0.8	Urban wind correction factor	m/s
addflux	0.	Urban Q_0 correction additive term	m2/s2
z10m	10.	10 meters above ground level	m
soimdef	1.0	Default Soil Moisture (no resuspension/erosion)	m3/m3
woff	0.5	Wind offset to smooth Richardson numbers	m/s
crhx	0.90	Min RH for cloud BLH enhancement	[0:1]
vkmax	500.	Maximum Kz	m2/s
odclw	180.0	Optical depth rate for liquid water	ad.
odcic	66.66	Optical depth rate for ice	ad.
topcldmax	1000.	Maximum altitude of low clouds top	m
cloh	1	High cloud option for attenuation	ad.
crhh	0.95	High cloud option for attenuation	ad.
cloh2	0.005	High clouds optical depth /m for RH=1	ad.
ztherm	25.0	Height of thermals start	m
ric	0.5	Troen and Mahrt suggestion for critical Ri for BL top	ad.
dvsca	1000.0	Entrain./Detrain. first guess vertical scale	m
vkmindry	0.01	Minimum Kz in the dry boundary layer	m2/s
vkminwet	1.0	Minimum Kz in cloudy boundary layer	m2/s
rlam	150.	Upper air mixing length	m

Table 9.2: *Constant values used for the calculation of additionnal parameters in the routine calc_turb.*

This flag induces a slight change for the 10m wind speed and Q_0 the surface sensible heat flux, only over urbanized areas as:

$$U_{10m,urb} = addwind \times U_{10m} \quad (9.11)$$

$$Q_{0,urb} = addflux + Q_0 \quad (9.12)$$

For the diagnostics calculations, some other parameters are fixed and depends on the landuse. They are tabulated in the src/calc_turb.F90 routine and for the 9 landuse classes of CHIMERE.

Category	1	2	3	4	5	6	7	8	9
Landuse	Agricultural	Grassland	Barren land	Inland water	Urban	Shrubs	Needleaf forest	Broadleaf forest	Ocean
z_0 (m)	monthly	0.1	0.01	0.0001	1.0	0.15	1.0	1.0	0.0001
UV albedo (no snow)	0.035	0.04	0.1	0.07	0.035	0.05	0.025	0.025	0.07
UV albedo (snow)	0.376	0.720	0.836	0.07	0.3	0.558	0.278	0.558	0.836

Table 9.3: *Tabulated values needed for the diagnostic of additional meteorological parameters. The values of UV albedo are extracted from (Laepple et al. 2005) for all meteorological conditions, except when snow is detected, where they are extracted from (Tanskannen et al. 2007).*

For the first landuse type, Agricultural, a typical monthly variability is tabulated as presented in Table 9.4.

Month	1	2	3	4	5	6	7	8	9	10	11	12
z_0 (m)	0.05	0.05	0.05	0.1	0.15	0.15	0.15	0.1	0.1	0.05	0.05	0.05

Table 9.4: *Tabulated monthly variability of the roughness length for the landuse category # 1 "Agricultural".*

9.2.2 Estimation of the vertical velocity

This calculation is done in the src/calc_winw.F90 routine. The vertical velocity is diagnosed by using the horizontal fluxes. A simple momentum conservation relation is applied to calculate the vertical flux for the top of each model box (assuming that the first one, near the ground, is zero).

9.2.3 Calculation of the solar zenithal angle

The solar zenithal angle has to be diagnosed for two different processes:

- The calculation of the photolysis rates using the FastJX module
- The calculation of the biogenic emissions

Its calculation is done following the method described in [Jacobson, 1999]. This calculation is done in the src/zenith.F90 routine.
The cosine of the solar zenithal angle is defined as:

$$cos(\theta_s) = sin(\phi)sin(\delta) + cos(\phi)cos(\delta)cos(H_a) \tag{9.13}$$

with:

- θ_s the solar zenithal angle
- ϕ the latitude
- δ the solar declination angle
- H_a the local hour angle of the sun

The solar declination angle is estimated as:

$$\delta = arcsin(sin(\epsilon_{ob})sin(\lambda_{ec})) \tag{9.14}$$

with:

- ϵ_{ob} the obliquity of the ecliptic
- λ_{ec} the ecliptic longitude of the Earth

The obliquity of the ecliptic, ϵ_{ob}, is calculated as:

$$\epsilon_{ob} = 23.439 - 10^7 \times N_{jD} \tag{9.15}$$

with N_{jD} the number of days since the the 1st January 2000. This estimation is automatically and hourly done using the src/calendar.F90 time calculations routines. The ecliptic longitude λ_{ec} is calculated as:

$$\lambda_{ec} = L_M + 1.915sin(g_M) + 0.02sin(2g_M) \tag{9.16}$$

with L_M and g_M the mean longitude of the sun and the mean anomaly, respectively. They also depend on the current Julian day and are estimated as:

$$L_M = 280.46 + 0.9856474N_{jD} \tag{9.17}$$
$$g_M = 357.528 + 0.9856003N_{jD} \tag{9.18}$$

Finally, the local hour angle of the sun H_a is calculated as:

$$H_a = \frac{2\pi t_s}{86400} \tag{9.19}$$

where t_s is the number of seconds past local noon.

9.2.4 Deep convection fluxes

The calculation of deep convection fluxes is a user's choice and can be activated or not in the chimere.par namelist file as:

```
[ideepconv]   Deep convection activation (1/0)   : 1
```

If the option is on, the calculations of deep convection fluxes are done in the calc_deepconv routine.

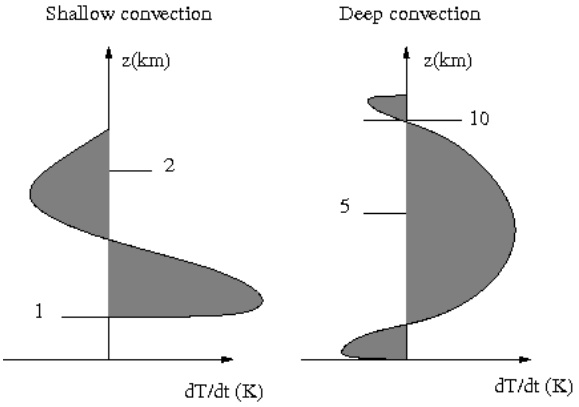


Figure 9.2: *Temperatures changes due to shallow and deep convection*

The deep convection scheme describes effects of subgrid scale clouds on tropospheric convection, after [Tiedtke, 1989] and as presented in Figure 9.2. Deep convection occurs when cumulus or cumulo-nimbus clouds (referenced as convective clouds) are present. These clouds are formed when air masses are unstable, when warm air is at the surface or cold air is transported in upper layers (cold front). High vertical wind speed are observed leading to vertically extended cloud structures. On the other hand, when clouds are only due to mechanical forcings (mountains, warm fronts), they are named stratiform clouds and generally exhibit low vertical speed values.

Air masses may be quickly mixed in the troposphere when convective unstabilities occured under a cloud. To describe this phenomenon, schemes generally consider a cloud (and the whole column including this cloud) and the environment. In the major part of deep convection parameterizations, the hypothesis of small cloud surface compared to the total studied surface is done.

Under the cloud, updrafts and downdrafts are observed, Figure 9.3. The updraft originates from air masses lighter than their environment when downdrafts represent fall of colder air (often with rain). In the updraft and the downdraft, air may be exchange between the cloud and the environment: if air of environment flows to the cloud, this is the **entrainment** and if air of clouds flows towards environment, this is the **detrainment**. In order to ensure mass conservation, a compensatory **subsidence** is observed in the environment.

In CHIMERE, the Tiedtke scheme is implemented. The main goal of this scheme is to estimated a convection mass flux:

$$M(z) = \rho(z)(a_{up}\overline{w_{up}(z)} + a_{dw}\overline{w_{dw}(z)}) = -\rho(z)a_{env}\overline{w_{env}(z)} \tag{9.20}$$

with $\overline{w_{up}(z)} > 0$, $\overline{w_{dw}(z)} < 0$ et $\overline{w_{ent}(z)} < 0$ the vertical wind speed in the updrafts, downdrafts and environment, respectively. The vertical gradient of this mass flux is:

$$\frac{\partial M(z)}{\partial z}(z) = E(z) - D(z) \tag{9.21}$$

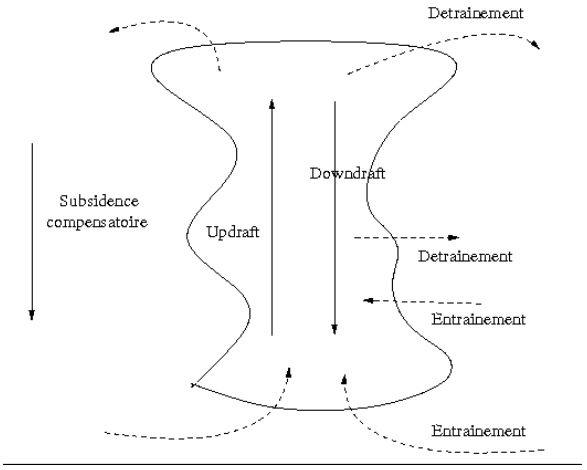


Figure 9.3: *Schematic view of a convective cloud*

with $E(z) > 0$ et $D(z) > 0$, the entrainment and detrainment fluxes. This equation works both for updrafts and downdrafts, with, for example for the updraft:

$$E(z) = E_{up}(z) + E_{dw}(z) \text{ and } D(z) = D_{up}(z) + D_{dw}(z) \tag{9.22}$$

An example of estimated fluxes are displayed in the Figure 9.4 .

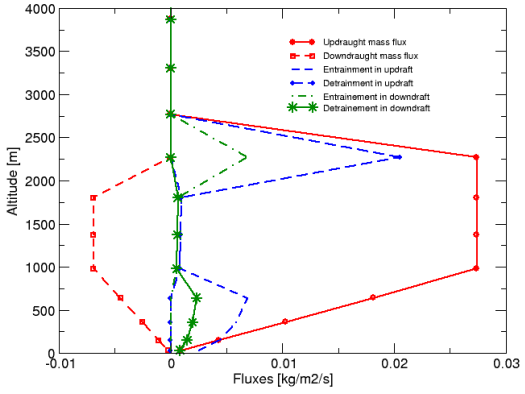


Figure 9.4: *Entrainment and detrainment fluxes in the updrafts and downdrafts.*

These fluxes are used to estimates chemical concentrations fluxes as:

$$\frac{\partial M_{up}(z)c_{up}(z)}{\partial z} = E_{up}(z)c_{env} - D_{up}(z)c_{up} \tag{9.23}$$

$$\frac{\partial M_{dw}(z)c_{dw}(z)}{\partial z} = E_{dw}(z)c_{env} - D_{dw}(z)c_{dw} \tag{9.24}$$

with the concentrations c_{up}, c_{dw} and c_{env} in the updraft, downdraft and environment, respectively. The parametrization is designed with the parameter names such as in the Figure 9.5 .

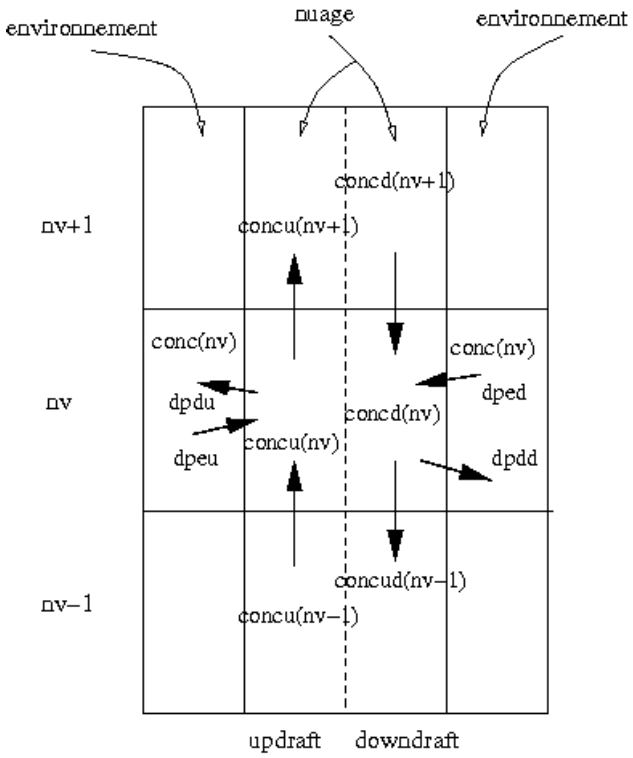


Figure 9.5: *Convective atmospheric column and its environment*

The net flux is first estimated in the src/locvalues.f90 routine. At this stage, the fluxes are in molecules.cm^{-2}.s^{-1} (after conversion in src/iniphys.f90). For each grid cell, the Equation 9.21 is applied to give 'updraught mass flux' (flxuloc) and 'downdraught mass flux' (flxdloc). The calculation is done from surface to top domain in order to ensure mass conservation following the relation:

$$\begin{aligned} FLXU(z) = & \frac{\partial M_{up}(z)}{\partial z}(z) = E_{up}(z) - D_{up}(z) + FLXU(z-1) \\ FLXD(z) = & \frac{\partial M_{dw}(z)}{\partial z}(z) = E_{dw}(z) - D_{dw}(z) + FLXD(z-1) \end{aligned} \tag{9.25}$$

The top level of the cloud and the detrainment (when $E_{dw}(z) > 0$) are estimated separately and names 'nvcloudtop' and 'nvdettop', respectively.
These fluxes are used in the src/transmix.f90 routine. One have to note that the 'concu', 'concd' parameters are not concentrations but ratios of pollutants molecules number on air molecules number. This conversion is done to ensure 'trpr' and 'trlo' production and loss fluxes terms in molecule.cm^{-3}.s^{-1}. 'concu' and 'cond' are estimated using the mass conservation relation, as for example:

$$\begin{aligned} FLXU(nv) \times concu(nv) = & FLXU(nv-1) \times concu(nv-1) \\ & + dpeu(nv) \times conc(nv) \\ & - dpdu(nv) \times concu(nv) \end{aligned} \tag{9.26}$$

and we have:

$$concu(nv) = \frac{FLXU(nv-1) \times concu(nv-1) + dpeu(nv) \times conc(nv)}{dpdu(nv) + FLXU(nv)} \tag{9.27}$$

9.3 Transport and mixing

9.3.1 Horizontal transport

9.3.1.1 Option activation

Three schemes for horizontal transport of chemical concentrations in the model are now available. The choice of the scheme is activated in the chimere.par file as:

```
[iadv]      Advection scheme (0..2) : 2
```

where the three possible values are:

1. iadv=0 : The **upwind scheme**. A simple first-order upwind scheme with a low computational cost but not very accurate and very diffusive.
2. iadv=1 : The third-order **PPM** scheme (PPM stands for 'Parabolic Piecewise Method'), proposed by [Colella and Woodward, 1984]): high computational cost but more accurate for long-live species, naturally diffusive in a chemistry-transport model
3. iadv=2 : The second-order **Van Leer** scheme: low computational cost and good accuracy for transport of high concentrations in plumes.

By default, all species are transported with the same scheme. But the user's has the option to manually change that, by modifying the second column of the ACTIVE_SPECIES file in its chemprep inputdata directory.
These schemes are defined in dedicated su-programs: src/upwind.F90 for upwind, src/ppm.F90 for PPM and src/vanleer.F90 for Van Leer. The diagnosed fluxes are then used for transport and mixing in the src/transmix.F90 program.

9.3.1.2 The transport equation

For a given chemical species with concentration c, the following conservation equation is numerically solved:

$$\partial_t (c\rho) + \partial_i \mathbf{F^i} = 0 \tag{9.28}$$

with ρ is the air density and F indicating the mass flux corresponding to velocity $\mathbf{v}$:

$$\mathbf{F} = \rho c \mathbf{v} \tag{9.29}$$

As CHIMERE is designed for structured grids where the grid cells are nearly parallelepipedic, this equation can be discretized and solved separately for each of the three orthogonal directions: zonal, meridional and vertical. This strategy is known as *operator splitting*. Even though the use of operator splitting may generate some numerical problems, this technique is very widely used in weather modelling and chemistry-transport modelling, both because it is more computationnally efficient and also sometimes more stable and accurate than a bi- or tri-dimensional approach, particularly when it is applied to high-order models ([Byun et al., 1999]). Therefore, the tendency c_t in the concentration c is equal to $c_t^{(1)} + c_t^{(2)} + c_t^{(3)}$, where $c_t^{(i)}$ is the time derivative of concentration due to transport in the i^{th} direction. It is also assumed that the time variations of ρ are much slower than the time variations of c ($|c\rho_t| \ll |\rho c_t|$), so that Eq. 9.28 becomes:

$$\rho c_t^{(i)} = -\partial_i \mathbf{F^i} \tag{9.30}$$

After time and space discretisation, if we note $\delta^{(i)}c$ the variation of c due to transport in direction i, the discretized transport equations are the following:

$$\delta^{(i)}c = -\left(\frac{F^i_{n+\frac{1}{2}}(t) - F^i_{n-\frac{1}{2}}(t)}{\Delta x}\right)\Delta t \tag{9.31}$$

The concentration increments are calculated successively for each direction from the initial concentration field (parallel strategy). This equation secures mass conservation because the inward and outward fluxes cancel out in each direction. The time integration is of order 1. The key issue in solving this equation is the estimation of the fluxes at the cell interfaces ($F^i_{n\pm\frac{1}{2}}(t)$). The way these fluxes are estimated numerically determines the characteristics of the transport scheme (scheme type and order, diffusivity, numerical stability etc.).
In chemistry-transport models, various types of numerical schemes have been tested and are proposed to users to solve the advection equations. These numerical schemes range from simple order-1 numerical schemes such as the classical upwind method to higher-order methods such as the Piecewise-parabolic method ([Colella and Woodward, 1984]) proposed in CHIMERE.
In the horizontal directions, it is assumed that the grid cell length does not vary substantially from one grid cell to its neighbours. As in the CHIMERE model, species concentrations and meteorological variables are represented on the same grid, the wind speed at the interfaces is interpolated linearly from the wind speeds at the centers of the two gridcells separated by the interface. The wind speed at the interface will be noted $u_{n\pm\frac{1}{2}}(t)$, and is assumed constant during each coarse time step. In the following we will drop the superscript i to indicate the direction. The definition of the wind speed at the cell interface is independent of the scheme used, so that the definition of the fluxes at the interfaces only depends on the evaluation of the concentration at the interface.
Three horizontal transport schemes are available in the model.

9.3.1.3 Upwind scheme

In the upwind scheme ([Courant et al., 1952]), the fluxes at the cell interfaces are defined by the following equations according to the sign of the wind speed at the cell interface:

- If $u_{n+\frac{1}{2}}(t) > 0$

$$F_{n\pm\frac{1}{2}}(t) = c_n \rho_n u_{n+\frac{1}{2}}(t) \tag{9.32}$$

- If $u_{n+\frac{1}{2}}(t) < 0$

$$F_{n\pm\frac{1}{2}}(t) = c_{n+1} \rho_n u_{n+\frac{1}{2}}(t) \tag{9.33}$$

The assumption made in this scheme is that the tracer concentration is uniform in each grid cell, so that the mass flux at the interface is the product of the wind at the interface by the tracer concentration in the upwind cell.

9.3.1.4 Van Leer scheme

The Van Leer scheme used in CHIMERE is commonly called Van Leer I because it is the first one described in the seminal paper of [Van Leer, 1979]. This scheme is of order 2 in space, it assumes that the concentration inside a grid cell is described by a linear slope between the two cell interfaces:

$$c_n(x) = c_n + (x - x_n)\Delta_n \tag{9.34}$$

where the slope Δ_n is determined according to the following cases. If $c_{n-1} \leq c_n \leq c_{n+1}$ or $c_{n-1} \geq c_n \geq c_{n+1}$ then:

$$\Delta_n = sign\left(c_{n+1} - c_{n-1}\right) \times \min\left(\frac{c_{n+1} - c_{n-1}}{2\Delta x}, \frac{c_{n+1} - c_n}{\Delta x}, \frac{c_n - c_{n-1}}{\Delta x}\right) \quad (9.35)$$

where, in this case, Δ_n is the smallest slope that can be estimated between cell n and its closest neighbours. Otherwise, c_n is an extremum of concentration and the concentration within cell n is assumed constant ($\Delta_n = 0$) which ensures that the scheme is monotonic.
This scheme, which is recognized in meteorology for its good numerical accuracy and smaller diffusion than the first-order upwind scheme, is also slightly more time-consuming than the first-order upwind scheme. In meteorology, it can be considered as a good compromise solution between numerical accuracy and computational efficiency for long-range transport ([Hourdin and Armengaud, 1999]).

9.3.1.5 The Parabolic Piecewise Method scheme

Another scheme that is proposed in CHIMERE for horizontal transport is the 3^{rd} order Parabolic Piecewise method (PPM) scheme, with slope-limiting and monotonicity-preserving conditions, such as presented in [Colella and Woodward, 1984]. This scheme is applied for each dimension separately, which formally limits the model to 2^d order accuracy in solving the two-dimensional transport problem because the cross derivative $\partial c^2/\partial x \partial y$ is not taken into account. However, since the scheme is symmetric, it can be considered that the errors due the neglect of cross-derivatives approximately compensate ([Ullrich et al., 2010]). Therefore, since the treatment of transport in each horizontal dimension has 3^{rd} order accuracy, the PPM scheme as implemented in CHIMERE is much less diffusive than the simple 2^d order Van Leer scheme (see, e.g. [Vuolo et al., 2009]).

9.3.2 Vertical transport

9.3.2.1 Option activation

Three schemes for horizontal transport of chemical concentrations in the model are now available. The choice of the scheme is activated in the chimere.par file as:

```
   [iadvv]  Vertical advection scheme (0..1)    : 1
```

where the two possible values are:

1. iadvv=0 : The **upwind scheme**. A simple first-order upwind scheme with a low computational cost but not very accurate and very diffusive.
2. iadvv=1 : The second-order **Van Leer** scheme: low computational cost and good accuracy for transport of high concentrations in plumes.

9.3.2.2 The transport equation

Vertical transport is assumed to balance horizontal mass divergence. The vertical mass flux of dry air is calculated columnwise for each cell interface in the vertical direction, successively from model bottom to model top, in the following way :

- In the lowest layer, the lateral mass imbalance is calculated by summing up all the incoming mass fluxes at the lateral boundaries of the cell and substracting the outgoing mass fluxes at lateral boundaries, the wind at the upper interface of the lowest model layer is then calculated in order to compensate this mass

imbalance by an opposite flux at the cell's upper boundary. This calculation is performed at the first order, assuming that the density of the air crossing a cell boundary is equal to the average density of the upstream cell, both for horizontal and vertical transport.

- The same calculation is then performed successively for each cell in all the column up to the model top, balancing the total imbalance of the mass flux from lateral and lower boundaries by an opposite mass flux at the upper boundary. These vertical transport mass fluxes (independent of species) are calculated first at each coarse time step in routine src/vtransport.f90

The calculation of the concentration tendancies due to vertical transport for each model species is then performed at each fine time step in routine src/transmix.f90. As the latter transport scheme needs two concentration values upstream of the considered boundary and one concentration value downstream, and this can not be secured next to model bottom and model top, CHIMERE switches back to upwind vertical transport for the cells where only one value of upstream concentration is available within the vertical simulation domain (including the boundary condition at model top).

9.3.3 Turbulent mixing

At each interface between layers k and k+1, one calculates an equivalent turbulent vertical velocity V_k and vertical mixing is expressed in layer k by the mass flux:

$$\text{Net Flux} = \frac{V_k(C_{k+1}.D_k/D_{k+1} - C_k)}{H_k} \tag{9.36}$$

where C denotes concentrations, D densities and H layer thicknesses. Density ratios are applied since turbulent mixing must conserve mass in each model cell. An equivalent formula is used for the upper layer. The turbulent velocity V_k is deduced from K(z) using:

$$V_k = \frac{K_z}{(\frac{1}{2}(H_k + H_{k+1}))} \tag{9.37}$$

When the top of the boundary layer is above the model top, H_{k+1} is replaced by h - <model-top> in the previous equation.
The K(z) profile is calculated in routine src/calc_turb.F90 and the turbulent velocity profile in routine src/mixing.F90. Vertical mixing mass fluxes (independent of species, first order) are calculated first at each coarse time step in routine src/vtransport.F90, then the complete calculation using the species concentration is performed at each fine time step in routine src/transmix.F90.

10 CHIMERE time integration

10.1 The several time-steps

CHIMERE simulation is split into two main parts: initialization and the time integration (Figure 10.1).

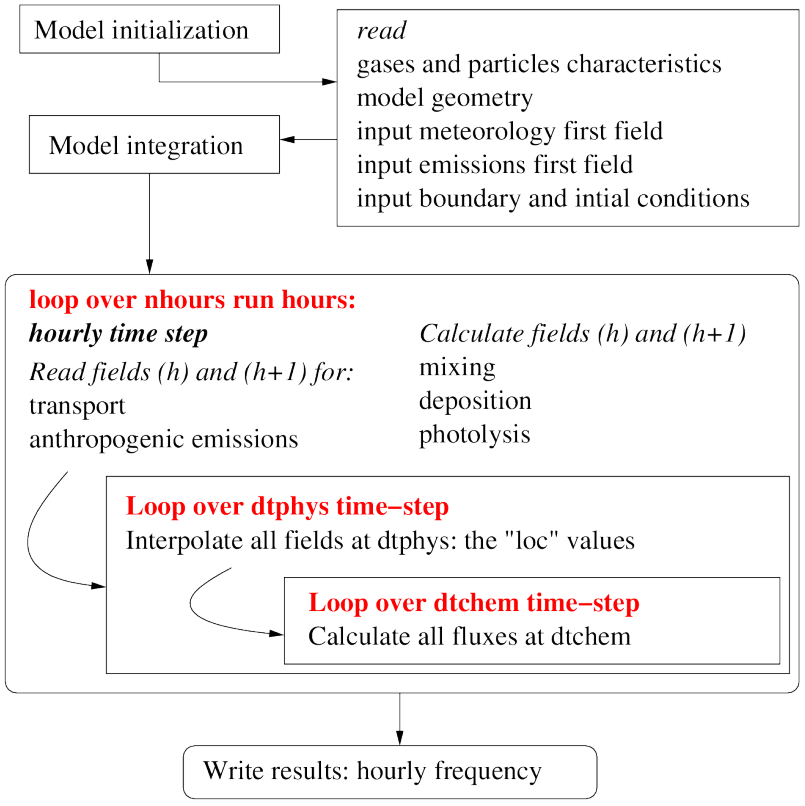


Figure 10.1: *General CHIMERE structure for the time integration of all processes*

At the **initialization** stage the model reads all input parameters, as well as two first meteorological and emissions fields (in order to start the run with realistic meteorological and concentrations fields). The **time integration** stage is itself split into two parts:

- A user-defined *physical* time step called dtphys
- A user-defined *chemical* time step called dtchem

These parameters can be changed in the chimere.par file as:

```
[dtphys]      Physical time steps (in mn)     : 15
[dtchem]      Chemical time step (in mn)      : 5
```

10.1.1 The physical time-step

In former release (prior to the CHIMERE2016 release) CHIMERE main time loop had an hourly frequency, due to input and output parameters. This hourly frequency was mandatory because of:

- The input parameters: the meteorological fields and the anthropogenic emissions are often provided at an hourly frequency. Note that if the meteorology has a lower frequency (i.e 3h), the meteo-prepwrf interface interpolates these fields to retrieve hourly frequency.
- The output parameters: for comparison to observations, the concentrations fields are written with an hourly frequency.

This hourly loop has been removed since the CHIMERE2016a release and replaced by a **do while** that is incremented in second at the physical time step frequency. However, this does not change the fact that some operations are required to be done with a hourly frequency. Therefore, a test on the current time in order to assess wether or not the current physical time step is the first of a new hour, is used for some operations. This suppression of the hourly loop has has been done in view of a future increase of some parameter frequency.

The physical time-step is a user-defined value and does not really depend on the transport. The forcing variables (wind, temperature, humidity, emissions) being hourly provided or diagnosed, this step is used to refine these values in order to have more realistic sub-hourly values. The refined values are calculated in src/locvalues.F90 with a simple linear interpolation as:

$$T_{loc} = w_2 \times T_{h1} + w_1 \times T_{h2} \tag{10.1}$$

with w_1 and w_2 are the linear interpolation weights, estimated as:

$$w_1 = thour \tag{10.2}$$
$$w_2 = 1 - w_1 \tag{10.3}$$

The parameter $thour$ is an increment (between 0 and 1) representing the exact time between two entire hours. This parameter is first defined in src/checkcfl.F90 as:

$$thour = \frac{0.5}{nphour} \tag{10.4}$$

then incremented during the physical loop in src/worker.F90 as:

$$thour = thour + \frac{1}{nphour} \tag{10.5}$$

The weak point of this approach is the linear interpolation of the meteorological and emissions data. In reality, all processes are not varying linearly from one hour to the next one. But, this is difficult to predict the real sub-hourly variability for most of the variables. The impact of lack of knowledge will have an impact on the results: more the physical time-step is small (then the $nphour$ parameter is high) and more the variable value will be closest to its high temporal frequency value. More the spatial resolution is high or the more the chemistry is fast and more it is recommended to decrease this physical time-step. Some arbitrary recommended values are of the order: dtphys=15 mn for a large domain, low chemistry and $\Delta x \approx 0.5^o$ to dtphys=5 mn for $\Delta x \approx 5$ km.

10.1.2 The chemical time-step and the CFL criteria

The chemical time-step called $dtchem$ has to respect the Courant-Freidrich Levy (CFL) conditions, since the fluxes (momentum, turbulent, deep convection) are used to update the chemical concentrations at this chemical

time-step. It the user can proposed a time-step, this is also calculated to have an adaptative time-step. There is two ways to manage this step:
If the user proposed:

```
[dtchem]      Chemical time step (in mn)      : 5
```

The adaptative time-step is calculated in src/checkcfl.F90 but if the value if found to be larger that the user request (here dtchem=5mn), the user request is finally saved for the model integration.
The other possible choice for the user is:

```
[dtchem]      Chemical time step (in mn)      : 0
```

The adaptative time-step is also calculated and is directly used. This ensures to have the lowest possible duration for the whole simulation. Note that since the adaptative time-step is diagnosed using the meteorological data with (h) and $(h+1)$, this time-step remains constant during one hour.
The CFL criteria is defined as:

$$u \times \frac{\Delta t}{\Delta x} < CFL_{max} \tag{10.6}$$

where CFL_{max}=1, u is the wind speed in a grid cell, Δt the time-step and Δx the horizontal resolution. The time-step has to be selected in order to have this criterion being respected. Originally used for horizontal transport only, we extended in CHIMERE this criterion to the vertical wind speed and the deep convection fluxes. The main goal of this estimation is to ensure that a parcel of air (including chemically active concentrations) is not allowed to travel accross a grid cell during a single time-step.
In order to ensure a maximum of robustness in the model, this criterion is increased with the following (tunable) value in the src/chimere_params.F90:

```
real(kind=iprec),parameter :: cflmax=0.8
```

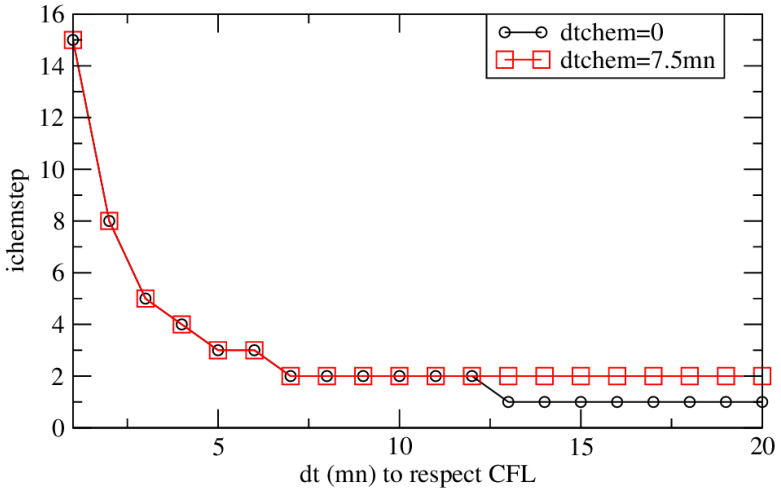


Figure 10.2: *Calculation of the number of integration chemical steps per physical steps to satisfy the CFL criterion.*

An example of adaptative time-step is displayed in Figure 10.2. For a specific meteorology, a $dtchem$ time-step is evaluated (here from 1 to 20mn). In this case, we consider that the user wants, at least, a time-step of 7.5mn. The physical time-step is fixed to 15mn. If $dtmin$=1, we have to have 15 $ichemstep$ values. The more the $dtmin$ increases the more the $ichemstep$ value decreases. If the user wants a full adaptative time-step

(i.e $dtchem$=0), $ichemstep$ may decrease until $ichemstep$=1 (for $dtmin$ >13). If the users wants at least $dtchem$=7.5, then $ichemstep$ is constrained and will decrease until $ichemstep$=2 only (even if it was found to be not necessary, following the CFL criterion).

10.2 The TWO-STEP time numerical solver

The numerical method for the temporal solution of the stiff system of partial differential equations is adapted from the second-order TWOSTEP algorithm originally proposed by [Verwer, 1994] for gas phase chemistry only. The calculation is performed in src/twostep_mod.F90. It is based on the application of a Gauss-Seidel iteration scheme to the two-step implicit backward differentiation (BDF2) formula:

$$c^{n+1} = \frac{4}{3}c^n - \frac{1}{3}c^{n-1} + \frac{2}{3}\Delta t R(c^{n+1}), \tag{10.7}$$

with c^n being the vector of chemical concentrations at time t_n, Δt the time step leading from time t_n to $t_n + 1$ and $R(c) = \dot{c} = P(c) - L(c)c$ the temporal evolution of the concentrations due to chemical production and emissions (P) and chemical loss and deposition (L). Note that L is a diagonal matrix here. After rearranging and introducing the production and loss terms this equation reads

$$c^{n+1} = \left(I + \frac{2}{3}\Delta t L(c^{n+1})\right)^{-1} \left(\frac{4}{3}c^n - \frac{1}{3}c^{n-1} + \frac{2}{3}\Delta t P(c^{n+1})\right). \tag{10.8}$$

The implicit nonlinear system obtained in this scheme can be solved pertinently with a Gauss-Seidel method.

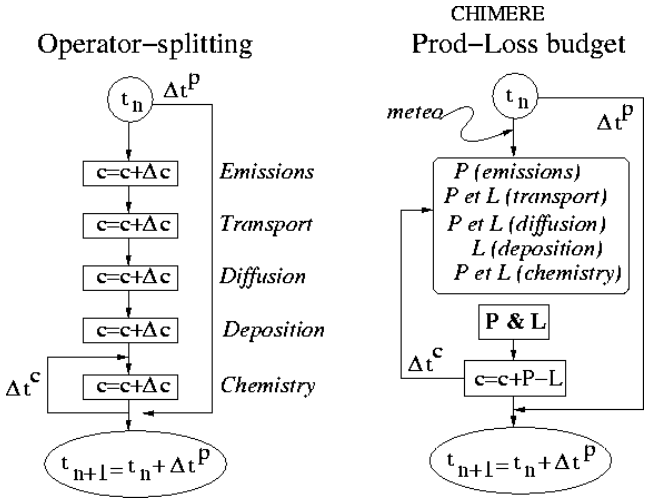


Figure 10.3: *Principle of 'operator-splitting' versus Chimere integration*

In CHIMERE the production and loss terms P and L in Equation 10.8 are replaced by the modified terms $\tilde{P} = P + P_h + P_v$ and $\tilde{L} = L + L_h + L_v$, respectively.

- P_h and P_v denote the temporal evolution of the concentrations due to horizontal (only advection) and vertical (advection and diffusion) inflow into the concerned grid box,
- L_h and L_v the temporal evolution due to the respective outflow divided by the concentration itself.

With this integration scheme, at each time step all physical and chemical processes are updated simultaneously. The "operator splitting" technique (see e.g. [McRae et al., 1982], which is still a standard way of solving

the 3D transport-chemistry-problem, and the associated "splitting error" are therefore avoided. Further advantages of the scheme are its stability even for quite long time steps due to the implicitness of the formulation and the simplicity of the code which facilitates the development of secondary models (adjoint, tangent linear) enormously.
It is strongly recommended, in order to have accurate results, to use 2 Gauss-Seidel iterations, which increases by 2 the computer time. This parameter has to be selected in the chimere.par file as:

```
[ngs]       Number of Gauss-Seidel iterations              : 2
[nsu]        - during spinup                               : 3
[irs]        - number of spinup hours                      : 1
```

This change affects mostly concentrations during morning. However, for values of ozone concentration, the proposed version does not appear to degrade simulations, especially during afternoon hours.
To ensure a correct initialization of the model (mostly when climatological boundary conditions are used for the first hour integration), it is also recommended to force a higher number of Gauss-Seidel iterations: here, for example, 3 Gauss-Seidel iterations for a spin-up time of 1 hour.

11 Gas-phase chemistry

11.1 Option activation

CHIMERE offers the option to include different gas phase chemical mechanisms. The choice of the mechanism is managed in the chimere.par file as:

```
[mecachim]    Chemistry mechanism (0..3)          : 3
```

with the following possibilities:

1. mecachim=0: no gas phase chemistry
2. mecachim=1: The complete MELCHIOR mechanism called MELCHIOR1
3. mecachim=2: The reduced MELCHIOR mechanism called MELCHIOR2
4. mecachim=3: The SAPRC-07-A mechanism

- **MELCHIOR1**:
  The original, complete MELCHIOR scheme ([Lattuati, 1997]) describes more than 300 reactions of 80 gaseous species.
  The hydrocarbon degradation is fairly similar to the EMEP gas phase mechanism ([Simpson, 1992]). Adaptations are made in particular for low NO_x conditions and NO_x-nitrate chemistry. All rate constants are updated according to [Atkinson et al., 1997] and [De Moore et al., 1994]. Heterogeneous formation of HONO from deposition of NO2 on wet surfaces is now considered, using the formulation of [Aumont et al., 2003].
- **MELCHIOR2**:
  In order to reduce the computing time a reduced mechanism, **MELCHIOR2**, with less than species and about 120 reactions is derived from MELCHIOR ([Derognat et al., 2003]), following the concept of "chemical operators" ([Carter, 1990]).
- **SAPRC**:
  The gas phase chemical mechanism SAPRC-07-A is also available, [Carter, 2010] [1]. It describes more than 275 reactions of 85 species and it is the most recent mechanism proposed in CHIMERE.

11.2 The MELCHIOR mechanims

11.2.1 Species list of the reduced MELCHIOR1 gas-phase chemical mechanism

Species	Definition
Inorganic compounds	
O3	ozone
H2O2	hydrogen peroxide
OH	hydroxy radical
HO2	hydroperoxy radical
NO	nitric oxide

[1] http://www.engr.ucr.edu/~carter/SAPRC/

NO2 ..... nitrogen dioxide
NO3 ..... nitrogen trioxide
N2O5 ..... dinitrogen pentoxide
HONO ..... nitrous acide
HNO3 ..... nitric acide
HNO4 ..... pernitric acide
CO ..... carbon monoxide
SO2 ..... sulfur dioxide
H2SO4 ..... sulfuric acid

Hydrocarbon species [2]

CH4 ..... methane
C2H6 ..... ethane
NC4H10 ..... n-butane
C2H4 ..... ethene
C3H6 ..... propene
OXYL ..... o-xylene
C5H8 ..... isoprene
APINEN ..... α-pinene
BPINEN ..... β-pinene
LIMONE ..... limonene
TERPEN ..... terpenes (lumped class)
HUMULE ..... Humulene (lumped class)
OCIMEN ..... Ocimene (lumped class)

Alcohol species

C2H5OH ..... ethanol
CH3OH ..... methanol

Carbonyls

HCHO ..... formaldehyde
CH3CHO ..... acetaldehyde
CH3COE ..... methyl ethyl ketone
CH3COY ..... dimethyl glyoxal
MEMALD 4-oxo-2-pentenal
MAC ..... methacroleine
MVK ..... methyl vinyl ketone
GLYOX ..... glyoxal
MGLYOX ..... methyl glyoxal
OFURAN 5-methyle-3H-furan-2-one

Organic nitrates

CH3NO3 ..... methyl nitrate
ETNO3 ..... ehtyl nitrate
BUNO3 ..... n-butyl-2-nitrate
ISNI ..... unsaturated nitrate from RO2P1
CARNIT ..... nitrate carbonyl taken as α-nitrooxy acetone
ORNIT1 ..... α-hydroperox nitrate
ORNIT2 ..... α-hydroperoxy nitrate from C5H8 and APINEN

(Per)oxy radicals

C2H5O2 ..... perxoy ethyl
CH2O2C ..... ethyl hydroperoxy
CH3O2 ..... methyl peroxy
CH3COO ..... peroxy acetyl radical
CH3CHX ..... propyl hydroperoxy
CH3COX ..... peroxy from butan-2-one
CH3COZ ..... peroxy from MACO2+NO reaction
SECBUO ..... 2-oxy butyl
SECC4H ..... peroxyl butyl
OXYL1 ..... peroxy radical from OXYL
RO2IP1 ..... peroxy radical from C5H8+OH reaction
MEMAL1 ..... adition of OH on MEMALD
MEMAL2 ..formed from the abstraction of an hydrogen in alpha position
MACO2 ..... peroxy radical from MAC+OH reaction
MVKO2 ..... peroxy radical from MVK
APIOH ..... Peroxy radical from APINEN+OH reaction

Peroxy nitrates

RNC2H4 ..... peroxy ethyl nitrate
RNC3H6 ..... peroxy propyl nitrate
RNC5H8 ..... peroxy from C5H8+NO3 reaction
ROXYL1 ..... peroxy from OXYL+NO3 reaction
ISNIR ..... peroxy from ISNI+OH reaction
APINO3 ..... Peroxy radical from APINEN+NO3 reaction

Pernitrates

PAN ..... peroxyacetyl nitrate
MACPAN ..... peroxy acyl nitrate from MAC
CH3NO4 ..... methyl pernitrate
MEMPAN ..... peroxy acyl nitrate from MEMAL2

Peroxide

APIO2H ..... hydroperoxyde from APINENOH+HO2 reaction
BUO2H ..... Butyl hydroperoxyde
CH3O2C ..... hydroxyethyl hydroperoxide
CH3O2H ..... methyl hydroperoxide
CH4CHX ..... hydroxypropyl hydroperoxide
CH4COX butan-2-one-3-hydroperoxide
CH4COZ ..... hydroperoxide from CH3COZ+HO2 reaction
ETO2H ..... ethyl hydroperoxide
MACO2H ..... hydroperoxy from MACO2+HO2 reaction
MEMAH2 ..... hydroperoxy from MEMAL2+HO2 reaction
MEMALH ..... hydroperoxy from MEMAL1+HO2 reaction
MVKO2H ..... hydroperoxy from MVKO2+HO2 reaction
OXYLH1 ..... hydroperoxy from OXYL1+HO2 reaction
PEROX ..... hydroperoxy from RO2P1+HO2 reaction
PPA ..... peroxy acetyl acid

11.2.2 Reaction list of the reduced MELCHIOR1 chemical mechanism

Reactions	Kinetic constants
Inorganic	
O3+NO→NO2	k(T)=A$e^{-B/T}$,A=1.8e-12,B=1370
O3+NO2→NO3	k(T)=A$e^{-B/T}$,A=1.2e-13,B=2450

[2] Hydrocarbon model species (except for CH4 and C2H4) represent groups of hydrocarbons with similar reactivity. As "definition" a typical representative of this group is given. This is also true for the degradation products.

Reactions	Kinetic constants
O3+OH→HO2	k(T)=A$e^{-B/T}$,A=1.9e-12,B=1000
O3+HO2→OH	k(T)=A$e^{-B/T}$,A=1.4e-14,B=600
NO+HO2→OH+NO2	k(T)=A$e^{-B/T}$,A=3.7e-12,B=-240
NO2+OH+M→HNO3	k(T,M)=mtroe(3.4e-30,0,3.2,4.77e-11,0,1.4,0.30)
HO2+OH→H2O	k(T)=A$e^{-B/T}$,A=4.8e-11,B=-250
H2O2+OH→HO2	k(T)=A$e^{-B/T}$,A=2.9e-12,B=160
HNO3+OH→NO3	k(T)=A$e^{-B/T}$,A=7.2e-15,B=-785
HNO3+OH+M→NO3	k(T,M)=troe(1.9e-33,-725,0,4.1e-16,-1440,0,1)
CO+OH→HO2+CO2	k(T)=A$e^{-B/T}$(300/T)^N,A=1.3e-13,B=0,N=1
CO+OH+M→HO2+CO2	k=3.21e-33
H2+OH→HO2	k(T)=A$e^{-B/T}$,A=7.7e-12,B=2100
HO2+HO2→H2O2	k(T)=A$e^{-B/T}$,A=2.2e-13,B=-600
HO2+HO2+M→H2O2	k(T)=A$e^{-B/T}$,A=1.7e-33,B=-1000
HO2+HO2+H2O→H2O2	k(T)=A$e^{-B/T}$,A=3.22e-34,B=-2800
HO2+HO2+H2O+M→H2O2	k(T)=A$e^{-B/T}$,A=2.38e-54,B=-3200
NO3+HO2→NO2+OH	k=4e-12
NO3+H2O2→HNO3+HO2	k=2e-15
NO3+O3→NO2	k=1e-17
NO3+NO→2*NO2	k(T)=A$e^{-B/T}$,A=1.8e-11,B=-110
NO3+NO3→2*NO2	k(T)=A$e^{-B/T}$,A=8.5e-13,B=2450
NO2+NO3→NO+NO2	k(T)=A$e^{-B/T}$,A=4.5e-14,B=1260
NO2+NO3+M→N2O5	k(T,M)=troe(2.7e-30,0,3.4,2e-12,0,-0.2,0.33)
N2O5+M→NO3+NO2	k(T,M)=troe(1e-3,11000,3.5,9.7e14,11080,-0.1,0.33)
NO2+HO2+M→HNO4	k(T,M)=troe(1.8e-31,0,3.2,4.7e-12,0,0,0.6)
HNO4+M→HO2+NO2	k(T,M)=troe(5e-6,10000,0,2.6e15,10900,0,0.6)
HNO4+OH→NO2	k(T)=A$e^{-B/T}$,A=1.5e-12,B=-360
NO+OH+M→HONO	k(T,M)=troe(7.e-31,0,2.6,1.5e-11,0,0.5,0.6)
HONO+OH→NO2	k(T)=A$e^{-B/T}$,A=1.8e-11,B=390
NO2→HONO+NO2	ks=0.5*depo(NO2)
SOx	
SO2+CH3O2→H2SO4+HCHO+HO2	k=4e-17
SO2+OH+M→H2SO4+HO2	k(T,M)=troe(4e-31,0,3.3,2e-12,0,0,0.45)
OH	
CH4+OH→CH3O2	k(T)=A$e^{-B/T}$,A=2.3e-12,B=1765
C2H6+OH→C2H5O2	k(T)=A$e^{-B/T}$,A=7.9e-12,B=1030
C2H4+OH+M→CH2O2C	k(T,M)=troe(7e-29,0,3.1,9e-12,0,0,0.7)
C3H6+OH+M→CH3CHX	k(T,M)=troe(8e-27,0,3.5,3e-11,0,0,0.5)
CH3OH+OH→HCHO+HO2	k(T)=A$e^{-B/T}$,A=3.1e-12,B=360
C2H5OH+OH→CH3CHO+HO2	k(T)=A$e^{-B/T}$,A=4.1e-12,B=70
OH	
HCHO+OH→CO+HO2	k(T)=A$e^{-B/T}$,A=8.6e-12,B=-20
CH3CHO+OH→CH3COO	k(T)=A$e^{-B/T}$,A=5.6e-12,B=-310
CH3COE+OH→CH3COX	k(T)=A$e^{-B/T}$(300/T)^N,A=2.92e-13,B=-414,N=-2
MEMALD+OH→MEMAL1	k=5.6e-11
GLYOX+OH→2*CO+HO2	k=1.1e-11
MGLYOX+OH→CH3COO+CO	k=1.5e-11
OFURAN+OH→MVKO2	k=6.9e-11
MAC+OH→0.5*MACO2	k(T)=A$e^{-B/T}$,A=1.86e-11,B=-175
MVK+OH→MVKO2	k(T)=A$e^{-B/T}$,A=4.1e-12,B=-453
CH3O2H+OH→CH3O2	k(T)=A$e^{-B/T}$,A=1.9e-12,B=-190
ETO2H+OH→C2H5O2	k(T)=A$e^{-B/T}$,A=1.9e-12,B=-190
PPA+OH→CH3COO	k(T)=A$e^{-B/T}$,A=1.9e-12,B=-190
BUO2H+OH→SECC4H	k(T)=A$e^{-B/T}$,A=1.9e-12,B=-190
CH4COX+OH→CH3COX	k(T)=A$e^{-B/T}$,A=1.9e-12,B=-190

Reactions	Kinetic constants
CH3O2C+OH→CH2O2C	k(T)=A$e^{-B/T}$,A=1.9e-12,B=-190
CH4CHX+OH→CH3CHX	k(T)=A$e^{-B/T}$,A=1.9e-12,B=-190
OXYLH1+OH→OXYL1	k(T)=A$e^{-B/T}$,A=1.9e-12,B=-190
MEMALH+OH→MEMAL1	k(T)=A$e^{-B/T}$,A=1.9e-12,B=-190
MEMAH2+OH→MEMAL2	k(T)=A$e^{-B/T}$,A=1.9e-12,B=-190
PEROX+OH→RO2IP1	k(T)=A$e^{-B/T}$,A=1.9e-12,B=-190
MACO2H+OH→MACO2	k(T)=A$e^{-B/T}$,A=1.9e-12,B=-190
MVKO2H+OH→MVKO2	k(T)=A$e^{-B/T}$,A=1.9e-12,B=-190
CH4COZ+OH→CH3COZ	k(T)=A$e^{-B/T}$,A=1.9e-12,B=-190
APIO2H+OH→APIOH	k(T)=A$e^{-B/T}$,A=1.9e-12,B=-190
CH3O2H+OH→HCHO+OH	k(T)=A$e^{-B/T}$,A=1.e-12,B=-190
ETO2H+OH→CH3CHO+OH	k(T)=A$e^{-B/T}$(300/T)^N,A=1.30e-13,B=-1176,N=-2
BUO2H+OH→CH3COE+OH	k(T)=A$e^{-B/T}$(300/T)^N,A=6.1e-14,B=-1681,N=-2
CH4COX+OH→CH3COY+OH	k(T)=A$e^{-B/T}$(300/T)^N,A=6.1e-14,B=-1533,N=-2
CH3O2C+OH→2*HCHO+OH	k(T)=A$e^{-B/T}$(300/T)^N,A=1.30e-13,B=-1238,N=-2
CH3O2C+OH→2*HCHO+OH	k(T)=A$e^{-B/T}$(300/T)^N,A=4.05e-13,B=-688,N=-2
CH4CHX+OH→HCHO+CH3CHO+OH	k(T)=A$e^{-B/T}$(300/T)^N,A=4.05e-13,B=-688,N=-2
CH4CHX+OH→HCHO+CH3CHO+OH	k(T)=A$e^{-B/T}$(300/T)^N,A=6.1e-14,B=-1681,N=-2
OXYLH1+OH→MEMALD+MGLYOX+OH	k=1.44e-10
MEMALH+OH→GLYOX+MGLYOX+OH	k(T)=A$e^{-B/T}$(300/T)^N,A=1.71e-13,B=-1403,N=-2
MEMAH2+OH→MALEIC+CH3O2	k=1.27e-11
PEROX+OH→0.43*MAC+0.57*MVK+HCHO+OH	k=8.22e-11
MACO2H+OH→CH3COZ	k=1.28e-11
MVKO2H+OH→0.28*HCHO+0.28*MGLYOX+0.28*OH+0.72*CH3CHO +0.72*CH3COO	k(T)=A$e^{-B/T}$(300/T)^N,A=4.05e-13,B=-1032,N=-2
MVKO2H+OH→0.28*HCHO+0.28*MGLYOX+0.28*OH+0.72*CH3CHO +0.72*CH3COO	k(T)=A$e^{-B/T}$(300/T)^N,A=6.1e-14,B=-1595,N=-2
CH4COZ+OH→CH3COE+OH	k=5.14e-11
APIO2H+OH→CH3CHO+CH3COE+OH	k(T)=A$e^{-B/T}$(300/T)^N,A=1.91e-13,B=-1193,N=-2
APIO2H+OH→CH3CHO+CH3COE+OH	k(T)=A$e^{-B/T}$(300/T)^N,A=3.82e-13,B=-882,N=-2
NO3	
CH4+NO3→CH3O2+HNO3	k=4e-19
C2H6+NO3→C2H5O2+HNO3	k=8e-18
NC4H10+NO3→SECC4H+HNO3	k=5.5e-17
C2H4+NO3→RNC2H4	k=2e-16
C3H6+NO3→RNC3H6	k=9.45e-15
OXYL+NO3→ROXYL1+HNO3	k=3.7e-16
C5H8+NO3→RNC5H8	k=7.8e-13
CH3OH+NO3→CH3O2+HNO3	k(T)=A$e^{-B/T}$,A=1.3e-12,B=2560
C2H5OH+NO3→C2H5O2+HNO3	k=9e-16
HCHO+NO3→CO+HNO3+HO2	k=5.8e-16
CH3CHO+NO3→CH3COO+HNO3	k=2.8e-15
CH3O2+NO3→HCHO+HO2+NO2	k=1.2e-12
C2H5O2+NO3→CH3CHO+NO2+HO2	k=1.2e-12
CH3COO+NO3→CH3O2+NO2+CO2	k=4e-12
CH2O2C+NO3→2*HCHO+NO2+HO2	k=1.2e-12
SECC4H+NO3→SECBUO+NO2	k=1.2e-12
CH3COX+NO3→CH3COY+NO2+HO2	k=1.2e-12
CH3CHX+NO3→HCHO+CH3CHO+NO2+HO2	k=1.2e-12
OXYL1+NO3→MEMALD+MGLYOX+NO2+HO2	k=1.2e-12
MEMAL1+NO3→GLYOX+MGLYOX+NO2+HO2	k=1.2e-12
MEMAL2+NO3→MALEIC+NO2+CH3O2	k=4e-12
MACO2+NO3→CH3COZ+NO2+CO2	k=4e-12
RO2IP1+NO3→0.38*MAC+0.50*MVK+0.88*HCHO+0.12*RO2IP1 +0.88*HO2+NO2	k=1.2e-12

Reactions	Kinetic constants
MVKO2+NO3→0.28*MGLYOX+0.28*HCHO+0.72*CH3CHO +0.72*CH3COO+0.28*HO2+NO2	k=1.2e-12
CH3COZ+NO3→CH3COE+HO2+NO2	k=1.2e-12
APIOH+NO3→CH3CHO+CH3COE+NO2+HO2	k=1.2e-12
RNC2H4+NO3→0.5*CARNIT+HCHO +1.5*NO2+0.5*HO2	k=1.2e-12
RNC3H6+NO3→0.5*CARNIT+0.5*CH3CHO+0.5*HCHO +1.5*NO2+0.5*HO2	k=1.2e-12
ROXYL1+NO3→BENZAL+NO2+HO2	k=1.2e-12
ISNIR+NO3→0.95*CH3CHO+0.475*CH3COE+0.475*MGLYOX +0.05*ISNI+0.05*HO2+1.9*NO2	k=1.2e-12
RNC5H8+NO3→0.85*ISNI+0.1*MAC+0.05*MVK+0.15*HCHO +1.1*NO2+0.8*HO2	k=1.2e-12
APINO3+NO3→CH3CHO+CH3COE+2*NO2	k=1.2e-12
O3	
C2H4+O3→HCHO+0.12*HO2+0.13*H2+0.44*CO	k(T)=A$e^{-B/T}$,A=9.1e-15,B=2580
C3H6+O3→0.53*HCHO+0.5*CH3CHO+0.31*CH3O2+0.28*HO2 +0.15*OH+0.065*H2+0.4*CO+0.7*CH4	k(T)=A$e^{-B/T}$,A=5.5e-15,B=1880
C5H8+O3→0.67*MAC+0.26*MVK+0.55*OH+0.07*C3H6+0.8*HCHO +0.06*HO2+0.05*CO+0.3*O3	k(T)=A$e^{-B/T}$,A=1.2e-14,B=2013
MAC+O3→0.8*MGLYOX+0.7*HCHO+0.215*OH+0.275*HO2 +0.2*CO+0.2*O3	k(T)=A$e^{-B/T}$,A=5.3e-15,B=2520
MVK+O3→0.82*MGLYOX+0.8*HCHO+0.04*CH3CHO+0.08*OH +0.06*HO2+0.05*CO+0.2*O3	k(T)=A$e^{-B/T}$,A=4.3e-15,B=2016
PEROX+O3→0.7*HCHO	k=8e-18
organic	
CH3O2+NO→HCHO+NO2+HO2	k(T)=A$e^{-B/T}$,A=4.2e-12,B=-180
C2H5O2+NO→CH3CHO+NO2+HO2	k=8.7e-12
CH3COO+NO→CH3O2+NO2+CO2	k=2e-11
CH2O2C+NO→2*HCHO+NO2+HO2	k=9e-12
SECC4H+NO→SECBUO+NO2	k=4e-12
SECC4H+NO+M→SECBUO+NO2	k(T,M)=troe(-3.76e-32,0,0,-3.3e-12,0,8.1,0.41)
SECBUO+M→CH3COE+HO2	k(T)=A$e^{-B/T}$,A=3.0e-14,B=200
SECBUO→CH3CHO+C2H5O2	k(T)=A$e^{-B/T}$,A=7.20e+12,B=5780
CH3COX+NO→CH3COY+NO2+HO2	k=4e-12
CH3CHX+NO→HCHO+CH3CHO+NO2+HO2	k=4e-12
OXYL1+NO→MEMALD+MGLYOX+NO2+HO2	k=4e-12
MEMAL1+NO→GLYOX+MGLYOX+NO2+HO2	k=4e-12
MEMAL2+NO→MALEIC+NO2+CH3O2	k=1.4e-11
MACO2+NO→CH3COZ+NO2+CO2	k=1.4e-11
RO2IP1+NO→0.32*MAC+0.42*MVK+0.74*HCHO+0.14*ISNI +0.12*RO2IP1+0.78*HO2+0.86*NO2	k(T)=A$e^{-B/T}$,A=1.4e-11,B=180
MVKO2+NO→0.266*MGLYOX+0.266*HCHO+0.684*CH3CHO +0.684*CH3COO+0.05*ISNI+0.266*HO2+0.95*NO2	k(T)=A$e^{-B/T}$,A=1.4e-11,B=180
CH3COZ+NO→CH3COE+HO2+NO2	k(T)=A$e^{-B/T}$,A=1.4e-11,B=180
APIOH+NO→0.8*CH3CHO+0.8*CH3COE+0.8*NO2+0.8*HO2+0.2*ISNI	k=4e-12
organic	
CH3O2+HO2→CH3O2H	k(T)=A$e^{-B/T}$,A=4.1e-13,B=-790
C2H5O2+HO2→ETO2H	k(T)=A$e^{-B/T}$,A=2.7e-13,B=-1000
CH3COO+HO2→0.67*PPA+0.33*O3	k(T)=A$e^{-B/T}$,A=4.3e-13,B=-1040
SECC4H+HO2→BUO2H	k(T)=A$e^{-B/T}$,A=2.7e-13,B=-1000
CH3COX+HO2→CH4COX	k(T)=A$e^{-B/T}$,A=2.7e-13,B=-1000
CH2O2C+HO2→CH3O2C	k(T)=A$e^{-B/T}$,A=2.7e-13,B=-1000
CH3CHX+HO2→CH4CHX	k(T)=A$e^{-B/T}$,A=2.7e-13,B=-1000
OXYL1+HO2→OXYLH1	k(T)=A$e^{-B/T}$,A=2.7e-13,B=-1000
MEMAL1+HO2→MEMALH	k(T)=A$e^{-B/T}$,A=2.7e-13,B=-1000

Reactions	Kinetic constants
MEMAL2+HO2→MEMAH2	k(T)=A$e^{-B/T}$,A=2.7e-13,B=-1000
RO2IP1+HO2→PEROX	k(T)=A$e^{-B/T}$,A=2.7e-13,B=-1000
MACO2+HO2→MACO2H	k(T)=A$e^{-B/T}$,A=2.7e-13,B=-1000
MVKO2+HO2→MVKO2H	k(T)=A$e^{-B/T}$,A=2.7e-13,B=-1000
CH3COZ+HO2→CH4COZ	k(T)=A$e^{-B/T}$,A=2.7e-13,B=-1000
APIOH+HO2→APIO2H	k(T)=A$e^{-B/T}$,A=2.7e-13,B=-1000
CH3O2+CH3O2→2*HCHO+2*HO2	k(T)=SPECIAL_1(1.1e-13,-365,25,1165)
CH3O2+CH3O2→HCHO+CH3OH	k(T)=SPECIAL_2(1.1e-13,-365,25,1165)
C2H5O2+CH3O2→CH3CHO+HCHO+2*HO2	k(T)=SPECIAL_3(6.4e-14,0,1.1e-13,-365,10.2,533,25,1165)
C2H5O2+CH3O2→CH3CHO+CH3OH	k(T)=SPECIAL_4(6.4e-14,0,1.1e-13,-365,10.2,533,25,1165)
C2H5O2+CH3O2→C2H5OH+HCHO	k(T)=SPECIAL_4(6.4e-14,0,1.1e-13,-365,25,1165,10.2,533)
CH3COO+CH3O2→CH3O2+CO2+HCHO+HO2	k(T)=SPECIAL_1(5.1e-12,-272,4.4e5,3910)
CH3COO+CH3O2→MECOOH+HCHO	k(T)=SPECIAL_2(5.1e-12,-272,4.4e5,3910)
SECC4H+CH3O2→SECBUO+HCHO+HO2	k(T)=SPECIAL_3(1.2e-12,1500,1.1e-13,-365,50,1165,25,1165)
SECC4H+CH3O2→CH3COE+CH3OH	k(T)=SPECIAL_4(1.2e-12,1500,1.1e-13,-365,50,1165,25,1165)
SECC4H+CH3O2→CH3COE+HCHO	k(T)=SPECIAL_4(1.2e-12,1500,1.1e-13,-365,25,1165,50,1165)
CH3COX+CH3O2→CH3COY+HCHO+2*HO2	k(T)=SPECIAL_3(5.5e-11,1500,1.1e-13,-365,50,1165,25,1165)
CH3COX+CH3O2→CH3COY+CH3OH	k(T)=SPECIAL_4(5.5e-11,1500,1.1e-13,-365,50,1165,25,1165)
CH3COX+CH3O2→CH3COY+HCHO	k(T)=SPECIAL_4(5.5e-11,1500,1.1e-13,-365,25,1165,50,1165)
CH2O2C+CH3O2→3*HCHO+2*HO2	k(T)=SPECIAL_3(2.3e-12,0,1.1e-13,-365,50,1165,25,1165)
CH2O2C+CH3O2→2*HCHO+CH3OH	k(T)=SPECIAL_4(2.3e-12,0,1.1e-13,-365,50,1165,25,1165)
CH2O2C+CH3O2→3*HCHO	k(T)=SPECIAL_4(2.3e-12,0,1.1e-13,-365,25,1165,50,1165)
CH3CHX+CH3O2→CH3CHO+2*HCHO+2*HO2	k(T)=SPECIAL_3(1.3e-10,2200,1.1e-13,-365,50,1165,25,1165)
CH3CHX+CH3O2→CH3CHO+HCHO+CH3OH	k(T)=SPECIAL_4(1.3e-10,2200,1.1e-13,-365,50,1165,25,1165)
CH3CHX+CH3O2→CH3CHO+2*HCHO	k(T)=SPECIAL_4(1.3e-10,2200,1.1e-13,-365,25,1165,50,1165)
RNC3H6+CH3O2→0.5*CARNIT+1.5*HCHO+0.5*CH3CHO +0.5*NO2+1.5*HO2	k(T)=SPECIAL_3(1.3e-10,2200,1.1e-13,-365,50,1165,25,1165)
RNC3H6+CH3O2→CARNIT+CH3OH	k(T)=SPECIAL_4(1.3e-10,2200,1.1e-13,-365,50,1165,25,1165)
RNC3H6+CH3O2→ORNIT1+HCHO	k(T)=SPECIAL_4(1.3e-10,2200,1.1e-13,-365,25,1165,50,1165)
OXYL1+CH3O2→MEMALD+MGLYOX+HCHO+2*HO2	k(T)=SPECIAL_3(2.1e-13,-600,1.1e-13,-365,50,1165,25,1165)
OXYL1+CH3O2→MEMALD+MGLYOX+CH3OH	k(T)=SPECIAL_4(2.1e-13,-600,1.1e-13,-365,50,1165,25,1165)
OXYL1+CH3O2→MEMALD+MGLYOX+HCHO	k(T)=SPECIAL_4(2.1e-13,-600,1.1e-13,-365,25,1165,50,1165)
MEMAL1+CH3O2→GLYOX+MGLYOX+HCHO+2*HO2	k(T)=SPECIAL_3(1.3e-11,800,1.1e-13,-365,50,1165,25,1165)
MEMAL1+CH3O2→GLYOX+MGLYOX+CH3OH	k(T)=SPECIAL_4(1.3e-11,800,1.1e-13,-365,50,1165,25,1165)
MEMAL1+CH3O2→GLYOX+MGLYOX+HCHO	k(T)=SPECIAL_4(1.3e-11,800,1.1e-13,-365,25,1165,50,1165)

Reactions	Kinetic constants
MEMAL2+CH3O2→MALEIC+CH3O2+HCHO+HO2	k(T)=SPECIAL_1(5.1e-12,-272,4.4e5,3910)
MEMAL2+CH3O2→MAA+HCHO	k(T)=SPECIAL_2(5.1e-12,-272,4.4e5,3910)
RO2IP1+CH3O2→0.3*MVK+0.3*MAC+1.6*HCHO+2*HO2	k(T)=SPECIAL_3(1.3e-11,800,1.1e-13,-365,50,1165,25,1165)
RO2IP1+CH3O2→0.3*MVK+0.3*MAC+0.6*HCHO+CH3OH	k(T)=SPECIAL_4(1.3e-11,800,1.1e-13,-365,50,1165,25,1165)
RO2IP1+CH3O2→0.3*MVK+0.3*MAC+1.6*HCHO	k(T)=SPECIAL_4(1.3e-11,800,1.1e-13,-365,25,1165,50,1165)
RNC5H8+CH3O2→0.6*ISNI+HCHO+2*HO2	k(T)=SPECIAL_3(1.3e-11,800,1.1e-13,-365,50,1165,25,1165)
RNC5H8+CH3O2→0.6*ISNI+CH3OH	k(T)=SPECIAL_4(1.3e-11,800,1.1e-13,-365,50,1165,25,1165)
RNC5H8+CH3O2→0.6*ISNI+HCHO	k(T)=SPECIAL_4(1.3e-11,800,1.1e-13,-365,25,1165,50,1165)
MACO2+CH3O2→CH3COZ+CO2+HCHO+HO2	k(T)=SPECIAL_1(5.1e-12,-272,4.4e5,3910)
MACO2+CH3O2→MAA+HCHO	k(T)=SPECIAL_2(5.1e-12,-272,4.4e5,3910)
MVKO2+CH3O2→MGLYOX+2*HCHO+2*HO2	k(T)=SPECIAL_3(5.5e-11,1500,1.1e-13,-365,50,1165,25,1165)
MVKO2+CH3O2→MGLYOX+HCHO+CH3OH	k(T)=SPECIAL_4(5.5e-11,1500,1.1e-13,-365,50,1165,25,1165)
MVKO2+CH3O2→MGLYOX+2*HCHO	k(T)=SPECIAL_4(5.5e-11,1500,1.1e-13,-365,25,1165,50,1165)
APIOH+CH3O2→CH3CHO+CH3COE+HCHO+2*HO2	k(T)=SPECIAL_3(1.8e-11,2200,1.1e-13,-365,1e9,0,25,1165)
APIOH+CH3O2→CH3CHO+CH3COE+HCHO	k(T)=SPECIAL_4(1.8e-11,2200,1.1e-13,-365,1e9,0,25,1165)
APINO3+CH3O2→CH3CHO+CH3COE+NO2+HCHO+HO2	k(T)=SPECIAL_3(1.8e-11,2200,1.1e-13,-365,1e9,0,25,1165)
APINO3+CH3O2→ORNIT2+HCHO	k(T)=SPECIAL_4(1.8e-11,2200,1.1e-13,-365,1e9,0,25,1165)
CH3COO+CH3COO→2.*CH3O2+2.*CO2	k(T)=Ae$^{-B/T}$,A=2.8e-12,B=-530
C2H5O2+CH3COO→CH3CHO+CH3O2+CO2+HO2	k(T)=SPECIAL_3(6.4e-14,0,2.8e-12,-530,10.2,533,1e9,0)
C2H5O2+CH3COO→CH3CHO+MECOOH	k(T)=SPECIAL_4(6.4e-14,0,2.8e-12,-530,1e9,0,10.2,533)
SECC4H+CH3COO→SECBUO+CH3O2+CO2	k(T)=SPECIAL_3(1.2e-12,1500,2.8e-12,-530,1e9,0,50,1165)
SECC4H+CH3COO→CH3COE+MECOOH	k(T)=SPECIAL_4(1.2e-12,1500,2.8e-12,-530,1e9,0,50,1165)
CH3COX+CH3COO→CH3COY+CH3O2+CO2+HO2	k(T)=SPECIAL_3(5.5e-11,1500,2.8e-12,-530,1e9,0,50,1165)
CH3COX+CH3COO→CH3COY+MECOOH	k(T)=SPECIAL_4(5.5e-11,1500,2.8e-12,-530,1e9,0,50,1165)
CH2O2C+CH3COO→2*HCHO+CH3O2+CO2+HO2	k(T)=SPECIAL_3(2.3e-12,0,2.8e-12,-530,1e9,0,50,1165)
CH2O2C+CH3COO→2*HCHO+MECOOH	k(T)=SPECIAL_4(2.3e-12,0,2.8e-12,-530,1e9,0,50,1165)
CH3CHX+CH3COO→CH3CHO+HCHO+CH3O2+CO2+HO2	k(T)=SPECIAL_3(1.2e-10,2200,2.8e-12,-530,1e9,0,50,1165)
CH3CHX+CH3COO→CH3CHO+HCHO+MECOOH	k(T)=SPECIAL_4(1.2e-10,2200,2.8e-12,-530,1e9,0,50,1165)
RNC3H6+CH3COO→0.5*CARNIT+0.5*HCHO+0.5*CH3CHO+0.5*NO2+CH3O2+CO2+0.5*HO2	k(T)=SPECIAL_3(1.2e-10,2200,2.8e-12,-530,1e9,0,50,1165)
RNC3H6+CH3COO→ORNIT1+MECOOH	k(T)=SPECIAL_4(1.2e-10,2200,2.8e-12,-530,1e9,0,50,1165)
OXYL1+CH3COO→MEMALD+MGLYOX+CH3O2+CO2+HO2	k(T)=SPECIAL_3(2.1e-13,-600,2.8e-12,-530,1e9,0,50,1165)
OXYL1+CH3COO→MEMALD+MGLYOX+MECOOH	k(T)=SPECIAL_4(2.1e-13,-600,2.8e-12,-530,1e9,0,50,1165)
MEMAL1+CH3COO→GLYOX+MGLYOX+CH3O2+CO2+HO2	k(T)=SPECIAL_3(1.3e-11,800,2.8e-12,-530,1e9,0,50,1165)

Reactions	Kinetic constants
MEMAL1+CH3COO→GLYOX+MGLYOX+MECOOH	k(T)=SPECIAL_4(1.3e-11,800,2.8e-12,-530,1e9,0,50,1165)
MEMAL2+CH3COO→MALEIC+2*CH3O2+CO2	k(T)=Ae$^{-B/T}$,A=5.6e-12,B=-530
RO2IP1+CH3COO→0.3*MVK+0.3*MAC+0.6*HCHO+HO2 +CH3O2+CO2	k(T)=SPECIAL_3(1.3e-11,800,2.8e-12,-530,1e9,0,50,1165)
RO2IP1+CH3COO→0.3*MVK+0.3*MAC+0.6*HCHO+MECOOH	k(T)=SPECIAL_4(1.3e-11,800,2.8e-12,-530,1e9,0,50,1165)
RNC5H8+CH3COO→0.6*ISNI+CH3O2+CO2	k(T)=SPECIAL_3(1.3e-11,800,2.8e-12,-530,1e9,0,50,1165)
RNC5H8+CH3COO→0.6*ISNI*+MECOOH	k(T)=SPECIAL_4(1.3e-11,800,2.8e-12,-530,1e9,0,50,1165)
MACO2+CH3COO→CH3O2+CH3COZ+2*CO2	k(T)=Ae$^{-B/T}$,A=5.6e-12,B=-530
MVKO2+CH3COO→MGLYOX+HCHO+HO2+CH3O2+CO2	k(T)=SPECIAL_3(5.5e-11,1500,2.8e-12,-530,1e9,0,50,1165)
MVKO2+CH3COO→MGLYOX+HCHO+MECOOH	k(T)=SPECIAL_4(5.5e-11,1500,2.8e-12,-530,1e9,0,50,1165)
APIOH+CH3COO→CH3CHO+CH3COE+HO2+CH3O2+CO2	k(T)=Ae$^{-B/T}$,A=1.4e-11,B=835
APINO3+CH3COO→CH3CHO+CH3COE+NO2+CH3O2+CO2	k(T)=Ae$^{-B/T}$,A=1.4e-11,B=835
C2H5O2+C2H5O2→2*CH3CHO+2*HO2	k(T)=SPECIAL_1(6.4e-14,0,10.2,533)
C2H5O2+C2H5O2→CH3CHO+C2H5OH	k(T)=SPECIAL_2(6.4e-14,0,10.2,533)
SECC4H+SECC4H→2*SECBUO	k(T)=SPECIAL_1(1.2e-12,1500,50,1165)
SECC4H+SECC4H→2*CH3COE	k(T)=SPECIAL_2(1.2e-12,1500,50,1165)
CH3COX+CH3COX→2*CH3COY+2*HO2	k(T)=SPECIAL_1(5.5e-11,1500,50,1165)
CH3COX+CH3COX→2*CH3COY	k(T)=SPECIAL_2(5.5e-11,1500,50,1165)
CH2O2C+CH2O2C→4*HCHO+2*HO2	k(T)=SPECIAL_1(2.3e-12,0,50,1165)
CH2O2C+CH2O2C→4*HCHO	k(T)=SPECIAL_2(2.3e-12,0,50,1165)
CH3CHX+CH3CHX→2*HCHO+2*CH3CHO+2*HO2	k(T)=SPECIAL_1(1.3e-10,2200,50,1165)
CH3CHX+CH3CHX→2*HCHO+2*CH3CHO	k(T)=SPECIAL_2(1.3e-10,2200,50,1165)
RNC3H6+RNC3H6→CARNIT+HO2+HCHO+CH3CHO+NO2	k(T)=SPECIAL_1(1.3e-10,2200,50,1165)
RNC3H6+RNC3H6→CARNIT+ORNIT1	k(T)=SPECIAL_2(1.3e-10,2200,50,1165)
OXYL1+OXYL1→2*MEMALD+2*MGLYOX+2*HO2	k(T)=SPECIAL_1(2.1e-13,-600.,50,1165)
OXYL1+OXYL1→2*MEMALD+2*MGLYOX	k(T)=SPECIAL_2(2.1e-13,-600.,50,1165)
MEMAL1+MEMAL1→2*GLYOX+2*MGLYOX+2*HO2	k(T)=SPECIAL_1(1.3e-11,800,50,1165)
MEMAL1+MEMAL1→2*GLYOX+2*MGLYOX	k(T)=SPECIAL_2(1.3e-11,800,50,1165)
MEMAL2+MEMAL2→2*MALEIC+2*CH3O2	k(T)=Ae$^{-B/T}$,A=2.8e-12,B=-530
RO2IP1+RO2IP1→0.6*MVK+0.6*MAC+1.2*HCHO+1.2*HO2	k(T)=SPECIAL_1(1.3e-11,800,50,1165)
RO2IP1+RO2IP1→0.6*MVK+0.6*MAC+1.2*HCHO	k(T)=SPECIAL_2(1.3e-11,800,50,1165)
RNC5H8+RNC5H8→1.2*ISNI+1.2*HO2	k(T)=SPECIAL_1(1.3e-11,800,50,1165)
RNC5H8+RNC5H8→1.2*ISNI	k(T)=SPECIAL_2(1.3e-11,800,50,1165)
MACO2+MACO2→2*CH3COZ+2*CO2	k(T)=Ae$^{-B/T}$,A=2.8e-12,B=-530
MVKO2+MVKO2→2*MGLYOX+2*HCHO+2*HO2	k(T)=SPECIAL_1(5.5e-11,1500,50,1165)
MVKO2+MVKO2→2*MGLYOX+2*HCHO	k(T)=SPECIAL_2(5.5e-11,1500,50,1165)
APIOH+APIOH→2*CH3CHO+2*CH3COE+2*HO2	k(T)=Ae$^{-B/T}$,A=1.8e-11,B=2200
APINO3+APINO3→2*CH3CHO+2*CH3COE+2*NO2	k(T)=Ae$^{-B/T}$,A=1.8e-11,B=2200
organic	
CH3O2+NO→CH3NO3	k(T)=Ae$^{-B/T}$,A=2.1e-14,B=-180
CH3NO3+OH→HCHO+HNO3+HO2	k(T)=Ae$^{-B/T}$,A=1.e-14,B=-1060
C2H5O2+NO→ETNO3	k=1.25e-13
ETNO3+OH→CH3CHO+HNO3+HO2	k(T)=Ae$^{-B/T}$,A=4.4e-14,B=-720
SECC4H+NO+M→BUNO3	k(T,M)=troe(3.76e-32,0,0,3.3e-12,0,8.1,0.41)
BUNO3+OH→RNC3H6	k=6.7e-13
RNC2H4+NO→0.5*CARNIT+HCHO+1.5*NO2+0.5*HO2	k=8.9e-12
RNC3H6+NO→0.5*CARNIT+0.5*CH3CHO+0.5*HCHO +1.5*NO2+0.5*HO2	k=4e-12
ROXYL1+NO→BENZAL+NO2+HO2	k=4e-12
ISNI+OH→ISNIR	k=3.4e-11

Reactions	Kinetic constants
ISNI+O3→0.5*ISNI+0.5*HCHO+0.5*MGLYOX+0.5*NO2 +0.08*OH+0.2*O3	k=5e-18
ISNIR+NO→0.95*CH3CHO+0.475*CH3COE+0.475*MGLYOX +0.05*ISNI+0.05*HO2+1.9*NO2	k(T)=Ae$^{-B/T}$,A=1.4e-11,B=180
RNC5H8+NO→0.85*ISNI+0.1*MAC+0.05*MVK+0.15*HCHO +1.1*NO2+0.8*HO2	k(T)=Ae$^{-B/T}$,A=1.4e-11,B=180
APINO3+NO→CH3CHO+CH3COE+2*NO2	k=4e-12
RNC5H8+HO2→ORNIT2	k(T)=Ae$^{-B/T}$,A=2.7e-13,B=-1000
RNC2H4+HO2→ORNIT1	k(T)=Ae$^{-B/T}$,A=2.7e-13,B=-1000
RNC3H6+HO2→ORNIT1	k(T)=Ae$^{-B/T}$,A=2.7e-13,B=-1000
ROXYL1+HO2→BENZYL	k(T)=Ae$^{-B/T}$,A=2.7e-13,B=-1000
ISNIR+HO2→ORNIT2	k(T)=Ae$^{-B/T}$,A=2.7e-13,B=-1000
APINO3+HO2→ORNIT2	k(T)=Ae$^{-B/T}$,A=2.7e-13,B=-1000
CH3COO+NO2+M→PAN	k(T,M)=troe(2.7e-28,0,7.1,1.2e-11,0,0.9,0.3)
PAN+M→CH3COO+NO2	k(T,M)=troe(4.9e-3,12100,0,5.4e16,13830,0,0.3)
PAN+OH→HCHO+NO3+CO2	k(T)=Ae$^{-B/T}$,A=9.5e-13,B=650
MACO2+NO2+M→MACPAN	k(T,M)=troe(2.7e-28,0,7.1,1.2e-11,0,0.9,0.3)
MACPAN+M→MACO2+NO2	k(T,M)=troe(4.9e-3,12100,0,5.4e16,13830,0,0.3)
MACPAN+OH→CH3COE+NO3+O3+CO2	k(T)=Ae$^{-B/T}$,A=3.25e-13,B=-500
MEMAL2+NO2+M→MEMPAN	k(T,M)=troe(2.7e-28,0,7.1,1.2e-11,0,0.9,0.3)
MEMPAN+M→MEMAL2+NO2	k(T,M)=troe(4.9e-3,12100,0,5.4e16,13830,0,0.3)
MEMPAN+OH→CH3COE+NO3+CO2	k(T)=Ae$^{-B/T}$,A=3.25e-13,B=-500
CH3O2+NO2+M→CH3NO4	k(T,M)=troe(2.5e-30,0,5.5,7.5e-12,0,0,0.36)
CH3NO4+M→CH3O2+NO2	k(T,M)=troe(9e-5,9690,0,1.1e16,10560,0,0.36)
ORNIT1+OH→CARNIT+OH	k(T)=Ae$^{-B/T}$(300/T)^{N},A=6.1e-14,B=-1743,N=-2
ORNIT1+OH→RNC3H6	k(T)=Ae$^{-B/T}$,A=1.9e-12,B=-190
ORNIT2+OH→0.95*CH3CHO+0.475*CH3COE+0.475*MGLYOX +0.05*ISNI+0.05*OH+0.95*NO2	k(T)=Ae$^{-B/T}$(300/T)^{N},A=6.1e-14,B=-1743,N=-2
ORNIT2+OH→ISNIR	k(T)=Ae$^{-B/T}$,A=1.9e-12,B=-190
photolytic	
O3→2*OH	J(T,Z,H2O)=photorate(O3)
NO2→NO+O3	J(Z)=photorate(NO2)
NO3→NO2+O3	J(Z)=photorate(NO3-2)
H2O2→2*OH	J(Z)=photorate(H2O2)
HNO3→NO2+OH	J(Z)=photorate(HNO3)
HCHO→CO+2*HO2	J(Z)=photorate(HCHO-1)
HCHO→CO+H2	J(Z)=photorate(HCHO-2)
CH3CHO→CH3O2+HO2+CO	J(Z)=photorate(CH3CHO)
CH3COE→CH3COO+C2H5O2	J(Z)=photorate(CH3COE)
CH3COY→2*CH3COO	J(Z)=photorate(CH3COY)
MGLYOX→CH3COO+HO2+CO	J(Z)=photorate(MGLYOX)
GLYOX→0.6*HO2+2*CO+1.4*H2	J(Z)=photorate(GLYOX)
MEMALD→0.5*OFURAN+0.5*MEMAL2+0.5*HO2	J(Z)=photorate(MEMALD)
NO3→NO	J(Z)=photorate(NO3-1)
N2O5→NO2+NO3	J(Z)=photorate(N2O5)
CH3O2H→HCHO+OH+HO2	J(Z)=photorate(CH3O2H)
ETO2H→CH3CHO+OH+HO2	J(Z)=photorate(CH3O2H)
BUO2H→CH3COE+OH+HO2	J(Z)=photorate(CH3O2H)
CH4COX→CH3COY+OH+HO2	J(Z)=photorate(CH3O2H)
CH3O2C→2*HCHO+OH+HO2	J(Z)=photorate(CH3O2H)
CH4CHX→HCHO+CH3CHO+OH+HO2	J(Z)=photorate(CH3O2H)
OXYLH1→MEMALD+MGLYOX+OH+HO2	J(Z)=photorate(CH3O2H)
MEMALH→GLYOX+MGLYOX+OH+HO2	J(Z)=photorate(CH3O2H)
MEMAH2→MALEIC+OH+CH3O2	J(Z)=photorate(CH3O2H)
PEROX→0.14*RO2IP1+0.488*CH3COE+0.372*MAC+0.86*HCHO +0.9*HO2+OH	J(Z)=photorate(CH3O2H)
MACO2H→CH3COZ+OH+CO2	J(Z)=photorate(CH3O2H)

Reactions	Kinetic constants
MVKO2H→0.28*HCHO+0.28*MGLYOX+0.28*HO2+0.72*CH3CHO +0.72*CH3COO+OH	J(Z)=photorate(CH3O2H)
CH4COZ→CH3COE+OH+HO2	J(Z)=photorate(CH3O2H)
APIO2H→CH3CHO+CH3COE+OH+HO2	J(Z)=photorate(CH3O2H)
PPA→CH3O2+CO2+OH	J(Z)=photorate(PPA)
HNO4→HO2+NO2	J(Z)=photorate(HNO4)
HONO→NO+OH	J(Z)=photorate(HONO)
CH3NO4→CH3O2+NO2	J(Z)=photorate(HNO4)
CH3NO3→HCHO+HO2+NO2	J(Z)=photorate(CH3NO3)
ETNO3→CH3CHO+HO2+NO2	J(Z)=photorate(ETNO3)
BUNO3→CH3COE+HO2+NO2	J(Z)=photorate(BUNO3)
PAN→CH3COO+NO2	J(Z)=photorate(PAN)
CARNIT→CH3COO+HCHO+NO2	J(Z)=photorate(CH3CHO)
ORNIT1→CH3CHO+HCHO+NO2+OH	J(Z)=photorate(CH3O2H)
ORNIT2→0.95*CH3CHO+0.475*CH3COE+0.475*MGLYOX+0.05*ISNI +0.05*HO2+0.95*NO2+OH	J(Z)=photorate(CH3O2H)
APINEN+NO3→APINO3	k(T)=Ae$^{-B/T}$,A=1.19e-12,B=-490
BPINEN+NO3→APINO3	k(T)=Ae$^{-B/T}$,A=1.19e-12,B=-490
LIMONE+NO3→APINO3	k(T)=Ae$^{-B/T}$,A=1.19e-12,B=-490
OCIMEN+NO3→APINO3	k(T)=Ae$^{-B/T}$,A=1.19e-12,B=-490
TERPEN+NO3→APINO3	k(T)=Ae$^{-B/T}$,A=1.19e-12,B=-490
HUMULE+NO3→APINO3	k(T)=Ae$^{-B/T}$,A=1.19e-12,B=-490
APINEN+OH→APIOH	k(T)=Ae$^{-B/T}$,A=1.21e-11,B=-444
BPINEN+OH→APIOH	k(T)=Ae$^{-B/T}$,A=1.21e-11,B=-444
LIMONE+OH→APIOH	k(T)=Ae$^{-B/T}$,A=1.21e-11,B=-444
OCIMEN+OH→APIOH	k(T)=Ae$^{-B/T}$,A=1.21e-11,B=-444
TERPEN+OH→APIOH	k(T)=Ae$^{-B/T}$,A=1.21e-11,B=-444
HUMULE+OH→APIOH	k(T)=Ae$^{-B/T}$,A=1.21e-11,B=-444
APINEN+O3→0.65*CH3CHO+0.53*CH3COE+0.14*CO+0.2*C2H5O2 +0.42*CH3CHX+0.85*OH+0.1*HO2	k(T)=Ae$^{-B/T}$,A=1.0e-15,B=736
BPINEN+O3→0.65*CH3CHO+0.53*CH3COE+0.14*CO+0.2*C2H5O2 +0.42*CH3CHX+0.85*OH+0.1*HO2	k(T)=Ae$^{-B/T}$,A=1.0e-15,B=736
LIMONE+O3→0.65*CH3CHO+0.53*CH3COE+0.14*CO+0.2*C2H5O2 +0.42*CH3CHX+0.85*OH+0.1*HO2	k(T)=Ae$^{-B/T}$,A=1.0e-15,B=736
TERPEN+O3→0.65*CH3CHO+0.53*CH3COE+0.14*CO+0.2*C2H5O2 +0.42*CH3CHX+0.85*OH+0.1*HO2	k(T)=Ae$^{-B/T}$,A=1.0e-15,B=736
OCIMEN+O3→0.65*CH3CHO+0.53*CH3COE+0.14*CO+0.2*C2H5O2 +0.42*CH3CHX+0.85*OH+0.1*HO2	k(T)=Ae$^{-B/T}$,A=1.0e-15,B=736
HUMULE+O3→0.65*CH3CHO+0.53*CH3COE+0.14*CO+0.2*C2H5O2 +0.42*CH3CHX+0.85*OH+0.1*HO2	k(T)=Ae$^{-B/T}$,A=1.0e-15,B=736
C5H8+OH→RO2IP1	k(T)=Ae$^{-B/T}$,A=2.55e-11,B=-410
NC4H10+OH→SECC4H	k(T)=Ae$^{-B/T}$(300/T)^{N},A=1.36e-12,B=-190,N=-2
OXYL+OH→OXYL1	k=1.37e-11

- The reactions O_3+hν→O(1D), O(1D)+H_2O→2OH, O(1D)+M→O(3P)+M and O(3P)+O_2+M→O_3+M have been combined to reaction O_3+hν→ O(1D) by taking into account H_2O and M concentrations in order to adjust the photolysis frequency.
- Due to lack of data, photolysis frequencies of higher organic peroxides are taken as that of CH_3OOH.
- Three body Troe reactions [1], given in the form :

$$k = \frac{k_0[M]}{1 + \frac{k_0[M]}{k_\infty}} f^Z$$

with

$$Z = \frac{1}{1 + \left(log_{10}\left(\frac{k_0(T)[M]}{k_\infty(T)}\right)\right)^2}$$

$$k_0 = A_0 e^{\left(-\frac{B_0}{T}\right)} \left(\frac{T}{300}\right)^{-n}, \text{ and } k_\infty = A_\infty e^{\left(-\frac{B_\infty}{T}\right)} \left(\frac{T}{300}\right)^{-m},$$

The parameters are given in the order $A_0, B_0, n, A_\infty, B_\infty, m, f$

- The reaction NO2+OH :

$$k = \frac{k_0[M]}{1 + \frac{k_0[M]}{k_\infty}} f^Z$$

with

$$Z = \frac{1}{1 + \left(\frac{log_{10}\left(\frac{k_0(T)[M]}{k_\infty(T)} - 0.12\right)}{1.2}\right)^2}$$

$$k_0 = A_0 e^{\left(-\frac{B_0}{T}\right)} \left(\frac{T}{300}\right)^{-n}, \text{ and } k_\infty = A_\infty e^{\left(-\frac{B_\infty}{T}\right)} \left(\frac{T}{300}\right)^{-m},$$

The parameters are given in the order $A_0, B_0, n, A_\infty, B_\infty, m, f$

- Radical recombinations SPECIAL_1 :

$$k\left(T\right) = k_1\left(T\right) \times \frac{k_2\left(T\right)}{1 + k_2\left(T\right)}$$

The parameters are given in the order A_1, B_1, A_2, B_2

- Radical recombinations SPECIAL_2 :

$$k\left(T\right) = \frac{k_1\left(T\right)}{1 + k_2\left(T\right)}$$

The parameters are given in the order A_1, B_1, A_2, B_2

- Radical recombinations SPECIAL_3 :

$$k\left(T\right) = 2 \times \sqrt{\frac{k_1\left(T\right) \times k_2\left(T\right) \times k_3\left(T\right) \times k_4\left(T\right)}{\left(1 + k_3\left(T\right)\right) \times \left(1 + k_4\left(T\right)\right)}}$$

The parameters are given in the order $A_1, B_1, A_2, B_2, A_3, B_3, A_4, B_4$

- Radical recombinations SPECIAL_4 :

$$k\left(T\right) = 2 \times \sqrt{k_1\left(T\right) \times k_2\left(T\right)} \times \frac{1 - \sqrt{\frac{k_3(T)}{1+k_3(T)} \times \frac{k_4(T)}{1+k_4(T)}} \times \left(1 - \frac{k_4(T)}{1+k_4(T)}\right)}{2 - \frac{k_3(T)}{1+k_3(T)} - \frac{k_4(T)}{1+k_4(T)}}$$

The parameters are given in the order $A_1, B_1, A_2, B_2, A_3, B_3, A_4, B_4$

11.2.3 Species list of the reduced MELCHIOR2 gas-phase chemical mechanism

Species ..... **Definition**

Inorganic compounds

O3 ..... ozone
H2O2 ..... hydrogen peroxide
OH ..... hydroxy radical
HO2 ..... hydroperoxy radical
NO ..... nitric oxide
NO2 ..... nitrogen dioxide
NO3 ..... nitrogen trioxide
N2O5 ..... dinitrogen pentoxide
HONO ..... nitrous acide
HNO3 ..... nitric acide
CO ..... carbon monoxide
SO2 ..... sulfur dioxide
H2SO4 ..... sulfuric acid

Hydrocarbon species [3]

CH4 ..... methane
C2H6 ..... ethane
NC4H10 ..... n-butane
C2H4 ..... ethene
C3H6 ..... propene
OXYL ..... o-xylene
C5H8 ..... isoprene
APINEN ..... α-pinene
BPINEN ..... β-pinene
LIMONE ..... limonene
TERPEN ..... terpenes (lumped class)
HUMULE ..... Humulene (lumped class)
OCIMEN ..... Ocimene (lumped class)

Carbonyls

HCHO ..... formaldehyde
CH3CHO ..... acetaldehyde
CH3COE ..... methyl ethyl ketone
GLYOX ..... glyoxal
MGLYOX ..... methyl glyoxal
CH3COY ..... dimethyl glyoxal
MEMALD ..... unsaturated dicarbonyls, reacting like 4-oxo-2-pentenal
MVK ..... methyl vinyl ketone
MAC ..... methacroleine

Organic nitrates

PAN ..... peroxyacetyl nitrate
CARNIT ..... nitrate carbonyl taken as α-nitrooxy acetone
ISNI ..... unsaturated nitrate from isoprene degradation

Organic peroxides

CH3O2H ..... methyl hydroperoxide
PPA ..... peroxy acetyl acid

(Per)oxy radicals

CH3O2 ..... methyl peroxy radical
CH3COO ..... peroxy acetyl radical

Operators [4]

oRO2 ..... representing peroxy radicals from OH attack to C2H5, NCHH10, C2H4, C3H6, OXYL, CH3COE, MEMALD, and MVK
oROOH ..... representing organic peroxides from oRO2+HO2 reactions
obio ..... representing peroxy radicals produced by C5H8 and APINEN + OH reaction
obioH . representing biogenic organic peroxides from obio+HO2 and obio+obio reactions
oPAN .. representing PAN homologue compounds (except PAN)
PANH ..... representing results from oPAN+HO2 reaction
toPAN ..... representing results from oPAN+NO2 reaction
oRN1 ..... representing organic nitrate peroxy radicals from NO3 attack to C2H4, C3H6, C5H8, APINEN, BPINEN, LIMONE, TERPEN, OCIMEN, HUMULE and OH attack to ISNI

11.2.4 Reaction list of the reduced MELCHIOR2 chemical mechanism

Reactions	Kinetic constants	Ref.
Inorganic chemistry		
O3+NO→NO2	$Ae^{-B/T}$,A=1.8e-12,B=1370	[1]
O3+NO2→NO3	$Ae^{-B/T}$,A=1.2e-13,B=2450	[1]
O3+OH→HO2	$Ae^{-B/T}$,A=1.9e-12,B=1000	[1]
O3+HO2→OH	$Ae^{-B/T}$,A=1.4e-14,B=600	[1]
NO+HO2→OH+NO2	$Ae^{-B/T}$,A=3.7e-12,B=-240	[1]
NO2+OH+M→HNO3	troe(3.4e-30,0,3.2,4.77e-11,0,1.4,0.30)	[2], n9
HO2+OH→H2O	$Ae^{-B/T}$,A=4.8e-11,B=-250	[1]
H2O2+OH→HO2	$Ae^{-B/T}$,A=2.9e-12,B=160	[1]
HNO3+OH→NO3	$Ae^{-B/T}$,A=5.5e-15,B=-985	[3], n1
CO+OH→HO2+CO2	$Ae^{-B/T}(300/T)^N$, A=2e-13, B=0, N=1	[3], n1

[3] Hydrocarbon model species (except for CH4 and C2H4) represent groups of hydrocarbons with similar reactivity. As "definition" a typical representative of this group is given. This is also true for the degradation products.

[4] For the concept of "chemical operators" see Carter (1990) and Aumont et al. (1997)

Reactions	Kinetic constants	Ref.
HO2+HO2→H2O2	$Ae^{-B/T}$,A=2.2e-13,B=-740	[1], n1
HO2+HO2+H2O→H2O2	$Ae^{-B/T}$,A=4.52e-34,B=-2827	[1], n1
NO3+HO2→NO2+OH	4e-12	[1]
NO3+H2O2→HNO3+HO2	2e-15	[3]
NO3+NO→2*NO2	$Ae^{-B/T}$,A=1.8e-11,B=-110	[1]
NO2+NO3→NO+NO2	$Ae^{-B/T}$,A=4.5e-14,B=1260	[3]
NO2+NO3+M→N2O5	troe(2.7e-30,0,3.4,2e-12,0,-0.2,0.33)	[1], n9
N2O5+M→NO3+NO2	troe(1e-3,11000,3.5,9.7e14,11080,-0.1,0.33)	[1], n9
N2O5+H2O→2*HNO3	2.6e-22	[4]
N2O5+H2O+H2O→2*HNO3	2e-39	[4]
NO+OH+M→HONO	troe(7.e-31,0,2.6,1.5e-11,0,0.5,0.6)	[1], n9
HONO+OH→NO2	$Ae^{-B/T}$,A=1.8e-11,B=390	[1]
NO+NO+O2→2*NO2	$Ae^{-B/T}$,A=3.30E-39,B=-530.0	[1]
NO2→HONO	0.5*depo(NO2)	[18]
SOx chemistry		
SO2+CH3O2→H2SO4+HCHO+HO2	4e-17	[3]
SO2+OH+M→H2SO4+HO2	troe(4e-31,0,3.3,2e-12,0,0,0.45)	[3], n9
OH attack to hydrocarbons		
CH4+OH→CH3O2	$Ae^{-B/T}$,A=2.3e-12,B=1765	[1]
C2H6+OH→CH3CHO+oRO2	$Ae^{-B/T}$,A=7.9e-12,B=1030	[1]
NC4H10+OH→0.9*CH3COE+0.1*CH3CHO+0.1*CH3COO+0.9*oRO2	$Ae^{-B/T}(300/T)^N$,A=1.36e-12, B=-190, N=-2	[5]
C2H4+OH+M→2*HCHO+oRO2	troe(7e-29,0,3.1,9e-12,0,0,0.7)	[1], n9
C3H6+OH+M→HCHO+CH3CHO+oRO2	troe(8e-27,0,3.5,3e-11,0,0,0.5)	[1], n9
OXYL+OH→ MEMALD+MGLYOX+oRO2	1.37e-11	[5]
C5H8+OH→0.32*MAC +0.42*MVK +0.74*HCHO +obio	$Ae^{-B/T}$, A=2.55e-11, B=-410	[1]
APINEN+OH→0.8*CH3CHO+0.8*CH3COE+obio	$Ae^{-B/T}$, A=1.21e-11, B=-444	[17]
BPINEN+OH→0.8*CH3CHO+0.8*CH3COE+obio	$Ae^{-B/T}$, A=1.21e-11, B=-444	[17]
LIMONE+OH→0.8*CH3CHO+0.8*CH3COE+obio	$Ae^{-B/T}$, A=1.21e-11, B=-444	[17]
HUMULE+OH→0.8*CH3CHO+0.8*CH3COE+obio	$Ae^{-B/T}$, A=1.21e-11, B=-444	[17]
OCIMEN+OH→0.8*CH3CHO+0.8*CH3COE+obio	$Ae^{-B/T}$, A=1.21e-11, B=-444	[17]
TERPEN+OH→0.8*CH3CHO+0.8*CH3COE+obio	$Ae^{-B/T}$, A=1.21e-11, B=-444	[17]
OH attack to carbonyls and peroxides		
HCHO+OH→CO+HO2	$Ae^{-B/T}$,A=8.6e-12,B=-20	[1]
CH3CHO+OH →CH3COO	$Ae^{-B/T}$,A=5.6e-12,B=-310	[1]
MEMALD+OH →GLYOX+MGLYOX+oRO2	5.6e-11	[1]
CH3COE+OH →CH3COY+oRO2	$Ae^{-B/T}(300/T)^N$, A=2.92e-13, B=-414, N=-2	[1]
GLYOX+OH→2*CO+HO2	1.1e-11	[1]
MGLYOX+OH→CH3COO+CO	1.5e-11	[1]
MVK+OH→0.266*MGLYOX +0.266*HCHO+0.684*CH3CHO +0.684*CH3COO+0.05*ISNI+0.95*oRO2	$Ae^{-B/T}$,A=4.1e-12,B=-453	[6]
MAC+OH→0.5*CH3COE+0.5*CO2+0.5*oPAN	$Ae^{-B/T}$,A=1.86e-11,B=-175	[6]
CH3O2H+OH→CH3O2	$Ae^{-B/T}$,A=1.9e-12,B=-190	[1]
PPA+OH→CH3COO	$Ae^{-B/T}$,A=1.9e-12,B=-190	n2
CH3O2H+OH→HCHO+OH	$Ae^{-B/T}$,A=1.e-12,B=-190	[1]
oROOH+OH→0.8*OH+0.2*oRO2	$Ae^{-B/T}$,A=4.35e-12,B=-455	n2
obioH+OH→OH	8e-11	n2
PANH+OH→0.2*oPAN	1.64e-11	n2

Reactions	Kinetic constants	Ref.
CARNIT+OH→CH3CHO+CO+NO2	k(T)=A$e^{-B/T}$,A=5.6e-12,B=-310	
NO3 attack to hydrocarbons and aldehydes		
C2H4+NO3→0.5*CARNIT+HCHO+oRN1	2e-16 [1]	
C3H6+NO3→0.5*CARNIT+1.5*HCHO+0.5*CH3CHO +0.5*HO2+oRN1	9.45e-15	[1]
APINEN+NO3→CH3CHO+CH3COE+oRN1	A$e^{-B/T}$,A=1.19e-12,B=490	[8]
BPINEN+NO3→CH3CHO+CH3COE+oRN1	A$e^{-B/T}$,A=1.19e-12,B=490	[8]
LIMONE+NO3→CH3CHO+CH3COE+oRN1	A$e^{-B/T}$,A=1.19e-12,B=490	[8]
OCIMEN+NO3→CH3CHO+CH3COE+oRN1	A$e^{-B/T}$,A=1.19e-12,B=490	[8]
HUMULE+NO3→CH3CHO+CH3COE+oRN1	A$e^{-B/T}$,A=1.19e-12,B=490	[8]
TERPEN+NO3→CH3CHO+CH3COE+oRN1	A$e^{-B/T}$,A=1.19e-12,B=490	[8]
C5H8+NO3→0.85*ISNI+0.1*MAC+0.05*MVK+0.15*HCHO +0.8*HO2+oRN1	7.8e-13	[6]
HCHO+NO3→CO+HNO3+HO2	5.8e-16	[1]
CH3CHO+NO3→CH3COO+HNO3	2.8e-15	[9]
CH3O2+NO3→HCHO+HO2+NO2	1.2e-12	[10]
CH3COO+NO3→CH3O2+NO2+CO2	4e-12	[10]
oRO2+NO3→NO2+HO2	1.2e-12	[10]
obio+NO3→NO2+HO2	1.2e-12	[10]
oPAN+NO3→NO2+HO2	4e-12	[10]
oRN1+NO3→1.5*NO2	1.2e-12	[10]
O3 attack to unsaturated hydrocarbons		
C2H4+O3→HCHO+0.12*HO2+0.13*H2+0.44*CO	A$e^{-B/T}$,A=9.1e-15,B=2580	[1]
C3H6+O3→0.53*HCHO+0.5*CH3CHO+0.31*CH3O2 +0.28*HO2+0.15*OH+0.065*H2+0.4*CO+0.7*CH4	A$e^{-B/T}$,A=5.5e-15,B=1880	[1]
C5H8+O3→0.67*MAC+0.26*MVK+0.55*OH+0.07*C3H6 +0.8*HCHO +0.06*HO2+0.05*CO+0.3*O3	A$e^{-B/T}$,A=1.2e-14,B=2013	[6]
MAC+O3→0.8*MGLYOX+0.7*HCHO+0.215*OH+0.275*HO2 +0.2*CO+0.2*O3	A$e^{-B/T}$,A=5.3e-15,B=2520	[6]
MVK+O3→0.82*MGLYOX+0.8*HCHO+0.04*CH3CHO +0.08*OH+0.06*HO2+0.05*CO+0.2*O3	A$e^{-B/T}$,A=4.3e-15,B=2016	[6]
APINEN+O3→1.27*CH3CHO+0.53*CH3COE+0.14*CO +0.62*oRO2+0.42*HCHO+0.85*OH+0.1*HO2	A$e^{-B/T}$,A=1.0e-15,B=736	[8]
BPINEN+O3→1.27*CH3CHO+0.53*CH3COE+0.14*CO +0.62*oRO2+0.42*HCHO+0.85*OH+0.1*HO2	A$e^{-B/T}$,A=1.0e-15,B=736	[8]
LIMONE+O3→1.27*CH3CHO+0.53*CH3COE+0.14*CO +0.62*oRO2+0.42*HCHO+0.85*OH+0.1*HO2	A$e^{-B/T}$,A=1.0e-15,B=736	[8]
TERPEN+O3→1.27*CH3CHO+0.53*CH3COE+0.14*CO +0.62*oRO2+0.42*HCHO+0.85*OH+0.1*HO2	A$e^{-B/T}$,A=1.0e-15,B=736	[8]
OCIMEN+O3→1.27*CH3CHO+0.53*CH3COE+0.14*CO +0.62*oRO2+0.42*HCHO+0.85*OH+0.1*HO2	A$e^{-B/T}$,A=1.0e-15,B=736	[8]
HUMULE+O3→1.27*CH3CHO+0.53*CH3COE+0.14*CO +0.62*oRO2+0.42*HCHO+0.85*OH+0.1*HO2	A$e^{-B/T}$,A=1.0e-15,B=736	[8]
organic radical conversion		
CH3O2+NO→HCHO+NO2+HO2	A$e^{-B/T}$,A=4.2e-12,B=-180	[1]
CH3COO+NO→CH3O2+NO2+CO2	2e-11	[1]
oRO2+NO→NO2+HO2	4e-12	n3
obio+NO→0.86*NO2+0.78*HO2+0.14*ISNI	A$e^{-B/T}$,A=1.4e-11,B=180	[6]
oPAN+NO→NO2+HO2	1.4e-11	n3
oRN1+NO→1.5*NO2	4e-11	n3
organic radical recombination		
CH3O2+HO2→CH3O2H	A$e^{-B/T}$,A=4.1e-13,B=-790	[1]
CH3COO+HO2→0.67*PPA+0.33*O3	A$e^{-B/T}$,A=4.3e-13,B=-1040	[1]

Reactions	Kinetic constants	Ref.
oRO2+HO2→ oROOH	$Ae^{-B/T}$,A=2.7e-13,B=-1000	n4
obio+HO2→obioH	$Ae^{-B/T}$,A=2.7e-13,B=-1000	n4
oPAN+HO2→PANH	$Ae^{-B/T}$,A=2.7e-13,B=-1000	n4
oRN1+HO2→X	$Ae^{-B/T}$,A=2.7e-13,B=-1000	n4
CH3O2+CH3O2→1.35*HCHO+0.7*HO2	$Ae^{-B/T}$,A=1.13e-13,B=-356	[1], n5
CH3COO+CH3O2→0.5*CH3O2+0.5*CO2+HCHO+0.5*HO2	$Ae^{-B/T}$,A=3.34e-12,B=-400	[1], n5
oRO2+CH3O2→0.65*HCHO+0.8*HO2+0.35*CH3OH	$Ae^{-B/T}$,A=1.5e-13,B=-220	n5
obio+CH3O2→0.8*HO2+0.5*HCHO	$Ae^{-B/T}$,A=2.44e-11,B=223	n5
oPAN+CH3O2→HCHO+0.5*HO2	$Ae^{-B/T}$,A=7.9e-12,B=-140	n5
CH3COO+CH3COO→2.*CH3O2+2.*CO2	$Ae^{-B/T}$,A=2.8e-12,B=-530	[1], n5
oRO2+CH3COO→0.8*CH3O2+0.8*CO2+0.8*HO2	$Ae^{-B/T}$,A=8.6e-13,B=-260	n5
obio+CH3COO→0.5*HCHO+1.5*HO2+0.7*CO2	$Ae^{-B/T}$,A=1.18e-11,B=127	n5
oPAN+CH3COO→CH3O2+CO2+HO2	$Ae^{-B/T}$,A=3.34e-12,B=-400	n5
oRO2+oRO2→1.3*HO2	6.4e-14	n5
organic nitrates and pernitrates		
CH3COO+NO2+M→PAN	troe(2.7e-28,0,7.1,1.2e-11,0,0.9,0.3)	[1], n9
oPAN+NO2+M→toPAN	troe(2.7e-28,0,7.1,1.2e-11,0,0.9,0.3)	n6 , n9
PAN+M→CH3COO+NO2	troe(4.9e-3,12100,0,5.4e16,13830,0,0.3)	[1], n9
toPAN+M→oPAN+NO2	troe(4.9e-3,12100,0,5.4e16,13830,0,0.3)	n6 , n9
PAN+OH→HCHO+NO3+CO2	$Ae^{-B/T}$,A=9.5e-13,B=650	[1]
toPAN+OH→NO3+CO2	$Ae^{-B/T}$,A=3.25e-13,B=-500	n6
ISNI+OH→0.95*CH3CHO+0.475*CH3COE+0.475*MGLYOX +0.05*ISNI+0.05*HO2+oRN1	3.4e-11	[6]
photolytic reactions		
O3→2*OH	photorate	[3], n7
NO2→NO+O3	photorate	[3]
NO3→NO2+O3	photorate	[3], [11]
NO3→NO	photorate	[3], [11]
N2O5→NO2+NO3	photorate	[3]
H2O2→2*OH	photorate	[3]
HNO3→NO2+OH	photorate	[3]
HONO→NO+OH	photorate	[3]
HCHO→CO+2*HO2	photorate	[3]
HCHO→CO+H2	photorate	[3]
CH3CHO→CH3O2+HO2+CO	photorate	[1]
CH3COE→CH3COO+CH3CHO+oRO2	photorate	[11], [12]
CH3COY→2*CH3COO	photorate	[13], [14]
MGLYOX→CH3COO+HO2+CO	photorate	[1]
GLYOX→0.6*HO2+2*CO+0.7*H2	photorate	[13], [14]
MEMALD→0.5*MVK+0.5*MALEIC+0.5*oPAN+0.5*HCHO +0.5*HO2	photorate	[15]
CH3O2H→HCHO+OH+HO2	photorate	[3]
PPA→CH3O2+CO2+OH	photorate	n8
oROOH→OH+HO2	photorate	n8
obioH→OH+HO2	photorate	n8

Reactions	Kinetic constants	Ref.
PANH→OH+HO2	photorate	n8
PAN→CH3COO+NO2	photorate	[3]

- [1] Atkinson et al., 1997
- [2] Donahue et al., 1997
- [3] DeMore et al., 1997
- [4] Mentel et al., 1996
- [5] Atkinson, 1990
- [6] Paulson and Seinfeld, 1992
- [7] Le Bras, 1997
- [8] Atkinson et al., 1994
- [9] DeMore et al., 1990
- [10] Canosa-Mas et al., 1996
- [11] Johnston et al., 1996
- [12] Martinez et al., 1992
- [13] Jenkins et al., 1997
- [14] Plum et al., 1983
- [15] Bierbach et al., 1994
- [16] Lightfoot et al., 1996
- [17] Kirchner and Stockwell, 1996
- [18] Aumont, 2002

- n1 : Rate constants containing a density dependent term in a minor reaction channel have been simplified by putting an average boundary layer molecular density of 2.5*10^{19} molecules/cm^3.
- n2 : For operator reactions with OH, oROOH is interpreted as 2-butyl hydrogen peroxide, obioH as a peroxide from isoprene degradation, PANH represents unsaturated organic peroxides; due to lack of data, the rate constants of these compounds and of peroxy acetyl acid have been estimated using structure reactivity relationships in Kwok and Atkinson (1995).
- n3 : The rate constant of the operator reaction oRO2+NO has been set to that of the i-C3H7O2+NO reaction given in [16], that of oPAN+NO to that of CH3COO2+NO [1], the rate constant for oRO2NO+NO is taken from that of ISNIR (nitrate peroxy radicals from isoprene degradation) + NO [6].
- n4 : The rate constants for the operator reactions oRO2, obio, RO2NI+HO2 have been set to that of the reaction C2H5O2+HO2 [1], that of oPAN+HO2 has been taken from CH3COO2+HO2 [1].
- n5 : Radical conserving and terminating pathways are combined to single reactions; rate constants in operator reactions are affected by interpreting oRO2 as 2-butyl peroxy radical [16], obio as a peroxy radical from isoprene degradation [6] and oPAN as CH3COO2.
- n6 : Reaction rates of the operators oPAN and OPAN have been set to those of the peroxy acetyl radical and PAN, respectively.
- n7 : The reactions O3+hν→O(1D), O(1D)+H2O→2OH, O(1D)+M→O(3P)+M and O(3P)+O2+M→O3+M have been combined to reaction O3+hν→O(1D) by taking into account H2O and M concentrations in order to adjust the photolysis frequency.
- n8 : Due to lack of data, photolysis frequencies of higher organic peroxides are taken as that of CH3OOH.
- n9 : Three body Troe reactions [1], given in the form:

$$k = \frac{k_0[M]}{1 + \frac{k_0[M]}{k_\infty}} f^Z$$

with

$$Z = \frac{1}{1 + \left(log_{10}\left(\frac{k_0(T)[M]}{k_\infty(T)}\right)\right)^2}$$

$$k_0 = A_0 e^{\left(-\frac{B_0}{T}\right)} \left(\frac{T}{300}\right)^{-n}, \text{ and } k_\infty = A_\infty e^{\left(-\frac{B_\infty}{T}\right)} \left(\frac{T}{300}\right)^{-m},$$

The parameters are given in the order $A_0, B_0, n, A_\infty, B_\infty, m, f$

11.3 The SAPRC mechanims

11.3.1 Species list of the SAPRC-07-A gas-phase chemical mechanism

Species	Definition
Inorganic compounds	
O3	ozone
H2O2	hydrogen peroxide
OH	hydroxy radical
HO2	hydroperoxy radical
NO	nitric oxide
NO2	nitrogen dioxide
NO3	nitrogen trioxide
N2O5	dinitrogen pentoxide
HONO	nitrous acide
HNO3	nitric acide
CO	carbon monoxide
SO2	sulfur dioxide
Hydrocarbon species	
CH4	Methane
C2H4	Ethen
ACYE	Acetylen
BENZ	Benzen
C5H8	Isoprene
APINEN	α-pinene
BPINEN	β-pinene
LIMONE	limonene
lumped class	
TERPEN	terpenes
HUMULE	Humulene
OCIMEN	Ocimene
ALK1	Ethane
ALK2	Propane
ALK3	Alkans 2.5x10^3 <k$_{OH}$< 5x10^3
ALK4	Alkans 5x10^3<k$_{OH}$<1x10^4
ALK5	Alkans 1x10^4<k$_{OH}$
ARO1	Aromatiques k$_{OH}$<2x10^4
ARO2	Aromatiques k$_{OH}$>2x10^4
OLE1	Alkens k$_{OH}$<7x10^4
OLE2	Alkens k$_{OH}$>7x10^3
AFG1	Lumped photoreactive monounsaturated dicarbonyl aromatic fragmentation products that photolyze to form radicals
AFG2	Lumped photoreactive monounsaturated dicarbonyl aromatic fragmentation products that photolyze to form non-radical products
AFG3	Lumped diunsaturatred dicarbonyl aromatic fragmentation product
RNO3	Lumped Organic Nitrates
PAN and PAN analogues	
PAN	Peroxy Acetyl Nitrate
PAN2	PPN and other higher alkyl PAN analogues
PBZN	PAN analogues formed from Aromatic Aldehydes
MAPAN	PAN analogues formed from Methacrolein
Carbonyls	
HCHO	Formaldehyde
MEK	Ketones and other non-aldehyde oxygenated products that react with OH radicals faster than 5x10^{-13} but slower than 5x10^{-12} cm^3.molec^{-2}.s^{-1}
GLY	Glyoxal
MACR	Methacrolein
MVK	Methyl Vinyl Ketone
CCHO	Acetaldehyde
RCHO	Lumped C3+ Aldehydes
ACET	Acetone
BACL	Biacetyl
BALD	Aromatic aldehydes
CRES	Phenols and Cresols
PRD2	Ketones (k$_{OH}$>0.7x10^4 ppm^{-1}.mn^{-1})
NPHE	Nitrophenols
IPRD	Lumped isoprene product species
MEOH	Methanol
Organic peroxides	
XOOH	Lumped organic hydroperoxide structure, used to represent the effect of photolysis of the hydroperoxide group in the SAPRC-99 peroxy radical representation (Carter, 2000).
COOH	Methyl Hydroperoxide
FACD	Formic Acid
PACD	Higher organic acids
AACD	Acetic Acid
(Per)oxy radicals	
TBUO	t-Butoxy Radicals
RCO3	Peroxy Propionyl and higher peroxy acyl Radicals
MEO2	Methyl Peroxy Radicals
MECO3	Acetyl Peroxy Radicals
MACO3	Peroxyacyl radicals formed from methacrolein and other acroleins
BZCO3	Peroxyacyl radical formed from Aromatic Aldehydes
BZO	Phenoxy Radicals
Operators [1]	
RO2N	Peroxy Radical Operator representing NO consumption with organic nitrate formation
RO2R	Peroxy Radical Operator representing NO to NO2 conversion with HO2 formation
R2O2	Peroxy Radical Operator representing NO to NO_2 conversion without HO_2 formation

11.3.2 Reaction list of the SAPRC-07-A chemical mechanism

[1] For the concept of "chemical operators" see Carter (1990) and Aumont et al. (1997)

Reactions	Kinetic constants
Inorganic chemistry	
O3+NO→NO2	k(T)=A$e^{-B/T}$,A=3.00e-12,B=1500
O3+NO2→NO3	k(T)=A$e^{-B/T}$,A=1.40e-13,B=2470
NO+NO3→2*NO2	k(T)=A$e^{-B/T}$,A=1.80e-11,B=-110
NO+NO+O2→2*NO2	k(T)=A$e^{-B/T}$,A=3.30e-39,B=-530
NO2+NO3+M→N2O5	k(T,M)=saprc_troe(3.60e-30,-4.10,0.,1.90e-12,0.20,0.,0.35,1.33)
N2O5+M→NO2+NO3	k(T,M)=saprc_troe(1.30e-03,-3.50,11000,9.70e+14,0.10,11080,0.35,1.33)
N2O5+H2O→2*HNO3	k=2.50e-22
N2O5+H2O+H2O→2*HNO3	k=1.80e-39
NO2+NO3→NO+NO2	k(T)=A$e^{-B/T}$,A=4.50e-14,B=1260
OH+NO+M→HONO	k(T,M)=saprc_troe(7.00e-31,-2.60,0.,3.60e-11,-0.10,0.,0.60,1.0)
OH+HONO→NO2	k(T)=A$e^{-B/T}$,A=2.50e-12,B=-260
OH+NO2+M→HNO3	k(T,M)=saprc_troe(1.80e-30,-3.00,0.,2.80e-11,0.,0.,0.60,1.0)
OH+NO3→HO2+NO2	k=2.00e-11
OH+HNO3→NO3	k(T)=saprc_2(2.40e-14,-460,2.70e-17,-2199,6.50e-34,-1335)
OH+CO→HO2+CO2	k(T)=saprc_1(1.44e-13,0.,3.43e-33,0.)
OH+O3→HO2	k(T)=A$e^{-B/T}$,A=1.70e-12,B=940
HO2+NO→OH+NO2	k(T)=A$e^{-B/T}$,A=3.60e-12,B=-270
HO2+NO2+M→HNO4	k(T,M)=saprc_troe(2.00e-31,-3.40,0.,2.90e-12,-1.10,0.,0.60,1.0)
HNO4+M→HO2+NO2	k(T,M)=saprc_troe(3.72e-05,-2.40,10650,5.42e+15,-2.30,11170,0.60,1.0)
HNO4+OH→NO2	k(T)=A$e^{-B/T}$,A=1.30e-12,B=-380
HO2+O3→OH	k(T)=A$e^{-B/T}$(300/T)^{N},A=2.03e-16,B=-693,N=-4.57
HO2+HO2→H2O2	k(T)=saprc_1(2.20e-13,-600,1.90e-33,-980)
HO2+HO2+H2O→H2O2	k(T)=saprc_1(3.08e-34,-2800,2.66e-54,-3180)
NO3+HO2→0.8*OH+0.8*NO2+0.2*HNO3	k=4.00e-12
NO3+NO3→2*NO2	k(T)=A$e^{-B/T}$,A=8.50e-13,B=2450
H2O2+OH→HO2	k=1.80e-12
OH+HO2→H2O	k(T)=A$e^{-B/T}$,A=4.80e-11,B=-250
OH+H2→HO2	k(T)=A$e^{-B/T}$,A=7.70e-12,B=2100
SOx chemistry	
OH+SO2+M→HO2+H2SO4	k(T,M)=saprc_troe(3.30e-31,-4.30,0.,1.60e-12,0.,0,0.60,1.0)
RO_2X operator	
RO2R+NO→NO2+HO2	k(T)=A$e^{-B/T}$,A=2.60e-12,B=-380
RO2R+HO2→XOOH	k(T)=A$e^{-B/T}$,A=3.80e-13,B=-900
RO2R+NO3→NO2+HO2	k=2.30e-12
RO2R+MEO2→HO2+0.75*HCHO+0.25*MEOH	k=2e-13
RO2R+RO2R→HO2	k=3.50e-14
RO2N+NO→RNO3	k(T)=A$e^{-B/T}$,A=2.60e-12,B=-380
RO2N+HO2→XOOH+PRD2	k(T)=A$e^{-B/T}$,A=3.80e-13,B=-900
RO2N+NO3→NO2+HO2+PRD2	k=2.30e-12
RO2N+MEO2→HO2+0.25*MEOH+PRD2+0.75*HCHO	k=2e-13
RO2N+RO2R→HO2+PRD2	k=3.50e-14
RO2N+RO2N→HO2+2*PRD2	k=3.50e-14
MECO3+RO2R→MEO2+CO2	k(T)=A$e^{-B/T}$,A=4.40e-13,B=-1070
MECO3+RO2N→MEO2+CO2+HO2+PRD2	k(T)=A$e^{-B/T}$,A=4.40e-13,B=-1070
MACO3+RO2R→CO2+HCHO+MECO3	k(T)=A$e^{-B/T}$,A=4.40e-13,B=-1070
MACO3+RO2N→CO2+HCHO+MECO3+HO2+PRD2	k(T)=A$e^{-B/T}$,A=4.40e-13,B=-1070

Reactions	Kinetic constants
R2O2+RO2R→RO2R	k=3.50e-14
R2O2+RO2N→RO2N	k=3.50e-14
R2O2+R2O2→X	k=3.50e-14
R2O2+MECO3→MECO3	k(T)=A$e^{-B/T}$,A=4.40e-13,B=-1070
R2O2+RCO3→RCO3	k(T)=A$e^{-B/T}$,A=4.40e-13,B=-1070
R2O2+BZCO3→BZCO3	k(T)=A$e^{-B/T}$,A=4.40e-13,B=-1070
R2O2+MACO3→MACO3	k(T)=A$e^{-B/T}$,A=4.40e-13,B=-1070
RCO3+RO2R→CO2+RO2R+CCHO	k(T)=A$e^{-B/T}$,A=4.40e-13,B=-1070
RCO3+RO2N→RO2R+CCHO+CO2+HO2+PRD2	k(T)=A$e^{-B/T}$,A=4.40e-13,B=-1070
BZCO3+RO2R→CO2+BZO+R2O2	k(T)=A$e^{-B/T}$,A=4.40e-13,B=-1070
BZCO3+RO2N→CO2+BZO+R2O2+HO2+PRD2	k(T)=A$e^{-B/T}$,A=4.40e-13,B=-1070
OH attack to hydrocarbons	
AFG1+OH→0.521*RO2R+0.201*MECO3+0.217*MACO3 +0.06*RO2N+0.202*R2O2+0.334*CO+0.407*RCHO+0.129*MEK +0.107*GLY+0.267*MGLY+0.284*XC	k=7.40e-11
AFG2+OH→0.521*RO2R+0.201*MECO3+0.217*MACO3 +0.06*RO2N+0.202*R2O2+0.334*CO+0.407*RCHO+0.129*MEK +0.107*GLY+0.267*MGLY+0.284*XC	k=7.40e-11
AFG3+OH→0.561*RO2R+0.117*MECO3+0.206*MACO3 +0.117*RO2N+0.172*R2O2+0.114*CO+0.274*GLY+0.153*MGLY +0.019*BACL+0.231*IPRD+0.195*AFG1+0.195*AFG2+0.938*XC	k=9.35e-11
CH4+OH→MEO2	k(T)=A$e^{-B/T}$,A=1.85e-12,B=1690
C2H4+OH+M→RO2R+1.61*HCHO+0.195*CCHO	k(T,M)=saprc_troe(1.00e-28,-4.50,0.,8.80e-12,-0.85,0.,0.60,1.0)
C5H8+OH→0.907*RO2R+0.093*RO2N+0.079*R2O2+0.624*HCHO +0.23*MACR+0.32*MVK+0.357*IPRD+-0.167*XC	k(T)=A$e^{-B/T}$,A=2.54e-11,B=-410
ACYE+OH+M→0.3*HO2+0.7*OH+0.3*CO+0.3*FACD+0.7*GLY	k(T,M)=saprc_troe(5.50e-30,-2.00,0.,8.30e-13,0.,0.,0.60,1.0)
BENZ+OH→0.57*HO2+0.29*RO2R+0.116*OH+0.024*RO2N +0.29*GLY+0.57*CRES+0.029*AFG1+0.261*AFG2+0.116*AFG3+-0.976*XC	k(T)=A$e^{-B/T}$,A=2.33e-12,B=193
ALK1+OH→RO2R+CCHO	k(T)=A$e^{-B/T}$(300/T)^N,A=1.34e-12,B=499,N=-2
ALK2+OH→0.965*RO2R+0.035*RO2N+0.261*RCHO+0.704*ACET+-0.105*XC	k(T)=A$e^{-B/T}$(300/T)^N,A=1.49e-12,B=87,N=-2
ALK3+OH→0.695*RO2R+0.236*TBUO+0.07*RO2N+0.558*R2O2 +0.026*HCHO+0.445*CCHO+0.122*RCHO+0.024*ACET+0.332*MEK+-0.046*XC	k(T)=A$e^{-B/T}$,A=1.51e-12,B=-126
ALK4+OH→0.83*RO2R+0.01*MEO2+0.011*MECO3+0.149*RO2N +0.933*R2O2+0.002*CO+0.029*HCHO+0.438*CCHO+0.236*RCHO +0.426*ACET+0.106*MEK+0.146*PRD2+-0.119*XC	k(T)=A$e^{-B/T}$,A=3.75e-12,B=-44
ALK5+OH→0.647*RO2R+0.353*RO2N+0.958*R2O2+0.04*HCHO +0.106*CCHO+0.209*RCHO+0.071*ACET+0.086*MEK +0.407*PRD2+2.004*XC	k(T)=A$e^{-B/T}$,A=2.70e-12,B=-374
OLE1+OH→0.904*RO2R+0.001*MEO2+0.095*RO2N+0.234*R2O2 +0.7*HCHO+0.301*CCHO+0.47*RCHO+0.005*ACET+0.119*PRD2 +0.026*MACR+0.008*MVK+0.006*IPRD+0.822*XC	k(T)=A$e^{-B/T}$,A=6.18e-12,B=-501
OLE2+OH→0.914*RO2R+0.086*RO2N+0.052*R2O2+0.209*HCHO +0.788*CCHO+0.481*RCHO+0.136*ACET+0.076*MEK+0.022*PRD2 +0.027*MACR+0.002*MVK+0.037*IPRD+0.111*XC	k(T)=A$e^{-B/T}$,A=1.26e-11,B=-488
ARO1+OH→0.166*HO2+0.482*RO2R+0.284*OH+0.068*RO2N +0.077*PRD2+0.218*GLY+0.138*MGLY+0.166*CRES+0.049*BALD +0.164*AFG1+0.193*AFG2+0.284*AFG3+0.002*XC	k=6.15e-12
ARO2+OH→0.108*HO2+0.58*RO2R+0.202*OH+0.11*RO2N +0.035*PRD2+0.116*GLY+0.286*MGLY+0.104*BACL+0.108*CRES +0.039*BALD+0.217*AFG1+0.21*AFG2+0.282*AFG3+1.486*XC	k=2.57e-11
OH attack to carbonyls and peroxides	

Reactions	Kinetic constants
GLY+OH→0.63*HO2+0.37*RCO3+1.26*CO+-0.37*XC	k=1.10e-11
MGLY+OH→MECO3+CO	k=1.50e-11
CRES+OH→0.8*RO2R+0.2*BZO+0.25*MGLY+5.05*XC	k(T)=Ae$^{-B/T}$,A=1.70e-12,B=-950
NPHE+OH→BZO+XN	k=3.50e-12
BALD+OH→BZCO3	k=1.20e-11
MACR+OH→0.5*RO2R+0.5*MACO3+0.416*CO+0.084*HCHO +0.416*MEK+0.084*MGLY+-0.416*XC	k(T)=Ae$^{-B/T}$,A=8.00e-12,B=-380
MVK+OH→0.3*RO2R+0.675*MECO3+0.025*RO2N+0.675*R2O2 +0.3*HCHO+0.675*RCHO+0.3*MGLY+-0.725*XC	k(T)=Ae$^{-B/T}$,A=2.60e-12,B=-610
IPRD+OH→0.67*RO2R+0.289*MACO3+0.041*RO2N+0.336*CO +0.055*HCHO+0.129*CCHO+0.013*RCHO+0.15*MEK+0.332*PRD2 +0.15*GLY+0.174*MGLY+-0.504*XC	k=6.19e-11
PRD2+OH→0.472*HO2+0.379*RO2R+0.029*MECO3+0.049*RCO3 +0.071*RO2N+0.094*R2O2+0.213*HCHO+0.084*CCHO+0.545*RCHO +0.115*MEK+0.336*PRD2+0.877*XC	k=1.55e-11
MEOH+OH→HO2+HCHO	k(T)=Ae$^{-B/T}$,A=2.85e-12,B=345
FACD+OH→HO2+CO2	k=4.50e-13
AACD+OH→0.491*RO2R+0.509*MEO2+0.509*CO2+0.491*MGLY+- 0.491*XC	k(T)=Ae$^{-B/T}$,A=4.20e-14,B=-855
PACD+OH→RO2R+0.143*CO2+0.142*CCHO+0.4*RCHO +0.457*BACL+-0.455*XC	k=1.20e-12
COOH+OH→0.3*OH+0.7*MEO2+0.3*HCHO	k(T)=Ae$^{-B/T}$,A=3.80e-12,B=-200
ACET+OH→MECO3+R2O2+HCHO	k(T)=Ae$^{-B/T}$(300/T)^{N},A=4.56e-14,B=-429,N=-3.65
RCHO+OH→0.035*RO2R+0.965*RCO3+0.035*CO+0.035*CCHO	k(T)=Ae$^{-B/T}$,A=5.10e-12,B=-405
CCHO+OH→MECO3	k(T)=Ae$^{-B/T}$,A=4.4e-12,B=-365
HCHO+OH→HO2+CO	k(T)=Ae$^{-B/T}$,A=5.4e-12,B=-135
MEK+OH→0.376*RO2R+0.51*MECO3+0.074*RCO3+0.039*RO2N +0.591*R2O2+0.088*HCHO+0.504*CCHO+0.376*RCHO+0.3*XC	k(T)=Ae$^{-B/T}$(300/T)^{N},A=1.3e-12,B=25,N=-2
XOOH+OH→OH	k=2.50e-11
organic nitrates and pernitrates	
RNO3+OH→0.189*HO2+0.305*RO2R+0.332*NO2+0.175*RO2N +0.671*R2O2+0.011*HCHO+0.429*CCHO+0.037*RCHO+0.004*ACET +0.18*MEK+0.039*PRD2+0.494*RNO3+0.174*XN+0.04*XC	k=7.20e-12
PAN+M→MECO3+NO2	k(T,M)=saprc_troe(4.90e-03,0.,12100,4.00e+16,0.,13600,0.30,1.41)
PAN2→RCO3+NO2	k(T)=Ae$^{-B/T}$,A=8.30e+16,B=13940
PBZN→BZCO3+NO2	k(T)=Ae$^{-B/T}$,A=7.9e+16,B=14000
MAPAN→MACO3+NO2	k(T)=Ae$^{-B/T}$,A=1.6e+16,B=13486
MECO3+NO2+M→PAN	k(T,M)=saprc_troe(2.70e-28,-7.10,0.,1.21e-11,- 0.90,0.,0.30,1.41)
RCO3+NO2→PAN2	k(T)=Ae$^{-B/T}$(300/T)^{N},A=1.21e-11,B=0,N=1.07
BZCO3+NO2→PBZN	k=1.37e-11
MACO3+NO2→MAPAN	k(T)=Ae$^{-B/T}$(300/T)^{N},A=1.21e-11,B=0,N=1.07
TBUO+NO2→RNO3+-2*XC	k=2.4e-11
BZO+NO2→NPHE	k(T)=Ae$^{-B/T}$,A=2.3e-11,B=-150
NO_3 attack	
MEO2+NO3→HCHO+HO2+NO2	k=1.30e-12
MECO3+NO3→MEO2+CO2+NO2	k=2.3e-12
RCO3+NO3→NO2+CCHO+RO2R+CO2	k=2.30e-12
BZCO3+NO3→NO2+CO2+BZO+R2O2	k=2.30e-12
MACO3+NO3→NO2+CO2+HCHO+MECO3	k=2.30e-12
R2O2+NO3→NO2	k=2.30e-12
HCHO+NO3→HNO3+HO2+CO	k(T)=Ae$^{-B/T}$,A=2e-12,B=2431
CCHO+NO3→MECO3+HNO3	k(T)=Ae$^{-B/T}$,A=1.40e-12,B=1860
RCHO+NO3→RCO3+HNO3	k(T)=Ae$^{-B/T}$,A=1.40e-12,B=1601
GLY+NO3→0.63*HO2+0.37*RCO3+HNO3+1.26*CO+-0.37*XC	k(T)=Ae$^{-B/T}$,A=2.80e-12,B=2376
MGLY+NO3→MECO3+HNO3+CO	k(T)=Ae$^{-B/T}$,A=1.40e-12,B=1895

Reactions	Kinetic constants
CRES+NO3→BZO+HNO3+XC	k=1.40e-11
BALD+NO3→BZCO3+HNO3	k(T)=A$e^{-B/T}$,A=1.34e-12,B=1860
MACR+NO3→0.5*RO2R+0.5*MACO3+0.5*HNO3+0.5*CO +0.5*XN+1.5*XC	k(T)=A$e^{-B/T}$,A=1.50e-12,B=1815
IPRD+NO3→0.799*RO2R+0.15*MACO3+0.051*RO2N+0.15*HNO3 +0.572*CO+0.227*HCHO+0.218*RCHO+0.008*MGLY+0.572*RNO3 +0.278*XN+-0.815*XC	k=1.00e-13
C2H4+NO3→RO2R+RCHO+XN+-1*XC	k(T)=A$e^{-B/T}$(300/T)^N,A=3.3e-12,B=2880,N=-2
OLE1+NO3→0.824*RO2R+0.176*RO2N+0.488*R2O2+0.009*CCHO +0.002*RCHO+0.024*ACET+0.546*RNO3+0.454*XN+0.572*XC	k(T)=A$e^{-B/T}$,A=4.73e-13,B=1047
OLE2+NO3→0.423*RO2R+0.409*NO2+0.033*MEO2+0.136*RO2N +0.762*R2O2+0.074*HCHO+0.546*CCHO+0.154*RCHO+0.11*ACET +0.002*MEK+0.026*MVK+0.007*IPRD+0.322*RNO3 +0.269*XN+0.114*XC	k(T)=A$e^{-B/T}$,A=2.20e-13,B=-382
ozonolysis	
AFG1+O3→0.522*HO2+0.826*OH+0.652*RCO3+0.652*R2O2 +0.522*CO+0.174*CO2+0.652*HCHO+0.432*GLY+0.568*MGLY+- 0.872*XC	k=9.66e-18
AFG2+O3→0.522*HO2+0.826*OH+0.652*RCO3+0.652*R2O2 +0.522*CO+0.174*CO2+0.652*HCHO+0.432*GLY+0.568*MGLY+- 0.872*XC	k=9.66e-18
AFG3+O3→0.554*HO2+0.095*RO2R+0.471*OH+0.013*MECO3 +0.163*RCO3+0.007*RO2N+0.163*R2O2+0.58*CO+0.19*CO2 +0.163*HCHO+0.366*GLY+0.279*MGLY+0.003*MACR+0.004*MVK +0.003*IPRD+0.35*AFG1+0.35*AFG2+0.139*AFG3+-0.575*XC	k=1.43e-17
MVK+O3→0.064*HO2+0.05*RO2R+0.164*OH+0.05*RCO3 +0.475*CO+0.124*CO2+0.1*HCHO+0.351*FACD+0.95*MGLY+- 0.05*XC	k(T)=A$e^{-B/T}$,A=8.50e-16,B=1520
IPRD+O3→0.4*HO2+0.285*OH+0.048*RCO3+0.048*R2O2 +0.498*CO+0.14*CO2+0.125*HCHO+0.047*CCHO+0.21*MEK +0.1*FACD+0.372*PACD+0.023*GLY+0.742*MGLY+-0.329*XC	k=4.18e-18
C2H4+O3→0.16*HO2+0.16*OH+0.51*CO+0.12*CO2+HCHO +0.37*FACD	k(T)=A$e^{-B/T}$,A=9.14e-15,B=2580
ACYE+O3→1.5*HO2+0.5*OH+1.5*CO+0.5*CO2	k(T)=A$e^{-B/T}$,A=1.00e-14,B=4100
OLE1+O3→0.116*HO2+0.04*RO2R+0.193*OH+0.104*MEO2 +0.004*RO2N+0.023*R2O2+0.368*CO+0.125*CO2+0.5*HCHO +0.154*CCHO+0.384*RCHO+0.002*ACET+0.006*MEK+0.189*PRD2 +0.185*FACD+0.022*AACD+0.112*PACD+0.69*XC	k(T)=A$e^{-B/T}$,A=3.15e-15,B=1701
OLE2+O3→0.093*HO2+0.039*RO2R+0.423*OH+0.29*MEO2 +0.147*MECO3+0.008*RCO3+0.003*RO2N+0.161*R2O2+0.297*CO +0.162*CO2+0.26*HCHO+0.495*CCHO+0.333*RCHO+0.048*ACET +0.032*MEK+0.042*PRD2+0.033*FACD+0.061*AACD +0.222*PACD+0.028*MACR+0.021*MVK+0.125*XC	k(T)=A$e^{-B/T}$,A=8.14e-15,B=1255
MACR+O3→0.108*HO2+0.208*OH+0.1*RCO3+0.1*R2O2 +0.45*CO+0.117*CO2+0.2*HCHO+0.333*FACD+0.9*MGLY+-0.1*XC	k(T)=A$e^{-B/T}$,A=1.40e-15,B=2100
organic radical conversion	
MEO2+NO→NO2+HCHO+HO2	k(T)=A$e^{-B/T}$,A=2.30e-12,B=-360
MECO3+NO→MEO2+CO2+NO2	k(T)=A$e^{-B/T}$,A=7.50e-12,B=-290
RCO3+NO→NO2+CCHO+RO2R+CO2	k(T)=A$e^{-B/T}$,A=6.70e-12,B=-340
BZCO3+NO→NO2+CO2+BZO+R2O2	k(T)=A$e^{-B/T}$,A=6.70e-12,B=-340
MACO3+NO→NO2+CO2+HCHO+MECO3	k(T)=A$e^{-B/T}$,A=6.70e-12,B=-340
R2O2+NO→NO2	k(T)=A$e^{-B/T}$,A=2.6e-12,B=-380
organic radical recombinaison	
MEO2+HO2→COOH	k(T)=A$e^{-B/T}$(300/T)^N,A=3.46e-13,B=-780,N=-0.36
MEO2+HO2→HCHO	k(T)=A$e^{-B/T}$(300/T)^N,A=3.34e-14,B=-780,N=3.53

Reactions	Kinetic constants
MEO2+MEO2→MEOH+HCHO	k(T)=A$e^{-B/T}$(300/T)^N,A=6.39e-14,B=-365,N=1.80
MEO2+MEO2→2*HCHO+2*HO2	k(T)=A$e^{-B/T}$,A=7.40e-13,B=520
MECO3+HO2→AACD+0.3*O3	k(T)=A$e^{-B/T}$,A=5.20e-13,B=-980
MECO3+MEO2→0.1*AACD+0.1*HCHO+0.9*HCHO+0.9*HO2 +0.9*MEO2+0.9*CO2	k(T)=A$e^{-B/T}$,A=2.00e-12,B=-500
MECO3+MECO3→2*MEO2+2*CO2	k(T)=A$e^{-B/T}$,A=2.90e-12,B=-500
RCO3+HO2→PACD+0.25*O3	k(T)=A$e^{-B/T}$,A=5.20e-13,B=-980
RCO3+MEO2→CO2+RO2R+CCHO+HCHO+HO2	k(T)=A$e^{-B/T}$,A=2.00e-12,B=-500
RCO3+MECO3→2*CO2+MEO2+CCHO+RO2R	k(T)=A$e^{-B/T}$,A=2.90e-12,B=-500
RCO3+RCO3→2*CCHO+2*RO2R+2*CO2	k(T)=A$e^{-B/T}$,A=2.90e-12,B=-500
BZCO3+HO2→PACD+0.25*O3+4*XC	k(T)=A$e^{-B/T}$,A=5.20e-13,B=-980
BZCO3+MEO2→CO2+BZO+R2O2+HCHO+HO2	k(T)=A$e^{-B/T}$,A=2.00e-12,B=-500
BZCO3+MECO3→2*CO2+MEO2+BZO+R2O2	k(T)=A$e^{-B/T}$,A=2.90e-12,B=-500
BZCO3+RCO3→2*CO2+CCHO+RO2R+BZO+R2O2	k(T)=A$e^{-B/T}$,A=2.90e-12,B=-500
BZCO3+BZCO3→2*BZO+2*R2O2+2*CO2	k(T)=A$e^{-B/T}$,A=2.90e-12,B=-500
MACO3+HO2→PACD+0.25*O3+XC	k(T)=A$e^{-B/T}$,A=5.20e-13,B=-980
MACO3+MEO2→2*HCHO+HO2+CO2+MECO3	k(T)=A$e^{-B/T}$,A=2.00e-12,B=-500
MACO3+MECO3→2*CO2+MEO2+HCHO+MECO3	k(T)=A$e^{-B/T}$,A=2.90e-12,B=-500
MACO3+RCO3→HCHO+MECO3+CCHO+RO2R+2*CO2	k(T)=A$e^{-B/T}$,A=2.90e-12,B=-500
MACO3+BZCO3→HCHO+MECO3+BZO+R2O2+2*CO2	k(T)=A$e^{-B/T}$,A=2.90e-12,B=-500
MACO3+MACO3→2*HCHO+2*MECO3+2*CO2	k(T)=A$e^{-B/T}$,A=2.90e-12,B=-500
BZO+HO2→CRES+-1*XC	k(T)=A$e^{-B/T}$,A=3.80e-13,B=-900
R2O2+HO2→HO2	k(T)=A$e^{-B/T}$,A=3.80e-13,B=-900
R2O2+MEO2→MEO2	k=2e-13
BZO→CRES+RO2R+-1*XC	k=1.e-3
TBUO→ACET+MEO2	k(T)=A$e^{-B/T}$,A=7.5e+14,B=8152
photolytic reactions	
NO2→NO+O3	J(Z)=photorate(NO2)
NO3→NO	J(Z)=photorate(NO3-1)
NO3→NO2+O3	J(Z)=photorate(NO3-2)
O3→2*OH	J(T,Z,H2O)=photorate(O3-1)
HONO→OH+NO	J(Z)=photorate(HONO)
HNO3→OH+NO2	J(Z)=photorate(HNO3)
HNO4→0.61*HO2+0.61*NO2+0.39*OH+0.39*NO3	J(Z)=photorate(HNO4)
H2O2→2*OH	J(Z)=photorate(H2O2)
PAN→0.6*MECO3+0.6*NO2+0.4*MEO2+0.4*CO2+0.4*NO3	J(Z)=photorate(PAN)
PAN2→0.6*RCO3+0.6*NO2+0.4*CCHO+0.4*RO2R+0.4*CO2+0.4*NO3	J(Z)=photorate(PAN2)
PBZN→0.6*BZCO3+0.6*NO2+0.4*CO2+0.4*BZO+0.4*R2O2+0.4*NO3	J(Z)=photorate(PBZN)
MAPAN→0.6*MACO3+0.6*NO2+0.4*CO2+0.4*HCHO+0.4*MECO3 +0.4*NO3	J(Z)=photorate(MAPAN)
HCHO→2*HO2+CO	J(Z)=photorate(HCHO-1)
HCHO→CO	J(Z)=photorate(HCHO-2)
CCHO→HO2+MEO2+CO	J(Z)=photorate(CCHO)
RCHO→HO2+RO2R+CO+CCHO	J(Z)=photorate(RCHO)
ACET→1.38*MEO2+0.62*MECO3+0.38*CO	J(Z)=photorate(ACET)
MEK→RO2R+MECO3+CCHO	J(Z)=photorate(MEK)
COOH→HO2+OH+HCHO	J(Z)=photorate(COOH)
XOOH→HO2+OH	J(Z)=photorate(XOOH)
GLY→2*HO2+2*CO	J(Z)=photorate(GLY-07R)
GLY→HCHO+CO	J(Z)=photorate(GLY-07M)
MGLY→HO2+MECO3+CO	J(Z)=photorate(MGLY)
BACL→2*MECO3	J(Z)=photorate(BACL)
NPHE→HONO+6*XC	J(Z)=photorate(NPHE)
NPHE→XN+6*XC	J(Z)=photorate(NPHE-2)
BALD→7*XC	J(Z)=photorate(BALD)

Reactions	Kinetic constants
AFG1→1.023*HO2+0.173*MEO2+0.305*MECO3+0.5*MACO3 +0.695*CO+0.195*GLY+0.305*MGLY+0.217*XC	J(Z)=photorate(AFG1)
AFG2→PRD2+-1*XC	J(Z)=photorate(AFG2)
MACR→0.67*HO2+0.33*OH+0.67*MECO3+0.33*MACO3 +0.33*R2O2+0.67*CO+0.67*HCHO	J(Z)=photorate(MACR)
MVK→0.4*MEO2+0.4*MACO3+0.6*CO+0.6*PRD2+-2.2*XC	J(Z)=photorate(MVK)
IPRD→1.233*HO2+0.467*MECO3+0.3*RCO3+1.233*CO+0.3*HCHO +0.467*CCHO+0.233*MEK+-0.233*XC	J(Z)=photorate(IPRD)
PRD2→0.913*RO2R+0.4*MECO3+0.6*RCO3+0.087*RO2N +0.677*R2O2+0.303*HCHO+0.163*CCHO+0.78*RCHO+-0.091*XC	J(Z)=photorate(PRD2)
RNO3→0.344*HO2+0.554*RO2R+NO2+0.102*RO2N+0.167*R2O2 +0.135*HCHO+0.444*CCHO+0.137*RCHO+0.008*ACET+0.207*MEK +0.451*PRD2+0.396*XC	J(Z)=photorate(RNO3)
O_3 attack to unsaturated hydrocarbons	
C5H8+O3→0.066*HO2+0.266*OH+0.192*MACO3+0.008*RO2N +0.192*R2O2+0.275*CO+0.122*CO2+0.592*HCHO+0.1*PRD2 +0.204*FACD+0.39*MACR+0.16*MVK+0.15*IPRD+-0.559*XC	k(T)=A$e^{-B/T}$,A=7.86e-15,B=1912
C5H8+NO3→0.749*RO2R+0.187*NO2+0.064*RO2N+0.187*R2O2 +0.936*IPRD+0.813*XN+-0.064*XC	k(T)=A$e^{-B/T}$,A=3.03e-12,B=448
TERPEN+OH→0.759*RO2R+0.042*RCO3+0.2*RO2N+0.388*R2O2 +0.001*CO+0.264*HCHO+0.533*RCHO+0.036*ACET+0.005*MEK +0.255*PRD2+0.009*MGLY+0.014*BACL+0.002*MVK +0.001*IPRD+5.056*XC	k(T)=A$e^{-B/T}$,A=1.87e-11,B=-435
TERPEN+O3→0.052*HO2+0.067*RO2R+0.585*OH+0.126*MECO3 +0.149*RCO3+0.203*RO2N+0.808*R2O2+0.185*CO+0.045*CO2 +0.229*HCHO+0.22*RCHO+0.165*ACET+0.004*MEK+0.409*PRD2 +0.107*FACD+0.043*PACD+0.001*GLY+0.002*MGLY+0.055*BACL +0.001*MACR+0.001*IPRD+3.526*XC	k(T)=A$e^{-B/T}$,A=9.57e-16,B=785
TERPEN+NO3→0.162*RO2R+0.421*NO2+0.019*RCO3+0.397*RO2N +1.347*R2O2+0.01*CO+0.017*HCHO+0.001*CCHO+0.509*RCHO +0.175*ACET+0.001*MGLY+0.003*MACR+0.001*MVK+0.002*IPRD +0.163*RNO3+0.416*XN+4.473*XC	k(T)=A$e^{-B/T}$,A=1.28e-12,B=-490
APINEN+OH→0.759*RO2R+0.042*RCO3+0.2*RO2N+0.388*R2O2 +0.001*CO+0.264*HCHO+0.533*RCHO+0.036*ACET+0.005*MEK +0.255*PRD2+0.009*MGLY+0.014*BACL+0.002*MVK +0.001*IPRD+5.056*XC	k(T)=A$e^{-B/T}$,A=1.87e-11,B=-435
APINEN+O3→0.052*HO2+0.067*RO2R+0.585*OH+0.126*MECO3 +0.149*RCO3+0.203*RO2N+0.808*R2O2+0.185*CO+0.045*CO2 +0.229*HCHO+0.22*RCHO+0.165*ACET+0.004*MEK+0.409*PRD2 +0.107*FACD+0.043*PACD+0.001*GLY+0.002*MGLY+0.055*BACL +0.001*MACR+0.001*IPRD+3.526*XC	k(T)=A$e^{-B/T}$,A=9.57e-16,B=785
APINEN+NO3→0.162*RO2R+0.421*NO2+0.019*RCO3+0.397*RO2N +1.347*R2O2+0.01*CO+0.017*HCHO+0.001*CCHO+0.509*RCHO +0.175*ACET+0.001*MGLY+0.003*MACR+0.001*MVK+0.002*IPRD +0.163*RNO3+0.416*XN+4.473*XC	k(T)=A$e^{-B/T}$,A=1.28e-12,B=-490
BPINEN+OH→0.759*RO2R+0.042*RCO3+0.2*RO2N+0.388*R2O2 +0.001*CO+0.264*HCHO+0.533*RCHO+0.036*ACET+0.005*MEK +0.255*PRD2+0.009*MGLY+0.014*BACL+0.002*MVK +0.001*IPRD+5.056*XC	k(T)=A$e^{-B/T}$,A=1.87e-11,B=-435
BPINEN+O3→0.052*HO2+0.067*RO2R+0.585*OH+0.126*MECO3 +0.149*RCO3+0.203*RO2N+0.808*R2O2+0.185*CO+0.045*CO2 +0.229*HCHO+0.22*RCHO+0.165*ACET+0.004*MEK+0.409*PRD2 +0.107*FACD+0.043*PACD+0.001*GLY+0.002*MGLY+0.055*BACL +0.001*MACR+0.001*IPRD+3.526*XC	k(T)=A$e^{-B/T}$,A=9.57e-16,B=785

Reactions	Kinetic constants
BPINEN+NO3→0.162*RO2R+0.421*NO2+0.019*RCO3+0.397*RO2N +1.347*R2O2+0.01*CO+0.017*HCHO+0.001*CCHO+0.509*RCHO +0.175*ACET+0.001*MGLY+0.003*MACR+0.001*MVK+0.002*IPRD +0.163*RNO3+0.416*XN+4.473*XC	k(T)=A$e^{-B/T}$,A=1.28e-12,B=-490
LIMONE+OH→0.759*RO2R+0.042*RCO3+0.2*RO2N+0.388*R2O2 +0.001*CO+0.264*HCHO+0.533*RCHO+0.036*ACET+0.005*MEK +0.255*PRD2+0.009*MGLY+0.014*BACL+0.002*MVK +0.001*IPRD+5.056*XC	k(T)=A$e^{-B/T}$,A=1.87e-11,B=-435
LIMONE+O3→0.052*HO2+0.067*RO2R+0.585*OH+0.126*MECO3 +0.149*RCO3+0.203*RO2N+0.808*R2O2+0.185*CO+0.045*CO2 +0.229*HCHO+0.22*RCHO+0.165*ACET+0.004*MEK+0.409*PRD2 +0.107*FACD+0.043*PACD+0.001*GLY+0.002*MGLY+0.055*BACL +0.001*MACR+0.001*IPRD+3.526*XC	k(T)=A$e^{-B/T}$,A=9.57e-16,B=785
LIMONE+NO3→0.162*RO2R+0.421*NO2+0.019*RCO3+0.397*RO2N +1.347*R2O2+0.01*CO+0.017*HCHO+0.001*CCHO+0.509*RCHO +0.175*ACET+0.001*MGLY+0.003*MACR+0.001*MVK+0.002*IPRD +0.163*RNO3+0.416*XN+4.473*XC	k(T)=A$e^{-B/T}$,A=1.28e-12,B=-490
OCIMEN+OH→0.759*RO2R+0.042*RCO3+0.2*RO2N+0.388*R2O2 +0.001*CO+0.264*HCHO+0.533*RCHO+0.036*ACET+0.005*MEK +0.255*PRD2+0.009*MGLY+0.014*BACL+0.002*MVK +0.001*IPRD+5.056*XC	k(T)=A$e^{-B/T}$,A=1.87e-11,B=-435
OCIMEN+O3→0.052*HO2+0.067*RO2R+0.585*OH+0.126*MECO3 +0.149*RCO3+0.203*RO2N+0.808*R2O2+0.185*CO+0.045*CO2 +0.229*HCHO+0.22*RCHO+0.165*ACET+0.004*MEK+0.409*PRD2 +0.107*FACD+0.043*PACD+0.001*GLY+0.002*MGLY+0.055*BACL +0.001*MACR+0.001*IPRD+3.526*XC	k(T)=A$e^{-B/T}$,A=9.57e-16,B=785
OCIMEN+NO3→0.162*RO2R+0.421*NO2+0.019*RCO3+0.397*RO2N +1.347*R2O2+0.01*CO+0.017*HCHO+0.001*CCHO+0.509*RCHO +0.175*ACET+0.001*MGLY+0.003*MACR+0.001*MVK+0.002*IPRD +0.163*RNO3+0.416*XN+4.473*XC	k(T)=A$e^{-B/T}$,A=1.28e-12,B=-490
HUMULE+OH→0.759*RO2R+0.042*RCO3+0.2*RO2N+0.388*R2O2 +0.001*CO+0.264*HCHO+0.533*RCHO+0.036*ACET+0.005*MEK +0.255*PRD2+0.009*MGLY+0.014*BACL+0.002*MVK+0.001*IPRD +5.056*XC	k(T)=A$e^{-B/T}$,A=1.87e-11,B=-435
HUMULE+O3→0.052*HO2+0.067*RO2R+0.585*OH+0.126*MECO3 +0.149*RCO3+0.203*RO2N+0.808*R2O2+0.185*CO+0.045*CO2 +0.229*HCHO+0.22*RCHO+0.165*ACET+0.004*MEK+0.409*PRD2 +0.107*FACD+0.043*PACD+0.001*GLY+0.002*MGLY+0.055*BACL +0.001*MACR+0.001*IPRD+3.526*XC	k(T)=A$e^{-B/T}$,A=9.57e-16,B=785
HUMULE+NO3→0.162*RO2R+0.421*NO2+0.019*RCO3+0.397*RO2N +1.347*R2O2+0.01*CO+0.017*HCHO+0.001*CCHO+0.509*RCHO +0.175*ACET+0.001*MGLY+0.003*MACR+0.001*MVK+0.002*IPRD +0.163*RNO3+0.416*XN+4.473*XC	k(T)=A$e^{-B/T}$,A=1.28e-12,B=-490

- The reactions O_3+hν→O(1D), O(1D)+H_2O→2OH, O(1D)+M→O(3P)+M and O(3P)+O_2+M→O_3+M have been combined to reaction O_3+hν→ O(1D) by taking into account H_2O and M concentrations in order to adjust the photolysis frequency.
- The reactions OH+CO→HO2+CO2, HO2+HO2→H2O2 et HO2+HO2+H2O→H2O2 :

$$k\left(T,M\right)=k_1\left(T\right)+k_2\left(T\right)\left[M\right]$$

  The parameters are given in the order A_1, B_1, A_2, B_2
- The reactions OH+HNO3→NO3 :

$$k\left(T,M\right)=k_0\left(T\right)+\frac{k_3\left(T\right)\left[M\right]}{\left(1+\frac{k_3(T)[M]}{k_2(T)}\right)}$$

The parameters are given in the order $A_0, B_0, A_2, B_2, A_3, B_3$

- Three body Troe reactions :

$$k(T,M) = \frac{k_0(T)[M]}{1+\frac{k_0(T)[M]}{k_\infty(T)}} \times F^Z$$

with

$$Z = \frac{1}{1+\left(\frac{log_{10}\left(\frac{k_0(T)[M]}{k_\infty(T)}\right)}{N}\right)^2}$$

$$k_0 = A_0 e^{\left(-\frac{B_0}{T}\right)}\left(\frac{T}{300}\right)^{-n}, \text{ and } k_\infty = A_\infty e^{\left(-\frac{B_\infty}{T}\right)}\left(\frac{T}{300}\right)^{-m},$$

The parameters are given in the order $A_0, n, B_0, A_\infty, m, B_\infty, F, N$

11.3.3 Species list of the chlorine SAPRC-07 gas-phase chemical mechanism

Species ..... **Definition**

Active Inorganic Species

CL2 ..... Chlorine molecules
CLNO ..... ClNO
CLONO ..... ClONO
CLNO2 ..... ClNO2
CLONO2 ..... ClONO2
HOCL ..... HOCl

Active Radical Species and Operators

CL ..... Chlorine atoms
CLO ..... ClO. Radicals

Steady state operators

xCL ..... Formation of Cl radicals from alkoxy radicals formed in peroxy radical reactions with NO and NO3 (100% yields) and RO2 (50% yields)
xCLCCHO ..... As above, but for CLCCHO
xCLACET ..... As above, but for CLACET

Active Organic Product Species

CLCCHO Chloroacetaldehyde (and other alpha-chloro aldehydes that are assumed to be similarly photoreactive)
CLACET Chloroacetone (and other alpha-chloro ketones that are assumed to be similarly photoreactive)

Low Reactivity Compounds Represented as Unreactive

HCL ..... Hydrochloric acid
CLCHO ..... Formyl Chloride (assumed to be unreactive)

11.3.4 Reaction list of the chlorine SAPRC-07-A chemical mechanism

Reactions	Kinetic constants
Base Chlorine Mechanism	
CL2→2*CL	J(Z)=photorate(CL2)
CL+NO→CLNO	k(T)=Aexp$^{-B/T}$(300/T)^N,A=7.60e-32,B=0.,N=-1.80
CLNO→CL+NO	J(Z)=photorate(CLNO)
CL+NO2+M→CLONO	k(T,M)=saprc_troe(1.30e-30,-2.00,0.,1.00e-10,-1.00,0.,0.60,1.00)
CL+NO2+M→CLNO2	k(T,M)=saprc_troe(1.80e-31,-2.00,0.,1.00e-10,-1.00,0.,0.60,1.00)
CLONO→CL+NO2	J(Z)=photorate(CLONO)
CLNO2→CL+NO2	J(Z)=photorate(CLNO2)
CL+HO2→HCL	k(T)=Aexp$^{-B/T}$(300/T)^N,A=3.44e-11,B=0.,N=-0.56
CL+HO2→CLO+OH	k(T)=Aexp$^{-B/T}$(300/T)^N,A=9.41e-12,B=0.,N=2.10
CL+O3→CLO	k(T)=Aexp$^{-B/T}$,A=2.80e-11,B=250
CL+NO3→CLO+NO2	k=2.40e-11
CLO+NO→CL+NO2	k(T)=Aexp$^{-B/T}$,A=6.20e-12,B=-295
CLO+NO2+M→CLONO2	k(T,M)=saprc_troe(1.80e-31,-3.40,0.,1.50e-11,-1.90,0.,0.60,1.00)

Reactions	Kinetic constants
CLONO2→CLO+NO2	J(Z)=photorate(CLONO2-1)
CLONO2→CL+NO3	J(Z)=photorate(CLONO2-2)
CLONO2+M→CLO+NO2	k(T,M)=saprc_troe(4.85e-5,-1.,1253,3.71e15,3.5,12530,0.60,1.00)
CL+CLONO2→CL2+NO3	k(T)=Aexp$^{-B/T}$,A=6.20e-12,B=-145
CLO+HO2→HOCL	k(T)=Aexp$^{-B/T}$,A=2.20e-12,B=-340
HOCL→OH+CL	J(Z)=photorate(HOCL)
CLO+CLO→0.29*CL2+1.42*CL	k(T)=Aexp$^{-B/T}$,A=1.25e-11,B=1960
OH+HCL→CL	k(T)=Aexp$^{-B/T}$,A=1.70e-12,B=230
CL+H2→HCL+HO2	k(T)=Aexp$^{-B/T}$,A=3.90e-11,B=2310
HCHO+CL→HCL+HO2+CO	k(T)=Aexp$^{-B/T}$,A=8.10e-11,B=30
CCHO+CL→HCL+MECO3	k=8.00e-11
MEOH+CL→HCL+HO2+HCHO	k=5.50e-11
RCHO+CL→HCL+0.1*RO2R+0.9*RCO3+0.1*CO+0.1*CCHO	k=1.23e-10
ACET+CL→HCL+MECO3+R2O2+HCHO	k(T)=Aexp$^{-B/T}$,A=7.70e-11,B=1000
MEK+CL→HCL+0.84*RO2R+0.085*MECO3+0.036*RCO3 +0.039*RO2N+0.135*R2O2+0.065*HCHO+0.07*CCHO +0.84*RCHO+0.763*XC	k=3.60e-11
RNO3+CL→HCL+0.055*HO2+0.547*RO2R+0.197*NO2 +0.202*RO2N+0.735*R2O2+0.045*HCHO+0.3*CCHO +0.029*RCHO+0.003*ACET+0.059*MEK+0.058*PRD2 +0.602*RNO3+0.201*XN+-0.149*XC	k=1.92e-10
PRD2+CL→HCL+0.314*HO2+0.541*RO2R+0.007*MECO3 +0.022*RCO3+0.116*RO2N+0.138*R2O2+0.237*HCHO +0.109*CCHO+0.789*RCHO+0.051*MEK+0.156*PRD2+1.262*XC	k=2.00e-10
GLY+CL→HCL+0.63*HO2+0.37*RCO3+1.26*CO+-0.37*XC	k(T)=Aexp$^{-B/T}$,A=8.10e-11,B=30
MGLY+CL→HCL+MECO3+CO	k=8.00e-11
CRES+CL→HCL+RO2R+-1*R2O2+BALD	k=6.20e-11
BALD+CL→HCL+BZCO3	k=8.00e-11
XOOH+CL→CL	k=1.66e-10
MACR+CL→0.25*HCL+0.802*RO2R+0.165*MACO3+0.033*RO2N +0.541*CO+0.082*IPRD+0.18*CLCCHO+0.541*CLACET +0.208*XC	k=3.85e-10
MVK+CL→0.322*RO2R+0.625*MECO3+0.053*RO2N +0.961*R2O2+0.947*CLCCHO+0.538*XC	k=2.32e-10
IPRD+CL→0.401*HCL+0.084*HO2+0.712*RO2R +0.154*MACO3+0.051*RO2N+0.018*R2O2+0.498*CO +0.195*HCHO+0.017*MGLY+0.115*IPRD+0.051*AFG1 +0.051*AFG2+0.14*CLCCHO+0.42*CLACET+0.709*XC	k=4.12e-10
CLCCHO→HO2+RO2CL+CO+HCHO	J(Z)=photorate(CLCCHO)
CLCCHO+OH→RCO3+-1*XC	k=3.10e-12
CLCCHO+CL→HCL+RCO3+-1*XC	k=1.29e-11
CLACET→RO2CL+MECO3+HCHO	J(Z)=photorate(CLACET)
RO2CL+NO→NO2+CL	k(T)=Aexp$^{-B/T}$,A=2.60e-12,B=-380
RO2CL+HO2→XOOH	k(T)=Aexp$^{-B/T}$,A=3.80e-13,B=-900
RO2CL+NO3→NO2+CL	k=2.30e-12
RO2CL+MEO2→0.5*CL+0.5*HO2+0.75*HCHO+0.25*MEOH	k=2e-13
RO2CL+RO2R→0.5*CL+0.5*HO2	k=3.50e-14
RO2CL+R2O2→RO2CL	k=3.50e-14
RO2CL+RO2N→0.5*CL+0.5*HO2+0.5*MEK+0.5*PRD2+XC	k=3.50e-14
RO2CL+RO2CL→CL	k=3.50e-14
RO2CL+MECO3→MEO2+CO2	k(T)=Aexp$^{-B/T}$,A=4.40e-13,B=-1070
RO2CL+RCO3→CO2+RO2R+CCHO	k(T)=Aexp$^{-B/T}$,A=4.40e-13,B=-1070
RO2CL+BZCO3→CO2+BZO+R2O2	k(T)=Aexp$^{-B/T}$,A=4.40e-13,B=-1070
RO2CL+MACO3→CO2+HCHO+MECO3	k(T)=Aexp$^{-B/T}$,A=4.40e-13,B=-1070
CH4+CL→HCL+MEO2	k(T)=Aexp$^{-B/T}$,A=7.30e-12,B=1280
C2H4+CL+M→RO2R+R2O2+HCHO+CLCHO	k(T,M)=saprc_troe(1.60e-29,-3.30,0.,3.10e-10,-1.00,0.,0.60,1.00)

Reactions	Kinetic constants
C5H8+CL→0.15*HCL+0.738*RO2R+0.177*RO2CL+0.085*RO2N +0.253*R2O2+0.275*HCHO+0.177*MVK+0.671*IPRD+0.067*CLCCHO +0.018*XC	k=4.80e-10
ACYE+CL+M→HO2+CO+XC	k(T,M)=saprc_troe(5.20e-30,-2.40,0.,2.20e-10,0.,0.,0.60,1.00)
Chlorine + Atmospheric Lumped VOC Mechanism	
ALK1+CL→HCL+RO2R+CCHO	k=5.95e-11
ALK2+CL→HCL+0.97*RO2R+0.03*RO2N+0.482*RCHO+0.488*ACET+-0.09*XC	k=1.37e-10
ALK3+CL→HCL+0.835*RO2R+0.094*TBUO+0.07*RO2N +0.526*R2O2+0.078*HCHO+0.34*CCHO+0.343*RCHO+0.075*ACET +0.253*MEK+0.18*XC	k=1.86e-10
ALK4+CL→HCL+0.827*RO2R+0.003*MEO2+0.004*MECO3 +0.165*RO2N+0.91*R2O2+0.003*CO+0.034*HCHO0.287*CCHO +0.412*RCHO+0.247*ACET+0.076*MEK+0.13*PRD2+0.327*XC	k=2.63e-10
ALK5+CL→HCL+0.647*RO2R+0.352*RO2N+0.894*R2O2 +0.022*HCHO+0.08*CCHO+0.258*RCHO+0.044*ACET +0.041*MEK+0.378*PRD2+2.368*XC	k=4.21e-10
OLE1+CL→0.308*HCL+0.902*RO2R+0.098*RO2N+0.518*R2O2 +0.025*HCHO+0.146*CCHO+0.051*RCHO+0.188*MACR+0.014*MVK +0.027*IPRD+0.225*CLCCHO+0.396*CLACET+1.361*XC	k=3.55e-10
OLE2+CL→0.263*HCL+0.447*RO2R+0.448*RO2CL+0.001*MEO2 +0.104*RO2N+0.619*R2O2+0.228*HCHO+0.361*CCHO+0.3*RCHO +0.081*ACET+0.04*MEK+0.049*MACR+0.055*MVK+0.179*IPRD +0.012*CLCCHO+0.18*CLACET+0.247*XC	k=3.83e-10
ARO1+CL→0.88*RO2R+0.12*RO2N+0.21*PRD2+0.671*BALD +0.323*XC	k=1.00e-10
ARO2+CL→0.842*RO2R+0.158*RO2N+0.224*PRD2+0.618*BALD +2.382*XC	k=2.18e-10
TERPEN+CL→0.548*HCL+0.252*RO2R+0.068*RO2CL+0.034*MECO3 +0.05*RCO3+0.016*MACO3+0.582*RO2N+1.938*R2O2+0.035*CO +0.158*HCHO+0.185*RCHO+0.274*ACET+0.007*GLY+0.003*BACL +0.003*MVK+0.158*IPRD+0.006*AFG1+0.006*AFG2+0.001*AFG3 +0.109*CLCCHO+3.543*XC	k=5.46e-10
HUMULE+CL→0.548*HCL+0.252*RO2R+0.068*RO2CL+0.034*MECO3 +0.05*RCO3+0.016*MACO3+0.582*RO2N+1.938*R2O2+0.035*CO +0.158*HCHO+0.185*RCHO+0.274*ACET+0.007*GLY+0.003*BACL +0.003*MVK+0.158*IPRD+0.006*AFG1+0.006*AFG2+0.001*AFG3 +0.109*CLCCHO+3.543*XC	k=5.46e-10
OCIMEN+CL→0.548*HCL+0.252*RO2R+0.068*RO2CL+0.034*MECO3 +0.05*RCO3+0.016*MACO3+0.582*RO2N+1.938*R2O2+0.035*CO +0.158*HCHO+0.185*RCHO+0.274*ACET+0.007*GLY+0.003*BACL +0.003*MVK+0.158*IPRD+0.006*AFG1+0.006*AFG2+0.001*AFG3 +0.109*CLCCHO+3.543*XC	k=5.46e-10
LIMONE+CL→0.548*HCL+0.252*RO2R+0.068*RO2CL+0.034*MECO3 +0.05*RCO3+0.016*MACO3+0.582*RO2N+1.938*R2O2+0.035*CO +0.158*HCHO+0.185*RCHO+0.274*ACET+0.007*GLY+0.003*BACL +0.003*MVK+0.158*IPRD+0.006*AFG1+0.006*AFG2+0.001*AFG3 +0.109*CLCCHO+3.543*XC	k=5.46e-10
BPINEN+CL→0.548*HCL+0.252*RO2R+0.068*RO2CL+0.034*MECO3 +0.05*RCO3+0.016*MACO3+0.582*RO2N+1.938*R2O2+0.035*CO +0.158*HCHO+0.185*RCHO+0.274*ACET+0.007*GLY+0.003*BACL +0.003*MVK+0.158*IPRD+0.006*AFG1+0.006*AFG2+0.001*AFG3 +0.109*CLCCHO+3.543*XC	k=5.46e-10

Reactions	Kinetic constants
APINEN+CL→0.548*HCL+0.252*RO2R+0.068*RO2CL+0.034*MECO3 +0.05*RCO3+0.016*MACO3+0.582*RO2N+1.938*R2O2+0.035*CO +0.158*HCHO+0.185*RCHO+0.274*ACET+0.007*GLY+0.003*BACL +0.003*MVK+0.158*IPRD+0.006*AFG1+0.006*AFG2+0.001*AFG3 +0.109*CLCCHO+3.543*XC	k=5.46e-10

12 Aerosol chemistry

12.1 The modelled aerosols

CHIMERE includes a sectional aerosol module. This module accounts for 7 species, listed in Table 12.1 :

Model species	Species	Type
pPPM	Anthropogenic primary species EC, OCp, and other industrial dusts	primary
pSOA	Anthropogenic and Biogenic secondary organic aerosol (ASOA+BSOA)	secondary
pH2SO4	Equivalent Sulfate(*)	secondary
pHNO3	Equivalent Nitrate(*)	secondary
pNH3	Equivalent Ammonium(*)	primary emitted, secondary transferred
pWATER	Water	

Table 12.1: *List of aerosol species. (*): ions, molecules, crystals*

Potentially, Chloride et Sodium can be included (high computing time). The physical processes accounted for are:

12.2 Option activation

CHIMERE offers the option to include aerosol chemical mechanisms. The choice is managed in the chimere.par file as:

```
[aero]      Chemically-active aerosols (1/0)    : 1
[nbins]     Number of aerosol size sections     : 10
```

12.3 Aerosols processes

- **Coagulation:**
  The flux of coagulation $J^{bin}_{coag,i}$ a compound i inside a bin b is computed with the size binning method:

$$J^{b}_{coag,i} = \sum_{j=1}^{b}\sum_{k=1}^{b} f^{b}_{j,k} K_{j,l} A^{j}_{p,i} Number^{k} - A^{b}_{p,i} \sum K_{bin,j} Number^{k} \tag{12.1}$$

  with $K_{j,l}$ the coagulation kernel coefficient between bins i and j and $f^{b}_{j,k}$ the partition coefficient (the fraction of the particle created from the coagulation of bins j and k which is redistributed inside bin b). The coagulation kernel and the partition coefficient are calculated as in [Debry et al., 2007].
- **Absorption:**
  Absorption is taken into account for both inorganic and organic species but their processing is different. For inorganic species, equilibrium concentrations are computed with the thermodynamic module ISORROPIA (or a tabulated version) presented in [Nenes et al., 1998]. For secondary organic species, equilibrium concentrations are calculated through a temperature dependent partitioning coefficient ([Pankow, 1994].

Please note that the ISORROPIA code is included in CHIMERE, please check the ISORROPIA web site for downloading the latest version.

- **Nucleation:**
  The parameterization of [Kulmala et al., 1998] for sulfuric acid nucleation is used. This process, favoured by cold humid atmospheric conditions, affects the number of ultrafine particles. The nucleated flux is added to the smallest bin in the sectional distribution. Although nucleation of condensable organic species has been clearly identified in many experimental studies ([Kavouras et al., 1998], there is no available parameterization. Since the sulfuric acid nucleation process competes with absorption processes, it is expected to occur in weakly particle polluted conditions.

12.3.1 Composition and mathematical representation of aerosols

Atmospheric aerosols are represented by their size distributions and compositions. The sectional representation described by [Gelbard and Seinfeld, 1980] has been used for the density distribution function. The sectional approach is quite useful to solve the governing equation for multicomponent aerosols. It discretizes the density distribution in a finite number of bins ([Warren, 1986]). All particles in section l are characterized by their mean mass median diameter dl. For a given x as $x = ln(m)$, with m the particle mass, q(x) is the density distribution as defined in Equation 12.2 , Q being the mass concentration function.

$$q(x) = \frac{dQ}{dx} \tag{12.2}$$

Q_l^k (μg m^{-3}) is the mass concentration of component k in section l and Q_l (μg m^{-3}) is the total mass concentration in section l (Equation 12.3).

$$Q_l = \int_{x_{l-1}}^{x_l} q(x)dx = \sum_k Q_l^k \tag{12.3}$$

Sulfate is formed through gaseous and aqueous oxidation of SO_2. Nitric acid is produced in the gas phase by NOx oxidation. N_2O_5 is converted into nitric acid via heterogeneous pathways by oxidation on aqueous aerosols. Ammonia is a primary emitted base converted in the aerosol phase by neutralization with nitric and sulfuric acids. Ammonia, nitrate and sulfate exist in aqueous, gaseous and particulate phases in the model. As an example, in the particulate phase the model species pNH_3 represents an equivalent ammonium as the sum of NH_4^+ ion, NH_3 liquid, NH_4NO_3 solid, etc.

12.3.2 Coagulation

Since Q_l^k is the mass concentration of component k in section l, the mass balance equation for coagulation [Gelbard and Seinfeld, 1980] follows Equation 12.4 :

$$\begin{aligned}\left[\frac{dQ_l^k}{dt}\right]_{coag} &= \frac{1}{2}\sum_{i=1}^{l-1}\sum_{j=1}^{l-1}\left[{}^{1a}\beta_{i,j,l}Q_j^k Q_i + {}^{1b}\beta_{i,j,l}Q_i^k Q_j\right] \\ &- \sum_{i=1}^{l-1}\left[{}^{2a}\beta_{i,l}Q_i Q_l^k - {}^{2b}\beta_{i,l}Q_l Q_i^k\right] \\ &- \frac{1}{2}{}^{3}\beta_{l,l}Q_l Q_l^k - Q_l^k\sum_{i=l+1}^{m}{}^{4}\beta_{i,l}Q_i\end{aligned} \tag{12.4}$$

The sectional coagulation coefficients ${}^{1a}\beta$,${}^{1b}\beta$,${}^{2a}\beta$,${}^{2b}\beta$,${}^{3}\beta and {}^{4}\beta$ (Fuch, 1964) depend on particle characteristics and meteorological data such as temperature, pressure and turbulence parameters. For submicronic particles, coagulation is essentially driven by Brownian motions. For coarse particles sedimentation is an efficient process.

12.3.3 Absorption

Absorption is described by the "bulk equilibrium" approach of [Pandis et al., 1993]. In this approach, all the bins for which condensation is very fast are merged into a "bulk particulate phase". Following [Debry et al., 2007], a cutting diameter of 1.25 μm is used to separate bins which are inside the "bulk particle" (with a diameter lower than the cutting diameter). Thermodynamic models are used to compute the partitioning between the gas phase and the particle phase and estimate the gas-phase concentrations at equilibrium.
For semi-volatile inorganic species (sulfate, nitrate, ammonium), the equilibrium concentration G_{eq} is calculated using the thermodynamic module ISORROPIA ([Nenes et al., 1998]). This model also determines the water content of particles. Interactions between inorganic and organic species are not taken into account, the thermodynamic of such mixtures still being poorly understood. Equilibrium concentrations for the semivolatile organic species k are related to particle concentrations through a temperature dependent partition coefficient K^p (in $m^3 \mu g^{-1}$) ([Pankow, 1994]):

$$G^k_{l,eq} = \frac{Q^k_l}{OM_l K^p_k} \tag{12.5}$$

with OM ($\mu g m^{-3}$) is the absorbent organic material concentration. Considering the thermodynamic equilibrium between the gas and particulate phases, this coefficient is given by

$$K^p_k = \frac{10^{-6}}{MW_{om}\zeta_k p^0_k} \tag{12.6}$$

with R is the ideal gas constant (8.206 10^{-5}m3 atm $mol^{-1}K^{-1}$), T the temperature (K), MW_{om} the mean molecular weight (g mol^{-1}), p^0_i the vapor pressure of product i as a pure liquid (atm) and ζ the activity coefficient of species in the bulk aerosol phase. The coefficient ζ, difficult to calculate, is assumed constant and equal to unity. Moreover, an empirical formulae can be used to estimate K_p:

$$log(K^p) = -0.61 log(p^0) - 4.74 \tag{12.7}$$

according to [Kaupp and Umlauf, 1992] for organic species.
The mass of compounds condensing into particles ΔA_p is redistributed over bins according to the kinetic of condensation into each bins whereas the mass of compounds evaporating from each bins is proportional to the amount of the compounds in the bins.
If the variation of particulate bulk concentration of compound i $\Delta A_{p,i} > 0$:

$$\Delta A^{bin}_{p,i} = \frac{k^{bin}}{\sum_j k^j_i} DeltaA_{p,i} \tag{12.8}$$

with k^{bin}_i the kinetic of condensation given by [Seinfeld and Pandis, 1998]:

$$k^{bin}_i = Number^{bin} \frac{2\pi D^{bin}_p D_i M_i}{RT} f(Kn, \alpha) \tag{12.9}$$

with $Number^{bin}$ the number of particles inside the bin, D^{bin}_p the mean diameter of the bin, D_i the diffusion coefficient for species i in air, M_i its molecular weight and f(Kn,α) is the correction dut to noncontinuum effects and imperfect surface accomodation.

If the variation of particulate bulk concentration of compound i $\Delta A_{p,i} < 0$:

$$\Delta A_{p,i}^{bin} = \frac{A_{p,i}^{bin}}{\sum_j A_{p,i}^j} DeltaA_{p,i} \tag{12.10}$$

The absorption flux J ($\mu g m^{-3} s^{-1}$) of a semi-volatile inorganic or organic species onto a bin computed with:

$$J = \frac{1}{\tau} \Delta A_{p,i}^{bin} \tag{12.11}$$

with τ the time to reach equilibrium. A time of 2 hours is used based on the results of [Aan de Brugh et al., 2012].
If the variation of particulate bulk concentration of compound i $\Delta A_{p,i} > 0$:

$$\Delta A_{p,i}^{bin} = \frac{k^{bin}}{\sum_j k_i^j} DeltaA_{p,i} \tag{12.12}$$

with k_i^{bin} the kinetic of condensation given by [Seinfeld and Pandis, 1998]:

$$k_i^{bin} = Number^{bin} \frac{2\pi D_p^{bin} D_i M_i}{RT} f(Kn, \alpha) \tag{12.13}$$

with $Number^{bin}$ the number of particles inside the bin, D_p^{bin} the mean diameter of the bin, D_i the diffusion coefficient for species i in air, M_i its molecular weight and f(Kn,α) is the correction dut to noncontinuum effects and imperfect surface accomodation.
If the variation of particulate bulk concentration of compound i $\Delta A_{p,i} < 0$:

$$\Delta A_{p,i}^{bin} = \frac{A_{p,i}^{bin}}{\sum_j A_{p,i}^j} DeltaA_{p,i} \tag{12.14}$$

The absorption flux J ($\mu g m^{-3} s^{-1}$) of a semi-volatile inorganic or organic species onto a bin computed with:

$$J = \frac{1}{\tau} \Delta A_{p,i}^{bin} \tag{12.15}$$

with τ the time to reach equilibrium. A time of 2 hours is used based on the results of [Aan de Brugh et al., 2012].

12.3.4 Nucleation

The parameterization of [Kulmala et al., 1998] for sulfuric acid nucleation is used. This process, favoured by cold humid atmospheric conditions, affects the number of ultrafine particles. The nucleated flux is added to the smallest bin in the sectional distribution. Nucleation of condensable organic species has been clearly identified in many experimental studies ([Kavouras et al., 1998], there is no available parameterization. Since, the sulfuric acid nucleation process competes with absorption processes, it is expected to occur in weakly particle polluted conditions.

Gas phase :	NH_3, HNO_3, HCl, H_2O.
Liquid phase :	NH_4^+, Na^+, H^+, Cl^-, NO_3^-, SO_4^{2-}, HSO_4^-, OH^-, H_2O, $HNO_{3(aq)}$, $HCl_{(aq)}$, $NH_{3(aq)}$, $H_2SO_{4(aq)}^2$.
Solid phase :	$(NH_4)_2SO_4$, NH_4HSO_4, $(NH_4)_3H(SO_4)_2$, NH_4NO_3, NH_4Cl, NaCl, $NaNO_3$, $NaHSO_4$, Na_2SO_4

12.4 Thermodynamic equilibrium

The inorganic part mainly containing ammonium, sulfates and nitrates is the major part of the particulate matter. This is particularly true in the fine mode (D < 2.5 μm). The thermodynamic equilibrium model ISORROPIA [Nenes et al., 1998], is used to determine the particle/gas partitioning of semi-volatil inorganic species. The model calculate the thermodynamical equilibrium of the system: sulfate-nitrate-ammonium-sodium-chloride-water at a given temperature and relative humidity. The possible species are the following:
Due to its low vapor pressure, sulfuric acid is entirely transfered in the condensed phase. Also, the Sodium is located in the particulate phase. Inorganic aerosols can be a mix of solid and liquid species depending on temperature and humidity. The solid/liquid phase transition is solved by ISORROPIA by computing the deliquescent relative humidities (transition relative humidity between the phases). In the CHIMERE model, the calculation of the thermodynamic equilibrium can be done by interpolating a look-up table (see characteristics in Table 12.2). This look-up table has been pre-calculated and is delivered with the model in the file AEROMIN.bin. The partitioning coefficient for the nitrates and ammonium, and the aerosol water content has been calculated for a range of temperature from 260 to 312K, for relative humidity from 0.3 to 0.99 and for concentrations from 10^{-2} to 65 $\mu.g.m^{-3}$. Because of numerical limits, Sodium and Chloride are not accounted for in this table. The active seasalt version needs the to use the on-line coupling.

Variable	Value		Increment
	Min.	Max.	
Temperature (K)	260	312	2.5
Relative Humidity	0.3	0.99	0.05
H_2SO_4, HNO_3, NH_3 ($\mu.g.m^{-3}$)	10^{-2}	65	x 1,5

Table 12.2: *Characteristics of the look-up table used for the calculation of the thermodynamic equilibrium with ISORROPIA.*

The use of the look-up table allows to run the model faster, some errors can occur around each deliquescent point. This approach has been compared to the on-line coupling and tested on an entire year (2001) at the regional scale (0,5^{o}x0,5^o) over Europe.

Species	DRH (298.15K)	Mixing	MDRH (298.15K)
$(NH_4)_2SO_4$	0.799		
NH_4NO_3	0.618	NH_4NO_3, $(NH_4)_2SO_4$	0.600
NH_4HSO_4	0.400	$(NH_4)_3H(SO_4)_2$, NH_4HSO_4	0.360
$(NH_4)_3H(SO_4)_2$	0.690	$(NH_4)_3H(SO_4)_2$, $(NH_4)_2SO_4$	0.675

Table 12.3: *Relative humidity at deliquescent points for the species used by ISORROPIA in the system sulfate-nitrate-ammonium-water.*

The comparison shows the use of an on-line coupling leads to a weak decrease of the mean concentrations

(13% for the nitrates, and no more than 2% for the sulfates) on the EMEP site. Ammonium concentrations are slightly increase (1 to 5%). In absolute values, the differences never exceed 0.5 $\mu.g.m^{-3}$ in average for the nitrates and 0.1 $\mu.g.m^{-3}$ for the sulfates and ammonium. The aerosol water content is slightly decreased (3 to 13% ; 0,1 to 2,8 $\mu.g.m^{-3}$.

The sensitivity tests showed very weak differences, less than $\pm$ 20%. The differences are higher in winter compare to summer. The highest differences are observed above 50-60% for the nitrates and ammonium corresponding to the main deliquescent points. Indeed, the look-up table is not enough refined in this zone to account for the strong variations of the concentrations. For the water, the highest differences are observed in the range 95-100% where the absorption of water can increase by a factor of 1000. The differences do not depend on the temperature (not shown here).

The differences obtained when comparing the on-line coupling and the look-up table are small enough compare to the uncertainties in the modelling of the other processes. The look-up table of ISORROPIA is able to determine the partition of NH_4/NH_3 and HNO_3/NO_3.

12.4.1 Humid diameter and density of aerosols

In many processes, the diameter and the density of aerosols are used (deposition, absorption, coagulation, etc...). These processes have to take into account that the diameter and the density of aerosols change with humidity due to the amount of water absorbed into the particles. The amount of water in each bins is computed with the "reverse mode" of ISORROPIA by using the composition of particles. The density of the aqueous phase of particles is computed according to composition following the method of [Semmler et al., 2006]. The density of the aqueous phase and the amount of water of each of the bins are used to wet diameters.

12.5 Multiphase chemistry

12.5.1 Sulfur aqueous chemistry

If the aerosol option of the model is selected, Aqueous sulphate chemistry is considered; Sulfate is produced in the following aqueous reactions ([Berge, 1993]; [Hoffmann and Calvert, 1985]; [Lee and Schwartz, 1983]):

$$\begin{aligned} SO_2^{aq} + O_3^{aq} &\rightarrow SO_4^{2-} \\ HSO_3^- + O_3^{aq} &\rightarrow SO_4^{2-} \\ SO_3^{2-} + O_3^{aq} &\rightarrow SO_4^{2-} \\ SO_2^{aq} + H_2O_2^{aq} &\rightarrow SO_4^{2-} \\ SO_2^{aq} + NO_2^{aq} &\rightarrow SO_4^{2-} \\ SO_3^{2-}(Fe^{3+}) &\rightarrow SO_4^{2-} \\ HSO_3^-(Mn^{2+}) &\rightarrow SO_4^{2-} \end{aligned} \tag{12.16}$$

SO_2, H_2O_2 and O_3 in the aqueous phase are in equilibrium with the concentrations in the gas phase. Moreover, aqueous SO_2 is dissociated into HSO_3^- and SO_3^{2-}. Catalyzed oxidation reactions of sulfur dioxide in aqueous droplets with iron and manganese are considered, following [Hoffmann and Calvert, 1985] among others. Henry's law coefficient and other aqueous equilibrium constants are used ([Seinfeld and Pandis, 1998]).

Sulfur chemistry is very pH sensitive. pH is computed according to concentrations of CO_2, SO_2, H_2SO_4, HNO_3, HCl, Na and NH_3.

12.5.2 Heterogeneous chemistry

Again with the aerosol option of the model, a few heterogeneous reactions are also considered. Nitric acid is produced onto existing particles and fog droplets. Although aerosol particles and cloud droplets occupy a very small fraction of the atmosphere, it is now well established that reactions involving gas species onto their surfaces may significantly contribute to atmospheric chemistry cycles. [Jacob, 2000] recommends for ozone model to include a minimal set of reactions with associated uptake coefficients given by [Harrison and Kito, 1990], and other references in [Jacob, 2000]:

$$\begin{aligned} HO_2 &\rightarrow 0.5H_2O_2 & \gamma &= 0.2 \\ NO_3 &\rightarrow HNO_3 & \gamma &= 0.001 \\ NO_2 &\rightarrow 0.5HNO_3 + 0.5HONO & \gamma &= 0.0001 \\ N_2O_5 &\rightarrow 2HNO_3 & \gamma &= 0.01 - 1 \end{aligned}$$

The first-order rate constant k for gas heterogeneous loss onto particles is given by:

$$k = \sum_l \left(\frac{d_l}{2D_g} + \frac{4}{V\gamma} \right)^{-1} A_l \tag{12.17}$$

with d_l, the particle diameter (m), D_g, the reacting gas molecular diffusivity (m2 s^{-1}), n, the mean molecular velocity (m s-1), A_l, the total surface area in the particle bin l and gamma the uptake coefficient of reactive species. The uptake coefficient for N_2O_5 is assumed to be temperature-dependent in the range 0.01 - 1 ([De Moore et al., 1994]) with increasing values for decreasing temperatures.
Finally, the study of [Aumont et al., 2003] suggested that NO_2 reactions on wet surfaces could be an important source for HONO production during wintertime smog episodes. An additional reaction is added in the gas-phase mechanism,.

12.6 Secondary organic aerosol (SOA)

The complete chemical scheme implemented in CHIMERE includes biogenic and anthropogenic precursors (Table 12.4).
Biogenic precursors include:

- APINEN (α-pinene and sabinene),
- BPINEN (β-pinene and δ^3-carene),
- LIMONE (limonene), OCI (myrcene and ocimene)
- C5H8 (isoprene).

Anthropogenic precursors include:

- TOL (benzene, toluene and other mono-substituted aromatics),
- TMB (Trimethylbenzene and other poly-substituted aromatics),
- NC4H10 (higher alkanes).

SOA formation is represented according to a single-step oxidation of the relevant precursors and gas-particle partitioning of the condensable oxidation products.
The gas-particle partitioning formulation has been described in detail by [Pun et al., 2006]. The overall approach consists in differentiating between hydrophilic SOA that are most likely to dissolve into aqueous inorganic particles and hydrophobic SOA that are most likely to absorb into organic particles.

Reactions	kinetic rates ($molec.cm^{-3}.s^{-1}$)
TOL+OH → 0.004×AnA0D + 0.001×AnA1D + 0.084×AnBmP + 0.013×AnBlP	1.81×10^{-12}exp(355/T)
TMB+OH → 0.002×AnA0D + 0.002× AnA1D + 0.001×AnA2D + 0.088×AnBmP + 0.006×AnBlP	9.80×10^{-9}/T
NC4H10+OH → 0.07×AnBmP	1.36×10^{-12}exp(190/T)$^{-2}$
APINEN+OH → 0.30×BiA0D + 0.17×BiA1D + 0.10×BiA2D	1.21×10^{-11}exp(444/T)
APINEN+O3 → 0.18×BiA0D + 0.16×BiA1D + 0.05×BiA2D	1.01×10^{-15}exp (-732/T)
APINEN+NO3 → 0.80×BiBmP	1.19×10^{-12}exp(490/T)
BPINEN+OH → 0.07×BiA0D + 0.08×BiA1D + 0.06×BiA2D	2.38×10^{-11}exp(357/T)
BPINEN+O3 → 0.09×BiA0D + 0.13×BiA1D + 0.04×BiA2D	1.50×10^{-17}
BPINEN+NO3 → 0.80×BiBmP	2.51×10^{-12}
LIMONE+OH → 0.20×BiA0D + 0.25×BiA1D + 0.005×BiA2D	1.71×10^{-10}
LIMONE+O3 → 0.09×BiA0D + 0.10×BiA1D	2×10^{-16}
OCIMEN+OH → 0.70×BiA0D + 0.075×BiA1D	$5.10\times^{-8}$/T
OCIMEN+O3 → 0.50×BiA0D + 0.055×BiA1D	7.50×10^{-14}/T
OCIMEN+NO3 → 0.70×BiA0D + 0.075×BiA1D	4.30×10^{-9}/T
HUMULE+OH → 0.74×BiBmP + 0.26×BiBlP	2.93×10^{-10}
C5H8+OH → 0.232×ISOPA1 + 0.0288×ISOPA2	2.55×10^{-11}exp(410/T)

Table 12.4: *Gas phase chemical scheme for SOA formation in CHIMERE. The surrogate SOA compounds consist of six hydrophilic species that include an anthropogenic nondissociative species (AnA0D), an anthropogenic once-dissociative species (AnA1D), an anthropogenic twice-dissociative species (AnA2D), a biogenic non dissociative species (BiA0D), a biogenic once-dissociative species (BiA1D) and a biogenic twice-dissociative species (BiA2D), three hydrophobic species that include an anthropogenic species with moderate saturation vapor pressure (AnBmP), an anthropogenic species with low saturation vapor pressure (AnBlP) and a biogenic species with moderate saturation vapor pressure (BiBmP), and two surrogate compounds for the isoprene oxidation products.*

The dissolution of hydrophilic SOA is governed by Henry's law whereas the absorption of hydrophobic particles is governed by Raoult's law. The large number of condensable organic compounds is represented by a set of surrogate compounds that cover the range of physico-chemical properties relevant for aerosol formation, i.e., water solubility and acid dissociation for hydrophilic compounds and saturation vapor pressure for hydrophobic compounds. These surrogate compounds were selected by grouping identified particulate-phase molecular products with similar properties. The molecular weight of each surrogate compound is determined based on its structure and functional groups. The Henry's law constant or the saturation vapor pressure of the surrogate species is derived from the average properties of the group. Other properties are estimated using the structure of each surrogate compound. Enthalpy of vaporization are given in brackets ($kJ.mol^{-1}$) for each SOA coumpounds : AnA0D (88), AnA1D(88), AnA2D(88), BiA0D(88), BiA1D(88), BiA2D(109), AnBmP(88), AnBlP(88), BiBmP(175). The full name of compounds are explicited in Table 12.4 caption.
The absorption process in CHIMERE is implemented as in [Bowman et al., 1997]. A dynamical approach is adopted to decribe the gas/particle conversion since the model time-step is about 5 min. and using the approach by [Bowman et al., 1997], the characteristic time for mass transfer can exceed 20 min. for coarse particles.

$$J_i = \frac{1}{\tau_i}(G_i - G_i^{eq}) \tag{12.18}$$

J_i ($\mu g.m^{-3}.s^{-1}$) is the absorption or desorption flux of species i, τ_i (s) is a characteristic time of the mass transfer that depends on particle size and the chemical properties of species i, G_i is the bulk gas-phase concentration of species i and G_i^{eq} is the gas-phase concentration of species i at thermodynamic equilibrium (i.e., at the surface of the particle). The equilibrium gas-phase concentrations are functions of the particle chemical composition, temperature and, for hydrophilic species, relative humidity, as described by [Pun et al., 2006].

The base SOA module was tested against the smog chamber data of [Odum et al., 1997] for anthropogenic compounds and those of [Griffin et al., 1999] for biogenic compounds and was shown to satisfactorily reproduce SOA formation for those compounds [Pun et al., 2006]. Higher alkanes and isoprene were added to the original chemical mechanism of [Pun et al., 2006]. The formation of SOA from higher alkanes follows the formulation of [Zhang et al., 2007] for the stoichiometric SOA yield and it is assumed that the SOA species can be represented by a hydrophobic surrogate compound with a moderate saturation vapor pressure. The formation of SOA from the oxidation of isoprene by hydroxyl radicals is represented with two surrogate products and follows the formulation of [Kroll et al., 2006, Zhang et al., 2007].

12.7 Radiative transfers and photochemical reaction rates

12.7.1 Radiative processes in the atmosphere

Up to version 2013b, CHIMERE worked exclusively with tabulated photochemical reaction rates, precalculated using the TUV model, and using a simple parameterization for attenuation by clouds. The photolysis rates were therefore assumed constant on the vertical, and depended only on the zenithal angle and on the presence of clouds, which were assumed to be over model top. These assumptions were justified by the fact that CHIMERE was historically a boundary-layer model.
Since version 2014a, CHIMERE can take into account the following effects on photolysis:

- Effect of ice- and liquid-water clouds on photolysis rates through Mie diffusion
- Effect of aerosols on photolysis rates through absorption and Mie diffusion
- Effect of absorption by ozone on photolysis rates, using real-time ozone concentrations within the model domain instead of climatologies

This has been obtained by including the Fast-JX model for radiative transfer (version 7.0b, see [Wild et al., 2000, Bian et al., 2002]) inside CHIMERE. This model is a model for radiative transfer and photochemical rates that has been designed with the purpose of its inclusions in CTMs, and is already used in models such as Polair3D, Geos-Chem, UKCA and PHOTOMCAT (e.g. [Voulgarakis et al., 2009, Real and Sartelet, 2011, Telford et al., 2013]). The photolysis rates calculated by fast-JX have been validated in the boundary layer ([Barnars et al., 2004]) as well as in the free troposphere ([Voulgarakis et al., 2009]). Fast-JX is designed to reduce as much as possible the computational cost as much as possible without inducing errors of more than 5% on photochemical reaction rates. Actually, in CHIMERE, the additional computation cost with online calculation of the photolytic rates compared to the former formulation with tabulated rates is below 10% of the total computation cost.
Since version 2016a, the precalculated photolytic rates are not available anymore. Photolytic rates are mandatorily calculated using the Fast-JX module, v. 7.0b, included in the distributed version of CHIMERE. This choice is due to various factors:

- The developers consider important to take into account the effect of cloud layers and aerosol layers on photochemistry. Aerosol layers were not taken into account in the previous formulation, and clouds were taken into account in a very simplified way.
- The new outputs that have been included in the new model version (Aerosol optical depth, LIDAR backscatter) need intermediary results of Fast-JX.

From a computational point of view, the calculation of photochemical reaction rates is performed in three steps (Figure 12.1):

1. Preprocessing of aerosol optical properties (Mie scattering and absorption) for each aerosol species and bin, generate input files for Fast-JX: necessary only when changing aerosol species or their optical properties

2. Initialisation of Fast-JX model (read input files): at the beginning of each run

3. Online calculation of photochemical reaction rates (every physical time step)

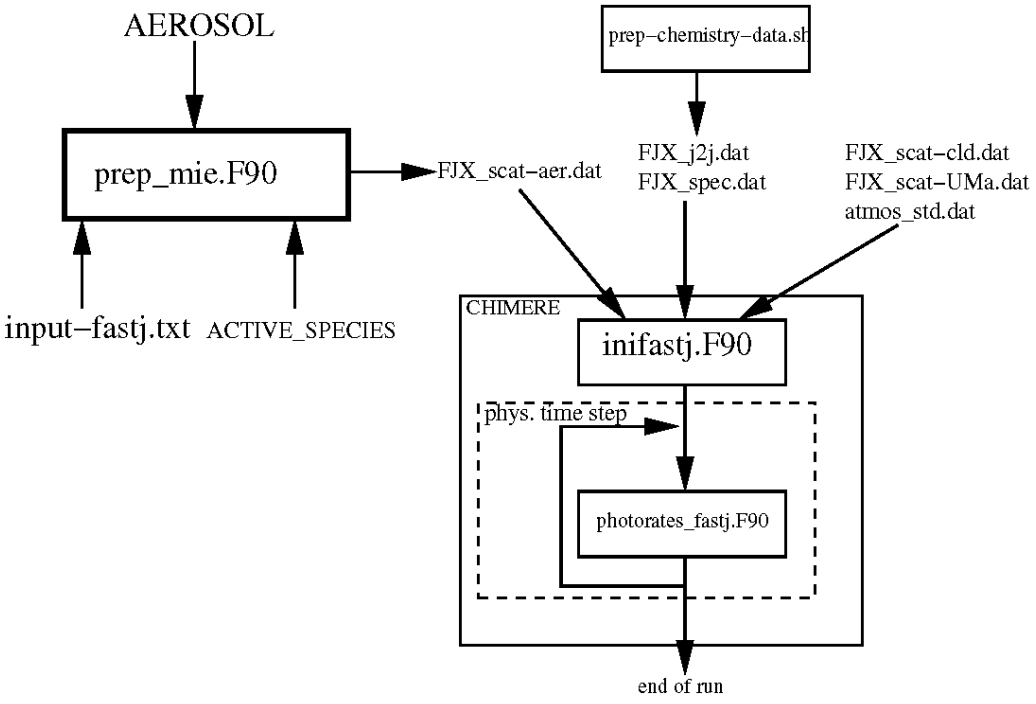


Figure 12.1: *Routines, files and scripts involved in the calculation of radiative transfers*

12.7.2 Optical preprocessing using prep_mie

The Mie calculations for each aerosol species and bins is performed by a short standalone program src/prep_mie.F90. This program is called by chimere-step1.sh and runs in the temporary execution directory. The name of its input and output files is stored in the prep_mie.nml file, in the same directory. src/prep_mie.F90 needs three input files:

1. AEROSOL:
   number of bins, their diameters and the list of the AEROSOL species,

2. input-fastj.txt:
   optical properties of each aerosol species (real and imaginary part of the refraction indices for 5 wavelength - 200 nm, 300 nm, 400 nm, 600 nm and 999 nm), as well as the density and Hanel size growth coefficient. This file needs to include these quantities for ALL aerosol species listed in the AEROSOL file. If the user adds a new aerosol specie, he will need to put its optical and physical properties in the input-fastj.txt file by editing it manually. Species in input-fastj.txt do not need to be in the same order as in the AEROSOL file, but it is requested that all aerosol species listed in the AEROSOL file shall be

present in the input-fastj.txt file, with exactly the same name. It is permitted that input-fastj.txt contains species that are not actually needed for the present run: input-fastj is used as a dictionnary of "all" the possible aerosol species and their physical and optical properties.

3. ACTIVE_SPECIES:
   list of the active species. This file is used only to check whether prep_mie writes its outputs with all the aerosol species in the right order.

It is worth noting that Fast-JX (as well as CHIMERE) treats distinct bins of a given aerosol species as distinct species. Therefore, prep_mie will perform the Mie calculations for $nbins \times naerospec$ species. The output file of src/prep_mie is stored in FJX_scat-aer.dat. This file includes, for each of the $nbins \times naerospec$ species, the effective radius, density, the efficiency factor Q, the single-scattering albedo and the first 7 terms of the Taylor expansion of the scattering phase function. These values are written in the exact same order as the order of the aerosol species in the ACTIVE_SPECIES file.
The Mie calculation is based on Michael Mischenko's spher.f code (which is distributed with CHIMERE as well). As it is a relatively long calculation (up to a couple of minutes depending on the computer and on the number of aerosol species and bins), it is performed only if the FJX_scat-aer.dat is absent in the inputdata directory. Therefore, if the user modifies the optical or physical properties of the aerosols in input-fastj.txt, he will need to remove the FJX_scat-aer.dat file from the inputdata directory in order to force recalculation of the scattering phase functions.

12.7.3 Fast-JX initialisation

Fast-JX initialisation is performed by the inifastj.F90 routine. This routine is a wrapper for the INIT_FJX routine of the module fjx_init_mod.F90. INIT_FJX reads the following input files:

1. FJX_spec.dat : cross-sections for photochemical reaction rates.
2. FJX_scat-cld.dat : cloud scattering data
3. FJX_scat-UMa.dat : University of Michigan aerosol scattering data (not used)
4. atmos_std.dat : temperature and ozone climatology - used for radiative transfers above the simulation domain
5. FJX_j2j.dat : file containing the information needed to reorder Fast-JX photochemical reaction rates in the order needed by the CTM - in this case, CHIMERE.

The values read from these input files are stored in arrays that are used for the online calculation of photochemical reaction rates at each physical time step.

12.7.4 Online calculation of photochemical reaction rates

The calculation of the photochemical reaction rates is performed by the routine photorates_fastj.F90, which calls the fast-jx PHOTO_JX routine (in fjx_sub_mod.f90) for each atmospheric column, after filling the input arrays of Fast-JX with the values from the meteorological model (for clouds) and from CHIMERE (for ozone and aerosols). photorates_fastj.F90 finally takes into account the clouds above model top by a simple calculation of the attenuation factor - whereas clouds within the CHIMERE domain are taken into account in details, separating water- and ice-clouds and performing an explicit Mie calculation.

Landuse		Albedo	
#	Description	(snow $<$ 1cm)	(snow $>$ 10 cm)
1	Agricultural land / crops	0.035	0.376
2	GrasslandLanduse type	0.04	0.720
3	Barren land/bare ground	0.10	0.836
4	Inland Water	0.07	-
5	Urban	0.035	0.3
6	Shrubs	0.05	0.558
7	Needleaf forest	0.025	0.278
8	Broadleaf forest	0.025	0.558
9	Ocean	0.07	-

Table 12.5: *Tabulated values from [Laepple et al., 2005] (for snow $<$ 1cm) and [Tanskannen and Manninen, 2007] (for snow $>$ 10 cm) used for the calculation of the albedo in the UV band*

12.7.5 surface albedo

In versions 2014a and 2014b, the surface albedo in the near UV band was assumed equal to 0.1, constant in space and time. However, it has been shown that the surface albedo in this wavelength band, which is the determinant band for the calculation of photolytic rates, is highly variable, according to the landuse and to the presence of snow. The surface albedo in the UV band is evaluated according to [Laepple et al., 2005] in the absence of snow, and from [Tanskannen and Manninen, 2007] in the presence of snow (Table 12.5).
The snow-depth is read from the meteorological inputs. In version 2016a, this feature has been coded only for WRF inputs. If any other model is used, the snow cover will be assumed inexistent. If the snow-cover is thinner than 1cm in the model, the albedo is assumed to be that of dry land. If the snow-cover is thicker than 10cm, the albedo is assumed to be that of snow-covered land. In-between, a linear interpolation is performed. The calculated value of the albedo is available in the CHIMERE outputs (variable “albedo”). Keep in mind that this albedo represents the albedo in the near-UV band, which is very different from the albedo in the visible band.

13 Additional diagnostic variables

During the model integration, some additional diagnostic variables are estimated:

- The Clouds Optical depth (COD) and the Aerosol Optical Depth (AOD)
- The lidar profiles (both in Nadir and Zenith lidar configuration).

13.1 The optical depth

The first step for modeling aerosol optical properties was to develop an aerosol optical scheme dedicated to the evaluation of vertically integrated particle loading (optical depth) as presented in [Pere et al., 2010].
This calculation is specifically designed to calculate aerosol properties directly comparable to AERONET data and satellite inversions (L2 products). It provides maps of aerosol optical depth (AOD) and other optical properties, such as the Single Scattering Albedo (SSA) and the asymmetry factor (g), based on simulated atmospheric chemical concentration fields.
The AOD or τ_{ext}, which represents the attenuation of the incident solar radiation light by atmospheric particles, depends on the wavelength (λ). For a layer thickness Δz, it is calculated as:

$$\tau_{\text{ext}}(\lambda, z) = \int_{\Delta z} \sigma_p^{\text{ext}}(\lambda, z')\mathrm{d}z' \tag{13.1}$$

This requires the calculation of the extinction coefficient (by particles), $\sigma_p^{\text{ext}}(z, \lambda)$ in m^{-1} as:

$$\sigma_p^{\text{ext}}(z, \lambda) = \int_{R_{\text{min}}}^{R_{\text{max}}} \pi R^2 Q_{\text{ext}}(\eta, R, \lambda) \cdot N_p(R, z)\mathrm{d}R \tag{13.2}$$

where Q_{ext} is the extinction efficiency, depending on the refractive index (η), the particles radius (R) and the wavelength (λ). N_p represents the particle concentration in number (m^{-3}). The complex refractive indices and density values are adaptated from FastJX database, depending on the specific CHIMERE model species.
The effect of relative humidity on the size of water soluble aerosols and therefore on the refractive index is accounted for by using a growth model as described in [Hänel, 1976]. A mean particle density is similarly defined. We consider a homogeneous internal mixing of the different chemical species. For the case of a homogeneous ensemble of spheres, the optical properties for the particles considered are computed using a Mie code [de Rooij and van der Stap, 1984]. Non-sphericity of particles such as mineral dust is theoretically and experimentally identified as a source of bias in simulated aerosol optical properties [Dubovik et al., 2002] but is not taken into account in this model version.

13.2 The lidar vertical profiles

13.2.1 Methodology

A general overview of the lidar signal modeling is displayed in Figure 13.1. The first column represents a model column, where aerosol concentrations (c_i) are available in grid cells for several model levels (z_i). This leads to a vertical concentration profile, where each c_i concentration represent the mean value between z_{i-1}

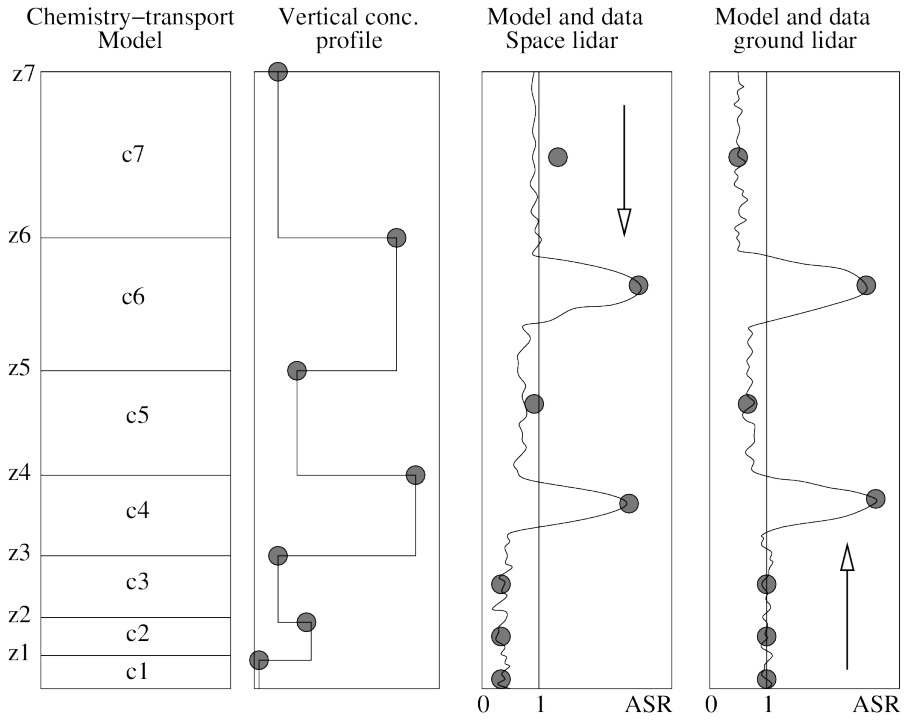


Figure 13.1: *Overview of the comparison methodology: example of the modelled Attenuated Scattering Ratio (ASR or $R'(z)$) estimation from initial concentration profiles (middle-left panel) on a specific model vertical grid (left panel) in the case of a space lidar (middle-right panel) or a ground lidar (right panel). The grey dots correspond to the value reported in the model simulation. After [Stromatas et al., 2012]*

and z_i (z_0 representing the ground). Based on this concentration profile, we simulate the lidar signal that would be observed by a lidar in space (third column) or by a ground based lidar (fourth column).
The calculation of the lidar signal from simulated aerosol concentration fields requires additional parameters than those used for the AOD.
In order to efficiently compare modeled and measured lidar profiles, the simulator is designed to calculate the Attenuated Scattering Ratio, $R'(z)$. By definition, $R'(z)$ is equal to 1 in absence of aerosols/clouds and when the signal is not attenuated. In the presence of aerosol, $R'(z)$ would be greater than one. Following [Winker et al., 2009], this ratio is expressed as:

$$R'(z) = \frac{\beta'(z)}{\beta'_{\mathrm{m}}(z)} \tag{13.3}$$

where

$$\beta'(z,\lambda) = \left[\frac{\sigma_{\mathrm{m}}^{\mathrm{sca}}(z,\lambda)}{S_{\mathrm{m}}(z,\lambda)} + \frac{\sigma_{\mathrm{p}}^{\mathrm{sca}}(z,\lambda)}{S_{\mathrm{p}}(z,\lambda)}\right] \cdot \exp\left(-2\left[\int_z^{\mathrm{TOA}} \sigma_{\mathrm{m}}^{\mathrm{ext}}(z',\lambda)\mathrm{d}z' + \eta' \int_z^{\mathrm{TOA}} \sigma_{\mathrm{p}}^{\mathrm{ext}}(z',\lambda)\mathrm{d}z'\right]\right) \tag{13.4}$$

and

$$\beta'_{\mathrm{m}}(z,\lambda) = \frac{\sigma_{\mathrm{m}}^{\mathrm{sca}}(z,\lambda)}{S_{\mathrm{m}}(z,\lambda)} \cdot \exp\left(-2\int_z^{\mathrm{TOA}} \sigma_{\mathrm{m}}^{\mathrm{ext}}(z',\lambda)\mathrm{d}z'\right) \tag{13.5}$$

$\beta'(z,\lambda)$ and $\beta'_{\rm m}(z,\lambda)$ are, respectively the total and molecular attenuated backscatter signal. $\sigma_{\rm p}^{\rm sca/ext}(z,\lambda)$ and $\sigma_{\rm m}^{\rm sca/ext}(z,\lambda)$ are the extinction/scattering coefficients for particles and molecules (in km^{-1}). $S_{\rm m}$ (respectively $S_{\rm p}$) is the molecular (respectively particular) extinction-to-backscatter ratio (in sr).
Finally, $\eta'(z)$ represents the particles multiple scattering and z represents the distance between the emitter and the studied point. Note that for the case of a space lidar the integration begins from the top of the atmosphere (TOA) while for a ground lidar the integration begins from 0 (ground level) to z.
The molecular contribution ($\sigma_{\rm m}$ and $S_{\rm m}$) is calculated theoretically. In order to remain consistent with the observations, the same equation as the one used to derive the molecular backscattering coefficient for producing the CALIOP attenuated backscatter profiles is implemented [Hostetler et al., 2006]. When the vertical distribution of pressure (P) and temperature (T) is known, the molecular backscattering coefficient can be expressed as:

$$\sigma_{\rm m}^{\rm sca} = \frac{P}{k_{\rm B}T} \cdot \frac{s_{\rm sca,mol}(\pi)}{S_{\rm m}} \tag{13.6}$$

with $k_{\rm B}$ being the Boltzmann constant and $s_{\rm sca,mol}$ the molecular scattering cross section (in m^2), given by:

$$s_{\rm sca,mol} = 4.5102 \cdot 10^{-31} \cdot \left(\frac{\lambda}{0.55}\right)^{-4.025-0.05627\cdot(\lambda/550)-1.647} \tag{13.7}$$

Note that $S_{\rm m} = (8\pi/3)k_{bw}(\lambda)$ where k_{bw} represents the dispersion of the refractive index and King factor of air.
The molecular extinction coefficient $\sigma_{\rm m}^{\rm ext}$ is given as a function of $\sigma_{\rm m}^{\rm sca}$:

$$\sigma_{\rm m}^{\rm ext} = \frac{8\pi}{3} \cdot \sigma_{\rm m}^{\rm sca} \tag{13.8}$$

The particles contribution ($\sigma_{\rm p}$ and $S_{\rm p}$) can be written as a function of the particle concentration ($N_{\rm p}$ in m^{-3}) and on the particle scattering/extinction efficiency ($Q_{\rm sca/ext}$) which depends on the refractive index, the size of particles and the wavelength (λ).
Note that multiple scattering effects are not taken into account here (η is set to 1 in Eq. 13.4). The single scattering approximation is adequate for small optical depths and non-absorbing aerosols [Gordon, 1997]. However, large scattering particles such as mineral dust could lead to non-negligible multiple scattering effects [Wandinger et al., 2010].
Finally, we also simulate the color ratio (χ') which corresponds to the ratio between two lidar profiles observed simultaneously at two different wavelengths ($\lambda_1 = 1064$ nm and $\lambda_2 = 532$ nm) :

$$\chi'(z) = \frac{R'_{\lambda_1}(z)}{R'_{\lambda_2}(z)} == \frac{\beta'_{\lambda_1}(z)}{\beta'_{\lambda_2}(z)} \tag{13.9}$$

Since scattering is more efficient when the wavelength is of the same order of magnitude as the particle diameter, this ratio provides information of the size of the particles in the backscattering layers and hence on their nature (cloud droplets, dust or pollution aerosols for instance). χ' is expected to be lower than 1 for small particles compared to wavelengths. It allows the qualitative identification of large/small particles but since there is a significant overlap between the distributions of χ' for different aerosol types, it cannot be used directly as an aerosol type identification tool [Omar et al., 2010].

13.2.2 The CHIMERE output results

All calculations are done in the src/lidar.F90 routine. This routine is called hourly and the results are hourly written in the out result file. Note that the lidar profile are calculated using the same wavelengths as those used for fastJX.
The input variables are mainly extracted from the FastJX routines or from the meteorology and are:

- thlaylocm: current cell thickness (in meters)
- CSCAtab: scattering cross section [m^2]
- CEXTtab: extinction cross section [m^2]
- PPItab: Backward scattering ratio [ad.]
- wavel(nwl): wavelengths (meters)
- temp: temperature in Kelvin
- presloc: Pressure field (Pa)
- numconc: the concentration in number of all aerosols in a bin and a cell (m^{-3})

The output variables are tables named:

- Nadir:
  - atb_mol_nad: Molecular attenuated backscatter signal ($m^{-1}.sr^{-1}$)
  - atb_tot_nad: Total attenuated backscatter signal (molecular + particles) ($m^{-1}.sr^{-1}$)
  - scat_ratio_nad: Attenuated scattering ratio
- Zenith:
  - atb_mol_zen: Molecular attenuated backscatter signal ($m^{-1}.sr^{-1}$)
  - atb_tot_zen: Total attenuated backscatter signal (molecular + particles) ($m^{-1}.sr^{-1}$)
  - scat_ratio_zen: Attenuated scattering ratio

Bibliography

[Aan de Brugh et al., 2012] Aan de Brugh, J. M. J., Henzing, J. S., Schaap, M., Morgan, W. T., van Heerwaarden, C. C., Weijers, E. P., Coe, H., and Krol, M. C. (2012). Modelling the partitioning of ammonium nitrate in the convective boundary layer. *Atmos. Chem. Phys.*, 12:3005–3023.

[Alfaro et al., 1997] Alfaro, S. C., Gaudichet, A., Gomes, L., and Maillé, M. (1997). Modeling the size distribution of a soil aerosol produced by sandblasting. *J of Geophysical Research*, 102:11,239–11,249.

[Alfaro et al., 1998] Alfaro, S. C., Gaudichet, A., Gomes, L., and Maillé, M. (1998). Mineral aerosol production by wind erosion: aerosol particle sizes and binding energies. *Geophys. Res. Lett*, 25:991–994.

[Alfaro and Gomes, 2001] Alfaro, S. C. and Gomes, L. (2001). Modeling mineral aerosol production by wind erosion: Emission intensities and aerosol size distribution in source areas. *J of Geophysical Research*, 106:18,075–18,084.

[Anav et al., 2011] Anav, A., Menut, L., Khvorostiyanov, D., and Viovy, N. (2011). Impact of tropospheric ozone on the Euro-Mediterranean vegetation. *Global Change Biology*, 17.

[Atkinson et al., 1997] Atkinson, R., Baulsch, D. L., Cox, R. A., Hampton, R. F., Kerr, J. A., Rossi, M. J., and Troe, J. (1997). Evaluated kinetics, photochemical and heterogeneous data. *J. Phys. Chem.*, 26(3):521–1012.

[Aumont et al., 2003] Aumont, B., Chervier, F., and Laval, S. (2003). Contribution of HONO sources to the NOx/HOx/O3 chemistry in the polluted boundary layer. *Atmospheric Environment*, 37(4):487 – 498.

[Baer and Nester, 1992] Baer, M. and Nester, K. (1992). Parameterization of trace gas dry deposition velocities for a regional mesoscale diffusion model. *Ann. Geophys.*, 10:912–923.

[Balkanski et al., 2007] Balkanski, Y., Schulz, M., Claquin, T., and Guibert, S. (2007). Reevaluation of mineral aerosol radiative forcings suggests a better agreement with satellite and aeronet data. *Atmospheric Chemistry and Physics*, 7(1):81–95.

[Barnars et al., 2004] Barnars, J. C., Chapman, E. G., Fast, J. D., Schmelzer, J. R., Slusser, J. R., and Shetter, R. E. (2004). An evaluation of the FAST-J photolysis algorithm for predicting nitrogen dioxide photolysis rates under clear and cloudy sky conditions. *Atmos Environ*, 38:3393–3403.

[Bauer et al., 2004] Bauer, S., Balkanski, Y., Schulz, M., Hauglustaine, D. A., , and Dentener, F. (2004). Heterogeneous chemistry on mineral aerosol surfacesă: a global modelling study on the influence on tropospheric ozone chemistry and comparison to observations. *J Geophys Res*, 109:D02304.

[Berge, 1993] Berge, E. (1993). Coupling of wet scavenging of sulphur to clouds in a numerical weather prediction model. *Tellus*, 45B:1–22.

[Bessagnet et al., 2004] Bessagnet, B., Hodzic, A., Vautard, R., Beekmann, M., Cheinet, S., Honoré, C., Liousse, C., and Rouil, L. (2004). Aerosol modeling with CHIMERE: preliminary evaluation at the continental scale. *Atmospheric Environment*, 38:2803–2817.

[Bessagnet et al., 2008] Bessagnet, B., Menut, L., Aymoz, G., Chepfer, H., and Vautard, R. (2008). Modelling dust emissions and transport within Europe: the Ukraine March 2007 event. *Journal of Geophysical Research*, 113:D15202.

[Bian et al., 2002] Bian, H., , and Prather, M. (2002). Fast-J2: accurate simulation of stratospheric photolysis in global chemical models. *J. Atmos. Chem.*, 41:281–296.

[Bicheron et al., 2011] Bicheron, P., Amberg, V., Bourg, L., Petit, D., Huc, M., Miras, B., Brockmann, C., Hagolle, O., Delwart, S., Ranera, F., Leroy, M., and Arino, O. (2011). Geolocation assessment of meris globcover orthorectified products. *IEEE Transactions on geoscience and remote sensing*, 49(8):2972–2982.

[Bowman et al., 1997] Bowman, F. m., Odum, J. R., Seinfeld, J. H., and Pandis, S. N. (1997). Mathematical model for gas-particle parttioning of secondary organic aerosols. *Atmos. Environ.*, 31:3921–3931.

[Byun et al., 1999] Byun, D. W., Young, J., Pleim, J., Odman, M. T., and Alapaty, K. (1999). Numerical transport algorithms for the community multiscale air quality (cmaq) chemical transport model in generalized coordinates. In *Science Algorithms of the EPA Models-3 Community Multiscale Air Quality (CMAQ) Modeling System*. US-EPA Office of Research and Development Washington, DC 20460, EPA/600/R-99/030.

[Cakmur et al., 2004] Cakmur, R. V., Miller, R. L., and Torres, O. (2004). Incorporating the effect of small-scale circulations upon dust emission in an atmospheric general circulation model. *J. Geophys. Res.*, 109:D07201.

[Carter, 2010] Carter, W. (2010). Development of the saprc-07 chemical mechanism. *Atmos Environ*, 44(40):5324 – 5335.

[Carter, 1990] Carter, W. P. L. (1990). A detail mechanism for the gas-phase atmospheric reactions of organic compounds. *Atmospheric Environment*, 24:481–518.

[Cheinet and Teixeira, 2003] Cheinet, S. and Teixeira, J. (2003). A simple formulation for the eddy-diffusivity parameterization of cloud-topped boundary layers. *GEOPHYSICAL RESEARCH LETTERS*, 30(18).

[Colella and Woodward, 1984] Colella, P. and Woodward, P. R. (1984). The piecewise parabolic method (PPM) for gas-dynamical simulations. *Journal of Computational Physics*, 11:38–39.

[Courant et al., 1952] Courant, R., Issacson, E., and Reees, M. (1952). On the solution of nonlinear hyperbolic differential equations by finite differences. *Comm. Pure Appl. Math.*, 5:243–255.

[Davidson et al., 1982] Davidson, C., Miller, J., and Pleskow, M. (1982). The influence of surface structure on predicted particle air deposition to natural grass canopies. *Water, Air and Soil Pollution*, 18:25–44.

[De Moore et al., 1994] De Moore, W. B., Sandetr, S. P., Golden, D. M., Hampton, R. F., Kurylo, M. J., Howard, C. J., Ravishankara, A. R., Kolb, C. E., and Molina, M. J. (1994). Chemical kinetics and photochimical data for use in stratospheric modelling evaluation. *JPL publication*, 94, 26, JPL, Pasadena, US.

[de Rooij and van der Stap, 1984] de Rooij, W. A. and van der Stap, C. C. A. H. (1984). Expansion of mie scattering matrices in generalized spherical functions. *Astronomy and Astrophysics*, 131(2):237–248.

[Debry et al., 2007] Debry, E., Fahey, K., Sartelet, K., Sportisse, B., and Tombette, M. (2007). Technical Note: A new SIze REsolved Aerosol Model (SIREAM). *Atmos. Chem. Phys.*, 7:1537–1547.

[Derognat et al., 2003] Derognat, C., Beekmann, M., Baeumle, M., Martin, D., and Schmidt, H. (2003). Effect of biogenic volatile organic compound emissions on tropospheric chemistry during the atmospheric pollution over the paris area (esquif) campaign in the ile-de-france region. *JOURNAL OF GEOPHYSICAL RESEARCH-ATMOSPHERES*, 108(D17).

[Dubovik et al., 2002] Dubovik, O., Holben, B. N., Lapyonok, T., Sinyuk, A., Mishchenko, M. I., Yang, P., and Slutsker, I. (2002). Non-spherical aerosol retrieval method employing light scattering by spheroids. *Geosphys. Res. Lett*, 29:1415.

[Ebel et al., 1994] Ebel, A., Friedrich, R., and Rodhe, H. (1994). Tropospheric modelling and emission estimation: Generation of european emission data for episodes (genemis) project, eurotrac annual report 1993, part 5.

[Emberson et al., 2000] Emberson, L.-D., Simpson, D., Tuovinen, J.-P., Ashmore, M.-R., and Cambridge, H.-M. (2000). Towards a model of ozone deposition and stomatal uptake over Europe. Technical report. EMEP/MSC-W 2000.

[Erisman et al., 1994] Erisman, J. W., van Pul, A., and Wyers, P. (1994). Parameterization of surface resistance for the quantification of atmospheric deposition of acidifying pollutants and ozone. *Atmospheric Environemnt*, 28:2595–2607.

[Fecan et al., 1999] Fecan, F., Marticorena, B., and Bergametti, G. (1999). Parameterization of the increase of aeolian erosion threshold wind friction velocity due to soil moisture for arid and semi-arid areas. *Annals of Geophysics*, 17:149–157.

[Folberth et al., 2006] Folberth, G. A., Hauglustaine, D. A., Lathière, J., and Brocheton, F. (2006). Interactive chemistry in the laboratoire de météorologie dynamique general circulation model: model description and impact analysis of biogenic hydrocarbons on tropospheric chemistry. *Atmos. Chem. Phys.*, 6:2273–2319.

[Gelbard and Seinfeld, 1980] Gelbard, F. and Seinfeld, J. H. (1980). Simulation of multicomponent aerosol dynamics. *Journal of colloid and Interface Science*, 78:485–501.

[Ginoux et al., 2001] Ginoux, P., Chin, M., Tegen, I., Prospero, J. M., Holben, B., Dubovik, O., and Lin, S. J. (2001). Sources and distributions of dust aerosols simulated with the GOCART model. *Journal of Geophysical Research*, 106:20255–20273.

[Giorgi, 1986] Giorgi, F. (1986). A particle dry deposition scheme for use in tracer transport models'. *J. Geophys. Res.*, 91:9794–9806.

[Gordon, 1997] Gordon, H. (1997). Atmospheric correction of ocean color imagery in the earth observing system era. *J. Geophys. Res.*, 102(D14):17081–17106.

[Griffin et al., 1999] Griffin, R. J., Cocker, E. R., Flagan, R. C., and Seinfeld, J. H. (1999). Organic aerosol formation from the oxidation of biogenic hydrocarbons. *Journal of Geophysical Research*, 104:3555–3567.

[Guenther et al., 2006] Guenther, A., Karl, T., Harley, P., Wiedinmyer, C., Palmer, P., and Geron, C. (2006). Estimates of global terrestrial isoprene emissions using MEGAN (Model of Emissions of Gases and Aerosols from Nature). *Atmos. Chem. Phys.*, 6:3181–3210.

[Hall et al., 1999] Hall, S., Khudaish, E., and Hart, A. (1999). Electrochemical oxidation of hydrogen peroxide at platinum electrodes. part iii: Effect of temperature. electrochim. *Electrochim. Acta*, 44:2455–2462.

[Hänel, 1976] Hänel, G. (1976). The properties of atmospheric particles as functions of the relative humidity at thermodynamic equilibrium with surrounding moist air. *Advances in Geophysics*, 19:73–188.

[Harrison and Kito, 1990] Harrison, R. and Kito, A. (1990). Field intercomparison of filter pack and denuder sampling methods for reactive gaseous and particulate pollutants. *Atmos. Environ.*, 24:2633–2640.

[Hauglustaine et al., 2014] Hauglustaine, D. A., Balkanski, Y., and Schulz, M. (2014). A global model simulation of present and future nitrate aerosols and their direct radiative forcing of climate. *Atmos Chem Phys*, 14:6863–6949.

[Hauglustaine et al., 2004] Hauglustaine, D. A., Hourdin, F., Jourdain, L., Filiberti, M.-A., Walters, S., Lamarque, J.-F., and Holland, E. A. (2004). Interactive chemistry in the Laboratoire de Meteorologie Dynamique general circulation model: Description and background tropospheric chemistry evaluation. *Journal of Geophysical Research*, 109(D04314). doi:10.1029/2003JD003,957.

[Henzig et al., 2006] Henzig, J. S., Olivié, D., and van Velthoven, P. (2006). A parameterization of size resolved below cloud scavenging of aerosols by rain. *Atmos. Chem. Phys.*, 6:3363–3375.

[Hicks et al., 1987] Hicks, B. B., Baldocchi, D. D., Meyers, T. P., Hosker Jr., R. P., and Matt, D. R. (1987). A preliminary multiple resistance routine for deriving dry deposition velocities from measured quantities. *Water, Air, Soil Pollut.*, 36.

[Hodzic et al., 2006a] Hodzic, A., Bessagnet, B., and Vautard, R. (2006a). A model evaluation of coarse-mode nitrate heterogeneous formation on dust particles. *Atmos. Environ.*, 40:4158–4171.

[Hodzic et al., 2010a] Hodzic, A., Jimenez, J., Madronich, S., Canagaratna, M., DeCarlo, P., Kleinman, L., and Fast, J. (2010a). Modeling organic aerosols in a megacity: potential contribution of semi-volatile and intermediate volatility primary organic compounds to secondary organic aerosol formation. *Atmos. Chem. Phys.*, 10.

[Hodzic et al., 2010b] Hodzic, A., Jimenez, J., Prevot, A., Szidat, S., Fast, J., and Madronich, S. (2010b). Can 3D Models Explain the Observed Fractions of Fossil and non-Fossil Carbon In and Near Mexico City? *Atmos. Chem. Phys.*, 10.

[Hodzic et al., 2009] Hodzic, A., Jimenez, J. L., Madronich, S., Aiken, A. C., Bessagnet, B., Curci, G., Fast, J., Lamarque, J.-F., Onasch, T. B., Roux, G., Schauer, J. J., Stone, E. A., and Ulbrich, I. M. (2009). Modeling organic aerosols during milagro: importance of biogenic secondary organic aerosols. *Atmospheric Chemistry and Physics*, 9(18):6949–6981.

[Hodzic et al., 2005] Hodzic, A., Vautard, R., Bessagnet, B., Lattuati, M., and Moreto, F. (2005). Long-term urban aerosol simulation versus routine particulate matter observations. *Atmospheric Environemnt*, 39:5851–5864.

[Hodzic et al., 2006b] Hodzic, A., Vautard, R., Chazette, P., Menut, L., and B.Bessagnet (2006b). Aerosol chemical and optical proprties over the Paris area within ESQUIF project. *Atmospheric Chemistry and Physics*, 6:3257–3280.

[Hoffmann and Calvert, 1985] Hoffmann, M. R. and Calvert, J. G. (1985). Chemical transformation modules for eulerian acid deposition models,. EPA/600/3-85/017.

[Honoré et al., 2008] Honoré, C., Rouïl, L., Vautard, R., Beekmann, M., Bessagnet, B., Dufour, A., Elichegaray, C., Flaud, J., Malherbe, L., Meleux, F., Menut, L., Martin, D., Peuch, A., Peuch, V., and Poisson, N. (2008). Predictability of European air quality: The assessment of three years of operational forecasts and analyses by the PREV'AIR system. *Journal of Geophysical Research*, 113:D04301.

[Honoré and Vautard, 2000] Honoré, C. and Vautard, R. (2000). Photochemical regimes in urban atmospheres: The influence of dispersion. *Geophys. Res. Letters*, 27:1895–1898.

[Horowitz, 2003] Horowitz, L. W., e. a. (2003). A global simulation of tropospheric ozone and related tracers: Description and evaluation of mozart, version 2. *J Geophys Res*, 108(D24):4784.

[Hostetler et al., 2006] Hostetler, C. A., Liu, Z., Reagan, J., Vaughan, M., Winker, D., Osborn, M., Hunt, W. H., Powell, K. A., , and Trepte, C. (2006). Caliop algorithm theoretical basis document, calibration and level 1 data products. *PC-SCI-201*, (NASA Langley Research Center):Hampton, VA 23681.

[Hourdin and Armengaud, 1999] Hourdin, F. and Armengaud, A. (1999). On the use of finite volume methods for atmospheric advection of trace species. Part I: Test of various formulations in a general circulation models. *Monthly Weather Review*, 127:822–837.

[Iversen and White, 1982] Iversen, J. D. and White, B. R. (1982). Saltation threshold on earth, mars and venus. *Sedimentology*, 29:111–119.

[Jacob, 2000] Jacob, D. J. (2000). Heterogeneous chemistry and tropospheric ozone. *Atmospheric Environment*, 34(34):2131–2159.

[Jacobson, 1999] Jacobson, M. (1999). *Fundamentals of Atmospheric Modeling*. Cambridge University Press.

[Kaupp and Umlauf, 1992] Kaupp, H. and Umlauf, G. (1992). Atmospheric gas-particle partitioning of organic compounds: a comparison of sampling methods. *Atmospheric Environment*, 26A:2259–2267.

[Kavouras et al., 1998] Kavouras, I., Mihalopoulos, N., and Stephanou, E. (1998). Formation of atmospheric particles from organic acids produced by forests. *Nature*, 395:683–686.

[Kok et al., 2014] Kok, J. F., Mahowald, N. M., Fratini, G., Gillies, J. A., Ishizuka, M., Leys, J. F., Mikami, M., Park, M.-S., Park, S.-U., Van Pelt, R. S., and Zobeck, T. M. (2014). An improved dust emission model Ž2013 part 1: Model description and comparison against measurements. *Atmospheric Chemistry and Physics*, 14(23):13023–13041.

[Kroll et al., 2006] Kroll, J. H., Ng, N. L., Murphy, S. M., Flagan, R. C., and Seinfeld, J. H. (2006). Secondary organic aerosol formation from isoprene photooxidation. *Environ. Sci. Technol.*, 40:1869–1877.

[Kulmala et al., 1998] Kulmala, M., A., L., and Pirjola, L. (1998). Parameterization for sulfuric acid / water nucleation rates. *J. Geophys. Res.*, 103(No D7):8301–8307.

[Kurtenbach et al., 2001] Kurtenbach, R., Becker, K., Gomes, J., Kleffmann, J., LŽrzer, J., Spittler, M., Wiesen, P., Ackermann, R., Geyer, A., and Platt, U. (2001). Investigations of emissions and heterogeneous formation of HONO in a road traffic tunnel. *Atmospheric Environment*, 35(20):9506 – 9517. 3385Ð3394.

[Laepple et al., 2005] Laepple, T., Schultz, M. G., Lamarque, J. F., Madronich, S., Shetter, R. E., Lefer, B. L., and Atlas, E. (2005). Improved albedo formulation for chemistry transport models based on satellite observations and assimilated snow data and its impact on tropospheric photochemistry. *J. Geophys. Res.*, 110:D11308.

[Lattuati, 1997] Lattuati, M. (1997). *Contribution à l'étude du bilan de l'ozone troposphérique à l'interface de l'Europe et de l'Atlantique Nord: modélisation lagrangienne et mesures en altitude*. Phd thesis, Université P.M.Curie, Paris, France.

[Lee and Schwartz, 1983] Lee, Y. N. and Schwartz, S. E. (1983). *Precipitation scavenging, dry deposition and resuspension, vol. 1.*, chapter Kinetics of oxidation of aqueous sulfur (IV) by nitrogen dioxide. Elsevier, New York.

[Li et al., 2003] Li, J., keng Liao, W., Choudhary, A., Ross, R., Thakur, R., Gropp, W., Latham, R., Siegel, A., Gallagher, B., and Zingale, M. (2003). Parallel netcdf: A high-performance scientific i/o interface. *SC Conference*, 0:39.

[Loosmore, 2003] Loosmore, G. (2003). Evaluation and development of models for resuspension of aerosols at short times after deposition. *Atmospheric Environment*, 37:639–647.

[Louis et al., 1982] Louis, J., Tiedke, M., and Geleyn, J. (1982). A short history of the pbl parametrization at ecmwf. In *ECMWF Workshop on Planetary Boundary Layer parametrization*, pages 59–80, University of Reading.

[Loveland et al., 2000] Loveland, T., Reed, B., Brown, J., Ohlen, D., Zhu, J., Yang, L., and Merchant, J. (2000). Development of a global land cover characteristics database and igbp discover from 1-km avhrr data. *International Journal of Remote Sensing*, 21(6/7):1303–1330.

[Mailler et al., 2016] Mailler, S., Menut, L., Khvorostyanov, D., Valari, M., Couvidat, F., Siour, G., Turquety, S., Briant, R., Tuccella, P., Bessagnet, B., Colette, A., Létinois, L., and Meleux, F. (2016). Chimere-2016: From urban to hemispheric chemistry-transport modeling. *Geoscientific Model Development Discussions*, 2016:1–41.

[Martensson et al., 2003] Martensson, E. M., Nilsson, E. D., de Leeuw, G., Cohen, L. H., and Hansson, H.-C. (2003). Laboratory simulations and parameterization of the primary marine aerosol production. *Journal of Geophysical Research*, 16:1–12.

[Marticorena and Bergametti, 1995] Marticorena, B. and Bergametti, G. (1995). Modeling the atmospheric dust cycle: 1 Design of a soil derived dust production scheme. *J. Geophys. Res.*, 100:16415–16430.

[McRae et al., 1982] McRae, G., Goodin, W., and Seinfeld, J. (1982). Development of a second generation mathematical model for urban air pollution: I. model formulation. *Atmospheric Environment*, 16:679–696.

[Menut, 2008] Menut, L. (2008). Sensitivity of hourly Saharan dust emissions to NCEP and ECMWF modelled wind speed. *J Geophys Res*, 113:D16201.

[Menut et al., 2013a] Menut, L., Bessagnet, B., Khvorostyanov, D., Beekmann, M., Blond, N., Colette, A., Coll, I., Curci, G., Foret, F., Hodzic, A., Mailler, S., Meleux, F., Monge, J., Pison, I., Siour, G., Turquety, S., Valari, M., Vautard, R., and Vivanco, M. (2013a). CHIMERE 2013: a model for regional atmospheric composition modelling. *Geoscientific Model Development*, 6:981–1028.

[Menut et al., 2005] Menut, L., C.Schmechtig, and B.Marticorena (2005). Sensitivity of the sandblasting fluxes calculations to the soil size distribution accuracy. *Journal of Atmospheric and Oceanic Technology*, 22:1875–1884.

[Menut et al., 2007] Menut, L., G.Foret, and G.Bergametti (2007). Sensitivity of mineral dust concentrations to the model size distribution accuracy. *Journal of Geophysical Research, Atmospheres*, 112:D10210.

[Menut et al., 2013b] Menut, L., Perez Garcia-Pando, C., Haustein, K., Bessagnet, B., Prigent, C., and Alfaro, S. (2013b). Relative impact of roughness and soil texture on mineral dust emission fluxes modeling. *J Geophys Res*, 118:6505–6520.

[Menut et al., 2000a] Menut, L., Vautard, R., Beekmann, M., and Honoré, C. (2000a). Sensitivity of Photochemical Pollution using the Adjoint of a Simplified Chemistry-Transport Model. *J. Geophys. Res.*, 105(D12):15379–15402.

[Menut et al., 2000b] Menut, L., Vautard, R., Flamant, C., Abonnel, C., Beekmann, M., Chazette, P., Flamant, P., Gombert, D., Guédalia, D., Lefebvre, M., Lossec, B., D., M., Mégie, G., Perros, P., Sicard, M., and Toupance, G. (2000b). Measurements and modelling of atmospheric pollution over the Paris area: an overview of the ESQUIF Project. *Annales Geophysicae*, 18(11):1467–1481.

[Middleton et al., 1990] Middleton, P., Stockwell, W. R., and Carter, W. P. (1990). Agregation and analysis of volatile organic compound emissions for regional modelling. *Atmospheric Environment*, 24:1107–1133.

[Mircea and Stefan, 1998] Mircea, M. and Stefan, S. (1998). A theoretical study of the microphysical parameterization of the scavenging coefficient as a function of precipitation type and rate. *Atmos. Env.*, 32:2931–2938.

[Monahan, 1986] Monahan, E. C. (1986). *In The Role of Air-Sea Exchange in Geochemical Cycling*, chapter The ocean as a source of atmospheric particles, pages 129–163. Kluwer Academic Publishers, Dordrecht, Holland.

[Nenes et al., 1998] Nenes, A., Pilinis, C., and Pandis, S. (1998). ISORROPIA: A new thermodynamic model for inorganic multicomponent atmospheric aerosols. *Aquatic Geochem.*, 4:123–152.

[Odum et al., 1997] Odum, J. R., Jungkamp, T. P. W., Griffin, R. J., Forster, H. J. L., Flagan, R. C., and Seinfeld, J. H. (1997). Aromatics, reformulated gasoline and atmospheric organic aerosol formation. *Environ. Sci. Technol.*, 31:1890–1897.

[Omar et al., 2010] Omar, A., Winker, D. M., Vaughan, M. A., Hu, Y., Trepte, C. R., Ferrare, R. A., Lee, K.-P., Hostetler, C. A., Kittaka, C., Rogers, R. R., Kuehn, R. E., and Liu, Z. (2010). The calipso automated aerosol classification and lidar ratio selection algorithm. *Journal of Atmospheric and Oceanic Technology*, 26(10):1994–2014.

[Pandis et al., 1993] Pandis, S., Wexler, A., and Seinfeld, J. (1993). Secondary organic aerosol formation and transport -ii. predicting the ambient secondary organic aerosol size distribution. *Atmos. Environ.*, 27A:2403–2416.

[Pankow, 1994] Pankow, J. F. (1994). An absorption model of gas/aerosol partition involved in the formation of secondary organic aerosol. *Atmos. Environ.*, 28:189–193.

[Passant, 2002] Passant, N. (2002). Speciation of uk emissions of nmvoc. (AEAT/ENV/R/0545).

[Pavia and O'Brien, 1986] Pavia, E. and O'Brien, J. (1986). Weibull statistics speed over the ocean. *Journal of Climate and Applied Meteorology*, 25:324–332.

[Pere et al., 2010] Pere, J., Mallet, M., Pont, V., and Bessagnet, B. (2010). Evaluation of an aerosol optical scheme in the chemistry-transport model CHIMERE. *Atmospheric Environment*, 44:3688–3699.

[Peters and Eiden, 1992] Peters, K. and Eiden, R. (1992). Modelling the dry deposition velocity of aerosol particles to a spruce forest. *Atmospheric Environment*, 26A(14):2555–2564.

[Petroff et al., 2008a] Petroff, A., Mailliat, A., Amielh, M., and Anselmet, F. (2008a). Aerosol dry deposition on vegetative canopies. Part I: Review of present knowledge. *Atmospheric Environment*, 42:3625–3653.

[Petroff et al., 2008b] Petroff, A., Mailliat, A., Amielh, M., and Anselmet, F. (2008b). Aerosol dry deposition on vegetative canopies. Part II: A new modelling approach and applications. *Atmospheric Environment*, 42:3654–3683.

[Priestley, 1949] Priestley, C. (1949). Heat transport and zonal stress between latitudes. *Quaterly Journal of the Royal Meteorology*, 75:28–40.

[Prigent et al., 2012] Prigent, C., Jiménez, C., and Catherinot, J. (2012). Comparison of satellite microwave backscattering (ASCAT) and visible/near-infrared reflectances (PARASOL) for the estimation of aeolian aerodynamic roughness length in arid and semi-arid regions. *Atmos. Meas. Tech.*, 5:2703–2712.

[Prigent et al., 2005] Prigent, C., Tegen, I., Aires, F., Marticorena, B., and Zribi, M. (2005). Estimation of the aerodynamic roughness length in arid and semi-arid regions over the globe with the ERS scatterometer. *J. Geophys. Res.*, 110:D09205.

[Pryor et al., 2005] Pryor, S., Schoof, J., and Barthelmie, R. (2005). Empirical downscaling of wind speed probability distributions. *J. Geophys. Res.*, 110:D19109.

[Pun et al., 2006] Pun, B. K., Seigneur, C., and Lohman, K. (2006). Modeling secondary organic aerosol formation via multiphase partitioning with molecular data. *Environ. Sci. Technol.*, 40:4722–4731.

[Real and Sartelet, 2011] Real, E. and Sartelet, K. (2011). Modeling of photolysis rates over europe: impact on chemical gaseous species and aerosols. *Atmos. Chem. Phys*, 11:1711–1727.

[Rouïl et al., 2009] Rouïl, L., Honoré, C., Vautard, R., Beekmann, M., Bessagnet, B., Malherbe, L., Meleux, F., Dufour, A., Elichegaray, C., Flaud, J., Menut, L., Martin, D., Peuch, A., Peuch, V., and Poisson, N. (2009). PREV'AIR : an operational forecasting and mapping system for air quality in Europe. *BAMS*, 90:73–83.

[Sander et al., 1999] Sander, G.C. and. Parlange, J.-Y., Smith, R.E.and Haverkamp, R., and Hogarth, W. (1999). Estimation of ponding time for constant surface flux. *Hydrology days Ed. AGU Pub. 19, San Francisco*, pages 402–410.

[Schaap et al., 2007] Schaap, M., Vautard, R., Bergstrom, R., van Loon, M., Bessagnet, B., Brandt, J., Christensen, H., Cuvelier, K., Foltescu, V., Graff, A., E., J. J., Kerschbaumer, A., Krol, M., Langner, J., Roberts, P., Rouil, L., Stern, R., Tarrason, L., Thunis, P., Vignati, E., White, L., Wind, P., and Builtjes, P. H. J. (2007). Evaluation of long-term aerosol simulations from seven air quality models and their ensemble in the eurodelta study. *Atmospheric Environemnt*, 41:2083–2097.

[Schmidt et al., 2001] Schmidt, H., Derognat, C., Vautard, R., and Beekmann, M. (2001). A comparison of simulated and observed ozone mixing ratios for the summer of 1998 in western Europe. *Atmospheric Environment*, 35:6277–6297.

[Schulz et al., 2006] Schulz, M., Textor, C., Kinne, S., Balkanski, Y., Bauer, S., Berntsen, T., Berglen, T., Boucher, O., Dentener, F., Guibert, S., Isaksen, I. S. A., Iversen, T., Koch, D., Kirkevag, A., Liu, X., Montanaro, V., Myhre, G., Penner, J. E., Pitari, G., Reddy, S., Seland, O., Stier, P., and Takemura, T. (2006). Radiative forcing by aerosols as derived from the aerocom present-day and pre-industrial simulations. *Atmos Chem Phys*, 6:5225–5246.

[Seinfeld and Pandis, 1998] Seinfeld, J. H. and Pandis, S. N. (1998). *Atmospheric chemistry and physics: From air pollution to climate change*. Wiley-Interscience, J.Wiley, New York.

[Semmler et al., 2006] Semmler, M., Luo, B. P., and Koop, T. (2006). Densities of liquid h+/nh4+/so42-/no3-/h2o solutions at tropospheric temperatures. *Atmos. Environ.*, 40:467–483.

[Shao and Lu, 2000] Shao, Y. and Lu, I. (2000). A simple expression for wind erosion threshold friction velocity. *J. Geophys. Res.*, 105:22,437–22,443.

[Simpson, 1992] Simpson, D. (1992). Long period modeling of photochemical oxidants in Europe, Calculations for July 1985. *Atmos. Environ.*, 26:1609–1634.

[Simpson et al., 2012] Simpson, D., Benedictow, A., Berge, H., Bergström, R., Emberson, L. D., Fagerli, H., Flechard, C. R., Hayman, G. D., Gauss, M., Jonson, J. E., Jenkin, M. E., Nyíri, A., Richter, C., Semeena, V. S., Tsyro, S., Tuovinen, J.-P., Valdebenito, A., and Wind, P. (2012). The emep msc-w chemical transport model - technical description. *Atmospheric Chemistry and Physics*, 12(16):7825–7865.

[Simpson et al., 2003] Simpson, D., Fagerli, H., Jonson, J.-E., Tsyro, S., Wind, P., and Tuovinen, J.-P. (2003). Transboundary Acidification, Eutrophication and Ground Level Ozone in Europe. Part I: Unified EMEP Model Description. Technical report. EMEP/ Status Report 2003.

[Slinn, 1982] Slinn, W. (1982). Predictions for particle deposition to vegetation surfaces. *Atmospheric Environment*, 23:1293–1304.

[Solazzo et al., 2012] Solazzo, E., Bianconi, R., Vautard, R., Appel, K. W., Moran, M. D., Hogrefe, C., Bessagnet, B., Brandt, J., Christensen, J. H., Chemel, C., Coll, I., van der Gon, H. D., Ferreira, J., Forkel, R., Francis, X. V., Grell, G., Grossi, P., Hansen, A. B., Jericevic, A., Kraljevic, L., Miranda, A. I., Nopmongcol, U., Pirovano, G., Prank, M., Riccio, A., Sartelet, K. N., Schaap, M., Silver, J. D., Sokhi, R. S., Vira, J., Werhahn, J., Wolke, R., Yarwood, G., Zhang, J., Rao, S., and Galmarini, S. (2012). Model evaluation and ensemble modelling of surface-level ozone in Europe and North America in the context of AQMEII. *Atmospheric Environment*, 53:60–74.

[Stromatas et al., 2012] Stromatas, S., Turquety, S., Menut, L., Chepfer, H., Cesana, G., Pere, J., and Bessagnet, B. (2012). Lidar signal simulation for the evaluation of aerosols in chemistry-transport models. *Geoscientific Model Development*, 5.

[Tanskannen and Manninen, 2007] Tanskannen, A. and Manninen, T. (2007). Effective UV surface albedo of seasonally snow-covered lands. *Atmos. Chem. Phys.*, 7:2759–2764.

[Tegen et al., 2002] Tegen, I., Harrison, S. P., Kohfeld, K., Prentice, I. C., Coe, M., and Heimann, M. (2002). Impact of vegetation and preferential source areas on global dust aerosol: Results from a model study. *J. Geophys. Res.*, 109.

[Telford et al., 2013] Telford, P. J., Abraham, N. L., Archibald, A. T., Braesicke, P., Dalvi, M., Morgenstern, O., OĆonnor, F. M., Richards, N. A. D., and Pyle, J. A. (2013). Implementation of the Fast-JX photolysis scheme (v6.4) into the UKCA component of the MetUM chemistry-climate model (v7.3). *Geoscientific Model Development*, 6:161–177.

[Tiedtke, 1989] Tiedtke, M. (1989). A comprehensive mass flux scheme for cumulus parameterization in large-scale models. *Monthly Weather Reviews*, 117:1779–1800.

[Troen and Mahrt, 1986] Troen, I. and Mahrt, L. (1986). A simple model of the atmospheric boundary layer: Sensitivity to surface evaporation. *Boundary-Layer Meteorology*, 37:129–148.

[Ullrich et al., 2010] Ullrich, P. A., Jablonowski, C., and Leer, B. V. (2010). High-order finite-volume methods for the shallow-water equations on the sphere. *J. Comput. Phys*, 229:6104–6134.

[Valari and Menut, 2010] Valari, M. and Menut, L. (2010). Transferring the heterogeneity of surface emissions to variability in pollutant concentrations over urban areas through a chemistry transport model. *Atmos Environ*, 44:3229–3238.

[Van Leer, 1979] Van Leer, B. (1979). Towards the ultimate conservative difference scheme. A second order sequel to Godunov's method. *J. Computational Phys.*, 32:101–136.

[Van Loon et al., 2007] Van Loon, M., Vautard, R., Schaap, M., Bergstrom, R., Bessagnet, B., Brandt, J., Builtjes, P., Christensen, J. H., Cuvelier, K., Graf, A., Jonson, J., Krol, M., Langner, J., Roberts, P., Rouil, L., Stern, R., Tarrason, L., Thunis, P., Vignati, E., White, L., and Wind, P. (2007). Evaluation of long-term ozone simulations from seven regional air quality models and their ensemble average. *Atmospheric Environment*, 41:2083–2097.

[Vautard et al., 2005a] Vautard, R., B.Bessagnet, M.Chin, and Menut, L. (2005a). On the contribution of natural Aeolian sources to particulate matter concentrations in Europe: testing hypotheses with a modelling approach. *Atmospheric Environment*, 39:3291–3303.

[Vautard et al., 2000] Vautard, R., Beekmann, M., and Menut, L. (2000). Applications of adjoint modelling in atmospheric chemistry: sensitivity and inverse modelling. *Environmental Modelling and Software*, 15:703–709.

[Vautard et al., 2001] Vautard, R., Beekmann, M., Roux, J., and Gombert, D. (2001). Validation of a hybrid forecasting system for the ozone concentrations over the Paris area. *Atmos. Environ.*, 35:2449–2461.

[Vautard et al., 2007] Vautard, R., Builtjes, P. H. J., Thunis, P., Cuvelier, K., Bedogni, M., Bessagnet, B., Honoré, C., Moussiopoulos, N., G., P., Schaap, M., Stern, R., Tarrason, L., and Van Loon, M. (2007). Evaluation and intercomparison of Ozone and PM10 simulations by several chemistry-transport models over 4 european cities within the City-Delta project. *Atmospheric Environment*, 41:173–188.

[Vautard et al., 2005b] Vautard, R., Honoré, C., Beekmann, M., and Rouil, L. (2005b). Simulation of ozone during the August 2003 heat wave and emission control scenarios. *Atmospheric Environment*, 39(16):2957–2967.

[Verwer, 1994] Verwer, J. (1994). Gauss-Seidel iteration for stiff odes from chemical kinetics. *Journal on Scientific Computing*, 15:1243–1250.

[Vestreng et al., 2005] Vestreng, V., Breivik, K., Adams, M., Wagner, A., Goodwin, J., Rozovskaya, O., and Oacyna, J. (2005). Inventory Review 2005 - Emission Data reported to CLRTAP and under the NEC Directive - Initial review for HMs and POPs . *EMEP Status report, Norwegian Meteorological Institute, Oslo*.

[Voulgarakis et al., 2009] Voulgarakis, A., Savage, N. H., Wild, O., Carver, G. D., Clemitshaw, K. C., and Pyle, J. A. (2009). Upgrading photolysis in the PHOTOMCAT CTM: model evaluation and assessment of the role of clouds. *Geoscientific Model Development*, 2:59–72.

[Vuolo et al., 2009] Vuolo, M., Menut, L., and Chepfer, H. (2009). Impact of transport schemes accuracy on modelled dust concentrations variability. *Journal of Atmospheric and Oceanic Technology*, 26:1135–1143.

[Wandinger et al., 2010] Wandinger, U., Tesche, M., Seifert, P., Ansmann, A., Müller, D., and Althausen, D. (2010). Size matters: Influence of multiple scattering on calipso lightâĂŘextinction profiling in desert dust. *Geophysical Research Letters*, 37(L10801).

[Warren, 1986] Warren, D. R. (1986). *Nucleation and growth of aerosols*. PhD thesis, Dissertation (Ph.D.), California Institute of Technology, Pasadena.

[Wesely, 1989] Wesely, M. (1989). Parameterization of Surface Resistances to Gaseous Dry Deposition in Regional-Scale Numerical Models. *Atmospheric Environment*, 23(23):1293–1304.

[White, 1986] White, B. R. (1986). Encyclopedia of fluid mechanics. *Gulf Publishing, Houston, TX, USA*, pages 239–282.

[Wild et al., 2000] Wild, O., Zhu, X., and Prather, J. (2000). Fast-J: accurate simulation of the in- and below-cloud photolysis in tropospheric chemical models. *J. Atmos. Chem.*, 37:245–282.

[Winker et al., 2009] Winker, D. M., M. A. Vaughan, A. O., Hu, Y., Powell, K. A., Liu, Z., Hunt, W. H., and Young, S. A. (2009). Overview of the calipso mission and caliop data processing algorithms. *Journal of Atmospheric and Oceanic Technology*, 26(2310-2323).

[Wolfe and Nickling, 1993] Wolfe, S. and Nickling, W. (1993). The protective role of sparse vegetation in wind erosion. *Progress in Physical Geography*, 17:50–68.

[Zhang et al., 2001] Zhang, L., Gong, S., Padro, J., and Barrie, L. (2001). A size-segregated particle dry deposition scheme for an atmospheric aerosol module. *Atmospheric Environment*, 35(3):549–560.

[Zhang et al., 2007] Zhang, Y., Huang, J.-P., Henze, D. K., and Seinfeld, J. H. (2007). Role of isoprene in secondary organic aerosol formation on a regional scale. *Journal of Geophysical Research Atmospheres*, 112(D20).

[Zyryanov et al., 2012] Zyryanov, D., Foret, G., Eremenko, M., Beekmann, M., Cammas, J.-P., M.D'Isidoro, Elbern, H., Flemming, J., Friese, E., Kioutsioutkis, I., Maurizi, A., D.Melas, Meleux, F., Menut, L., Moinat, P., Peuch, V.-H., Poupkou, A., Razinger, M., Schultz, M., Stein, O., Suttie, A. M., Valdebenito, A., Zerefos, C., Dufour, G., Bergametti, G., and Flaud, J.-M. (2012). 3D evaluation of tropospheric ozone simulations by an ensemble of regional Chemistry Transport Model. *Atmos Chem Phys*, 12:3219–3240.

List of Figures

1.1 *General principle of a chemistry-transport model such as CHIMERE. In the box 'Meteorology', u_* stands for the friction velocity, Q_0 the surface sensible heat flux, L the Monin-Obukhov length and BLH the boundary layer height. c_{mod} and c_{obs} are for the chemical concentrations fields for the model and the observations, respectively.* 13

2.1 Figures to validate the March 2009 Test Case simulation 33

3.1 *General structure of CHIMERE model* 36
3.2 *Interaction between master and workers processes and input and output files. Note that workers processes also communicate with each other and that these interraction are not represented here.* 41
3.3 *Detailed list of CHIMERE routines and time loops* 43

4.1 *Examples of horizontal domains. The dots represent the MM5 EUR1 grid cells centers and the rectangle represents the boundaries of the CHIMERE CONT3 domain.* 51
4.2 *Example of aeolian roughness length z_0 derived from GARLAP dataset and projected on a CHIMERE grid.* 55
4.3 *Example of erodibility factor derived from MODIS dataset and projected on a CHIMERE grid.* 55

5.1 *Example of an aerosol size distribution with ten bins. The intervals represent the boundaries of the distribution (nbins+1 values) and the red dots represent the Mean Mass Median Diameter (MMD) of the distribution (nbins values).* 69
5.2 *Distribution factors used to project the three aerosol emitted modes on the CHIMERE bins size distribution.* 70

6.1 *Top-down processing of EMEP anthropogenic emissions with the emiSURF interface* 75
6.2 *Top-down processing of HTAP anthropogenic emissions with the emiSURF interface* 76
6.3 *The STATSGO-FAO soil types data regridded to $1^o \times 1^o$ resolution. The values correspond to the surface types explained in the Table 6.5. For each cell, only the most important relative surface is displayed.* 83
6.4 *[top] the USGS landuse classes (from 1 to 23) over the domain: (1) urban and built-up land, (2) dryland cropland and pasture, (3) irrigated cropland and pasture, (4) mixed dryland/irrigated cropland and pasture, (5) cropland/grassland mosaic, (6) cropland/woodland mosaic, (7) grassland, (8) shrubland, (9) mixed shrubland/grassland, (10) savanna, (11) deciduous broadleaf forest, (12) deciduous needleleaf forest, (13) evergreen broadleaf forest, (14) evergreen needleleaf forest, (15) mixed forest, (16) water bodies, (17) herbaceous wetland, (18) wooded wetland, (19) barren or sparsely vegetated, (20) herbaceous tundra, (21) wooded tundra, (22) mixed tundra, (23) bare ground tundra. [bottom] The relative percentage of USGS class 19 surface (for barren soils). This class is used as a desert mask for the dust fluxes calculation when using the USGS data.* 86
6.5 *Function defined to moderate the mineral dust emissions fluxes after a precipitation event.* . . 87

7.1 *Main principle of dry deposition for gas and particles. For each model species, three resistances are estimated: deposition occurs if the sum of all these resistances is low. For particles, the settling velocity is added.* 93
7.2 *Function used to define the hourly variability of the LAI and the phenological function. The required parameters are shown using their names in the model: SGS and EGS for the start and end of the growing season, LAImin and LAImax for the minimum and maximum of LAI value, SGSlength and EGSlength for the length of the start and end of the growing season. The phenological parameters are PHENa, PHENb, and PHENc to define the minimum value, the length, the start, and the end of the season.* 99

8.1 *Flowchart of the several options to build the initial and boundary conditions.* 110
8.2 *Surface ozone concentrations modelled with LMDz-INCA and MACC for july.* 113
8.3 *Surface mineral dust concentrations modelled with GOCART and LMDzINCA for july.* 114

9.1 *Flow chart of the meteorological CHIMERE pre-processor.* 118
9.2 *Temperatures changes due to shallow and deep convection* 125
9.3 *Schematic view of a convective cloud* 125
9.4 *Entrainment and detrainment fluxes in the updrafts and downdrafts.* 126
9.5 *Convective atmospheric column and its environment* 127

10.1 *General CHIMERE structure for the time integration of all processes* 133
10.2 *Calculation of the number of integration chemical steps per physical steps to satisfy the CFL criterion.* 135
10.3 *Principle of 'operator-splitting' versus Chimere integration* 136

12.1 *Routines, files and scripts involved in the calculation of radiative transfers* 176

13.1 *Overview of the comparison methodology: example of the modelled Attenuated Scattering Ratio (ASR or $R'(z)$) estimation from initial concentration profiles (middle-left panel) on a specific model vertical grid (left panel) in the case of a space lidar (middle-right panel) or a ground lidar (right panel). The grey dots correspond to the value reported in the model simulation. After [Stromatas et al., 2012]* 180

List of Tables

1.1 *Main properties of the CHIMERE model* . . . 12

2.1 *Useful URL adresses for the development and the use of the CHIMERE model and its modules* 20
2.2 *Links between the user's flags and the programs used* . . . 23
2.3 List of CHIMERE parameters . . . 23
2.4 List of output meteorological variables . . . 30

4.1 *Landuse categories used in CHIMERE* . . . 53
4.2 *Projection factors from the Globcover database to CHIMERE.* . . . 54
4.3 *Projection factors from the USGS database to CHIMERE.* . . . 54

5.1 *List of primary data files in the chemprep/data directory.* . . . 59
5.2 *Parameters needed for the semi-volatil compounds and the Secondary Organic Aerosols (SOA) formation. These species are not dependent on the chemical mechanism, their reactions being added whatever the chemical mechanism chosen.* . . . 60
5.3 List of possible chemical reactions . . . 63
5.4 Values of the diameter bins obtained for $D_{min} = 0.01\,\mu\mathrm{m}$, $D_{max} = 40\,\mu\mathrm{m}$, and twelve different values of N. . . . 67
5.5 *Aerosols emissions with the three modes describing their size distribution: fine, coarse and big. The mean mass median diameter D_p is expressed in μm, σ is unitless.* . . . 70

6.1 *Gas and particle emissions required for MELCHIOR and SAPRC* . . . 74
6.2 *List of the biogenic emitted species with the MEGAN parameterization.* . . . 79
6.3 *List of the sea salt emitted species.* . . . 81
6.4 *Mandatory informations for the mineral dust emissions fluxes calculations* . . . 82
6.6 List of tunable parameters for the mineral dust emissions fluxes . . . 83
6.5 *Description of the USGS soil types. CS = Coarse sand; FMS = Fine medium sand. Note that only the first 12 soiltype are really used in the mineral dust fluxes calculation. The α value is not used in this model version (but here just for consistency with older model version).* . . . 85

7.1 *The (chemprep/data/DEPO_SPEC.meca) data file. The main characteristics of the dry deposited species with their names, dMx the molar mass of the model species, dHx the effective Henry's law constant (M atm^{-1}) for the gas, df0 the normalised (0 to 1) reactivity factor for the dissolved gas. Note that all peroxides (with *) are treated as SO_2. $dRwat$ is a resistance to the solution of gases in water', en s m^{-1} and is not used in the current model version.* . . . 95
7.2 *List of acronyms used in the deposition parameters data file. T/B stands for "temperate or boreal", Med for Mediterranean.* . . . 97
7.3 *Dry deposition constants set in chemprep/data/DEPO_PARS.univ dependingon the vegetation type: (0) estimated for CHIMERE; (1) taken from the EMEP model documentation (EMEP website); (2) EMEP data with corrections applied for the growing season for the DF type: EGS=300 instead of 270, SGS_len=30 instead of 56.* . . . 98

7.4 *Parameters for the wet deposition with their model species names, charspec, the type of the species, in cloud scavenging constants and the molar mass.* 106
7.5 *Constants used for the calculation of the wet scavenging fluxes for gas and aerosols* 106

9.1 *Mandatory and optional variables in exdomout.nc meteo file. Note that all meteorological 3D variables must be provided at half-layers levels. If the optional variable are not provided by the raw meteorological model, there are intialized to zero and diagnosed if possible.* 119
9.2 *Constant values used for the calculation of additionnal parameters in the routine calc_turb.* . . 123
9.3 *Tabulated values needed for the diagnostic of additional meteorological parameters. The values of UV albedo are extracted from (Laepple et al. 2005) for all meteorological conditions, except when snow is detected, where they are extracted from (Tanskannen et al. 2007).* 123
9.4 *Tabulated monthly variability of the roughness length for the landuse category # 1 "Agricultural".* 123

12.1 *List of aerosol species. (*): ions, molecules, crystals* 167
12.2 *Characteristics of the look-up table used for the calculation of the thermodynamic equilibrium with ISORROPIA.* 171
12.3 *Relative humidity at deliquescent points for the species used by ISORROPIA in the system sulfate-nitrate-ammonium-water.* 171
12.4 *Gas phase chemical scheme for SOA formation in CHIMERE. The surrogate SOA compounds consist of six hydrophilic species that include an anthropogenic nondissociative species (AnA0D), an anthropogenic once-dissociative species (AnA1D), an anthropogenic twice-dissociative species (AnA2D), a biogenic non dissociative species (BiA0D), a biogenic once-dissociative species (BiA1D) and a biogenic twice-dissociative species (BiA2D), three hydrophobic species that include an anthropogenic species with moderate saturation vapor pressure (AnBmP), an anthropogenic species with low saturation vapor pressure (AnBlP) and a biogenic species with moderate saturation vapor pressure (BiBmP), and two surrogate compounds for the isoprene oxidation products.* 174
12.5 *Tabulated values from [Laepple et al., 2005] (for snow $<$ 1cm) and [Tanskannen and Manninen, 2007] (for snow $>$ 10 cm) used for the calculation of the albedo in the UV band* 178

A References using CHIMERE

A.1 Reference papers

For CHIMERE description overview: see [Menut et al., 2013, GMD]
http://www.geosci-model-dev.net/6/981/2013/gmd-6-981-2013.html

- Menut L, B.Bessagnet, D.Khvorostyanov, M.Beekmann, N.Blond, A.Colette, I.Coll, G.Curci, G.Foret, A.Hodzic, S.Mailler, F.Meleux, J.L.Monge, I.Pison, G.Siour, S.Turquety, M.Valari, R.Vautard and M.G.Vivanco, 2013, CHIMERE 2013: a model for regional atmospheric composition modelling, Geoscientific Model Development, 6, 981-1028, doi:10.5194/gmd-6-981-2013

For CHIMERE used in real-time forecast: see [Rouil et al, 2009] or [Menut and Bessagnet, 2010]

- Rouil L., C.Honore, R.Vautard, M.Beekmann, B.Bessagnet, L.Malherbe, F.Meleux, A.Dufour, C.Elichegaray, J-M.Flaud, L.Menut, D.Martin, A.Peuch, V-H.Peuch, N.Poisson, 2009, PREV'AIR : an operational forecasting and mapping system for air quality in Europe, BAMS, DOI: 10.1175/2008BAMS2390.1
- Menut L. and B.Bessagnet, 2010, Atmospheric composition forecasting in Europe , Annales Geophysicae, 28, 61-74

For CHIMERE used for health impacts: see [Valari et al., 2010]

- Valari M. and L.Menut, 2010, Transferring the heterogeneity of surface emissions to variability in pollutant concentrations over urban areas through a chemistry transport model, Atmospheric Environment, Volume 44, Issue 27, Pages 3229-3238

For CHIMERE used for fires emissions: see [Turquety et al., 2014, GMD]

- Turquety S., L.Menut, B.Bessagnet, A.Anav, N.Viovy, F.Maignan and M.Wooster, 2014, APIFLAME v1.0: High resolution fire emission model and application to the Euro-Mediterranean region, Geosci. Model. Dev., in press

For CHIMERE used for dust: see [Menut et al., 2013, JGR]

- Menut L., C.Perez Garcia-Pando, K.Haustein, B.Bessagnet, C.Prigent and S.Alfaro, 2013, Relative impact of roughness and soil texture on mineral dust emission fluxes modeling, Journal of Geophysical Research Atmospheres, 118, 6505-6520, doi:10.1002/jgrd.50313

A.2 List of papers using CHIMERE

1. Berchet,A., Pison, I., Chevallier, F., Bousquet, P., Bonne, J.-L., and Paris, J.-D.: Objectified quantification of uncertainties in Bayesian atmospheric inversions, Geosci. Model Dev., 8, 1525-1546, doi:10.5194/gmd-8-1525-2015, 2015.
2. Breon, F. M., Broquet, G., Puygrenier, V., Chevallier, F., Xueref-Remy, I., Ramonet, M., Dieudonné, E., Lopez, M., Schmidt, M., Perrussel, O., and Ciais, P.: An attempt at estimating Paris area CO2 emissions from atmospheric concentration measurements, Atmos. Chem. Phys., 15, 1707-1724, doi:10.5194/acp-15-1707-2015, 2015.

3. Cuesta J., M. Eremenko, C. Flamant, G. Dufour, B. Laurent, G. Bergametti, M. Hopfner, J. Orphal, D. Zhou, Three-dimensional distribution of a major desert dust outbreak over East Asia in March 2008 derived from IASI satellite observations, J. Geophys. Res. Atmos., 120, doi:10.1002/2014JD022406, 2015.

4. Hamaoui-Laguel L., Robert Vautard, Li Liu, Fabien Solmon, Nicolas Viovy, Dmitry Khvorostyanov, Franz Essl, Isabelle Chuine, Augustin Colette, Mikhail A. Semenov, Alice Schaffhauser, Jonathan Storkey, Michel Thibaudon, Michelle M. Epstein, Effects of climate change and seed dispersal on airborne ragweed pollen loads in Europe, Nature Clim. Change, 2015/05/25 online, 1758-6798, 10.1038/nclimate2652, 2015.

5. Likhvar, V., Pascal, M., Markakis, K., Colette, A., Hauglustaine, D., Valari, M., Klimont, Z., Medina, S., Kinney, P.: A multi-scale health impact assessment of air pollution over the 21st century, Science of the Total Environment, 514, 439449, 2015. http://www.ncbi.nlm.nih.gov/pubmed/25687670

6. Mailler S., L. Menut, A. G. Di Sarra, S. Becagli, T. Di Iorio, P. Formenti, B. Bessagnet, R. Briant, J. L. Gomez-Amo, M. Mallet, G. Rea, G. Siour, D. M. Sferlazzo, R. Traversi, R. Udisti, and S. Turquety, On the radiative impact of aerosols on photolysis rates: comparison of simulations and observations in the Lampedusa island during the CharMEx/ADRIMED campaign, Atmos. Chem. Phys. Discuss., 15, 7585-7643, 2015, doi:10.5194/acpd-15-7585-2015

7. Marécal V., V.-H. Peuch, C. Andersson, S. Andersson, J. Arteta, M. Beekmann, A. Benedictow, R. Bergstrom, B . Bessagnet, A. Cansado, F. Chéroux, A. Colette, A. Coman, R. L. Curier, H. A. C. Denier van der Gon, A. Drouin, H. Elbern, E. Emili, R. J. Engelen, H. J. Eskes, G. Foret, E. Friese, M. Gauss, C. Giannaros, M. Joly, E. Jaumouillé, B. Josse, N. Kadygrov, J. W. Kaiser, K. Krajsek, J. Kuenen, U. Kumar, N. Liora, E. Lopez, L. Malherbe, I. Martinez, D. Melas, F. Meleux, L. Menut, P. Moinat, T. Morales, J. Parmentier, A. Piacentini, M. Plu, A. Poupkou, S. Queguiner, L. Robertson, L. Rouil, M. Schaap, A. Segers, M. Sofiev, M. Thomas, R. Timmermans, A. Valdebenito, P. van Velthoven, R. van Versendaal, J. Vira, and A. Ung, A regional air quality forecasting system over Europe: the MACC-II daily ensemble production, Geosci. Model Dev. Discuss., 8, 2739-2806, 2015, doi:10.5194/gmdd-8-2739-2015

8. Markakis, K., Valari, M., Perrussel, O., Sanchez, O., Honore, C.: Climate forced air-quality modeling at urban scale: sensitivity to model resolution, emissions and meteorology, Atmos. Chem. Phys., 15, 7703-7723, 2015. http://www.atmos-chem-phys.net/15/7703/2015/acp-15-7703-2015.html

9. Menut L., S.Mailler, G.Siour, B.Bessagnet, S.Turquety, G.Rea, R.Briant, M.Mallet, J.Sciare and P.Formenti, Ozone and aerosols tropospheric concentrations variability analyzed using the ADRIMED measurements and the WRF-CHIMERE models, Atmos. Chem. Phys., 15, 6159-6182, 2015, www.atmos-chem-phys.net/15/6159/2015/, doi:10.5194/acp-15-6159-2015, .

10. Menut L., G.Rea, S.Mailler, D.Khvorostyanov, S.Turquety, Variability of aerosols forecast over the Mediterranean area and during July 2013 (ADRIMED/CHARMEX), Atmos. Chem. Phys. Discuss., 15, 10341-10388, 2015, doi:10.5194/acpd-15-10341-2015,

11. Petetin H., M. Beekmann, A. Colomb, H. A. C. Denier van der Gon, J.-C. Dupont, C. Honoré, V. Michoud, Y. Morille, O. Perrussel, A. Schwarzenboeck, J. Sciare, A. Wiedensohler, and Q. J. Zhang, Evaluating BC and NOx emission inventories for the Paris region from MEGAPOLI aircraft measurements, Atmos. Chem. Phys., 15, 9799-9818, 2015

12. Rea G, S.Turquety, L.Menut, R.Briant, S.Mailler and G.Siour, Source contributions to summertime aerosols in the Euro-Mediterranean region, Atmos. Chem. Phys. Discuss., 15, 8191-8242, 2015, , doi:10.5194/acpd-15-8191-2015

13. Shaiganfar R., S. Beirle, Herve Petetin, Q. Zhang, Matthias Beekmann, T. Wagner, New concepts for the comparison of tropospheric NO2 column densities derived from car-MAX-DOAS observations, OMI satellite observations and the regional model CHIMERE during two MEGAPOLI campaigns in Paris 2009/10, Atmos. Meas. Techn., 8, 2827-2852, 2015

14. Schaap, M., C. Cuvelier, C. Hendriks, B. Bessagnet, J.M. Baldasano, A. Colette, P. Thunis, D. Karam, H. Fagerli, A. Graff, R. Kranenburg, A. Nyiri, M.T. Pay, L. Rouil, M. Schulz, D. Simpson, R. Stern, E. Terrenoire and P. Wind, Performance of European chemistry transport models as function of horizontal resolution, Atmospheric Environment 112(2015), pp. 90-105

15. Schucht, S., A. Colette, S. Rao, M. Holland, W. Schoepp, P. Kolp, Z. Klimont, B. Bessagnet, S. Szopa, R. Vautard, J.-M. Brignon and L. Rouil, Moving towards ambitious climate policies: Monetised health benefits from improved air quality could offset mitigation costs in Europe, Environmental Science and Policy 50(2015), pp. 252-269

16. Sofiev M., U. Berger, M. Prank, J. Vira, J. Arteta, J. Belmonte, K.-C. Bergmann, F. Chéroux, H. Elbern, E. Friese, C. Galan, R. Gehrig, D. Khvorostyanov, R. Kranenburg, V. Marécal, F. Meleux, L. Menut, A.-M. Pessi, L. Robertson, O. Ritenberga, V. Rodinkova, A. Saarto, A. Segers, E. Severova, I. Sauliene, P. Siljamo, B. M. Steensen, E. Teinemaa, M. Thibaudon, and V.-H. Peuch, MACC regional multi-model ensemble simulations of birch pollen dispersion in Europe, Atmos. Chem. Phys. Discuss., 15, 8243-8281, 2015, , doi:10.5194/acpd-15-8243-2015

17. Terrenoire E., B.Bessagnet, L.Rouil, F.Tognet, G.Pirovano, L.Letinois, A.Colette, P.Thunis, M.Amann, and L.Menut, High resolution air quality simulation over Europe with the chemistry transport model CHIMERE, Geosci. Model Dev., 8, 21-42, doi:10.5194/gmd-8-21-2015, 2015,

18. Watson L., Gwendoline Lacressonniere, Michael Gauss, Magnuz Engardt, Camilla Andersson, Beatrice Josse, Virginie Marecal, Agnes Nyiri, Stefan Sobolowski, Guillaume Siour, Robert Vautard, The impact of meteorological forcings on gas phase air pollutants over Europe, Atmospheric Environment, Volume 119, October 2015, Pages 240-257, ISSN 1352-2310, http://dx.doi.org/10.1016/j.atmosenv.2015.07.037.
19. Wang R., Shu Tao, Yves Balkanski, Philippe Ciais, Olivier Boucher, Junfeng Liu, Shilong Piao, Huizhong Shen, Maria Raffaella Vuolo, Myrto Valari, Han Chen, Yuanchen Chen, Anne Cozic, Ye Huang, Bengang Li, Wei Li, Guofeng Shen, Bin Wang, and Yanyan Zhang (2014), Exposure to ambient black carbon derived from a unique inventory and high-resolution model, PNAS, 111, 7, 2459-2463.
20. Boichu M., Lieven Clarisse, Dmitry Khvorostyanov, and Cathy Clerbaux, Improving volcanic sulfur dioxide cloud dispersal forecasts by progressive assimilation of satellite observations, Geophysical Research Letters, 10.1002/2014GL059496, 2014.
21. Bessagnet, B., Beauchamp, M., Guerreiro, C., de Leeuw, F., Tsyro, S., Colette, A., Meleux, F., Rouil, L., Ruyssenaars, P., Sauter, F., Velders, G. J. M., Foltescue, V. L., van Aardennee, J. (2014b) Can further mitigation of ammonia emissions reduce exceedances of particulate matter air quality standards?, Environmental Science and Policy, Volume 44, Pages 149-163.
22. Jacob D., J.Petersen, B.Eggert, A.Alias, O.B.Christensen, L.M.Bouwer, A.Braun, A.Colette, M.Deque, G.Georgievski, E.Georgopoulou, A.Gobiet, L.Menut, G.Nikulin, A.Haensler, N.Hempelmann, C.Jones, K.Keuler, S.Kovats, N.Kroner, S.Kotlarski, A.Kriegsmann, E.Martin, E. van Meijgaard, C.Moseley, S.Pfeifer, S.Preuschmann, C.Radermacher, K.Radtke, D.Rechid, M.Rounsevell, P.Samuelsson, S.Somot, J.-F.Soussana, C.Teichmann, R.Valentini, R.Vautard, B.Weber, P.Yiou, 2014, EURO-CORDEX: New high-resolution climate change projections for European impact research, Regional Environmental Change, Volume: 14, Issue: 2, Pages: 563-578.
23. Bentayeb M., M. Stempfelet, V. Wagner, M. Zins, S. Bonenfant, C. Songeur, O. Sanchez, A. Rosso, G. Brulfert, I. Rios, E. Chaxel, J. Virga, A. Armengaud, P. Rossello, E. Rivière, M. Bernard, F. Vasbien, R. Deprost, Retrospective modeling outdoor air pollution at a fine spatial scale in France, 1989-2008, Atmospheric Environment, Volume 92, Pages 267-279, 2014.
24. Colette A., B. Bessagnet, F. Meleux, E. Terrenoire, and L. Rouil, Frontiers in air quality modelling, Geosci. Model Dev., 7, 203-210, 2014
25. Foret, G., M. Eremenko, J. Cuesta, P. Sellitto, J. Barré, B. Gaubert, A. Coman, G. Dufour, X. Liu, M. Joly, C. Doche, M. Beekmann, Ozone pollution: What can we see from space? A case study, J. Geophys. Res. Atmos., 119, 8476-8499, doi:10.1002/2013JD021340, 2014.
26. Gaubert, B., A. Coman, G. Foret, F. Meleux, A. Ung, L. Rouil, A. Ionescu, Y. Candau, and M. Beekmann, Regional scale ozone data assimilation using an ensemble Kalman filter and the CHIMERE chemical transport model,Geosci. Model Dev., 7, 283-302, 2014.
27. Hamaoui-Laguel L., F. Meleux, Matthias Beekmann, B. Bessagnet, S. Génermont, P. Cellier and L. Létinois, Improving ammonia emissions in air quality modelling for France, Atmos. Environ., 94, 584-595, 2014
28. Konovalov I. B., E. V. Berezin, P. Ciais, G. Broquet, M. Beekmann, J. Hadji-Lazaro, C. Clerbaux, M. O. Andreae, J. W. Kaiser, and E.-D. Schulze, Constraining CO2 emissions from open biomass burning by satellite observations of co-emitted species: a method and its application to wildfires in Siberia, Atmos. Chem. Phys., 14, 10383-10410, 2014
29. Markakis, K., Valari, M., Colette, A., Sanchez, O., Perrussel, O., Honore, C., Vautard, R., Klimont, Z. and Rao, S. Air quality in the mid-21st century for the city of Paris under two climate scenarios; from the regional to local scale, Atmos. Chem. Phys. 14, 7323-7340, 2014.
30. Péré J. C., Bessagnet, B., Mallet, M., Waquet, F., Chiapello, I., Minvielle, F., Pont, V., and Menut, L., 2014, Direct radiative effect of the Russian wildfires and their impact on air temperature and atmospheric dynamics during August 2010, Atmos. Chem. Phys., 14, 1999-2013, 2014, doi:10.5194/acp-14-1999-2014
31. Petetin H., M. Beekmann, J. Sciare, M. Bressi, A. Rosso, O. Sanchez, and V. Ghersi, A novel model evaluation approach focusing on local and advected contributions to urban PM2.5 levels: application to Paris, France, Geosci. Model Dev., 7, 1483-1505, 2014
32. Turquety S., L.Menut, B.Bessagnet, A.Anav, N.Viovy, F.Maignan and M.Wooster, 2014, APIFLAME v1.0: High resolution fire emission model and application to the Euro-Mediterranean region, Geosci. Model. Dev., 7, 587-612, doi:10.5194/gmd-7-587-2014
33. Cuesta J., M. Eremenko, X. Liu, G. Dufour, Z. Cai, M. Hopfner, T. von Clarmann, P. Sellitto, G. Foret, B. Gaubert, M. Beekmann, J. Orphal, K. Chance, R. Spurr, and J.-M. Flaud, 2013, Satellite observation of lowermost tropospheric ozone by multispectral synergism of IASI thermal infrared and GOME-2 ultraviolet measurements over Europe, Atmos. Chem. Phys., 13, 9675-9693, 2013
34. Boichu M., L. Menut, D. Khvorostyanov, L. Clarisse, C. Clerbaux, S. Turquety, and P.-F. Coheur, 2013, Inverting for volcanic SO2 flux at high temporal resolution using spaceborne plume imagery and chemistry-transport modelling: the 2010 Eyjafjallajokull eruption case-study, Atmos. Chem. Phys., 13, 6553-6588, 13, 8569-8584, doi:10.5194/acp-13-8569-2013

35. Broquet, G., Chevallier, F., Breon, F.-M., Kadygrov, N., Alemanno, M., Apadula, F., Hammer, S., Haszpra, L., Meinhardt, F., Morgui, J. A., Necki, J., Piacentino, S., Ramonet, M., Schmidt, M., Thompson, R. L., Vermeulen, A. T., Yver, C., and Ciais, P.: Regional inversion of CO2 ecosystem fluxes from atmospheric measurements: reliability of the uncertainty estimates, Atmos. Chem. Phys., 13, 9039-9056, doi:10.5194/acp-13-9039-2013, 2013. on-line paper

36. Colette A., B.Bessagnet, R.Vautard, S.Szopa, S.Rao, S.Schucht, Z.Klimont, L.Menut, G.Clain, F.Meleux, L.Rouil, 2013, European atmosphere in 2050, a regional air quality and climate perspective under CMIP5 scenarios, Atmos. Chem. Phys., 13, 7451-7471

37. Dall'Osto, M., X. Querol, A. Alastuey, M.C. Minguillon, M. Alier, F. Amato, M. Brines, M. Cusack, J.O. Grimalt, A. Karanasiou, T. Moreno, M. Pandolfi, J. Pey, C. Reche, A. Ripoll, R. Tauler, B.L. Van Drooge, M. Viana, R.M. Harrison, J. Giet, D. Beddows, W. Bloss, C. O'Dowd, D. Ceburnis, G. Martucci, N.L. Ng, D. Worsnop, J. Wenger, E. Mc Gillicuddy, J. Sodeau, R. Healy, F. Lucarelli, S. Nava, J.L. Jimenez, F. Gomez-Moreno, B. Artinano, A.S.H. Prevot, L. Pfaffenberger, S. Frey, F. Wilsenack, D. Casabona, P. Jimenez-Guerrero, D. Gross, N. Cots, 2013. Presenting SAPUSS: Solving Aerosol Problem by Using Synergistic Strategies in Barcelona, Spain. Atmos. Chem. Phys. 13, 8991-9019, doi:10.5194/acp-13-8991-2013.

38. Jerez, S., P. Jimenez-Guerrero, J.P. Montavez, R.M. Trigo., 2013. Impact of the North Atlantic Oscillation on the variations of aerosol ground levels through local processes over Europe. Atmos. Chem. Phys. 13, doi:10.5194/acp-13-1-2013.

39. Jimenez-Guerrero, P., S. Jerez, J.P. Montavez, R. M. Trigo, 2013. Uncertainties in future ozone and PM10 projections over Europe from a regional climate multi-physics ensemble. Geophys. Res. Lett. 40, 1-6, , doi:10.1002/2013GL057403.

40. Jimenez-Guerrero, P., J.J. Gomez-Navarro, R. Baro, R. Lorente, N. Ratola, J.P. Montavez, 2013. Is there a common pattern of future gas-phase air pollution in Europe under diverse climate change scenarios? Clim. Change, DOI 10.1007/s10584-013-0944-8.

41. Menut L, B.Bessagnet, D.Khvorostyanov, M.Beekmann, N.Blond, A.Colette, I.Coll, G.Curci, G.Foret, A.Hodzic, S.Mailler, F.Meleux, J.L.Monge, I.Pison, G.Siour, S.Turquety, M.Valari, R.Vautard and M.G.Vivanco, 2013, CHIMERE 2013: a model for regional atmospheric composition modelling, Geoscientific Model Development, 6, 981-1028, doi:10.5194/gmd-6-981-2013, on-line paper

42. Mailler S., D.Khvorostyanov, and L.Menut, 2013, Impact of the vertical emission profiles on background gas-phase pollution simulated from the EMEP emissions over Europe, Atmos. Chem. Phys., 13, 5987-5998, doi:10.5194/acp-13-5987-2013

43. Siour G, A.Colette, L.Menut, B.Bessagnet, I.Coll, F.Meleux, 2013, Bridging the scales in an eulerian air quality model to assess megacity export of pollution, Env. Mod. Software, 46, 271-282

44. Menut L., C.Perez Garcia-Pando, K.Haustein, B.Bessagnet, C.Prigent and S.Alfaro, 2013, Relative impact of roughness and soil texture on mineral dust emission fluxes modeling, Journal of Geophysical Research Atmospheres, 118, 6505-6520, doi:10.1002/jgrd.50313

45. Menut L., B.Bessagnet, A.Colette and D.Khvorostyanov, 2013, On the impact of the vertical resolution on chemistry transport modelling, Atmospheric Environment, 67, 370-384

46. Zhang Q.J., M. Beekmann, F. Drewnick, F. Freutel, J. Schneider, M. Crippa, A. Prevot, U. Baltensperger, L. Poulain, A. Wiedensohler, J. Sciare, V. Gros, A. Borbon, A. Colomb, V. Michoud, J-F. Doussin, H. A. C. Denier van dr Gon, M. Haeffelin, J.-C. Dupont, G. Siour, H. Petetin, B. Bessagnet, S.N. Pandis, A. Hodzic, O. Sanchez, C. Honore, and O. Perrussel, 2013, Formation of organic aerosol in the Paris region during the MEGAPOLI summer campaign: evaluation of the volatility-basis-set approach within the CHIMERE model, Atmos. Chem. Phys., 13, 5767-5790.

47. Anav A., L. Menut, D. Khvorostyanov, N. Viovy, Comparison of two canopy conductance parameterizations to quantify the interactions between surface ozone and vegetation over Europe, Journal of Geophysical Research - Biogeosciences, 117, G03027, 20 PP., doi:10.1029/2012JG001976

48. Coman, C, G.Foret, M.Beekmann, M.Eremenko, G.Dufour, B.Gaubert, A.Ung, C.Schmechtig, J.-M.Flaud, and G.Bergametti, Assimilation of IASI partial tropospheric columns with an Ensemble Kalman Filter over Europe, Atmos. Chem. Phys.,12,2513-2532,2012.

49. Delcloo A.W., Alex Deckmyn, Rafiq Hamdi, Herman Van Langenhove, Gilles Foret and Hugo De Backer, Coupling of the CTM CHIMERE to the High Resolution LAM ALADIN for Belgium, Air Pollution Modeling and its Application XXI, NATO Science tor Peace and Security Series C: Environmental Security, 2012, Volume 4, Part 2,315-319, DOl: 10.1007/978-94-007-1359-8 54.

50. Drobinski P., Anav A., Lebeaupin Brossier C., Samson G., Stefanon M., Bastin S., Baklouti M., Beranger K., Beuvier J., Bourdalle-Badief R., Coquart L., D'Andrea F., de Noblet N., Diaze F., Dutay J.C., Ethe C., Foujols M.J., Khvorostiyanov D., Madec G., Maisonnave E., Mancip M., Masson S., Menut L., Palmieri J., Polcher J., Turquety S., Valcke S., Viovy N., Model of the Regional Coupled Earth system (MORCE): application to process and climate studies in vulnerable regions, Env. Mod. Software, 35, 1-18

51. Konovalov, I. B., M. Beekmann, B. D'anna, And C. George, Significant light induced ozone loss on biomass burning aerosol: evidence from chemistry-transport modeling based on new laboratory studies, Geophys. Res. Lett., doi:10.1029/2012GL052432, 2012

52. Jimenez-Guerrero, P., J.P. Montavez, J.J. Gomez-Navarro, S. Jerez, R. Lorente-Plazas, 2012. Impacts of climate change on ground level gas-phase pollutants and aerosols in the Iberian Peninsula for the late XXI century. Atmos. Environ. 55, 483-495, doi:10.1016/j.atmosenv.2012.02.048.

53. Menut L., O.P.Tripathi, A.Colette, R.Vautard, E.Flaounas, B.Bessagnet, 2012, Evaluation of regional climate simulations for air quality modelling purposes, Climate Dynamics, in press, .

54. Menut L., A.Goussebaile, B.Bessagnet, D.Khvorostiyanov, A.Ung, 2012, Impact of realistic hourly emissions profiles on modelled air pollutants concentrations, Atmospheric Environment, pp. 233-244, doi:10.1016/j.atmosenv.2011.11.057

55. Schere, K., J. Flemming, R. Vautard, C. Chemel, A. Colette, C. Hogrefe, B. Bessagnet, F. Meleux, R. Mathur, S. Roselle, R.-M. Hu, R. S. Sokhi, S. T. Rao and S. Galmarini, 2011: Trace gas/aerosol boundary concentrations and their impacts on continental-scale AQMEII modeling domains. Atmosheric Environment, in press.

56. Solazzo, E., R. Bianconi, G. Pirovano, V. Matthias, R. Vautard, M. D. Moran, K. Wyat Appel, B. Bessagnet, J. Brandt, J. H. Christensen, C. Chemel, I. Coll, J. Ferreira, R. Forkel, X. V. Francis and 18 other authors, Operational model evaluation for particulate matter in Europe and North America in the context of AQMEII, Atm. Env., Vol 53, pp 75-92, 2012

57. Solazzo, E., R. Bianconi, R. Vautard, K. Wyat Appel, M. D. Moran, C. Hogrefe, B. Bessagnet, J. Brandt, J.H. Christensen, C. Chemel, I. Coll, H. Denier van der Gon, J. Ferreira, R. Forkel and 22 other authors, Model evaluation and ensemble modelling of surface-level ozone in Europe and North America in the context of AQMEII, Atm. Env., Vol 53, pp 60-74, 2012

58. Tuccella P., G.Curci, G.Visconti, B.Bessagnet, L.Menut and R.Park, 2012, Modelling of gas and aerosol with WRF/Chem over Europe: evaluation against one year of ground-based measurements, Journal of Geophysical Research Atmosphere, vol. 117, D03303, doi:10.1029/2011JD016302

59. Vautard, R., Moran, M. D., Solazzo, E., Gilliam, R. C., Matthias, V., Bianconi, R., Chemel, C., Ferreira, J., Geyer, B., Hansen, A. B., Jericevic, A., Prank, M., Segers, A., Silver, J. D., Werhahn, J., Wolke, R., Rao, S. T., and S. Galmarini, 2012, Evaluation of the meteorological forcing used for the Air Quality Model Evaluation InternationaI Initiative (AQMEII) air quality simulations. Atmos. Environ., doi:10.1016/j.atmosenv.2011.10.065.

60. Wilson R. C., Z. L. Fleming, P. S. Monks, G. Clain, S. Henne, I. B. Konovalov, S. Szopa, and L. Menut, 2012, Have primary emission reduction measures reduced ozone across Europe? An analysis of European rural background ozone trends 1996-2005, , ACP, 12, 437-454

61. Zyryanov D., G. Foret, M. Eremenko, M. Beekmann, J-P Cammas, M.D'Isidoro, H. Elbern, J. Flemming, E. Friese, I. Kioutsioutkis, A. Maurizi, D.Melas, F. Meleux, L. Menut, P. Moinat, V-H Peuch, A. Poupkou, M. Razinger, M. Schultz, O. Stein, A. M. Suttie, A. Valdebenito, C. Zerefos, G. Dufour, G. Bergametti and J-M. Flaud, 2012, 3D evaluation of tropospheric ozone simulations by an ensemble of regional Chemistry Transport Model, Atmospheric Chemistry and Physics, 12, 3219-3240

62. Hodzic, A. and Jimenez, J. L.: Modeling anthropogenically controlled secondary organic aerosols in a megacity: a simplified framework for global and climate models, Geosci. Model Dev., 4, 901-917, doi:10.5194/gmd-4-901-2011, 2011, article

63. Anav A., L.Menut, D.Khvorostiyanov and N.Viovy, Impact of tropospheric ozone on the Euro-Mediterranean vegetation, Global Change Biology, vol. 17, issue 6, DOI: 10.1111/j.1365-2486.2010.02387.x, .

64. Boynard, A., M. Beekmann, G. Foret, A. Ung, S. Szopa, C. Schmechtig, A. Coman, An ensemble assessment of regional ozone model uncertainty with an explicit error representation , Atmos. Env.,Volume 45, Issue 3, January 2011, Pages 784-793.

65. Borrego, C., Monteiro, A., Pay, M.T., Ribeiro, I., Miranda, A.I., Basart, S., Baldasano, J.M.. (2011). How bias-correction can improve air quality forecast over Portugal. Atmospheric Environment, 45, 37, 6629-6641. Broquet, G., F. Chevallier, P. Rayner, C. Aulagnier, I. Pison, M.Ramonet,M. Schmidt, A. T. Vermeulen, and P.

66. Ciais (2011), A European summertime CO2 biogenic flux inversion at mesoscale from continuous in situ mixing ratio measurements, J. Geophys. Res., 116, D23303, doi:10.1029/2011JD016202.

67. Carvalho, A., Monteiro, A., Flannigan, M., Solman, S., Miranda, A.I., Borrego, C. (2011). Forest fires in a changing climate and their impacts on air quality. Atmospheric Environment 45, 5545-5553.

68. Colette A., O.Favez, F.Meleux, L.Chiappini, M.Haeffelin, Y.Morille, L.Malherbe, A.Papin, B.Bessagnet, L.Menut, E.Leoz, L.Rouil, 2010, Assessing in near real time the impact of the April 2010 Eyjafjallajokull ash plume on air quality, Atmospheric Environment, 45, 1217-1221.

69. Jimenez-Guerrero, P., O. Jorba, M.T. Pay, J.P. Montavez, S. Jerez, J.J. Gomez-Navarro, J.M. Baldasano, 2011. Comparison of two different sea-salt aerosol schemes as implemented in air quality models applied to the Mediterranean. Atmos. Chem. Phys. 11, 4833-4850, doi: 10.5194/acp-11-4833-2011.

70. Jimenez-Guerrero, P., J.J. Gomez-Navarro, S. Jerez, R. Lorente-Plazas, J.A. Garcia-Valero, J.P. Montavez, 2011. Isolating the effects of climate change in the variation of secondary inorganic aerosols (SIA) in Europe for the 21st century (1991-2100). Atmos. Environ. 45(4), 1059-1063, doi:10.1016/j.atmosenv.2010.11.022.

71. Kukkonen J., T. Balk, D. M. Schultz, A. Baklanov, T. Klein, A. I. Miranda, A. Monteiro, M. Hirtl, V. Tarvainen, M. Boy, V.-H. Peuch, A. Poupkou, I. Kioutsioukis, S. Finardi, M. Sofiev, R. Sokhi, K. Lehtinen, K. Karatzas, M. Astitha, G. Kallos, M. Schaap, E. Reimer, H. Jakobs, K. Eben. (2011). Operational, regional-scale, chemical weather forecasting models in Europe. Atmos. Chem. Phys. Discuss., 11, 5985-6162.

72. de Fouquet C., L.Malherbe and A.Ung, 2011, Geostatistical analysis of the temporal variability of ozone concentrations. Comparison between CHIMERE model and surface observations, Atmospheric Environment, 45, 3434-3446.

73. Jiménez-Guerrero, P., O. Jorba, M.T. Pay, J.P. Montavez, S. Jerez, J.J. Gomez-Navarro, J.M. Baldasano, 2011. Comparison of two different sea-salt aerosol schemes as implemented in air quality models applied to the Mediterranean. Atmos. Chem. Phys. 11, 4833-4850, doi: 10.5194/acp-11-4833-2011.

74. Jiménez-Guerrero, P., J.J. Gomez-Navarro, S. Jerez, R. Lorente-Plazas, J.A. Garcia-Valero, J.P. Montavez, 2011. Isolating the effects of climate change in the variation of secondary inorganic aerosols (SIA) in Europe for the 21st century (1991-2100). Atmos. Environ. 45(4), 1059-1063, doi:10.1016/j.atmosenv.2010.11.022.

75. Konovalov, I. B., M. Beekmann, I. N. Kuznetsova, A. Yurova, And A. M. Zvyagintsev, Atmospheric impacts of the 2010 Russian wildfires: integrating modelling and measurements of an extreme air pollution episode in the Moscow region, Atmos. Chem. Phys., 11, 10036-10051, 2011.

76. Konovalov I.B., Beekmann, ?., Kuznetsova, I. N., Glazkova, A.?., Vivchar ?.V., ZaripovR.B. (2011) Estimation of an impact of wildfires on air pollution in the Moscow megacity region by the combined use of a chemistry transport model and measurement data, Izvestia, Atmos. Ocean. Phys., 47(4).

77. Kuznetsova, I.N., Konovalov, I.B., Artamonova, A.A., Nakhaev, M.I., Lezina, E.A., Zvyagintsev, A.M., Beekmann, M., The observed and simulated variability of PM10 concentration in Moscow and Zelenograd, Russian Meteorology and Hydrology, 36 (3), 175-184, 2011.

78. Royer,P., Chazette,P., Sartelet,K., Zhang,Q.J., Beekmann,M., And Raut,J.-C., Lidar-derived PM10 and comparison with regional modeling in the frame of the MEGAPOLI Paris summer campaign, Atmos. Chem. Phys., 11, 10705-10726, 2011.

79. Schmechtig, C., B. Marticorene, B. Chatenet, G. Bergametti, J. L. Rajot,and A. Coman, (2011), Simulation of the mineral dust content over Western Africa from the event to the annual scale with the CHIMERE-DUST model, Atmos. Chem. Phys., 11,7185-7207.

80. Valari M., E.Chatignoux and L.Menut, 2011, Using a chemistry transport model to account for the spatial variability of exposure-concentrations in epidemiologic air pollution studies, Journal of the Air and Waste Management Association, 61, 164-179

81. Aulagnier, C., P. Rayner, P. Ciais, R. Vautard, L. Rivier, and M. Ramonet (2010), Is the recent build-up of atmospheric CO2 over Europe reproduced by models, Part 2: An overview with the atmospheric mesoscale transport model CHIMERE, Tellus, Ser. B, 62, 14-25, 2010.

82. Beekmann, M., and R. Vautard, 2010: A modelling study of photochemical regimes over Europe: robustness and variability. Atmos. Chem. Phys. Disc., 10, 10067-10084.

83. Bessagnet B., C.Seigneur, L.Menut, 2010, Impact of dry deposition of semi-volatile organic compounds on secondary organic aerosols, Atmospheric Environment, 10.1016/j.atmosenv.2010.01.027.

84. Coll, I., C. Rousseau, B. Barletta, S. Meinardi and D. R. Blake, Evaluation of an urban NMHC emission inventory by measurements and impact on CTM results, Atm. Env., Vol 44 (31), pp 3843-3855, 2010.

85. Curci, G., Palmer, P. I., Kurosu, T. P., Chance, K., and Visconti, G.: Estimating European volatile organic compound emissions using satellite observations of formaldehyde from the Ozone Monitoring Instrument, Atmos. Chem. Phys., 10, 11501-11517, doi:10.5194/acp-10-11501-2010, 2010

86. Curci, G., Beekmann, M., Vautard, R., Smiatek, G., Steinbrecher, R., Theloke, J., Friedrich, R. (2009), Modelling study of the impact of isoprene and terpene biogenic emissions on European ozone levels, Atmospheric Environment, 43, 1444-1455, doi:10.1016/j.atmosenv.2008.02.070

87. Huijnen, V., H. J. Eskes, A. Poupkou, H. Elbern, K. F. Boersma, G. Foret, M. Sofiev, A. Valdebenito, J. Flemming, O. Stein, A. Gross, L. Robertson, M. D'Isidoro, I. Kioutsioukis, E. Friese, B. Amstrup, R. Bergstrom, A. Strunk, J. Vira, D. Zyryanov, A. Maurizi, D. Melas, V.-H. Peuch, and C. Zerefos, Comparison of OMI NO2 tropospheric columns with an ensemble of global and European regional air quality models Atmos. Chem. Phys., 10, 3273-3296, 2010.

88. Hodzic A, Jimenez JL, Prevot ASH, et al., 2010, Can 3-D models explain the observed fractions of fossil and non-fossil carbon in and near Mexico City?, Atmospheric chemistry and physics Volume: 10 Issue: 22 Pages: 10997-11016

89. Hodzic A, Jimenez JL, Madronich S, et al., 2010, Modeling organic aerosols in a megacity: potential contribution of semi-volatile and intermediate volatility primary organic compounds to secondary organic aerosol formation, Atmospheric chemistry and physics Volume: 10 Issue: 12 Pages: 5491-5514 Konovalov, I. B., M. Beekmann, A. Richter, J. P. Burrows And A. Hilboll, Multi-annual changes of NOx emissions in megacity regions: nonlinear trend analysis of satellite measurement based estimates, Atmos. Chem. Phys., 10, 8481-8498, 2010.

90. Leitao, J., A. Richter, M. Vrekoussis, A. Kokhanovsky, Q. J. Zhang, M. Beekmann, and J. P. Burrows, On the improvement of NO2 satellite retrievals - aerosol impact on the airmass factors, Atmos. Measurement Technics, 3, 475-493, 2010.

91. Menut L. and B.Bessagnet, 2010, Atmospheric composition forecasting in Europe , Annales Geophysicae, 28, 61-74

92. Rolland M.-N., Gabrielle, B., Laville, P., Cellier, P., Beekmann, M., Gilliot, J.-M., Michelin, J., Hadjar, D., Curci, G., Biophysical modeling of NO emissions from agricultural soils for use in regional chemistry-transport models, Environmental Pollution, 158 (3), 711-722, 2010.

93. Sciare,J., D'argouges,O., Zhang,Q.J., Sarda-Esteve,R., Gaimoz,C., Gros,V., Beekmann,M., And Sanchez,O., Comparison between simulated and observed chemical composition of fine aerosols in Paris (France) during springtime: contribution of regional versus continental emissions, Atmos. Chem. Phys., 10, 11987-12004, 2010. Valari M. and L.Menut, 2010, Transferring the heterogeneity of surface emissions to variability in pollutant concentrations over urban areas through a chemistry transport model, Atmospheric Environment, Volume 44, Issue 27, Pages 3229-3238,

94. Borrego, C., Sa, E., Monteiro, A., Ferreira, J., Miranda, A.I. (2009). Forecasting Human Exposure to Atmospheric Pollutants - a modelling approach. Atmospheric Environment, doi:10.1016/j.atmosenv.2009.07.049.

95. Dufour,G., Wittrock,F., Camredon,M., Beekmann,M., Richter,A., and Burrows,J., SCIAMACHY formaldehyde observations: constraint for isoprene emissions over Europe ? Atmos. Chem. Phys., 9, 1647-1664, 2009.

96. Curci, G., M. Beekmann, R. Vautard, G. Smiatek, R. Steinbrecher, J. Theloke, R. Friedrich, Modelling study of the impact of isoprene and terpene biogenic emissions on European ozone levels, Atmos. Environ. 48, 1444-1455, 2009.

97. Flaounas, E., I. Coll, A. Armengaud and C. Schmechtig, The representation of dust transport and missing urban sources as major issues for the simulation of PM episodes in a Mediterranean area, Atmospheric Chemistry and Physics, Vol 9, pp8091-8101, 2009.

98. Bessagnet B., L.Menut, G.Curci, A.Hodzic, B.Guillaume, C.Liousse, S.Moukhtar, B.Pun, C.Seigneur, M.Schulz, 2009, Regional modeling of carbonaceous aerosols over Europe - Focus on Secondary Organic Aerosols Journal of of Atmospheric Chemistry,

99. Coll, I., Lasry, F., Fayet, S., Armengaud, A., and R. Vautard, 2009, Simulation and evaluation of 2010 emission control scenarios in a Mediterranean area. Atmos. Environ., 43, 4194-4204.

100. de Meij A., Gzella, A., Cuvelier, C., Thunis, P., Bessagnet, B., Vinuesa, J.F., Menut, L., Kelder H., 2009, The impact of MM5 and WRF meteorology over complex terrain on CHIMERE model calculations. ACP ,

101. Foret, G., Hamaoui, L., Schmechtig, C., Eremenko, M., Keim, C., Dufour, G., Boynard, A., Coman, A., Ung, A. and Beekmann, M.: Evaluating the potential of IASI ozone observations to constrain simulated surface ozone concentrations, Atmos. Chem. Phys., 9, 8479-8491, 2009.

102. Hodzic A, Jimenez JL, Madronich S, et al., 2009, Modeling organic aerosols during MILAGRO: importance of biogenic secondary organic aerosols, ATMOSPHERIC CHEMISTRY AND PHYSICS Volume: 9 Issue: 18 Pages: 6949-6981 Konovalov I. B., M. Beekmann, F. Meleux, A. Dutot and G. Foret, Combining deterministic and statistical approaches for PM10 forecasting in Europe, Atm. Env., 43, 2009.

103. Konovalov, I.B., Elanskii, N. F., Zvyagintsev, A. M., Belikov, I. B., and Beekmann, M.: Validation of chemistry transport model of the lower atmosphere in the Central European region of Russia using ground-based and satellite measurement data, Russian Meteorology and Hydrology, 34 (4), 236-242, 2009.

104. Menut L., O.Masson, B.Bessagnet, 2009, Contribution of Saharan dust on radionuclides aerosols activity levels in Europe? The 21-22 February 2004 case study, J. Geophys. Res., 114, D16202, doi:10.1029/2009JD011767.

105. Menut L., I. Chiapello and C. Moulin, 2009, Previsibility of mineral dust concentrations: The CHIMERE-DUST forecast during the first AMMA experiment dry season, Journal of Geophysical Research - Atmospheres, 114, D07202

106. Rouil L., C.Honore, R.Vautard, M.Beekmann, B.Bessagnet, L.Malherbe, F.Meleux, A.Dufour, C.Elichegaray, J-M.Flaud, L.Menut, D.Martin, A.Peuch, V-H.Peuch, N.Poisson, 2009, PREV'AIR : an operational forecasting and mapping system for air quality in Europe, BAMS, DOI: 10.1175/2008BAMS2390.1,

107. Steinbrecher, R., Smiatek, G., Koble, R., Seufert, G., Theloke, J., Hauff, K., Ciciolli, P., Vautard, R., 2009: Intra- and inter-annual variability of VOC emissions from natural and semi-natural vegetation in Europe and neighbouring countries. Atmos. Environ., 43, 1380-1391.

108. Szopa S., G.Foret, L.Menut, A.Cozic, 2009, Impact of large scale circulation on European summer surface ozone: consequences for modeling, Atmospheric Environment, Volume 43, Issue 6, Pages 1189-1195, doi:10.1016/j.atmosenv.2008.10.039,

109. Timmermans, R. M. A., Segers, A. J., Builtjes, P. H. J., Vautard, R., Siddans, R., Elbern, H., Tjemkes, S. A. T., and M. Schaap, 2009, The added value of a proposed satellite imager for ground-level particulate matter analyses and forecasts. IEEE J-STAR, 2, 271-283.

110. Timmermans, R. M. A., Schaap, M., Elbern, H., Siddans, R., Tjemkes, S., Vautard, R., and P. Builtjes, 2009: An observing system simulation experiment (OSSE) for aerosol optical depth from satellites. J. Atmos. Ocean. Technol,26, 2673-2682.

111. Vautard, R., M. Schaap, R Bergstrom, B. Bessagnet, J. Brandt, P.J.H. Builtjes, J.H. Christensen, C. Cuvelier, V. Foltescu, A. Graf, A. Kerschbaumer, M. Krol, P. Roberts, L. Rouil, R. Stern, L. Tarrason, P. Thunis, E. Vignati, P. Wind, 2009, Skill and uncertainty of a regional air quality model ensemble. Atmos. Environ., 43, 4822-4832.

112. Vivanco, M., Palomino, I., Vautard, R., Bessagnet, B., Martin, F., Menut, L., Jimenez, S., 2009: Multi-year assessment of photochemical air quality simulation over Spain, Environmental Modeling and Software, 24, 63-73. Vuolo M.R., H.Chepfer, L.Menut and G.Cesana, 2009, Comparison of mineral dust layers vertical structures modelled with CHIMERE-DUST and observed with the CALIOP lidar, Journal of Geophysical Research - Atmospheres , Vol. 114, D09214, doi:10.1029/2008JD011219,

113. Vuolo M.R., L.Menut and H.Chepfer, 2009, Impact of transport schemes accuracy on modelled dust concentrations variability Journal of Atmospheric and Oceanic Technology, 26, p.1135-1143, doi:10.1175/2008JTECHA1197.1, 2008

114. Bessagnet B., L.Menut, G.Aymoz, H.Chepfer and R.Vautard, 2008, Modelling dust emissions and transport within Europe: the Ukraine March 2007 event, Journal of Geophysical Research - Atmospheres, 113, D15202, doi:10.1029/2007JD009541,

115. Bessagnet, B., L. Menut, G. Curci, A. Hodzic, B. Guillaume, C. Liousse, S. Moukhtar, B. Pun, C. Seigneur and M. Schulz (2008), Regional modeling of carbonaceous aerosols over Europe - Focus on Secondary Organic Aerosols, Journal of Atmospheric Chemistry, 61, 175-202

116. Colette A., Menut L., Haeffelin M., Morille Y., 2008, Impact of the transport of aerosols from the free troposphere towards the boundary layer on the air quality in the Paris area, Atmospheric Environment, Vol 42/2 pp 390-402, DOI: 10.1016/j.atmosenv.2007.09.044,

117. Curci, G., Beekmann, M., Vautard, R., Smiatek, G., Steinbrecher, R., Theloke, J., and R. Friedrich, 2008: Modeling study of the impact of isoprene and terpene emissions on European ozone levels. Atmos. Environ., 43, 1444-14

118. Eremenko, M., Dufour, G., Foret, G., Keim, C., Orphal, J., Beekmann, M., Bergametti, G., and Flaud, J.-M.: Tropospheric ozone distributions over Europe during the heat wave in July 2007 observed from infrared nadir spectra recorded by IASI, Geophys. Res. Lett., 35, doi:10.1029/2008GL034803, 2008.

119. Honoré C., L.Rouil, R.Vautard, M.Beekmann, B.Bessagnet, A.Dufour, C.Elichegaray , J-M.Flaud, L.Malherbe, F.Meleux, L.Menut, D.Martin, A.Peuch, V.-H.Peuch, N.Poisson, 2008 Predictability of European air quality: The assessment of three years of operational forecasts and analyses by the PREV'AIR system, Journal of Geophysical Research, Atmospheres , 113, D04301, http://dx.doi.org/10.1029/2007JD008761,

120. Menut L., 2008, Sensitivity of hourly Saharan dust emissions to NCEP and ECMWF modeled wind speed, Journal of Geophysical Research - Atmospheres, 113, D16201, doi:10.1029/2007JD009522,

121. Valari M. and L. Menut, 2008, Does increase in air quality models resolution bring surface ozone concentrations closer to reality?, Journal of Atmospheric and Oceanic Technology, DOI: 10.1175/2008JTECHA1123.1,

122. Vivanco M.G., Palomino I., Vautard R., Bessagnet R., Martin F., Menut L., Jimenez S., 2008, Multi-year assessment of photochemical air quality simulation over Spain, Env. Mod. and Software, doi:10.1016/j.envsoft.2008.05.004

123. Hodzic A., S. Madronich, B. Bohn, S. Massie, L. Menut, and C. Wiedinmyer, 2007, Wildfire particulate matter in Europe during summer 2003: Meso-scale modeling of smoke emissions, transport and radiative effects, Atmospheric Chemistry and Physics, 7

124. Pison I., L.Menut and G.Bergametti, 2007 Inverse modeling of surface NOx anthropogenic emissions fluxes in the Paris area during the ESQUIF campaign, J. Geophys. Res., 112, D24302, doi:10.1029/2007JD008871.

125. Vautard R., M.Maidi, L.Menut, M.Beekmann, A.Colette, 2007 Boundary layer photochemistry simulated with a two-stream convection scheme, Atmospheric Environment, Volume 41, Issue 37, Pages 8275-8287.

126. Pirovano G., I. Coll, M. Bedogni, S. Alessandrini, M. P. Costa, V. Gabusi, F. Lasry, L. Menut, R. Vautard, 2007, On the influence of meteorological input on photochemical modelling of a severe episode over a coastal area, Atmospheric Environment, Volume 41, Issue 30, September 2007, Pages 6445-6464

127. Menut L., G.Forêt and G.Bergametti, 2007, Sensitivity of mineral dust concentrations to the model size distribution accuracy, Journal of Geophysical Research, Atmospheres, 112, D10210, doi:10.1029/2006JD007766.

128. Drobinski P., F. Said, G. Ancellet, J. Arteta, P. Augustin, S. Bastin, A. Brut, J.L. Caccia, B. Campistron, S. Cautenet, A. Colette, B. Cros, U. Corsmeier, I. Coll, A. Dabas, H. Delbarre, A. Dufour, P. Durand, V. Guenard, M. Hasel, N. Kalthoff, C. Kottmeier, A. Lemonsu, F. Lohou, V. Masson, L. Menut, C. Moppert, V.H. Peuch, V. Puygrenier, O. Reitebuch, R. Vautard, 2007, Regional transport and dilution during high pollution episodes in southeastern France: Summary of findings from the ESCOMPTE experiment, Journal of Geophysical Research, Atmospheres, 112, D13105, doi:10.1029/2006JD007494.

129. Deguillaume L., M. Beekmann, L. Menut, Bayesian Monte Carlo analysis applied to regional scale inverse emission modelling for reactive trace gases, Journal of Geophysical Research, Atmospheres, Vol. 112, No. D2, D02307. http://dx.doi.org/10.1029/2006JD007518

130. Konovalov I. B., M. Beekmann, A. Richter, J. P. Burrows, 2005, Inverse modelling of the spatial distributions of NOx emissions on a continental scale using satellite data, Atmposheric Chemistry and Physics , 6, 1747-1770, 2006.

131. Cuvelier, C., Thunis, P., Vautard, R., Amann, M., Bessagnet, B., Bedogni, M., Berkowicz, R., Brandt, J., Brocheton, F., Builtjes, P., Coppalle, A., Denby, B., Douros G., Graf, A., Hellmuth, O., Honoré, C., Hodzic, A., Jonson, J., Kerschbaumer, A., de Leeuw, F., Minguzzi, E., Moussiopoulos, N., Pertot, C., Pirovano, G., Rouil, L., Schaap, M., Stern, R., Tarrason, L., Vignati, E., Volta, M., White, L., Wind, P., Zuber, A., 2006: CityDelta: A model intercomparison to explore the impact of emission reductions in 2010 in European cities in 2010, Atmospheric Environment, in press.

132. Vautard, R., Builtjes, P. H. J., Thunis, P., Cuvelier, K., Bedogni, M., Bessagnet, B., Honoré, C., Moussiopoulos, N., Pirovano G., Schaap, M., Stern, R., Tarrason, L., Van Loon, M., 2006: Evaluation and intercomparison of Ozone and PM10 simulations by several chemistry-transport models over 4 european cities within the City-Delta project, Atmospheric Environment, in press.

133. Hodzic A., B.Bessagnet and R.Vautard, A model evaluation of coarse-mode nitrate heterogeneous formation on dust particles, 1006, Atm.Env, 40, 4158-4171

134. Colette A., Ancellet G., L. Menut and S.R.Arnold, A Lagrangian analysis of the impact of transport and transformation on the ozone stratification observed in the free troposphere during the ESCOMPTE campaign, Atmos. Chem. Phys., 6, 3487-3503, 2006

135. Hodzic A., R. Vautard, P. Chazette, L. Menut and B.Bessagnet, Aerosol chemical and optical properties over the Paris area within ESQUIF project, Atmospheric Chemistry and Physics, 2006, pp.3257-3280. SRef-ID: 1680-7324/acp/2006-6-3257

136. Szopa S., D.Hauglustaine, R.Vautard and L. Menut, Future global tropospheric ozone changes and impact on European air quality, Geophysical Research Letter, 2006, 33, L14805, doi:10.1029/2006GL025860

137. Vautard R., S. Szopa, M. Beekmann, L. Menut, D. A. Hauglustaine, L. Rouil, M. Roemer (2006), Are decadal anthropogenic emission reductions in Europe consistent with surface ozone observations?, Geophys. Res. Lett., 33, L13810, doi:10.1029/2006GL026080

138. Pison I., L. Menut and N.Blond, Inverse modeling of emissions for local photo-oxidant pollution: Testing a new methodology with kriging constraints, Annales Geophysicae, 2006, 24, 1523-1535

139. Hodzic A., R. Vautard, H. Chepfer, P. Goloub, L. Menut, P. Chazette, J.L. Deuze, A. Apituley, P. Couvert, Evolution of aerosol optical thickness over Europe during the August 2003 heat wave as seen from CHIMERE model simulations and POLDER data, Atmospheric Chemistry and Physics, 2006, 1853-1864. SRef-ID: 1680-7324/acp/2006-6-1853

140. Blond, N., Boersma, K. F., Eskes, H. J., van der A, R., Van Rosendael, M., De Smedt, I., Bergametti, G., Vautard, R., 2005. Intercomparison of SCHIAMACHY nitrogen dioxide observations, in-situ measurements and air quality modelling results over Western Europe. J. Geophys. Res., in press.

141. Hodzic, A., Vautard, R., Bessagnet, B., Lattuati, M., and F. Moreto, 2005: On the quality of long-term urban particulate matter simulation with the CHIMERE model. Atmospheric Environment, 39, 5851-5864.

142. Bessagnet B., A.Hodzic, O.Blanchard, M.Lattuati, O.LeBihan, H.Marfaing and L.Rouil, 2005, Origin of particulate matter pollution episodes in wintertime over the Paris basin, Atm.Env., 39, 6159-6174.

143. Menut L., I. Coll and S. Cautenet, 2005, Impact of meteorological data resolution on the forecasted ozone concentrations during the ESCOMPTE IOP 2a and 2b, Atmospheric Research - ESCOMPTE Special Issue, 74, 139-159, 2005

144. Vautard, R., C. Honoré, M. Beekmann, L. Rouil, 2005: Simulation of ozone during the August 2003 heat wave and emission control scenarios, Atmospheric Environment, in press.

145. Vautard R., B.Bessagnet, M.Chin and L. Menut, On the contribution of natural Aeolian sources to particulate matter concentrations in Europe: testing hypotheses with a modelling approach, Atm. Environ., 39, Issue 18, 3291-3303, 2005

146. Monteiro, A., Vautard, R., Borrego, C., and A. I. Miranda, 2005: Long-term simulations of photo oxidant pollution over Portugal using the CHIMERE model, Atmospheric Environment., 39, 3089-3101.

147. Hodzic A., Vautard, R., Bessagnet, B., Lattuati, M., Moreto, F., Long-term urban aerosol simulation versus routine particulate matter observations. Atmospheric Environment, 39, 5851-5864, 2005

148. Vautard R., B.Bessagnet, M.Chin and L.Menut, On the contribution of natural Aeolian sources to particulate matter concentrations in Europe: testing hypotheses with a modelling approach, Atm. Env., 39, Issue 18, 3291-3303, 2005

149. Menut L., I. Coll and S. Cautenet, Impact of meteorological data resolution on the forecasted ozone concentrations during the ESCOMPTE IOP 2a and 2b, Atmospheric Research - ESCOMPTE Special Issue, 74, 139-159, 2005.

150. Bessagnet B., A.Hodzic, R.Vautard, M.Beekmann, S.Cheinet, C.Honoré, C.Liousse and L.Rouil, Aerosol modeling with CHIMERE - preliminary evaluation at the continental scale, Atmospheric Environment, 38, 2803-2817, 2004

151. Blond, N. and R.Vautard, Three-dimensional ozone analyses and their use for short-term ozone forecasts, J. Geophys. Res., 109, D17303, doi:10.1029/2004JD004515, 2004.

152. Wackernagel, H., C. Lajaunie, N. Blond, C. Roth and R. Vautard, Geostatistical risk mapping with chemical transport model output and ozone station data, Ecological Modelling, 179, 177-185, 2004.

153. Hodzic A., Chepfer H., Vautard R., Chazette P., Beekmann M., Bessagnet B., Chatenet B., Cuesta J., Drobinski P., Goloub P., Haeffelin M., Morille Y., 2004: Comparisons of aerosol chemistry-transport model simulations with lidar and sun photometer observations at a site near Paris., J. Geophys. Res., 109, D23201,doi:10.1029/2004JD004735, 2004

154. Konovalov, I., Beekmann, M., Vautard, R., Burrows, J., Richter, A., Nuess, H., and N. Nelansky, 2004: The comparison and evaluation of modelled and GOME measurement derived tropospheric NO2 columns over western and eastern Europe Atmospheric Chemistry and Physics, in press.

155. Labouze, E., C. Honoré, L. Moulay, B. Couffignal, and M. Beekmann, 2004. Photochemical ozone creation potentials: a new set of characterization factors for different gas species at the scale of the Western Europe, Int. Journal of Life Cycle Assessment, Vol.9, Nr.3, 187-195.

156. Monteiro, A., Borrego, C., Vautard, R., and A. I. Miranda, 2004: long-term simulations of photooxidant pollution over Portugal using the CHIMERE model. Atmospheric Environment, submitted.

157. Pison I. and L.Menut, Quantification of the impact of aircraft traffic emissions on tropospheric ozone over Paris area, Atmospheric Env., 38-7, 971-983, 2004

158. Vautard, R., C. Honoré, M. Beekmann, L. Rouil, 2004: Simulation of ozone during the August 2003 heat wave and emission control scenarios, Atmospheric Environment, in press.

159. Zhang, B.-N., R. Vautard and N.-T. Kim Oanh, 2004: Comparison of the UAM-V/SAIMM and CHIMERE/ECMWF Photochemical Modeling System Performance in a Tropical Urban Area, J. Air and Waste Management, in press

160. Beekmann M. and C.Derognat, Monte carlo uncertainty analysis of a regional scale transport chemistry model constrained by measurements from the ESQUIF campaign, Journal of Geophysical Research, ESQUIF special section, 2003

161. Blond, N., Bel, L. and Vautard, R., Three-dimensional ozone data analysis with an air quality model over the Paris area, J. Geophys. Res., 108(D23), 4744, doi:10.1029/2003JD003679, 2003.

162. Derognat C., M.Beekmann, H.Schmidt, R.Vautard, D.Martin, B.Neininger, Effect of biogenic VOC emissions on the tropospheric chemistry during elevated ozone periods in Ile-de-france, Journal of Geophysical Research, ESQUIF special section, 2003

163. Menut L., Adjoint modelling for atmospheric pollution processes sensitivity at regional scale during the ESQUIF IOP2, Journal of Geophysical Research, ESQUIF special section, 2003

164. Sillman S., R. Vautard, L. Menut and D. Kley, O3-NOx-VOC sensitivity and NOx-VOC indicators in Paris: results from models and ESQUIF measurements, Journal of Geophysical Research, ESQUIF special section, 2003

165. Schmidt H. and D.Martin, Continental scale adjoint sensitivity of ozone concentrations in the paris region during the ESQUIF episodes, Journal of Geophysical Research, ESQUIF special section, 2003

166. Vautard R., D. Martin, M. Beekmann, R. Friedrich, A. Jaubertie, D. Kley, M. Lattuati, P. Moral, B. Neininger and J. Theloke, Paris emission inventory diagnostic from the ESQUIF airborne measurements and a chemistry-transport model, Journal of Geophysical Research, ESQUIF special section, 2003

167. Vautard R. et al., A synthesis of the ESQUIF field campaign, Journal of Geophysical Research, ESQUIF special section, 2003

168. Kurtenbach R., K.H Becker, J.A.G. Gomes, J. Kleffmann, J.C. L´orzer, M. Spittler, P. Wiesen, R. Ackermannb, A. Geyer, U. Platt, 'Investigations of emissions and heterogeneous formation of HONO in a road traffic tunnel', Atmospheric Environment, 35 33853394, 2001

169. Schmidt H., C. Derognat, R.Vautard and M.Beekmann, 'A comparison of simulated and observed ozone mixing ratios for the summer of 1998 in western Europe', Atmospheric Environment, 2001

170. Vautard R., M. Beekmann, J. Roux, D. Gombert, 'Validation of a deterministic forecasting system for the ozone concentrations over the Paris area', Atmospheric Environment, 35 2449-2461, 2001.

171. Honoré, C., Vautard, R., Beekmann, M., Low and High Nox chemical regimes in an urban environment, Environmental Modelling and Software, 15, 559-564, 2000

172. Honoré, C., Vautard, R. and Beekmann, M., Photochemical regimes in urban atmospheres: the influence of dispersion. Geophys. Res. Letters, 27, 1895-1898, 2000.

173. Menut L., R.Vautard, M.Beekmann and C.Honoré, 'Sensitivity of Photochemical Pollution using the Adjoint of a Simplified Chemistry-Transport Model', Journal of Geophysical Research - Atmospheres 105, D12, 15,379-15,402, 2000

174. Menut L., R. Vautard, C. Flamant, C. Abonnel, M. Beekmann, P. Chazette, P. H. Flamant, D. Gombert, D. Guedalia, D. Kley, M.P. Lefebvre, B. Lossec, D. Martin, G. Megie, M. Sicard, P. Perros, G. Toupance, 'Atmospheric pollution over the Paris area: The ESQUIF project', Annales Geophysicae, 18, 1467-1481, 2000

175. Vautard R., M.Beekmann and L. Menut, 'Applications of adjoint modelling in atmospheric chemistry: sensitivity and inverse modelling', Environmental Modeling and Sofware, 15, pp 703-709, 2000

B History

This section tracks the model evolution over the last versions.

B.1 Development of the mineral dust emissions

Historically, there was no dust emissions in CHIMERE before 2005. Between 2005 and 2008, two model developments were done in parallel:

- a **simple dust emissions scheme for Europe**, in order to close the aerosol mass budget for air quality studies ([Vautard et al., 2005b]). This development was done over Europe only due to the availability of anthropogenic emissions (EMEP only for the CHIMERE version previous to 2008). The parameterization were chosen to be simple in order to ensure fast calculations considering that all gaseous and particles species are calculated. The main goal was not to have the best emissions schemes but a scheme able to unbiase the modelled aerosols masses over Europe, and enough robust and stable to make confident forecasts.
- the **transport model CHIMERE-dust** dedicated to long range transport of dust over the northern hemisphere ([Menut et al., 2005, Menut et al., 2007, Menut, 2008, Menut et al., 2013a]). This model was developed for studies of mineral aerosols processes (emissions and transport) over the Northern Atlantic.

In 2010, the development of CHIMERE-dust was frozen. Its specific parameterizations were implemented into CHIMERE (specific dry deposition velocities, saltation and sandblasting, Weibull distribution for wind speed used for emissions, the Tiedke deep convection scheme). Previous model version thus proposed the two models into a single one. However, the developments were not yet finished: the mineral dust database used is only valid for arid and semi-arid areas over Africa and the erosion scheme over Europe remains simple.
For the 2016 version, development has been made to homogenize the mineral dust emissions computations over the globe. The European dust production model was removed and the African dust production model was extent to any domain by adapting all required databases.

B.2 chimere2008

Version *chimere2008* contained the following improvements and new processes.

- New functionality:
  - ◇ Due to integration of the MEGAN model biogenic emission potentials data and emission rates parameterizations, Chimere can now be used outside Europe if the user provides anthropogenic emissions in the region of interest
  - ◇ Automatic preparation of the file **LANDUSE_<domain>** from the original GLCF global land use database for the desired Chimere domain
  - ◇ Meteorological interface to the WRF model **prepwrf** has been added
  - ◇ Possibility to use aerosol boundary and initial conditions from the LMDz model output
  - ◇ A new mode of **exachim** to display various data slices by a simple mouse click
- Process changes:

- ◇ Updated Secondary Organic Aerosols (SOA) chemistry: the full MEGAN SOA scheme is now used

- Computational changes:
  - ◇ New format of the emissions interface **emiSURF** and **prepemis**. The emission files are now separated by individual species, which makes the **prepemis** interface simpler and easier to modify. If a simulation spans two consequent months, emissions for each day are now taken from a corresponding month rather than from the first month for all days. One can also choose emission types to use independently: either surface, point, or fire emissions. Hourly changes of fire emissions are now allowed. If emissions are not available for a given species, they are set to zero, and the simulation continues
  - ◇ Reorganized boundary and initial conditions interface for more convenience and code simplicity. User can now choose a global database for each species
  - ◇ Revised vertical interpolations in the boundary and initial conditions interface
  - ◇ Running Open MPI or LAM depending on user system settings. If both realizations are found, preference is given to Open MPI
  - ◇ Simulation parameters are now organized in the form of an array in the top calling script **chimere.sh**. This allows more convenient parameter specification, especially for simulations for several, possibly nested, model domains
  - ◇ The script **chimere-run.sh** has been split into parts corresponding to Chimere components: compilation, meteorological interfaces, emissions, initial and boundary conditions, and Chimere core. It is now possible to run individually one or more of these components.

B.3 V200606

B.3.1 Parallelization

Version V200606 represented a major breakthrough in the model computational speed, since it has been parallelized and can now run on distributed memory clusters and shared memory machines, ranging from the local home-made cluster of PCs, to large supercomputers. However, there are no changes neither in the scientific core of the model, nor in the I/O file formats.
The rationale of the parallelization was :

- the increasing computation time of the aerosol version and of nextcoming, more sophisticated versions,
- the user requirements for higher resolution domains,
- the requirements of air pollution forecast agencies, in terms of forecast computation time.

CHIMERE uses the distributed memory scheme, and an MPI message passing library. It has been tested with Open MPI and LAM/MPI, but should work, with minor changes in the scripts, with MPICH or other MPI compatible parallel environments.
There is one master program, which calls several worker subroutines, each worker been in charge of the processing of a subdomain. Subdomains are the result of a Cartesian division of the main geographical domain by the number of processors.
The master program is in charge of the initializations and file I/O. The workers are in charge of the scientific processing and inter-subdomains boundary conditions updates.
As described above, CHIMERE is basically an MPMD (multiple program, multiple data) application. However, MPMD is only available with MPI-2 compatible environments. To increase CHIMERE portability, its interface has been tweaked to mimic the appearance of an SPMD (single program, multiple data) application, which makes it compatible with widely spread MPI-1 parallel environments.
Despite the tremendous architectural change in the code structure, most scientific subroutines, now called by the worker main subroutine, have remained unchanged.

As far as the user interface is concerned, the only apparent modifications are :

- definition of subdomains in **chimere-mm5** script : **nzdoms** and **nmdoms** parameters.
- use of an MPI library : MPI must be installed for running CHIMERE, even if it runs on only one processor with only one subdomain.

B.3.2 Toolbox

There is a new processing inside **exachim** : the COARDS intermediate file is no longer necessary. Instead, GrADS compliant files are built directly. A new utility, chm2grads.f90, replaces chm2coards.f90. All kinds of CHIMERE grids may be used, not only rectilinear ones. More sophisticated command line options allows for displaying only selected variables and time slots.
The udunits library is no longer used.
A new tool to transform the old CHIMERE binary files into netCDF files, **chmbin2cdf.f90**, has been included in the distribution.
An older tool, **chim2fig**, which used to be distributed with pre-netCDF versions of CHIMERE, has been upgraded to accept netCDF files.

B.3.3 Scripts

New top-level scripts have been added, to run CHIMERE on PC clusters with a PBS-like batch scheduler.
Despite the fact that an interface to ECMWF meteorology is not yet provided in this version, a script to run CHIMERE on ECMWF HPCD computer is provided as an example for running CHIMERE under IBM LoadLeveler and POE environments.

B.3.4 makefiles changes

The directory structure of the src/ tree has been modified, and Makefiles have been rationalized. This allows now for using the parallel compilation capability of the GNU make utility. Also, the meteo interface is run in background, during model compilation. This reduces dramatically the compilation time on multiprocessor machines, allowing for more sophisticated optimizations. Minor bugs have been corrected in Makefile headers.

C Some scripts used in the CHIMERE suite

C.1 The *domains/makeCOORDdomains* script for horizontal grid definition

To **create a new COORD file**, you first have to add a new line in the **domainlist.nml** file describing your new domain. After that, run manually the **domains-makeCOORDdomains.sh** script (in the **scripts/** directory or here below) with the required domain name:

```
domains-makeCOORDdomains new_domain_name new_COORD_file
```

with the following *makeCOORDdomains* script:

```
#!/bin/sh

if [ $# -eq 0 ] ; then
  echo "define the domain name"
  exit 0
else
  dom=$1
fi

nzo=`gawk '$1=="'${dom}'" {print $2}' domainlist.nml`
nme=`gawk '$1=="'${dom}'" {print $3}' domainlist.nml`
dx=`gawk '$1=="'${dom}'" {print $4}' domainlist.nml`
dy=`gawk '$1=="'${dom}'" {print $5}' domainlist.nml`
xbotleft=`gawk '$1=="'${dom}'" {print $6}' domainlist.nml`
ybotleft=`gawk '$1=="'${dom}'" {print $7}' domainlist.nml`

touch COORD
\rm COORD
[[ -z ${nzo} || -z ${nme} || -z ${dx} || -z ${dy} || -z ${xbotleft} || -z ${ybotleft} ]] &&\
   { echo "Error reading domainlist.nml. Probably domain ${dom} is not defined. Bye" ; exit 1 ; }

echo "   making horizontal COORD file"
echo "       geometry definition:"
echo "             nodes="${nzo}"x"${nme}
echo "             resol="${dx}"x"${dy}
echo "             south-west point="${xbotleft}"x"${ybotleft}

gawk -v xbotleft=${xbotleft} -v ybotleft=${ybotleft} -v dx=${dx} -v dy=${dy} -v nzo=${nzo} -v nme=${
  for(j=1;j<=nme;j++){
  for(i=1;i<=nzo;i++){
     x=(i-1)*dx
     y=(j-1)*dy
     xlon=xbotleft+x
     xlat=ybotleft+y
     print  xlon "  " xlat >> "COORD"
  }
  }
}'

mv COORD COORD_${dom}
cp COORD_${dom} HCOORD
```

C.2 The *util/define_geom* script for vertical grid definition

To make your own VCOORD file, go to the directory **util/**, edit the **define_geom** script and adapt the top pressure level to the one you need.
N.B.: It is recommended to have a maximum ptop of 200 hPa since the global model used for boundary conditions delivered data only up to this value.
The define_geom script:

```
#!/bin/sh

#  Defines a geometrical-progression vertical layering
#  For the CHIMERE model. It actually produces sets of
#  Hybrid sigma-p coefficients Ak and Bk such that the
#  pressure at top of layer k is Pk = Ak*1e5 + Bk*Ps in Pa
#  where Ps is Surface pressure

#  Define the parameters below and run the script by just typing "define_geom"

ptop=700    # Pressure at model top
nlay=8      # Number of layers
pre1=995    # Pressure (hPa) of the first layer top when Ps = 1000 hPa
fout=../data/vgrid/VCOORD.8GEOM700

echo ${nlay} ${pre1} ${ptop} | gawk -f geom.awk > ${fout}
```

Recommendations

- When defining manually the hybrid coefficients the user shall verify that under all possible meteorological conditions these layers do not cross one another or get mixed up.
- It is highly recommended that top level be a pressure level ($b_k = 0$), since it has been found to minimize mass loss through top boundary.
- Using the MOZART and LMDz-INCA boundary conditions, one should not use a model top above 200 hPa
- In the present formulation for cloud/radiation/photolysis, it is assumed that the model domain is *below the clouds*, i.e. no cloud albedo is taken into account. This puts constraints on model top to be not too high. This will be changed in future releases.

D How To install NetCDF under GNU/Linux

D.1 Background

Since CHIMERE requires a NetCDF package. This note describes how to install NetCDF for the supported compilers.
NetCDF installation has been tested with :

- ifort 32 bits (version 8.1.028)
- ifort 64 bits (version 8.1.027)
- gfortran 32 bits (version 4.4.2 20091027)
- gfortran 64 bits (version 4.1.2 20080704)
- netcdf (version 3.6.3 or 4.1.1 with hdf5-1.8.5)

D.2 Download

- **Download NetCDF** (source package) from the URL :

```
http://www.unidata.ucar.edu/downloads/netcdf/index.jsp
```

  For the Parallel NetCDF, please check the following web sites, for download and information, respectively:

```
http://cucis.ece.northwestern.edu/projects/PnetCDF/download.html
https://trac.mcs.anl.gov/projects/parallel-netcdf/wiki/Download
```

- **Decompress and detar**

```
tar xvfz netcdf.tar.gz
tar xvfz parallel-netcdf-1.7.0.tar.gz
```

D.3 Configure NetCDF

As an example for the NetCDF-3 family version 3.6.3:

```
cd netcdf-3.6.3/src
```

The configuration process depends on several environment variables that you shall set according to your compiler. Although it may be possible to link CHIMERE executables compiled with compiler A with the NetCDF library compiled with compiler B, we strongly recommend to use the same compiler. The time you will spend to install a new NetCDF library is negligible compared to the time you could loose trying to match inconsistent libraries.

We suppose you want to install netcdf somewhere under `/opt` . If you choose to install under `/usr/local`, or under you home directory, replace `/opt` your installation path in the following text.
We also suppose your shell is like `bash` or `ksh` . If you use `csh`, modify the `export` statements according to your shell syntax.

D.3.1 ifort 64 bit on Intel EMT64 or AMD Opteron

As root :

```
mkdir /opt/netcdf-3.6.3-ifort
```

As an ordinary user :

```
export FC=ifort
export F90=ifort
export CFLAGS="-O -m64"
export FFLAGS="-mp"
export CPPFLAGS="-DNDEBUG -DpgiFortran"
./configure --prefix=/opt/netcdf-3.6.3-ifort
make
make test
```

As root :

```
make install
```

Parallel NetCDF:

```
export LD_LIBRARY_PATH=/opt/openmpi-1.10.2-ifort/lib:/opt/openmpi-1.10.2-ifort/lib/

export FC=ifort
export F90=ifort

# The same C/C++ compilers as for Open MPI!
export CC=icc
export CXX=icpc
export MPICC=/opt/openmpi-1.10.2-ifort/bin/mpicc
export MPICXX=/opt/openmpi-1.10.2-ifort/bin/mpicxx
export MPIF77=/opt/openmpi-1.10.2-ifort/bin/mpif77
export MPIF90=/opt/openmpi-1.10.2-ifort/bin/mpif90
export CFLAGS='-O -m64 -mcmodel=medium'
export CXXFLAGS='-O -m64 -mcmodel=medium'
export FFLAGS='-O -g -m64 -mcmodel=medium'
export FCLAGS='-O -g -m64 -mcmodel=medium'
export LDFLAGS='-O -g -mcmodel=medium'
./configure --prefix=/opt/pnetcdf-1.7.0-ifort-64-medium
make clean && make && make testing
```

As root :

```
make install
```

D.3.2 gfortran (4.7.2 or later) 64 bit on Intel EMT64 or AMD Opteron

```
export CC=/opt/centos/devtoolset-1.1/root/usr/bin/gcc
export CXX=/opt/centos/devtoolset-1.1/root/usr/bin/g++
export FC=/opt/centos/devtoolset-1.1/root/usr/bin/gfortran
export F77=/opt/centos/devtoolset-1.1/root/usr/bin/gfortran

export CFLAGS='-O -m64 -mcmodel=medium'
export LDFLAGS='-O -g -fno-second-underscore -mcmodel=medium'
export CPPFLAGS='-DNDEBUG -DgFortran'
export FCFLAGS='-O -g -m64 -fno-second-underscore -mcmodel=medium'
export FFLAGS='-O -g -m64 -fno-second-underscore -mcmodel=medium'

./configure --prefix=/opt/netcdf-3.6.3-gfortran-64-medium
make clean && make && make check && make install
```

As root :

```
  make install
```

Parallel NetCDF:

```
export FC=/opt/centos/devtoolset-1.1/root/usr/bin/gfortran
export F90=/opt/centos/devtoolset-1.1/root/usr/bin/gfortran
export CC=/opt/centos/devtoolset-1.1/root/usr/bin/gcc
export CXX=/opt/centos/devtoolset-1.1/root/usr/bin/g++

export MPICC=/opt/openmpi-1.10.2-gfortran/bin/mpicc
export MPICXX=/opt/openmpi-1.10.2-gfortran/bin/mpicxx
export MPIF77=/opt/openmpi-1.10.2-gfortran/bin/mpif77
export MPIF90=/opt/openmpi-1.10.2-gfortran/bin/mpif90
export CFLAGS='-O -m64 -mcmodel=medium'
export CXXFLAGS='-O -m64 -mcmodel=medium'
export FFLAGS='-O -g -m64 -fno-second-underscore -mcmodel=medium'
export FCLAGS='-O -g -m64 -fno-second-underscore -mcmodel=medium'
export LDFLAGS='-O -g -fno-second-underscore -mcmodel=medium'

./configure --prefix=/opt/pnetcdf-1.7.0-64-gfortran-medium
make clean && make && make testing
```

As root :

```
  make install
```

D.4 Manually Configure CHIMERE

Automatic configuration of CHIMERE using config.sh is described in §2.2, p. 19. Here we explain how to configure the model manually.
In the directory `makefiles.hdr/`, you will find 9 files :

```
Makefile.hdr.g95-64-lam
Makefile.hdr.g95-64-ompi
Makefile.hdr.g95-lam
Makefile.hdr.g95-ompi
Makefile.hdr.gfortran-64-lam
Makefile.hdr.gfortran-64-ompi
Makefile.hdr.ifort-64-lam
Makefile.hdr.ifort-64-ompi
Makefile.hdr.ifort-ompi
```

After linking to `Makefile.hdr` the file corresponding to your compiler, MPI library, and system (32 or 64 bit), for instance:

```
ln -sf makefiles.hdr/Makefile.hdr.gfortran-64-ompi Makefile.hdr
```

modify the lines `my_netcdflib=` and `my_netcdfinc=` in the file mychimere.sh to point to your NetCDF directory. Modify also the PATHs to your HDF5 library given by variables `my_hdflib` and `my_hdfinc`. For instance :

```
export my_netcdfdir=/opt/netcdf-3.6.3-gfortran
```

If you are using NetCDF4/HDF5:

```
export my_hdfdir=/opt/hdf5-1.8.5-gfortran
```

Follow the comments in `Makefile.hdr.xxxx` for other options. 1

E How To install MPI under GNU/Linux

E.1 Background

CHIMERE is now parallelized, using the distributed memory scheme, and requires an MPI compatible Message Passing Library to be installed and configured on the host or cluster it will run on.
MPI is required even if CHIMERE is planned to run on a single processor machine !
Several free MPI libraries are available for download. MPICH and LAM/MPI are well known. The newer OpenMPI is claimed to be the continuation of LAM/MPI.
CHIMERE has been tested with LAM/MPI and Open MPI. This HOW-TO describes briefly the installation and basic configuration process for LAM/MPI and Open MPI on a RedHat-like GNU-Linux distribution.
We recommend the precompiled package installation for RedHat-like distributions. However, some 64 bit Linux distributions have a precompiled LAM-MPI binary which is not compatible with other libraries. In that case, you will have to install the LAM-MPI package from source, as described at the end of the document.

Tested with:

- Fedora Core 4
- LAM-7.1.1

E.2 LAM/MPI Installation

RedHat-like distributions include a RPM for LAM/MPI. It is generally called "lam".
Here is the installation process for a Fedora Core 4 system. You must have administrative privileges to perform it.

- If you use YUM as a package tool:

```
yum install lam
```

- If you use RPM:
  - ◇ download lam-7.1.1-7.FC4.i386.rpm from your Fedora repository
  - ◇ you may also want libaio-devel-0.3.104-2.i386.rpm
  - ◇ install :

```
rpm -Uvh libaio-devel-0.3.104-2.i386.rpm lam-7.1.1-7.FC4.i386.rpm
```

- Edit `/etc/lam/lam-bhost.def` to set the list of hosts you will include in your LAM cluster. For instance, for a cluster of 3 bi-processors, `lam-bhost.def` would contain :

```
host1.mycluster.mydomain.edu cpu=2
host2.mycluster.mydomain.edu cpu=2
host3.mycluster.mydomain.edu cpu=2
```

For a uniprocessor machine, `lam-bhost.def` would only contain :

```
localhost
```

- Instead of using the system wide lam-bhost.def, you can create and use your own hosts file, and boot LAM/MPI using this file. A file named "nodelist.example" is provided as a template in this distribution. Edit it according to your environment.

E.3 Testing

- type:

  ```
  lamboot
  ```

  to boot you LAM/MPI environment using system-wide hosts list, or

  ```
  lamboot <my_host_list>
  ```

  to boot your own host list defined in file `<my_host_list>`
- type:

  ```
  lamnodes
  ```

  to verify that all nodes declared in the hosts file are up.

If cas of insuccess, get LAM/MPI documentation from their web site.
Most problems occur because the user is not allowed to perform **rsh** or **ssh** connexions to the hosts listed in hostfile.
Check with your system administrator that you can **ssh** to the target hosts. If the hosts are connected to a private network, ask her/him to allow **rsh** on these hosts. The advantage of using **rsh** is that you can schedule unattended jobs using `cron` or `at` . Otherwise you need to change your ssh passphrase for an empty one, which can be a security issue.

E.4 Uniprocessor users

Parallelism is mainly useful for Air Pollution Forecast Agencies, or for scientists running long periods of reanalysis. For the users who just want to run CHIMERE as they were accustomated to, on a single processor machine, here is a simple summary of what they shall do with LAM/MPI:

- install LAM/MPI as described above

  ```
  yum install lam
  ```

- check that ssh is installed on your machine

  ```
  ssh localhost
  ```

Most modern linux distributions come with ssh installed and configured.

- edit **/etc/lam/lam-bhost.def** to keep only the line

```
localhost
```

- boot LAM/MPI

```
lamboot
```

- Enjoy CHIMERE !

E.5 Installation from source

Thanks to Gabriele Curci at aquila.infn.it

Some 64 bit linux vendors have compiled the lam package with the "second-underscore" option. This leads to an incompatibility between lam and netcdf libraries. If you get error messages like this in your make.log file, you are probably in that case :

```
twostep_mod.f90:(.text+0xbdb6): undefined reference to `mpi_irecv_'
twostep_mod.f90:(.text+0xc2cb): undefined reference to `mpi_issend_'
twostep_mod.f90:(.text+0xc33a): undefined reference to `mpi_irecv_'
twostep_mod.f90:(.text+0xc7f0): undefined reference to `mpi_issend_'
```

To overcome this problem, you have to install LAM-MPI from source. Here is the process, copied from Gabriele's message :

- login as root
- download LAM source, I installed latest version 7.1.2 (wget http://www.lam-mpi.org/download/files/lam-7.1.2.tar.bz2)
- unzip the source (tar jxvf lam-7.1.2.tar.bz2)
- `cd lam-7.1.2`
- `./configure "FC=g77 -fno-second-underscore" --prefix=/usr/local`
- `make`
- `make install`

E.6 Open MPI installation

This section briefly explains how to install Open MPI with g95 and ifort compilers from sources. The sources can be downloaded from the Open MPI home page [http://www.open-mpi.org].

With g95 on a 32 bit system

```
export COMPILO=g95
./configure CC=gcc CXX=g++ F77=$COMPILO  FC=$COMPILO \
            --prefix=/opt/openmpi-1.2.5-$COMPILO \
            --with-mpi-f90-size=medium
make all
```

```
make install
edit /etc/profile to set the PATH variable
edit /etc/ld.so.conf.d/openmpi.conf
ldconfig
```

With g95 on a 64 bit system

```
export COMPILO=g95
./configure CC=gcc CXX=g++ F77=$COMPILO FC=$COMPILO \
             CFLAGS=-m64 CXXFLAGS=-m64 FFLAGS=-m64 FCFLAGS=-m64 \
            --prefix=/opt/openmpi-1.2.5-$COMPILO \
            --with-mpi-f90-size=medium
make all
make install
edit /etc/profile to set the PATH variable
edit /etc/ld.so.conf.d/openmpi.conf
ldconfig
```

Build options with ifort for 64 and a 32 bit systems

For a 64 bit system:

```
export CC=gcc
export CXX=g++
export CFLAGS='-O2 -m64'
export CXXFLAGS='-O2 -m64'
export LDFLAGS='-O2'
export FC=ifort
export FCFLAGS='-O2 -m64'
export F77=ifort
export FFLAGS='-O2 -m64'
./configure --prefix=/opt/openmpi-1.2.5-ifort-64 --with-mpi-f90-size=medium
```

For a 32 bit system you need to remove the -m64 flag from the options above.

F Notes on using CHIMERE with LAM MPI

You need to make sure that LAM MPI is booted on your system, with the right number of processors. The command to use is:

```
lamnodes
```

The system should respond with a list of active nodes and the number of processors per node. The total number of declared processors should be superior or equal to **nzdoms*nmdoms** (see p.43).
If it does not, boot your MPI environment. With LAM/MPI, to boot the default nodes list, type:

```
lamhalt
lamboot
```

A file named **nodelist.example** is provided here as a template if you want to boot different nodes. To use this file, first edit it according to your environment, taking care to declare at least **nzdoms*nmdoms** processors. Once your **nodelist.example** file is edited, type:

```
lamhalt
lamboot nodelist.example
```

If you want to have an understanding of the impacts of the hostlist file (nodelist.example) read the recommendations in p.43

F.1 Specific case of single node envrionment

In the trivial case of a single node environment, the node list file, either **/etc/lam/lam-bhosts.def** or your own **nodelist.example** should contain only this single line:

```
localhost
```

And you should set **nzdoms=1** and **nmdoms=1** in **chimere.sh**.

In the other trivial case of a single bi-processor node, the node list file, should contain only this single line:

```
localhost cpu=2
```

And you should set **nzdoms=2** and **nmdoms=1** in **chimere.sh**.

G Structure of the CHIMERE netCDF files

G.1 Known issues

Using colon (or other special characters) in input file names is not compatible with the use of the PnetCDF library. The following error may occur:

```
pncvar.F90: netCDF error on source line         246 Unknown Error
Erreur code is         -220
```

G.2 EMIS.[domain].[MM].[SPEC].s.nc and EMIS.[domain].[MM].[SPEC].p.nc

```
netcdf EMIS.CONT5.05.NO2.s {
dimensions:
Time = 24 ;
west_east = 79 ;
south_north = 47 ;
bottom_top = 7 ;
type_day = 7 ;
SpStrLen = 23 ;
variables:
float lon(south_north, west_east) ;
lon:units = "degrees_east" ;
lon:long_name = "Longitude" ;
float lat(south_north, west_east) ;
lat:units = "degrees_north" ;
lat:long_name = "Latitude" ;
float EMEP_levels(bottom_top) ;
EMEP_levels:units = "meters" ;
EMEP_levels:long_name = "Cut_off_heights_for_redistribution" ;
float NO2(Time, type_day, bottom_top, south_north, west_east) ;
NO2:units = "molecule/cm2/s" ;
NO2:long_name = "NO2 Emission" ;

// global attributes:
:Title = "CHIMERE emissions" ;
:Sub-title = "Hourly surfacic emission" ;
:Chimere_type = "EMISSIONS" ;
:Generating_process = "Generated by sectoremis" ;
:Conventions = "None" ;
:Domain = "CONT5" ;
:Year = "2003" ;
:Landuse_for_Reggriding = "glcf" ;
:history = "" ;
}

netcdf EMIS.CONT5.01.NO2.p {
dimensions:
Time = 24 ;
west_east = 79 ;
south_north = 47 ;
```

```
Sources = 8 ;
type_day = 3 ;

variables:
float lon(south_north, west_east) ;
lon:units = "degrees_east" ;
lon:long_name = "Longitude" ;
float lat(south_north, west_east) ;
lat:units = "degrees_north" ;
lat:long_name = "Latitude" ;
long Sources_PIG(Sources) ;
Sources_PIG:units = "flag-0-1" ;
Sources_PIG:long_name = "Pig_treatment" ;
float Sources_lat(Sources) ;
Sources_lat:units = "Degrees" ;
Sources_lat:long_name = "Y_coordinate_of_source_point" ;
long Sources_ilat(Sources) ;
Sources_ilat:units = "cell_number" ;
Sources_ilat:long_name = "Y_coordinate_of_source_point" ;
float Sources_lon(Sources) ;
Sources_lon:units = "Degrees" ;
Sources_lon:long_name = "X_coordinate_of_source_point" ;
long Sources_ilon(Sources) ;
Sources_ilon:units = "cell_number" ;
Sources_ilon:long_name = "X_coordinate_of_source_point" ;
float Sources_Temp(Sources) ;
Sources_Temp:units = "Celcius_degree" ;
Sources_Temp:long_name = "Temperature_of_source_point" ;
float Sources_Height(Sources) ;
Sources_Height:units = "Meter" ;
Sources_Height:long_name = "Height_of_source_point" ;
float Sources_Diameter(Sources) ;
Sources_Diameter:units = "Meter" ;
Sources_Diameter:long_name = "Diameter_of_source_point" ;
float Sources_Velocity(Sources) ;
Sources_Velocity:units = "Meter/s" ;
Sources_Velocity:long_name = "Velocity_of_source_point_emission" ;
float NO2(Time, type_day, Sources) ;
NO2:units = "molecule/cm2/s" ;
NO2:long_name = "NO2 Emission" ;

// global attributes:
:Title = "CHIMERE SUITE" ;
:Sub-title = "Hourly point emission" ;
:Chimere_type = "EMISSIONS" ;
:Generating_process = "Generated by distribemis" ;
:Conventions = "None" ;
:Domain = "CONT5" ;
:Emission_version = "2008b" ;
:history = "" ;
}
```

G.3 exdomout.nc

```
netcdf exdomout {
dimensions:
Time = UNLIMITED ; // (13 currently)
DateStrLen = 19 ;
```

```
west_east = 67 ;
south_north = 46 ;
bottom_top = 32 ;
variables:
char Times(Time, DateStrLen) ;
float lon(south_north, west_east) ;
lon:units = "degrees_east" ;
lon:long_name = "Longitude" ;
float lat(south_north, west_east) ;
lat:units = "degrees_north" ;
lat:long_name = "Latitude" ;
float sshf(Time, south_north, west_east) ;
sshf:units = "W/m^2" ;
sshf:long_name = "Surface sensible heat flux" ;
float slhf(Time, south_north, west_east) ;
slhf:units = "W/m^2" ;
slhf:long_name = "Surface latent heat flux" ;
float usta(Time, south_north, west_east) ;
usta:units = "m/s" ;
usta:long_name = "Frictional velocity" ;
float tem2(Time, south_north, west_east) ;
tem2:units = "K" ;
tem2:long_name = "2m air temperature" ;
float soim(Time, south_north, west_east) ;
soim:units = "m^3/m^3" ;
soim:long_name = "Soil Moisture level 1" ;
float hght(Time, south_north, west_east) ;
hght:units = "m" ;
hght:long_name = "PBL height from MM5" ;
float rh2m(Time, south_north, west_east) ;
rh2m:units = "fraction" ;
rh2m:long_name = "Relative Humidity at 2m" ;
float lspc(Time, south_north, west_east) ;
lspc:units = "kg/m^2" ;
lspc:long_name = "Large scale precipitation" ;
float copc(Time, south_north, west_east) ;
copc:units = "kg/m^2" ;
copc:long_name = "convective precipitation" ;
float u10m(Time, south_north, west_east) ;
u10m:units = "m/s" ;
u10m:long_name = "10 m U wind" ;
float v10m(Time, south_north, west_east) ;
v10m:units = "m/s" ;
v10m:long_name = "10 m V wind" ;
float temp(Time, bottom_top, south_north, west_east) ;
temp:units = "K" ;
temp:long_name = "Temperature" ;
float cliq(Time, bottom_top, south_north, west_east) ;
cliq:units = "kg/kg" ;
cliq:long_name = "Cloud liquid water mixing ratio" ;
float rain(Time, bottom_top, south_north, west_east) ;
rain:units = "kg/kg" ;
rain:long_name = "Rain water mixing ratio" ;
float sphu(Time, bottom_top, south_north, west_east) ;
sphu:units = "kg/kg" ;
sphu:long_name = "Specific humidity" ;
float cice(Time, bottom_top, south_north, west_east) ;
cice:units = "kg/kg" ;
cice:long_name = "Ice mixing ratio" ;
```

```
float pres(Time, bottom_top, south_north, west_east) ;
pres:units = "Pa" ;
pres:long_name = "Pressure" ;
float alti(Time, bottom_top, south_north, west_east) ;
alti:units = "m" ;
alti:long_name = "Altitude of half-sigma level" ;
float winz(Time, bottom_top, south_north, west_east) ;
winz:units = "m/s" ;
winz:long_name = "Zonal wind" ;
float winm(Time, bottom_top, south_north, west_east) ;
winm:units = "m/s" ;
winm:long_name = "Meridional wind" ;

// global attributes:
:Title = "CHIMERE SUITE" ;
:Sub-title = "Interpolated Meteo file" ;
:Generating_process = "Generated by prepexmm5" ;
:Conventions = "" ;
:Domain = "CONT3" ;
:history = "File exdomout.nc was generated on",
                   "Tue Nov 15 14:25:27 2005 by <user> on <host>",
                    "from input file EUR1/MMOUT_EUR1_20030730_20030803_S\n" ;
:mm5_nxx = 85 ;
:mm5_nxx_DOT = 86 ;
:mm5_nyy = 75 ;
:mm5_nyy_DOT = 76 ;
:mm5_nlev = 32 ;
}
```

G.4 meteo.nc

```
netcdf meteo.20090312_20090319_test {
dimensions:
Time = UNLIMITED ; // (193 currently)
DateStrLen = 19 ;
west_east = 79 ;
south_north = 47 ;
bottom_top = 8 ;
variables:
float lon(south_north, west_east) ;
lon:units = "degrees_east" ;
lon:long_name = "Longitude" ;
float lat(south_north, west_east) ;
lat:units = "degrees_north" ;
lat:long_name = "Latitude" ;
char Times(Time, DateStrLen) ;
float hght(Time, south_north, west_east) ;
hght:units = "m" ;
hght:long_name = "Boundary layer height" ;
float u10m(Time, south_north, west_east) ;
u10m:units = "m/s" ;
u10m:long_name = "10m zonal wind speed" ;
float v10m(Time, south_north, west_east) ;
v10m:units = "m/s" ;
v10m:long_name = "10m meridional wind speed" ;
float w10m(Time, south_north, west_east) ;
w10m:units = "m/s" ;
w10m:long_name = "10m vertical wind speed" ;
```

```
float usta(Time, south_north, west_east) ;
usta:units = "m/s" ;
usta:long_name = "Friction velocity u*" ;
float wsta(Time, south_north, west_east) ;
wsta:units = "m/s" ;
wsta:long_name = "Convection velocity w*" ;
float tem2(Time, south_north, west_east) ;
tem2:units = "K" ;
tem2:long_name = "2m temperature" ;
float soim(Time, south_north, west_east) ;
soim:units = "m^3/m^3" ;
soim:long_name = "Soil moisture" ;
float sreh(Time, south_north, west_east) ;
sreh:units = "%" ;
sreh:long_name = "Surface relative humidity" ;
float psfc(Time, south_north, west_east) ;
psfc:units = "Pa" ;
psfc:long_name = "Surface pressure" ;
float sshf(Time, south_north, west_east) ;
sshf:units = "W/m2" ;
sshf:long_name = "Surface sensible heat flux" ;
float slhf(Time, south_north, west_east) ;
slhf:units = "W/m2" ;
slhf:long_name = "Surface latent heat flux" ;
float copc(Time, south_north, west_east) ;
copc:units = "mm/h" ;
copc:long_name = "Convective precipitation" ;
float lspc(Time, south_north, west_east) ;
lspc:units = "kg/m^2/h" ;
lspc:long_name = "Large scale precipitation" ;
float topc(Time, south_north, west_east) ;
topc:units = "kg/m^2/h" ;
topc:long_name = "Precipitation" ;
float aerr(Time, south_north, west_east) ;
aerr:units = "s/m" ;
aerr:long_name = "Aerodynamic resistance" ;
float atte(Time, south_north, west_east) ;
atte:units = "[0-1]" ;
atte:long_name = "Radiation attenuation factor" ;
float swrd(Time, south_north, west_east) ;
swrd:units = "W/m2" ;
swrd:long_name = "Shortwave radiation" ;
float winz(Time, bottom_top, south_north, west_east) ;
winz:units = "m/s" ;
winz:long_name = "Zonal wind" ;
float winm(Time, bottom_top, south_north, west_east) ;
winm:units = "m/s" ;
winm:long_name = "Meridional wind" ;
float winw(Time, bottom_top, south_north, west_east) ;
winw:units = "m/s" ;
winw:long_name = "Vertical wind" ;
float temp(Time, bottom_top, south_north, west_east) ;
temp:units = "K" ;
temp:long_name = "Temperature" ;
float sphu(Time, bottom_top, south_north, west_east) ;
sphu:units = "kg/kg" ;
sphu:long_name = "Specific humidity" ;
float airm(Time, bottom_top, south_north, west_east) ;
airm:units = "molecule/m**3" ;
```

```
airm:long_name = "Air density" ;
float hlay(Time, bottom_top, south_north, west_east) ;
hlay:units = "m" ;
hlay:long_name = "Layer top altitude" ;
float kzzz(Time, bottom_top, south_north, west_east) ;
kzzz:units = "m2/s2" ;
kzzz:long_name = "Kz diffusion coefficient" ;
float clwc(Time, bottom_top, south_north, west_east) ;
clwc:units = "kg/kg" ;
clwc:long_name = "Liquid (+ice) water content" ;
float cliq(Time, bottom_top, south_north, west_east) ;
cliq:units = "kg/kg" ;
cliq:long_name = "Cloud liquid water mixing ratio" ;
float rain(Time, bottom_top, south_north, west_east) ;
rain:units = "kg/kg" ;
rain:long_name = "Rain water mixing ratio" ;
float pres(Time, bottom_top, south_north, west_east) ;
pres:units = "Pa" ;
pres:long_name = "Pressure" ;
float cice(Time, bottom_top, south_north, west_east) ;
cice:units = "kg/kg" ;
cice:long_name = "Ice liquid water mixing ratio" ;
float thlay(Time, bottom_top, south_north, west_east) ;
thlay:units = "m" ;
thlay:long_name = "Layer thickness" ;
float dpeu(Time, bottom_top, south_north, west_east) ;
dpeu:units = "kg/m2/s" ;
dpeu:long_name = "Entrainment in updraft" ;
float dped(Time, bottom_top, south_north, west_east) ;
dped:units = "kg/m2/s" ;
dped:long_name = "Entrainment in downdraft" ;
float dpdu(Time, bottom_top, south_north, west_east) ;
dpdu:units = "kg/m2/s" ;
dpdu:long_name = "Detrainment in updraft" ;
float dpdd(Time, bottom_top, south_north, west_east) ;
dpdd:units = "kg/m2/s" ;
dpdd:long_name = "Detrainment in downdraft" ;
float flxu(Time, bottom_top, south_north, west_east) ;
flxu:units = "kg/m2/s" ;
flxu:long_name = "updraft mass flux" ;
float flxd(Time, bottom_top, south_north, west_east) ;
flxd:units = "kg/m2/s" ;
flxd:long_name = "downdraft  mass flux" ;

// global attributes:
:Title = "CHIMERE SUITE" ;
:Sub-title = "Hourly output meteo file" ;
:Chimere_type = "Chimere Meteo" ;
:Generating_process = "Generated by chimere" ;
:Conventions = "None" ;
:Domain = "CONT5" ;
:Chimere_version = "chimere2014b" ;
:history = "unknown" ;
}
```

G.5 AEMISSIONS.nc

```
netcdf AEMISSIONS {
```

```
dimensions:
Time = UNLIMITED ; // (24 currently)
west_east = 79 ;
south_north = 47 ;
bottom_top = 8 ;
SpStrLen = 23 ;
DateStrLen = 19 ;
Species = 24 ;

variables:
char Times(Time, DateStrLen) ;
char species(Species, SpStrLen) ;
float lon(south_north, west_east) ;
lon:units = "degrees_east" ;
lon:long_name = "Longitude" ;
float lat(south_north, west_east) ;
lat:units = "degrees_north" ;
lat:long_name = "Latitude" ;
float APINEN(Time, bottom_top, south_north, west_east) ;
APINEN:units = "molecule/cm2/s" ;
APINEN:long_name = "APINEN Emission" ;
float C2H4(Time, bottom_top, south_north, west_east) ;
C2H4:units = "molecule/cm2/s" ;
C2H4:long_name = "C2H4 Emission" ;
float C2H6(Time, bottom_top, south_north, west_east) ;
C2H6:units = "molecule/cm2/s" ;
C2H6:long_name = "C2H6 Emission" ;
float C3H6(Time, bottom_top, south_north, west_east) ;
C3H6:units = "molecule/cm2/s" ;
C3H6:long_name = "C3H6 Emission" ;
float C5H8(Time, bottom_top, south_north, west_east) ;
C5H8:units = "molecule/cm2/s" ;
C5H8:long_name = "C5H8 Emission" ;
float CH3CHO(Time, bottom_top, south_north, west_east) ;
CH3CHO:units = "molecule/cm2/s" ;
CH3CHO:long_name = "CH3CHO Emission" ;
float CH3COE(Time, bottom_top, south_north, west_east) ;
CH3COE:units = "molecule/cm2/s" ;
CH3COE:long_name = "CH3COE Emission" ;
float CH4(Time, bottom_top, south_north, west_east) ;
CH4:units = "molecule/cm2/s" ;
CH4:long_name = "CH4 Emission" ;
float CO(Time, bottom_top, south_north, west_east) ;
CO:units = "molecule/cm2/s" ;
CO:long_name = "CO Emission" ;
float HCHO(Time, bottom_top, south_north, west_east) ;
HCHO:units = "molecule/cm2/s" ;
HCHO:long_name = "HCHO Emission" ;
float HONO(Time, bottom_top, south_north, west_east) ;
HONO:units = "molecule/cm2/s" ;
HONO:long_name = "HONO Emission" ;
float NC4H10(Time, bottom_top, south_north, west_east) ;
NC4H10:units = "molecule/cm2/s" ;
NC4H10:long_name = "NC4H10 Emission" ;
float NH3(Time, bottom_top, south_north, west_east) ;
NH3:units = "molecule/cm2/s" ;
NH3:long_name = "NH3 Emission" ;
float NO(Time, bottom_top, south_north, west_east) ;
NO:units = "molecule/cm2/s" ;
```

```
NO:long_name = "NO Emission" ;
float NO2(Time, bottom_top, south_north, west_east) ;
NO2:units = "molecule/cm2/s" ;
NO2:long_name = "NO2 Emission" ;
float OXYL(Time, bottom_top, south_north, west_east) ;
OXYL:units = "molecule/cm2/s" ;
OXYL:long_name = "OXYL Emission" ;
float SO2(Time, bottom_top, south_north, west_east) ;
SO2:units = "molecule/cm2/s" ;
SO2:long_name = "SO2 Emission" ;
float H2SO4_fin(Time, bottom_top, south_north, west_east) ;
H2SO4_fin:units = "molecule/cm2/s" ;
H2SO4_fin:long_name = "H2SO4_fin Emission" ;
float PPM_big(Time, bottom_top, south_north, west_east) ;
PPM_big:units = "molecule/cm2/s" ;
PPM_big:long_name = "PPM_big Emission" ;
float PPM_coa(Time, bottom_top, south_north, west_east) ;
PPM_coa:units = "molecule/cm2/s" ;
PPM_coa:long_name = "PPM_coa Emission" ;
float OCAR_fin(Time, bottom_top, south_north, west_east) ;
OCAR_fin:units = "molecule/cm2/s" ;
OCAR_fin:long_name = "OCAR_fin Emission" ;
float BCAR_fin(Time, bottom_top, south_north, west_east) ;
BCAR_fin:units = "molecule/cm2/s" ;
BCAR_fin:long_name = "BCAR_fin Emission" ;
float TOL(Time, bottom_top, south_north, west_east) ;
TOL:units = "molecule/cm2/s" ;
TOL:long_name = "TOL Emission" ;
float TMB(Time, bottom_top, south_north, west_east) ;
TMB:units = "molecule/cm2/s" ;
TMB:long_name = "TMB Emission" ;

// global attributes:
:Title = "CHIMERE SUITE" ;
:Sub-title = "Emissions file - Surfacic + Point sources + Fires" ;
:Generating_process = "Generated by prepemis" ;
:Conventions = "" ;
:Domain = "CONT5" ;
:history = "" ;
}
```

G.6 BEMISSIONS.nc

```
netcdf BEMISSIONS {
dimensions:
Time = UNLIMITED ; // (13 currently)
DateStrLen = 19 ;
west_east = 67 ;
south_north = 46 ;
biospecies = 13 ;
variables:
        char Times(Time, DateStrLen) ;
        float lon(south_north, west_east) ;
        float lat(south_north, west_east) ;
        float C5H8(Time, south_north, west_east) ;
        float APINEN(Time, south_north, west_east) ;
        float BPINEN(Time, south_north, west_east) ;
        float LIMONE(Time, south_north, west_east) ;
```

```
        float TERPEN(Time, south_north, west_east) ;
        float OCIMEN(Time, south_north, west_east) ;
        float HUMULE(Time, south_north, west_east) ;
        float NO(Time, south_north, west_east) ;
        float SALT_coa(Time, south_north, west_east) ;
        float NA_coa(Time, south_north, west_east) ;
        float HCL_coa(Time, south_north, west_east) ;
        float H2SO4_coa(Time, south_north, west_east) ;
        float WATER_coa(Time, south_north, west_east) ;

// global attributes:
:Title = "CHIMERE SUITE" ;
:Sub-title = "Bioemissions file" ;
:Generating_process = "Generated by calbio" ;
:Conventions = "" ;
:Domain = "CONT3" ;
:history = "File BEMISSIONS.nc",
                  "was generated on Tue Nov 15 14:25:40 2005 ",
                  "by <user> on <host> from input file",
                  "meteo.nc\n",
}
```

G.7 BOUN_CONCS.nc

```
netcdf BOUN_CONCS {
dimensions:
        Time = UNLIMITED ; // (121 currently)
        DateStrLen = 19 ;
        SpStrLen = 23 ;
        west_east = 101 ;
        south_north = 111 ;
        bottom_top = 20 ;
        h_boundary = 424 ;
        Species = 169 ;

variables:
        char Times(Time, DateStrLen) ;
        char species(Species, SpStrLen) ;
        float lon(south_north, west_east) ;
        float lat(south_north, west_east) ;
        float top_conc(Time, south_north, west_east, Species) ;
        float lat_conc(Time, bottom_top, h_boundary, Species) ;

// global attributes:
                :Title = "CHIMERE SUITE" ;
                :Sub-title = "Fine boundary concentrations file" ;
                :Generating_process = "Generated by prep_CHIMERE" ;
}
```

G.8 end.nc

```
netcdf end.20030730_20030803_heat-wave {
dimensions:
Time = UNLIMITED ; // (1 currently)
DateStrLen = 19 ;
```

```
SpecStrLen = 16 ;
Species = 119 ;
west_east = 67 ;
south_north = 46 ;
bottom_top = 8 ;
variables:
float lon(south_north, west_east) ;
lon:units = "degrees_east" ;
lon:long_name = "Longitude" ;
float lat(south_north, west_east) ;
lat:units = "degrees_north" ;
lat:long_name = "Latitude" ;
char species_name(Species, SpecStrLen) ;
char Times(Time, DateStrLen) ;
float APINEN(Time, bottom_top, south_north, west_east) ;
APINEN:units = "molecules/cm3" ;
float C2H4(Time, bottom_top, south_north, west_east) ;
C2H4:units = "molecules/cm3" ;
float C2H6(Time, bottom_top, south_north, west_east) ;
C2H6:units = "molecules/cm3" ;
float C3H6(Time, bottom_top, south_north, west_east) ;
C3H6:units = "molecules/cm3" ;
float C5H8(Time, bottom_top, south_north, west_east) ;
C5H8:units = "molecules/cm3" ;
float CARNIT(Time, bottom_top, south_north, west_east) ;
CARNIT:units = "molecules/cm3" ;
float CH3CHO(Time, bottom_top, south_north, west_east) ;
CH3CHO:units = "molecules/cm3" ;
float CH3COE(Time, bottom_top, south_north, west_east) ;
CH3COE:units = "molecules/cm3" ;
float CH3COO(Time, bottom_top, south_north, west_east) ;
CH3COO:units = "molecules/cm3" ;
float CH3COY(Time, bottom_top, south_north, west_east) ;
CH3COY:units = "molecules/cm3" ;
float CH3O2(Time, bottom_top, south_north, west_east) ;
CH3O2:units = "molecules/cm3" ;
float CH3O2H(Time, bottom_top, south_north, west_east) ;
CH3O2H:units = "molecules/cm3" ;
float CH4(Time, bottom_top, south_north, west_east) ;
CH4:units = "molecules/cm3" ;
float CO(Time, bottom_top, south_north, west_east) ;
CO:units = "molecules/cm3" ;
float DUSTAQ(Time, bottom_top, south_north, west_east) ;
DUSTAQ:units = "molecules/cm3" ;
float GLYOX(Time, bottom_top, south_north, west_east) ;
GLYOX:units = "molecules/cm3" ;
float H2O2(Time, bottom_top, south_north, west_east) ;
H2O2:units = "molecules/cm3" ;
float H2SO4(Time, bottom_top, south_north, west_east) ;
H2SO4:units = "molecules/cm3" ;
float H2SO4AQ(Time, bottom_top, south_north, west_east) ;
H2SO4AQ:units = "molecules/cm3" ;
float HCHO(Time, bottom_top, south_north, west_east) ;
HCHO:units = "molecules/cm3" ;
float HNO3(Time, bottom_top, south_north, west_east) ;
HNO3:units = "molecules/cm3" ;
float HNO3AQ(Time, bottom_top, south_north, west_east) ;
HNO3AQ:units = "molecules/cm3" ;
float HO2(Time, bottom_top, south_north, west_east) ;
```

```
HO2:units = "molecules/cm3" ;
float HONO(Time, bottom_top, south_north, west_east) ;
HONO:units = "molecules/cm3" ;
float ISNI(Time, bottom_top, south_north, west_east) ;
ISNI:units = "molecules/cm3" ;
float MAC(Time, bottom_top, south_north, west_east) ;
MAC:units = "molecules/cm3" ;
float MEMALD(Time, bottom_top, south_north, west_east) ;
MEMALD:units = "molecules/cm3" ;
float MGLYOX(Time, bottom_top, south_north, west_east) ;
MGLYOX:units = "molecules/cm3" ;
float MVK(Time, bottom_top, south_north, west_east) ;
MVK:units = "molecules/cm3" ;
float N2O5(Time, bottom_top, south_north, west_east) ;
N2O5:units = "molecules/cm3" ;
float NC4H10(Time, bottom_top, south_north, west_east) ;
NC4H10:units = "molecules/cm3" ;
float NH3(Time, bottom_top, south_north, west_east) ;
NH3:units = "molecules/cm3" ;
float NH3AQ(Time, bottom_top, south_north, west_east) ;
NH3AQ:units = "molecules/cm3" ;
float NO(Time, bottom_top, south_north, west_east) ;
NO:units = "molecules/cm3" ;
float NO2(Time, bottom_top, south_north, west_east) ;
NO2:units = "molecules/cm3" ;
float NO3(Time, bottom_top, south_north, west_east) ;
NO3:units = "molecules/cm3" ;
float O3(Time, bottom_top, south_north, west_east) ;
O3:units = "molecules/cm3" ;
float obio(Time, bottom_top, south_north, west_east) ;
obio:units = "molecules/cm3" ;
float obioH(Time, bottom_top, south_north, west_east) ;
obioH:units = "molecules/cm3" ;
float OH(Time, bottom_top, south_north, west_east) ;
OH:units = "molecules/cm3" ;
float oPAN(Time, bottom_top, south_north, west_east) ;
oPAN:units = "molecules/cm3" ;
float oRN1(Time, bottom_top, south_north, west_east) ;
oRN1:units = "molecules/cm3" ;
float oRO2(Time, bottom_top, south_north, west_east) ;
oRO2:units = "molecules/cm3" ;
float oROOH(Time, bottom_top, south_north, west_east) ;
oROOH:units = "molecules/cm3" ;
float OXYL(Time, bottom_top, south_north, west_east) ;
OXYL:units = "molecules/cm3" ;
float PAN(Time, bottom_top, south_north, west_east) ;
PAN:units = "molecules/cm3" ;
float PANH(Time, bottom_top, south_north, west_east) ;
PANH:units = "molecules/cm3" ;
float PPA(Time, bottom_top, south_north, west_east) ;
PPA:units = "molecules/cm3" ;
float PPMAQ(Time, bottom_top, south_north, west_east) ;
PPMAQ:units = "molecules/cm3" ;
float SO2(Time, bottom_top, south_north, west_east) ;
SO2:units = "molecules/cm3" ;
float SOA(Time, bottom_top, south_north, west_east) ;
SOA:units = "molecules/cm3" ;
float SOAAQ(Time, bottom_top, south_north, west_east) ;
SOAAQ:units = "molecules/cm3" ;
```

```
float toPAN(Time, bottom_top, south_north, west_east) ;
toPAN:units = "molecules/cm3" ;
float p1PPM(Time, bottom_top, south_north, west_east) ;
p1PPM:units = "molecules/cm3" ;
float p1DUST(Time, bottom_top, south_north, west_east) ;
p1DUST:units = "molecules/cm3" ;
float p1SOA(Time, bottom_top, south_north, west_east) ;
p1SOA:units = "molecules/cm3" ;
float p1H2SO4(Time, bottom_top, south_north, west_east) ;
p1H2SO4:units = "molecules/cm3" ;
float p1HNO3(Time, bottom_top, south_north, west_east) ;
p1HNO3:units = "molecules/cm3" ;
float p1NH3(Time, bottom_top, south_north, west_east) ;
p1NH3:units = "molecules/cm3" ;
float p1WATER(Time, bottom_top, south_north, west_east) ;
p1WATER:units = "molecules/cm3" ;
float p2PPM(Time, bottom_top, south_north, west_east) ;
p2PPM:units = "molecules/cm3" ;
float p2DUST(Time, bottom_top, south_north, west_east) ;
p2DUST:units = "molecules/cm3" ;
float p2SOA(Time, bottom_top, south_north, west_east) ;
p2SOA:units = "molecules/cm3" ;
float p2H2SO4(Time, bottom_top, south_north, west_east) ;
p2H2SO4:units = "molecules/cm3" ;
float p2HNO3(Time, bottom_top, south_north, west_east) ;
p2HNO3:units = "molecules/cm3" ;
float p2NH3(Time, bottom_top, south_north, west_east) ;
p2NH3:units = "molecules/cm3" ;
float p2WATER(Time, bottom_top, south_north, west_east) ;
p2WATER:units = "molecules/cm3" ;
float p3PPM(Time, bottom_top, south_north, west_east) ;
p3PPM:units = "molecules/cm3" ;
float p3DUST(Time, bottom_top, south_north, west_east) ;
p3DUST:units = "molecules/cm3" ;
float p3SOA(Time, bottom_top, south_north, west_east) ;
p3SOA:units = "molecules/cm3" ;
float p3H2SO4(Time, bottom_top, south_north, west_east) ;
p3H2SO4:units = "molecules/cm3" ;
float p3HNO3(Time, bottom_top, south_north, west_east) ;
p3HNO3:units = "molecules/cm3" ;
float p3NH3(Time, bottom_top, south_north, west_east) ;
p3NH3:units = "molecules/cm3" ;
float p3WATER(Time, bottom_top, south_north, west_east) ;
p3WATER:units = "molecules/cm3" ;
float p4PPM(Time, bottom_top, south_north, west_east) ;
p4PPM:units = "molecules/cm3" ;
float p4DUST(Time, bottom_top, south_north, west_east) ;
p4DUST:units = "molecules/cm3" ;
float p4SOA(Time, bottom_top, south_north, west_east) ;
p4SOA:units = "molecules/cm3" ;
float p4H2SO4(Time, bottom_top, south_north, west_east) ;
p4H2SO4:units = "molecules/cm3" ;
float p4HNO3(Time, bottom_top, south_north, west_east) ;
p4HNO3:units = "molecules/cm3" ;
float p4NH3(Time, bottom_top, south_north, west_east) ;
p4NH3:units = "molecules/cm3" ;
float p4WATER(Time, bottom_top, south_north, west_east) ;
p4WATER:units = "molecules/cm3" ;
float p5PPM(Time, bottom_top, south_north, west_east) ;
```

```
p5PPM:units = "molecules/cm3" ;
float p5DUST(Time, bottom_top, south_north, west_east) ;
p5DUST:units = "molecules/cm3" ;
float p5SOA(Time, bottom_top, south_north, west_east) ;
p5SOA:units = "molecules/cm3" ;
float p5H2SO4(Time, bottom_top, south_north, west_east) ;
p5H2SO4:units = "molecules/cm3" ;
float p5HNO3(Time, bottom_top, south_north, west_east) ;
p5HNO3:units = "molecules/cm3" ;
float p5NH3(Time, bottom_top, south_north, west_east) ;
p5NH3:units = "molecules/cm3" ;
float p5WATER(Time, bottom_top, south_north, west_east) ;
p5WATER:units = "molecules/cm3" ;
float p6PPM(Time, bottom_top, south_north, west_east) ;
p6PPM:units = "molecules/cm3" ;
float p6DUST(Time, bottom_top, south_north, west_east) ;
p6DUST:units = "molecules/cm3" ;
float p6SOA(Time, bottom_top, south_north, west_east) ;
p6SOA:units = "molecules/cm3" ;
float p6H2SO4(Time, bottom_top, south_north, west_east) ;
p6H2SO4:units = "molecules/cm3" ;
float p6HNO3(Time, bottom_top, south_north, west_east) ;
p6HNO3:units = "molecules/cm3" ;
float p6NH3(Time, bottom_top, south_north, west_east) ;
p6NH3:units = "molecules/cm3" ;
float p6WATER(Time, bottom_top, south_north, west_east) ;
p6WATER:units = "molecules/cm3" ;
float M(Time, bottom_top, south_north, west_east) ;
M:units = "molecules/cm3" ;
float O2(Time, bottom_top, south_north, west_east) ;
O2:units = "molecules/cm3" ;
float N2(Time, bottom_top, south_north, west_east) ;
N2:units = "molecules/cm3" ;
float H2O(Time, bottom_top, south_north, west_east) ;
H2O:units = "molecules/cm3" ;
float TOTPAN(Time, bottom_top, south_north, west_east) ;
TOTPAN:units = "molecules/cm3" ;
float NOX(Time, bottom_top, south_north, west_east) ;
NOX:units = "molecules/cm3" ;
float OX(Time, bottom_top, south_north, west_east) ;
OX:units = "molecules/cm3" ;
float HOX(Time, bottom_top, south_north, west_east) ;
HOX:units = "molecules/cm3" ;
float NOY(Time, bottom_top, south_north, west_east) ;
NOY:units = "molecules/cm3" ;
float ROOH(Time, bottom_top, south_north, west_east) ;
ROOH:units = "molecules/cm3" ;
float HCNM(Time, bottom_top, south_north, west_east) ;
HCNM:units = "molecules/cm3" ;
float PM10(Time, bottom_top, south_north, west_east) ;
PM10:units = "molecules/cm3" ;
float PM25(Time, bottom_top, south_north, west_east) ;
PM25:units = "molecules/cm3" ;
float PM10_anth(Time, bottom_top, south_north, west_east) ;
PM10_anth:units = "molecules/cm3" ;
float PM25_anth(Time, bottom_top, south_north, west_east) ;
PM25_anth:units = "molecules/cm3" ;
float PPM10_anth(Time, bottom_top, south_north, west_east) ;
PPM10_anth:units = "molecules/cm3" ;
```

```
float PPM25_anth(Time, bottom_top, south_north, west_east) ;
PPM25_anth:units = "molecules/cm3" ;
float pPPM(Time, bottom_top, south_north, west_east) ;
pPPM:units = "molecules/cm3" ;
float pDUST(Time, bottom_top, south_north, west_east) ;
pDUST:units = "molecules/cm3" ;
float pSOA(Time, bottom_top, south_north, west_east) ;
pSOA:units = "molecules/cm3" ;
float pH2SO4(Time, bottom_top, south_north, west_east) ;
pH2SO4:units = "molecules/cm3" ;
float pHNO3(Time, bottom_top, south_north, west_east) ;
pHNO3:units = "molecules/cm3" ;
float pNH3(Time, bottom_top, south_north, west_east) ;
pNH3:units = "molecules/cm3" ;
float pWATER(Time, bottom_top, south_north, west_east) ;
pWATER:units = "molecules/cm3" ;

// global attributes:
:Title = "CHIMERE SUITE" ;
:Sub-title = "Final concentrations file" ;
:Chimere_type = "end" ;
:Generating_process = "Generated by chimere" ;
:Conventions = "None" ;
:Domain = "CONT3" ;
:history = "File end.20030730_20030803_heat-wave.nc",
                  "was generated on Tue Nov  8 12:27:58 2005",
                  "by <user> on <host>\n" ;
}
```

G.9 Fire emissions EMIS.[domain].[MM].[SPEC].f.nc

```
netcdf EMIS.MEDa.06.CO.f {
dimensions:
        west_east = 119 ;
        south_north = 84 ;
        days = 30 ;
        hours = 24 ;
        sources = 315 ;
variables:
        float lon(south_north, west_east) ;
                lon:units = "degrees_east" ;
                lon:long_name = "Longitude" ;
        float lat(south_north, west_east) ;
                lat:units = "degrees_north" ;
                lat:long_name = "Latitude" ;
        float ilatsources(sources) ;
                ilatsources:units = "index" ;
                ilatsources:long_name = "Latitude_of_sources" ;
        float ilonsources(sources) ;
                ilonsources:units = "index" ;
                ilonsources:long_name = "Longitude_of_sources" ;
        float CO(hours, days, sources) ;
                CO:units = "molecule/cm2/s" ;
                CO:long_name = "CO Emission" ;
```